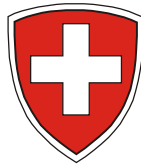


Switzerland

Swiss Geodetic Commission



Suisse

Commission Géodésique Suisse

**Swiss National Report on the
GEODETIC ACTIVITIES
in the years 2011 to 2015**

Presented to the XXVI General Assembly
of the International Union of Geodesy and Geophysics
in Prague, Czech Republic, June/July 2015



**Rapport National Suisse sur les
ACTIVITÉS GÉODÉSIQUES
exécutées de 2011 à 2015**

Présenté à la vingt-sixième Assemblée générale
de l'Union Géodésique et Géophysique Internationale
tenue à Prague, République Tchèque, Juin/Juillet 2015

Zurich 2015

Swiss Geodetic Commission/Commission Géodésique Suisse

ETH Zurich

Robert-Gnehm-Weg 15

8093 Zurich

Switzerland

<http://www.sgc.ethz.ch/publications>

Edited by:

J. Mueller-Gantenbein

A. Wiget

U. Marti

M. Rothacher

P.-Y. Gilliéron

Secretary of the SGC

(Commission 1)

(Commission 2)

(Commission 3)

(Commission 4)

In addition to the bibliographies at the end of each section we recommend the following
www-sites:

Astronomical Institute of the University of Bern (AIUB): <http://www.aiub.unibe.ch/>

Institute of Geodesy and Photogrammetry,
Eidgenössische Technische Hochschule, ETH Zurich: <http://www.igp.ethz.ch/>

Office federal de topographie (swisstopo)
Federal Office of Topography (swisstopo): <http://www.swisstopo.ch/>

Geodetic Engineering Laboratory,
École polytechnique fédérale de Lausanne EPFL: <http://topo.epfl.ch/>

Haute Ecole d'Ingénierie et de Gestion du Canton de Vaud: <http://www.heig-vd.ch/>

University of Applied Sciences Northwestern Switzerland,
Fachhochschule Nordwestschweiz: <http://www.fhnw.ch/>

ISBN 978-3-908440-39-0

Printed by: adag, Zurich

©2015 Swiss Geodetic Commission

PREFACE

The Swiss Geodetic Commission (SGC) is an organisation within the Swiss Academy of Sciences (SCNAT). It is devoted to research into scientific problems of geodesy including the transfer to practical applications in national surveying. Of particular importance is the promotion of international cooperation and national coordination. The SGC has close links to the Swiss Geophysical Commission, in particular in the field of gravimetry where research projects are being pursued jointly on an interdisciplinary basis.

For the compilation of the national report covering the scientific activities of the past 4 years it was decided to follow the structure of previous national reports and divide it into 4 commissions according to the structure of the International Association of Geodesy (IAG):

- 1 Reference Frames
- 2 Gravity Field
- 3 Earth Rotation and Geodynamics
- 4 Positioning & Applications

These main chapters were compiled by an editorial staff consisting of A. Wiget (Commission 1), U. Marti (Commission 2), M. Rothacher (Commission 3), P.-Y. Gilliéron (Commission 4). Our special thanks go to J. Mueller-Gantenbein, secretary of SGC, for the careful editing and preparation of the layout. Without her efforts this report could not have been realized in due time.

The SGC expresses its appreciative thanks to all colleagues who have contributed to this report and who are promoting Geodetic Sciences in Switzerland. Financial support was provided by the SCNAT. Its valuable help is gratefully acknowledged.

On behalf of the Swiss Geodetic Commission, June 2015

Urs Marti
Vice-President of SGC

Alain Geiger
President of SGC

1	REFERENCE FRAMES	11
	CODE CONTRIBUTIONS TO THE IGS.....	11
	<i>S. Schaer¹², D. Arnold¹, C. Baumann¹³, H. Bock¹⁴, R. Dach¹, L. Prange¹, S. Lutz¹³, E. Orliac¹, D. Thaller¹⁴, A. Villiger¹</i>	
	EUREF ACTIVITIES AT CODE.....	15
	<i>S. Schaer¹², R. Dach¹, S. Lutz¹³, A. Villiger¹</i>	
	REPROCESSING ACTIVITIES AT CODE.....	17
	<i>S. Lutz¹², P. Steigenberger³⁴, R. Dach¹, S. Schaer¹⁵, K. Sośnica¹⁶</i>	
	UPDATING THE EMPIRICAL CODE ORBIT MODEL AND VALIDATION OF GPS AND GLONASS ORBITS USING SATELLITE LASER RANGING DATA	19
	<i>D. Arnold¹, G. Beutler¹, K. Sośnica¹², M. Meindl³, S. Lutz¹⁴, R. Dach¹</i>	
	CODE FIVE SYSTEM SOLUTION FOR IGS MGEX	21
	<i>L. Prange¹, E. Orliac¹, R. Dach¹, S. Schaer¹², K. Sośnica¹³</i>	
	AIUB CONTRIBUTION TO THE TGVF/OVF	23
	<i>L. Prange¹, E. Orliac¹, R. Dach¹</i>	
	THE SWISS OPTICAL GROUND STATION AND GEODYNAMICS OBSERVATORY ZIMMERWALD	25
	<i>T. Schildknecht¹, A. Jäggi¹, M. Ploner¹, E. Brockmann²</i>	
	SATELLITE LASER RANGING AT ZIMMERWALD.....	27
	<i>M. Ploner¹, T. Schildknecht¹, A. Jäggi¹, P. Lauber¹, J. Utzinger¹, M. Prohaska¹, E. Brockmann²</i>	
	COMBINATION OF SLR, GPS, AND GLONASS OBSERVATIONS USING CO-LOCATIONS IN SPACE AS A CONTRIBUTION TO THE ITRF	30
	<i>K. Sośnica¹², D. Thaller¹³, R. Dach¹, A. Maier¹, A. Jäggi¹</i>	
	GNSS CLOCK MODELLING AND ESTIMATION.....	33
	<i>K. Wang and M. Rothacher</i>	
	GNSS REPROCESSING.....	35
	<i>K. Wang and M. Rothacher</i>	
	CO-LOCATION OF SPACE GEODETIC TECHNIQUES ON GROUND AND IN SPACE	37
	<i>B. Männel and M. Rothacher</i>	
	ANALYSIS OF PERMANENT GNSS NETWORKS AT SWISSTOPO (PNAC)	40
	<i>E. Brockmann, D. Ineichen, S. Lutz, S. Schaer</i>	
	MULTI-GNSS ACTIVITIES AT SWISSTOPO.....	44
	<i>S. Lutz, E. Brockmann, D. Ineichen, S. Schaer</i>	
	REPROCESSING ACTIVITIES AT SWISSTOPO	47
	<i>D. Ineichen, E. Brockmann, S. Lutz, S. Schaer</i>	
	REVISION AND UPDATES OF THE NETWORKS OF THE NATIONAL GEODETIC SURVEY	50
	<i>A. Wiget</i>	
	MEASUREMENTS FOR THE NATIONAL HEIGHT SYSTEM	52
	<i>A. Schlatter and A. Wiget</i>	
	THE NATIONWIDE CHANGE OF THE REFERENCE FRAME FROM LV03 TO LV95	54
	<i>A. Wiget</i>	

TOWARDS A DISTORTION FREE NATIONAL SPATIAL DATA INFRASTRUCTURE IN SWITZERLAND: APPROACH,
DEVELOPED TOOLS AND INTERNET SERVICES FOR THE CHANGE OF THE REFERENCE FRAME 55
M. Kistler, U. Marti, J. Ray, Ch. Baumann and A. Wiget

BIBLIOGRAPHY COMMISSION 1 61

2 GRAVITY FIELD.....	73
ABSOLUTE AND RELATIVE GRAVITY MEASUREMENTS.....	73
<i>U. Marti¹, H. Baumann², B. Bürki³ and S. Guillaume³</i>	
GRAVIMETRIC CALIBRATION LINE INTERLAKEN-JUNGFRAUJOCH	75
<i>U. Marti¹, B. Bürki² and H. Baumann³</i>	
GRAVITY MEASUREMENTS FOR THE VERTICAL NETWORK.....	77
<i>U. Marti¹ and A. Schlatter¹</i>	
PROCESSING FACILITY FOR ESA'S GOCE GRAVITY FIELD EXPLORER MISSION.....	78
<i>H. Bock¹², U. Meyer¹, A. Jäggi¹, R. Dach¹ and G. Beutler¹</i>	
COMBINED GLOBAL GRAVITY FIELD DETERMINATION BASED ON THE GRACE-, GOCE-MISSIONS.....	80
<i>U. Meyer¹, A. Jäggi¹, G. Beutler¹ and L. Mervart²</i>	
TIME-VARIABLE GLOBAL GRAVITY FIELDS DERIVED FROM GRACE- AND GOCE-MEASUREMENTS	82
<i>U. Meyer¹, A. Jäggi¹, G. Beutler¹ and L. Mervart²</i>	
TEMPORAL EARTH'S GRAVITY FIELD VARIATIONS FROM SLR OBSERVATIONS.....	84
<i>K. Sośnica¹², A. Jäggi¹, U. Meyer¹, D. Thaller¹³, A. Maier¹, G. Beutler¹ and R. Dach¹</i>	
SWARM-MISSION: ORBIT DETERMINATION AND DERIVED GRAVITY FIELD	88
<i>D. Arnold¹, C. Dahle¹², H. Bock¹³, A. Jäggi¹</i>	
ANALYZING GRAIL DATA: FIRST LUNAR GRAVITY FIELD SOLUTIONS AT AIUB.....	90
<i>D. Arnold¹, S. Bertone¹, A. Jäggi¹, G. Beutler¹ and L. Mervart²</i>	
GPS-ONLY GRAVITY FIELD RECOVERY WITH GOCE, CHAMP, AND GRACE	93
<i>A. Jäggi¹, H. Bock¹², U. Meyer¹ and G. Beutler¹</i>	
TANDEM-X BASELINE SOLUTIONS USING DIFFERENTIAL GPS	95
<i>A. Jäggi¹, O. Montenbruck², Y. Moon³ and D. Bodenmann¹</i>	
GEOID AND HYDROGRAPHY IN LACUSTRINE AREAS.....	97
<i>A. Geiger¹, Ph. Limpach¹, M. Pozzi¹, M. Wessels², F. Anselmetti³</i>	
ULTRA PRECISE GEOID DETERMINATION FOR A NEW GENERATION OF FUTURE LINEAR COLLIDER: A FEASIBILITY STUDY AT CERN.....	99
<i>S. Guillaume¹, A. Geiger¹, B. Bürki¹ and M. Jones²</i>	
DIGITAL ASTRONOMICAL DEFLECTION MEASURING SYSTEM CODIAC AT ETH ZURICH.....	103
<i>B. Bürki, S. Guillaume, A. Wolf, P. Sorber, and H.P. Oesch</i>	
SCIEX PROJECT REG FOR REGIONAL GRAVITY FIELD MODELLING.....	106
<i>J. Kaminskis^{1,2}, M. Rothacher¹, A. Zarins², B. Bürki¹, S. Guillaume¹</i>	
KINEMATIC GRAVITY DETERMINATION BY GNSS/INS INTEGRATION.....	108
<i>J. Skaloud¹, E. Pares², M. Blazquez², I. Colomina²</i>	
BIBLIOGRAPHY COMMISSION 2	111

3 EARTH ROTATION AND GEODYNAMICS FRAMES	117
CODE CONTRIBUTIONS TO EARTH ROTATION MONITORING	117
<i>S. Schaer¹², R. Dach¹, S. Lutz¹³, M. Meindl⁴, D. Thaller¹⁵, G. Beutler¹</i>	
IMPACT OF ORBIT MODELING ON GNSS-DERIVED GEODYNAMIC PARAMETERS.....	119
<i>D. Arnold¹, S. Lutz¹², G. Beutler¹, S. Schaer¹³, R. Dach¹</i>	
GEOCENTER ESTIMATION FROM GNSS DATA	121
<i>S. Schaer¹², G. Beutler¹, R. Dach¹, M. Meindl³, S. Lutz¹⁴</i>	
GEOCENTER COORDINATES AND EARTH ROTATION PARAMETERS FROM HIGH AND LOW ORBITING SLR SATELLITES	123
<i>K. Sośnica¹², A. Jäggi¹, D. Thaller¹³, R. Dach¹, A. Maier¹, G. Beutler¹</i>	
THE BLUE-SKY EFFECT AND THE IMPACT OF THE ATMOSPHERIC PRESSURE LOADING ON SLR SOLUTIONS.....	126
<i>K. Sośnica¹², R. Dach¹, D. Thaller¹³, A. Jäggi¹, G. Beutler¹</i>	
HIGH-RATE GPS FOR SEISMOLOGY	128
<i>S. Häberling and M. Rothacher</i>	
GNSS TIME SERIES OF THE TOHOKU EARTHQUAKE	129
<i>M. Meindl, P. Psimoulis, N. Houlié, M. Rothacher</i>	
GNSS REFERENCE STATIONS FOR GEODYMICS AND SEISMOLOGY IN THE SWISS ALPS.....	130
<i>P. Limpach, A. Villiger and A. Geiger</i>	
THE GEODETIC THREE DIMENSIONAL STRAIN-RATE FIELD IN SWITZERLAND: NEW METHODS AND RESULTS	132
<i>A. Villiger¹, A. Geiger¹, E. Brockmann², A. Wiger², U. Marti²</i>	
STRAIN RATE AND STRESS FIELD OF SWITZERLAND	134
<i>N. Houlié^{1,2}, J. Woessner³, M. Rothacher² and D. Giardini¹</i>	
ASSESSMENT OF HIGH-RATE GPS TIME SERIES AT LONG PERIODS.....	136
<i>K. Kelevitz¹, N. Houlié^{1,2}, D. Giardini¹ and M. Rothacher²</i>	
LITHOSPHERE-ASTHENOSPHERE INTERACTIONS NEAR THE SAN ANDREAS FAULT	138
<i>N. Houlié^{1,2}, Chamberlain³, C. and T. Stern³</i>	
LONG-PERIOD SURFACE MOTION OF THE MULTI-PATCH Mw9.0 TOHOKU-OKI EARTHQUAKE	140
<i>P. Psimoulis, N. Houlié, M. Meindl and M. Rothacher</i>	
RECENT CRUSTAL VERTICAL MOVEMENTS FROM LEVELLING AND GNSS PERMANENT NETWORKS.....	142
<i>E. Brockmann, A. Schlatter</i>	
BIBLIOGRAPHY COMMISSION 3	145

4 POSITIONING AND APPLICATIONS	151
MICRO AERIAL VEHICLE, ADVANCED SENSOR ORIENTATION	151
<i>J. Skaloud, M. Rehak, R. Mabillard</i>	
STOCHASTIC MODELING OF INERTIAL SENSORS.....	153
<i>Y. Stebler, S. Guerrier, J. Skaloud</i>	
VEHICLE TRAJECTORY ANALYSIS BASED ON INERTIAL TECHNIQUES	155
<i>Y. Stebler, J. Skaloud</i>	
DRONES FOR SEARCH AND RESCUE	157
<i>J. Skaloud, Y. Stebler.</i>	
FAULT DETECTION AND ISOLATION IN MULTIPLE MEMS-IMUS CONFIGURATIONS	159
<i>J. Skaloud, A. Waegli, S. Guerrier</i>	
AUTOMATED ASSESSMENT OF DIGITAL TERRAIN MODELS FROM AIRBORNE LASER SCANNING	161
<i>Ph. Schaer, J. Skaloud</i>	
SNOW MOISTURE & SNOW PROPERTIES DETERMINATION WITH GNSS IN ALPINE ENVIRONMENT.....	164
<i>J. Skaloud, C. Botteron</i>	
PREDICTION OF PHASE AMBIGUITY RESOLUTION.....	165
<i>J. Skaloud, D. Willi</i>	
HYPERSPECTRAL REMOTE SENSING OF CROP PROPERTIES WITH UNMANNED AERIAL VEHICLES.....	167
<i>Y. Akhtman, D. Constantin, M. Rehak</i>	
UAV BASED MULTISPECTRAL IMAGING OVER A CORAL REEF LAGOON IN REUNION ISLAND.....	168
<i>Y. Akhtman, D. Constantin, M. Rehak</i>	
INVESTIGATION OF HEAVY METALS DISTRIBUTION IN SUSPENDED MATTER AND MACROPHYTES OF THE SELENGA RIVER DELTA USING AIRBORNE HYPERSPECTRAL REMOTE SENSING	169
<i>Y. Akhtman, D. Constantin, M. Rehak</i>	
SATELLITE POSITIONING PERFORMANCE ASSESSMENT FOR ROAD TRANSPORT, SAPPART COST ACTION TU 1302	170
<i>P.-Y. Gilliéron¹ and U. Wild²</i>	
BERNESE GNSS SOFTWARE.....	172
<i>R. Dach¹, D. Arnold¹, C. Baumann¹², S. Bertone¹, H. Bock¹³, Y. Jean¹, A. Jäggi¹, S. Lutz¹², A. Maier¹, M. Meindl¹⁴, L. Mervart¹⁵, U. Meyer¹, E. Orliac¹, E. Ortiz-Geist¹⁶, L. Ostini¹, L. Prange¹, S. Schaer¹⁷, K. Sošnica¹⁸, D. Thaller¹⁹, P. Walser¹, A. Villiger¹, G. Beutler¹</i>	
CODE CONTRIBUTIONS TO GLOBAL IONOSPHERE MONITORING.....	174
<i>S. Schaer¹², A. Villiger¹</i>	
AMBIGUITY RESOLUTION FOR GLONASS	178
<i>S. Schaer¹²</i>	
CLOCK MODELLING IN GNSS PROCESSING	180
<i>E. Orliac¹, R. Dach¹</i>	
GNSS DATA PROCESSING IN THE NATIONAL MULTI-HAZARD EARLY WARNING SYSTEM IN THE SULTANATE OF OMAN	182
<i>D. Arnold¹, R. Dach¹, J. Steinborn², A. Kloth²</i>	

UPDATING THE IGS ORBIT COMBINATION FOR A MULTI-SYSTEM AND MULTI-FREQUENCY ENVIRONMENT.....	185
<i>E. Ortiz-Geist^{1,2}, R. Dach¹, E. Schönemann², W. Enderle²</i>	
LOCAL UPLIFT RATES IN THE SWISS ALPS (WILDHORN-DECKE)	188
<i>B. Sievers</i>	
USE OF LOW-COST GNSS-R FOR LIMNIMETRY	195
<i>M. Kasser, E. Rodrigues</i>	
DIACHRONIC DIGITAL IMAGE CORRELATION FOR MONITORING OF INFRASTRUCTURES.	198
<i>M. Kasser, J. Compte</i>	
HOW THIS SURFACE MOVES: THE LASER SCANNING AS A SURVEILLANCE TOOL	201
<i>V. Barras, N. Delley, G. Chapotte, M. Jeanneret</i>	
LOW COST GNSS SOLUTION FOR LANDSLIDE MONITORING - GEOMON	203
<i>P.-H. Cattin, M. Jeanneret</i>	
CONTRIBUTIONS OF SWISSTOPO TO GNSS METEOROLOGY.....	204
<i>E. Brockmann, D. Ineichen, S. Lutz and S. Schaer</i>	
CONTRIBUTIONS OF SWISSTOPO TO GNSS CLIMATOLOGY: COST PROJECT GNSS4SWEC	206
<i>E. Brockmann, D. Ineichen, S. Lutz and S. Schaer</i>	
SWISS POSITIONING SERVICE (SWIPOS).....	209
<i>U. Wild, D. Andrey, C. Biberstein-Pedroni, L. Kislig and Chr. Mislin</i>	
GEODETIC DAM MONITORING	212
<i>A. Wiget and M. Kistler</i>	
GNSS INTERFERENCE DETECTION WITH HELICOPTER FLIGHTS:	213
<i>M. Scaramuzza, M. Troller, H. Wipf</i>	
MOBILE MULTILATERATION	214
<i>M. Scaramuzza¹, M. Loeser², D. Früh², S. Mühlemann², T. Anliker², Ch. Frick²</i>	
GNSS PERFORMANCE MODEL.....	216
<i>M. Scaramuzza¹, H. Wipf¹, A. Geiger²</i>	
THE CUBE SATELLITE MISSION CUBETH.....	217
<i>D. Willi, Ch. Hollenstein, B. Männel, M. Rothacher</i>	
ACTIVE DEBRIS REMOVAL (GSTP 5.4).....	220
<i>K. Wang, Ch. Hollenstein, M. Rothacher</i>	
IONOSPHERE GRADIENTS FOR GBAS.....	222
<i>K. Wang¹, M. Meindl¹, A. Geiger¹, M. Rothacher¹, M. Scaramuzza², M. Troller² and P. Truffer²</i>	
GNSS-LoC.....	224
<i>K. Wang, M. Meindl and M. Rothacher</i>	
TRIPLE-FREQUENCY AMBIGUITY RESOLUTION	226
<i>K. Wang and M. Rothacher</i>	
TROPOSPHERIC SOUNDING WITH GNSS AND WATER VAPOUR DISTRIBUTION.....	228
<i>F. Hurter¹, A. Geiger¹, D. Perler¹, K. Wilgan²</i>	

ATMOSPHERIC WATER VAPOUR SENSING BY MEANS OF SOLAR LUNAR ABSORPTION SPECTROSCOPY USING A COMPACT HIGH-RESOLVING NIR SPECTROGRAPH.....	230
<i>S. Münch¹, B. Bürki¹, M. Rothacher¹, A. Geiger¹, P. Sorber¹, St. Florek², H. Becker-Ross², M. Okruss², R. Tischendorf²</i>	
IMAGE BASED GEOMONITORING.....	232
<i>F. Neyer, Ph. Limpach, A. Geiger</i>	
GNSS FOR DEFORMATION AND GEOHAZARD MONITORING IN THE SWISS ALPS	234
<i>P. Limpach and A. Geiger</i>	
FAST DETECTION OF SUDDEN MOVEMENTS WITH GNSS IN VIEW OF HAZARD MONITORING	235
<i>R. Hohensinn, A. Geiger</i>	
GNSS REMOTE SENSING OF SNOW COVERAGE ON GROUND AND GLACIER SURFACES.....	237
<i>L. Steiner¹, P. Limpach¹, A. Geiger¹, M. Rothacher¹, M. Huss²</i>	
QDAEDALUS: A VERSATILE USABLE DIGITAL CLIP-ON MEASURING SYSTEM FOR TOTAL STATIONS.....	238
<i>S. Guillaume, B. Bürki, A. Wolf, P. Sorber, H-P. Oesch, and A. Geiger</i>	
LASER ALIGNMENT MULTIPOINT BASED DESIGN APPROACH LAMBDA PROJECT.....	243
<i>G. Stern^{1,2}, A. Geiger¹, H. Mainaud-Durand², S. Guillaume¹</i>	
FSI AND MICRO-TRIANGULATION STUDY FOR THE PRE-ALIGNMENT OF CLIC IN THE PACMAN PROJECT	244
<i>S. W. Kamugasa and V. Vlachakis</i>	
BIBLIOGRAPHY COMMISSION 4.....	247

1 Reference Frames

CODE Contributions to the IGS

S. Schaer^{1,2}, D. Arnold¹, C. Baumann^{1,3}, H. Bock^{1,4}, R. Dach¹, L. Prange¹, S. Lutz^{1,3}, E. Orliac¹, D. Thaller^{1,4}, A. Villiger¹

¹Astronomical Institute, University of Bern

²Federal Office of Topography, swisstopo

³Now with Federal Office of Topography, swisstopo

⁴Now with PosiTim UG

⁵Now with Federal Agency for Cartography and Geodesy, BKG

The consortium Center of Orbit Determination in Europe (CODE) consists of four institutions:

- Astronomical Institute of University Bern (AIUB), Switzerland
- Federal Office of Topography (swisstopo), Switzerland
- Federal Agency of Cartography and Geodesy (BKG), Germany
- Institut für Astronomische und Physikalische Geodäsie at Technische Universität München (IAPG/TUM), Germany

CODE is an Analysis Center (AC) of the International GNSS Service (IGS, [Dow et al., 2009]) generating operationally series of Global Navigation Satellite System (GNSS) products since 1992. The major products, computed at CODE and delivered to the IGS, are GNSS orbits, Earth orientation parameters (EOPs), receiver station coordinates, model parameters describing the troposphere and global ionosphere maps, phase-consistent satellite and receiver clock corrections (up to a time resolution of 5 seconds), and differential code biases (DCB). A complete list of all our products is available on our ftp server (ftp://ftp.unibe.ch/aiub/AIUB_AFTP.TXT).

We aim to deliver the best possible solutions to the IGS leading to a steady development of the processing routines and used software. Therefore, we use the development version of the Bernese GNSS Software (BSW, [Dach et al., 2007]), which is further developed and maintained at our institute. Because of this, we can benefit from the latest implementations and adapt the software in order to support the best possible processing strategies. A complete overview of the development steps during the covered reporting period can be obtained in the IGS technical reports [Dach et al. 2012, 2013, and 2014]. The following improvements are a brief selection of the most important ones:

- GLONASS ambiguity resolution enabled (February 2011, see also Schaer 2015)
- GLONASS-GPS bias parameters for station coordinates and troposphere zenith path delay parameters are setup and stored in final normal equation files (NEQs) (February 2011)
- Traditional three-day solution based on three-day coordinate set instead of weekly set (September 2012)
- NEQ manipulation/combination sequences completely revised/rewritten for the final analysis (September 2012)
- New GNSS observation selection scheme activated for all analysis lines (July 2013)
- Albedo model according to Rodriguez-Solano et al. (2012) and antenna thrust activated (June 2013)
- Substantial improvements concerning the generation of the rapid and ultra-rapid products (in 2014)
- NEQ manipulation/combination sequences completely revised/rewritten for the rapid/ultra-rapid analysis (June 2014)
- Extended ECOM (empirical CODE orbit model, see Arnold et al. 2015a) enabled (January 2015)

Another milestone regarding the processing of GLONASS satellites was achieved on February 2013. It was the first time where we processed 32 GPS and 25 GLONASS satellites for one day. Figure 1.1 displays the cumulative numbers of satellites which were processed in the operational routines. Since 2011 we observe a stabilization of the number of operational satellites which corresponds to the reaching of the full constellation of GLONASS on the 31. October 2011 [IGSMAIL 6486]. Due to our goal to deliver products of all active satellites we process all data even if satellites are flagged as unhealthy and only tracked by a limited number of stations.

The processing of the IGS products relies on a global network of GNSS stations. Figure 1.2 shows the global distribution of the IGS network distinguishing between 183 GPS/GLONASS and 69 GPS-only stations as it was used in February 2015.

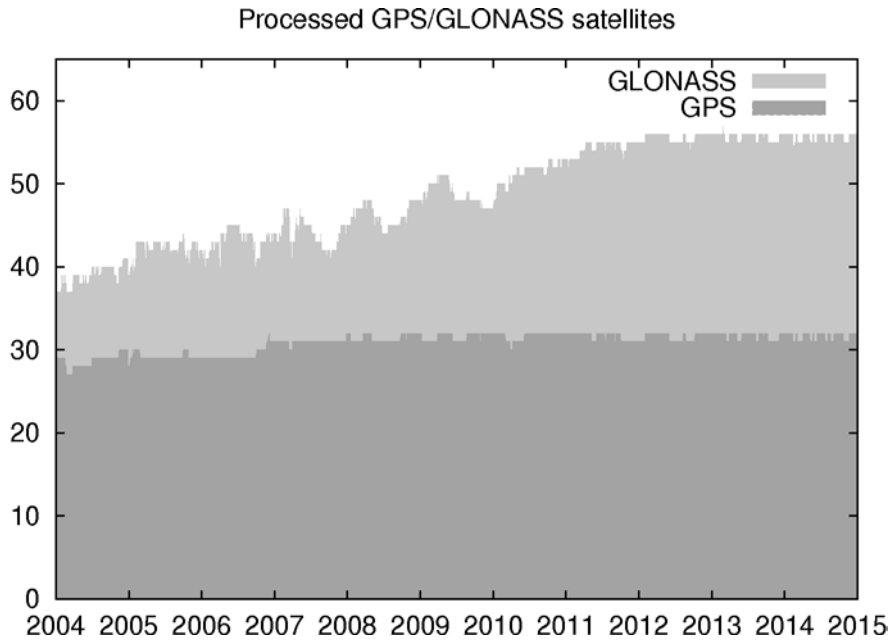


Figure 1.1: Cumulative diagram of the GPS/GLONASS constellation: Number of satellites which have been considered and delivered in the products for the IGS final solutions.

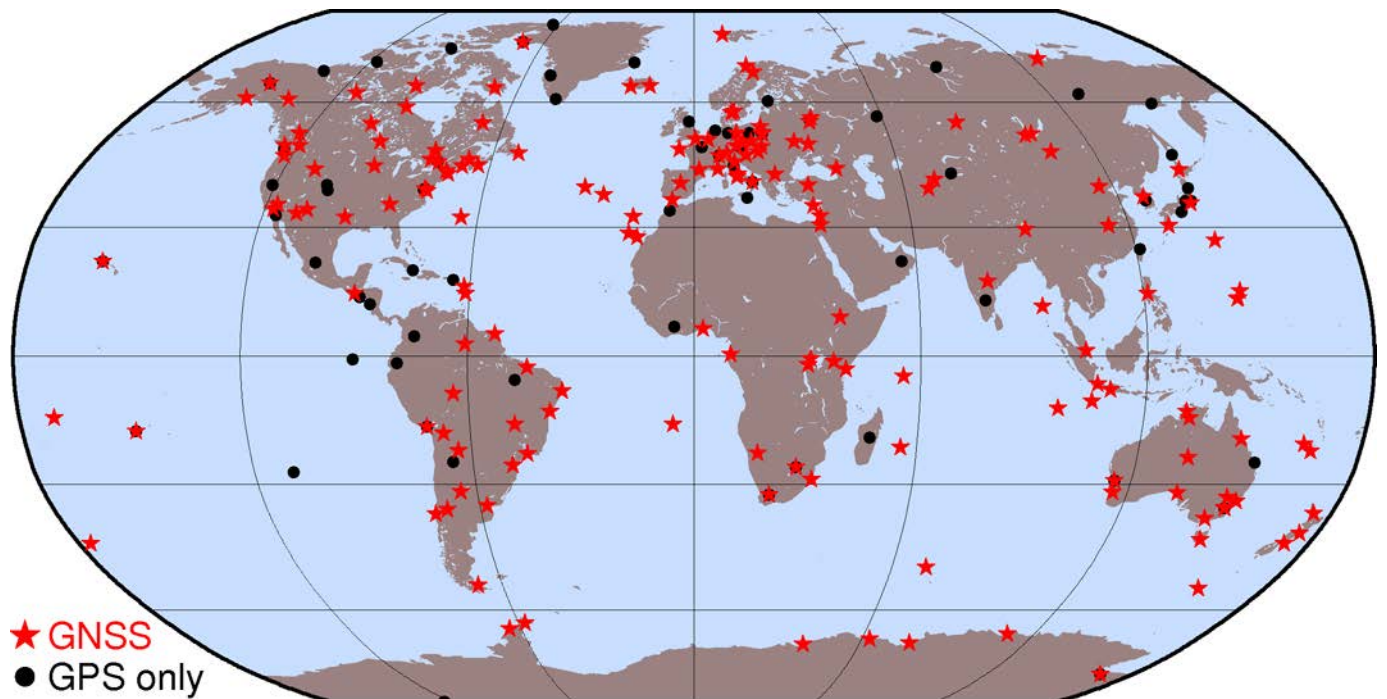


Figure 1.2: IGS network processed at CODE (status of February 2015).

The organization and realization of a first IGS Workshop on GNSS Biases was a key challenge and achievement in 2012 [Schaer 2013]. This workshop was held at the University of Bern on 18–19 January 2012. All related information, including all presentations, may be found at:

<http://www.biasws2012.unibe.ch>

One main focus of this workshop was on biases specific to GLONASS:

- IGS AC GLONASS inter-frequency code bias results were compared for the first time. It could be shown that the generation of an IGS-combined GLONASS clock product should be possible (even with current IGS AC GLONASS clock products).
- The “GLONASS interoperability issue” was another key subject. There was finally a clear consensus that the causing bias must be addressed as differential code-phase bias (DCPB).



Figure 1.3: 37 participants of the IGS Workshop on GNSS Biases on 18th January 2012 in front of the main building of the University of Bern, Switzerland.

EUREF Activities at CODE

S. Schaer^{1,2}, R. Dach¹, S. Lutz^{1,3}, A. Villiger¹

¹*Astronomical Institute, University of Bern*

²*Federal Office of Topography swisstopo*

³*Now with Federal Office of Topography, swisstopo*

EUREF is an integrated component of the Subcommittee 1.3, Regional Reference Frames, of the IAG (International Association of Geodesy). A key component is the EUREF Permanent Network (EPN, [Bruyninx 2004 and Bruyninx et al., 2012]), consisting of 265 GNSS tracking stations (status March 2015). The data is analyzed in a distributed processing scheme between 16 local analysis centers (LACs). It is worth mentioning that all but one LAC are using the Bernese GNSS Software [Dach et al, 2007] from version 5.2 up to the current development version developed at AIUB.

CODE, the Center for Orbit Determination in Europe, is one of the EUREF LACs. It is a joint venture between the Astronomical Institute of the University of Bern (AIUB, Switzerland), the Swiss Federal Office of Topography (swisstopo, Wabern, Switzerland), the Federal Agency for Cartography and Geodesy (BKG, Frankfurt am Main, Germany), and the Institut für Astronomische und Physikalische Geodäsie at Technische Universität München (IAPG, TUM, Munich, Germany).

CODE processes parts of the EPN network operationally using the Bernese development version and delivers the results to the combination center. The weekly station coordinates are generated using a combined GPS/GLONASS solution. The precise orbits, used during the processing steps, are taken from CODE which are also submitted to the IGS for the final combination products. Our contribution contains 58 stations (38 GPS/GLONASS and 20 GPS only) shown in Figure 1.4. The EPN network has its focus on Europe, therefore, most stations are located on the western part of the Eurasian plate. The development of the processed network at CODE during the last four years is shown in Figure 1.5.

Ambiguity resolution for GLONASS is an essential analysis feature not only for global solutions but also for the EUREF regional analysis at CODE (see Schaer, 2015). It has been activated for our EUREF activities in February 2011. Consideration of GLONASS-GPS bias parameters for station coordinates and troposphere zenith delay parameters in the archived NEQ results created a new dataset for further studies.

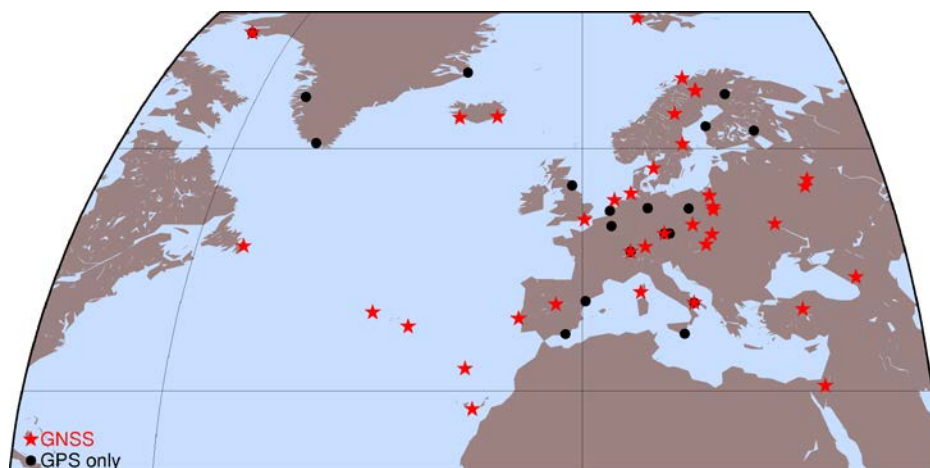


Figure 1.4: GNSS receiver network processed at AIUB and contributed to the EPN network (status of February 2015).

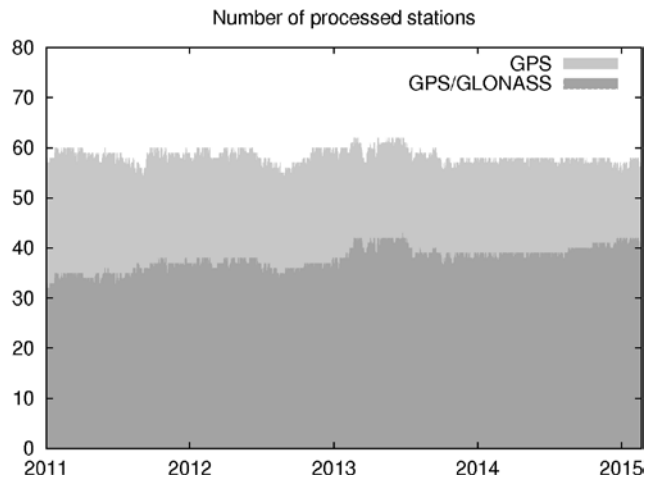


Figure 1.5: EPN GPS-only and GPS/GLONASS-combined receivers processed at AIUB.

Reprocessing activities at CODE

S. Lutz^{1,2}, P. Steigenberger^{3,4}, R. Dach¹, S. Schaer^{1,5}, K. Sośnica^{1,6}

¹ Astronomical Institute, University of Bern

² Now with Federal Office of Topography, swisstopo

³ Institut für Astronomische und Physikalische Geodäsie, Technische Universität München

⁴ Now with German Aerospace Center, German Space Operations Center

⁵ Federal Office of Topography, swisstopo

⁶ Now with Institute of Geodesy and Geoinformatics, Wrocław University of Environmental and Life Sciences

The Center for Orbit Determination in Europe (CODE) is one of the global analysis centers participating in the reprocessing efforts of the International GNSS Service (IGS). Major motivation for the 2nd IGS reprocessing campaign (repro2) is the preparation of a new release of the International Terrestrial Reference Frame, namely ITRF2014. The CODE contribution to IGS repro2 covers the time period from January 1994 to December 2013 (7305 days), complemented with the operational final CODE solutions for 2014, and includes a total of 372 globally distributed stations (Figure 1.6). The number of stations per day varies between 40 in 1994 and 290 in 2010. Whereas only GPS is considered in the first eight years, GLONASS starts contributing in January 2002. Nevertheless, GPS is dominating the solutions over all years.

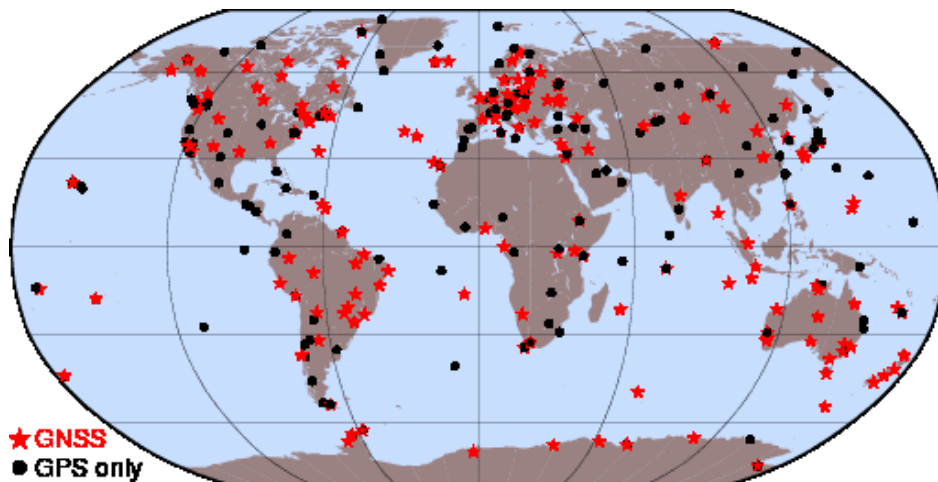


Figure 1.6: Network used for the GNSS reprocessing from CODE. The station selection is based on the priority list of the IGS reference frame coordinator. However, in particular additional GPS/GLONASS stations were included to improve the GLONASS coverage.

The CODE contribution to IGS repro2 was computed with the development version of the Bernese GNSS Software (Dach et al. 2007) and follows the strategy from the operational CODE final processing scheme as it was in June 2013. It generally applies the IERS 2010 conventions (Petit and Luzum 2010) as well as the guidelines from the IGS (<http://acc.igs.org/reprocess2.html>). As for the operational final processing, two different product lines were generated: a pure 1-day solution and a 3-day long-arc solution.

The orbit quality, in particular the radial component, of the satellites equipped with laser retro-reflector arrays is assessed using Satellite Laser Ranging (SLR). There is almost no difference between the 1-day and 3-day solutions for the orbits of the GPS satellites, whereas the GLONASS orbits in the early years with its sparse tracking network are substantially better using 3-day compared to 1-day arcs (Figure 1.7).

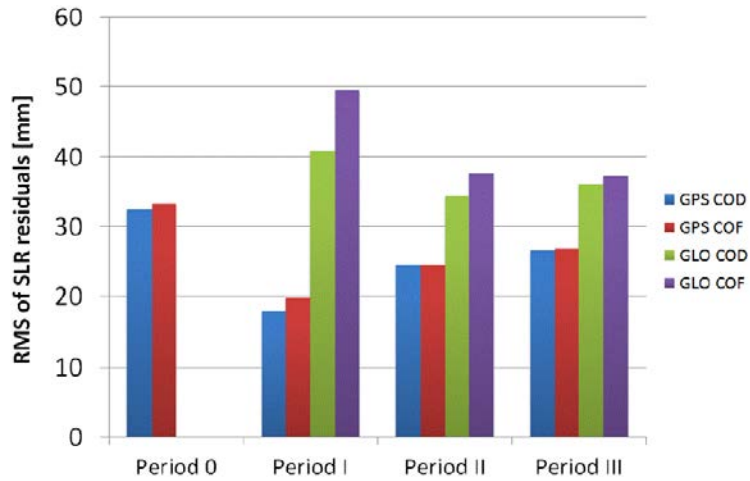


Figure 1.7: RMS of SLR residuals to GPS and GLONASS satellites from 3-day (COD) and 1-day (COF) solutions in the time intervals 1994-1999 (Period 0), 2000-2008 (Period I), 2009-2011 (Period II), and 2012-2013 (Period III).

The median repeatabilities of weekly station coordinates between 2002 and 2014 are scaled down by 40 percent in the 3-day long-arc solution with respect to the pure 1-day solution, what corresponds to the expectation from the data usage $1/\sqrt{3} = 0.57$. Furthermore, spurious signatures in the earth rotation parameters, especially the rates, derived from the 1-day solution are significantly reduced with the long-arc approach (Lutz et al., 2015a).

Updating the empirical CODE orbit model and validation of GPS and GLONASS orbits using Satellite Laser Ranging data

D. Arnold¹, G. Beutler¹, K. Sośnica^{1,2}, M. Meindl³, S. Lutz^{1,4}, R. Dach¹

¹Astronomical Institute, University of Bern

²Now with Institute of Geodesy and Geoinformatics, Wrocław University of Environmental and Life Sciences

³Institute of Geodesy and Photogrammetry, IGP, ETH Zurich

⁴Federal Office of Topography, swisstopo

The Empirical CODE Orbit Model (ECOM, Beutler et al. 1994) was developed in the early 1990s. The development was motivated by the lack of reliable satellite information. The model is widely used in the IGS community and allows for a successful absorption of non-gravitational accelerations, in particular induced by solar radiation pressure, acting on GPS satellites. Since 2002 the Russian Global Navigation Satellite System GLONASS is included in the CODE solutions for the IGS in a correctly combined GPS-GLONASS solution and therefore has an impact on all CODE products generated for the IGS.

Figure 1.8 illustrates the development of the number of GPS and GLONASS satellites in the CODE analysis since 1994.

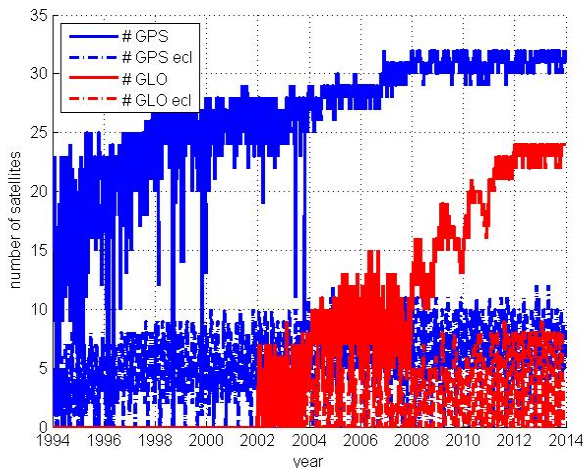


Figure 1.8: Number of GPS and GLONASS satellites

The number of GPS satellites grew from about 15 in 1994 to about 25 in 1997. Since 2006 the GPS constellation is stable at a level of about 30 satellites. The available number of GLONASS satellites grew almost linearly until the end of 2011, when the system became operational with 22-24 satellites. Figure 1.8 also shows the number of satellites in eclipse, separately for GPS and GONASS. Because all satellites of one orbital plane go simultaneously into eclipse, this number is either zero or eight for the fully deployed GLONASS and zero or eight to twelve for GPS.

The Empirical CODE Orbit Model (ECOM) is documented in Beutler et al. (1994). It decomposes Solar Radiation Pressure (SRP) into the three orthogonal directions e_D (unit vector from the Sun to the satellite), e_Y (unit vector along the solar panels axes), and e_B , orthogonal to both vectors, e_D and e_Y . In the frame of the classic ECOM SRP can be modeled by a constant and a general once-per-revolution acceleration in each axis. Springer et al. (1999) showed that only five out of the nine accelerations are needed in the analysis, namely the constant accelerations and the once-per-revolution accelerations in the e_B direction.

The 5-parameter ECOM was and is perfectly suited to account for SRP acting on the GPS satellites. Meindl et al. (2013) showed, however, that the geocenter derived from GLONASS-only solutions in 2008-2011 had strong spurious excursions > 10 cm in amplitude with a frequency of three cycles per year (cpy) – see also Arnold et al. (2015c) in this volume. Roriguez-Solano et al. (2014) confirmed that the ECOM was primarily responsible for that

problem. This was the motivation for Arnold et al. (2015b) to thoroughly analyze the old ECOM and to come up with a revised version, which solves for a constant acceleration in each of the three orthogonal directions and, in addition, for even-order periodic accelerations along e_D , and for odd-order accelerations along e_B . The revised ECOM is used for all CODE contributions to the IGS since January 4, 2015 (beginning of GPS week 1826).

The GLONASS orbits generated with the old and the new ECOM were validated by Sosnica et al. (2015) using the Satellite Laser Ranging (SLR) observations of the global tracking network of the ILRS (International Laser Ranging Service) of the years 2012 and 2013. The SLR residuals of orbits calculated with the old ECOM show a strong systematic behavior as a function of the angle ε between Sun and satellite, as measured from the center of the Earth. No such biases are seen when using the revised ECOM. Figure 1.9 illustrates this result: The old ECOM is biased at $\varepsilon = 30^\circ$ by -50 mm, at $\varepsilon = 180^\circ$ by $+50$ mm. This slope virtually disappears for the new ECOM. The color code provides in addition the elevation angle of the Sun above the orbital plane. Small mean biases of a few millimeters remain even with the new ECOM. They originate mainly from the satellite signature effect, which is caused by a spread of the laser pulse due to reflection from multiple reflectors. The satellite signature effect can be as large as 15 mm for multi-photon SLR detectors when ranging to GLONASS-M satellites (Sosnica et al., 2015).

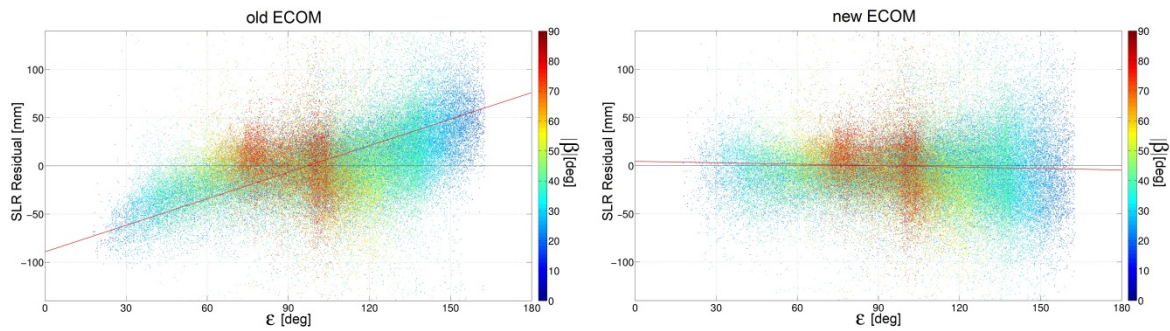


Figure 1.9: Validation of old and new ECOM using SLR (from Sosnica et al, (2015))

CODE five system solution for IGS MGEX

L. Prange¹, E. Orliac¹, R. Dach¹, S. Schaer^{1,2}, K. Sośnica^{1,3}

¹*Astronomical Institute, University of Bern*

²*Federal Office of Topography, swisstopo*

³*Now with Institute of Geodesy and Geoinformatics, Wrocław University of Environmental and Life Sciences*

The International GNSS service (IGS, Dow et al. 2009) provides precise reference products for the established Global Navigation Satellite System (GNSS) GPS since about 20 years (and a bit less for GLONASS). These orbit, clock, coordinate reference frame, troposphere, and ionosphere products are freely distributed and widely used by scientific, administrative, and commercial users from all over the world. The IGS facilities needed for data collection, product generation, product combination, as well as data and product dissemination are well established. The Center for Orbit Determination in Europe (CODE, Dach et al. 2013) is one of the Analysis Centers (AC) of the IGS since the beginning. It generates GPS and GLONASS reference products using the Bernese GNSS Software (BSW, Dach et al, 2007). In the recent years new GNSS, regional overlay systems (like QZSS or IRNSS), and Space Based Augmentation Systems (SBAS) are being built up. The existing GNSS are under modernization (e.g., better satellite clocks, new signals). The new signals offer new opportunities, but also require investments into the existing IGS infrastructure.

In order to exploit the potential of the new GNSS and their signals and to prepare for their integration into the existing processing chains, the IGS has set up the Multi-GNSS EXperiment (MGEX, Montenbruck et al. 2013) in 2012 and has updated its standardized Receiver INdependent EXchange data format (RINEX3, MacLeod and Agrotis 2013). CODE participates in the MGEX – benefitting and contributing at the same time. We benefit from the availability of more and more GNSS data tracked by the fast growing network of MGEX stations (see Figure 1.10) and provided in the new RINEX3 format. This data allows us to confront our software (BSW) and processing chains with the new signals. The challenge is to find a good strategy to handle all these new signals in order to get the best possible benefit for the resulting products. On the other hand we contribute to MGEX by providing the results of our raw data monitoring and our data analysis – allowing it to compare them with results of other groups.

The focus of CODE's MGEX activities was on the European Galileo system in the beginning. In order to generate Galileo orbit and clock products, the BSW had to be enabled to accept data provided in the new RINEX3 data format. Furthermore a frequency- and observation-type selection and bookkeeping was added and internal data formats had to be changed. These improvements left its mark on the meanwhile distributed version 5.2 of the BSW. Later developments aimed on the extension of the BSW in order to allow the processing of more than three GNSS at the same time. The CODE MGEX orbit and clock processing chains have been updated accordingly and are now able to process data of the GNSS GPS, GLONASS, Galileo, BeiDou (MEO and IGSO), and QZSS together in a fully integrated solution. This capability has been demonstrated by reprocessing MGEX data of the whole year 2014.

The processing of multi-GNSS data revealed some issues, however: In order to ensure an optimal station distribution for each GNSS with a limited number of stations (limited computation time) an advanced station selection had to be introduced. The limitations of the ECOM solar radiation pressure model (Springer, 1999) are even more obvious for some of the new GNSS (mainly Galileo and QZSS) than demonstrated for GLONASS by Arnold et al. (2015b). The (BSW) assumption that GNSS satellites always maintain the Yaw-attitude mode leads to large orbit determination errors for satellites flying in orbit normal attitude steering mode, which is the case for QZSS and BeiDou at low beta angles. On the other hand the MGEX results confirm that the clocks of some new GNSS spacecraft (i.e., Galileo, QZSS, GPS Block IIF) are so stable that their estimated clock corrections can even be used for orbit validation (Prange et al., 2014)(see also Figure 1.11).

The CODE-MGEX ("com") products are made available for public use via the IGS data center CDDIS (<http://cddis.gsfc.nasa.gov/gnss/products/mgex>). Until late 2014 the products were provided irregularly in a batch mode. Since the beginning of 2015 the delay is reduced to about two weeks.

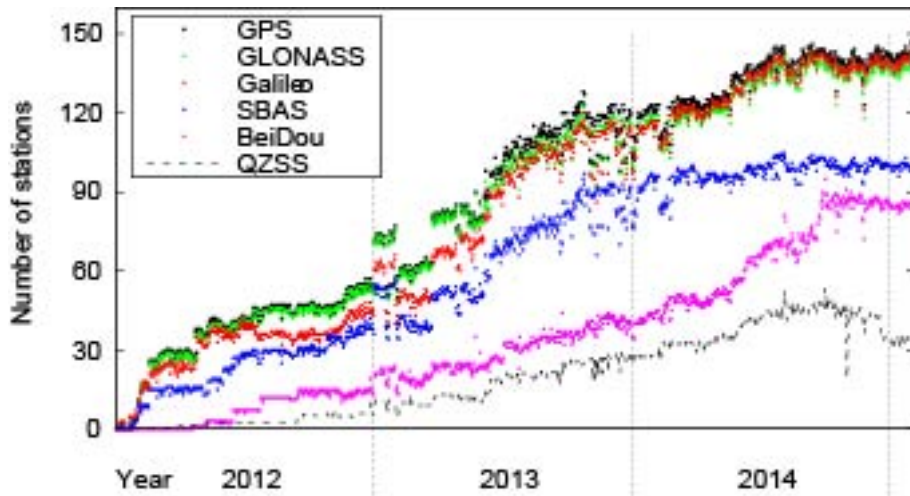


Figure 1.10: Number of RINEX3 stations included in CODEs data monitoring.

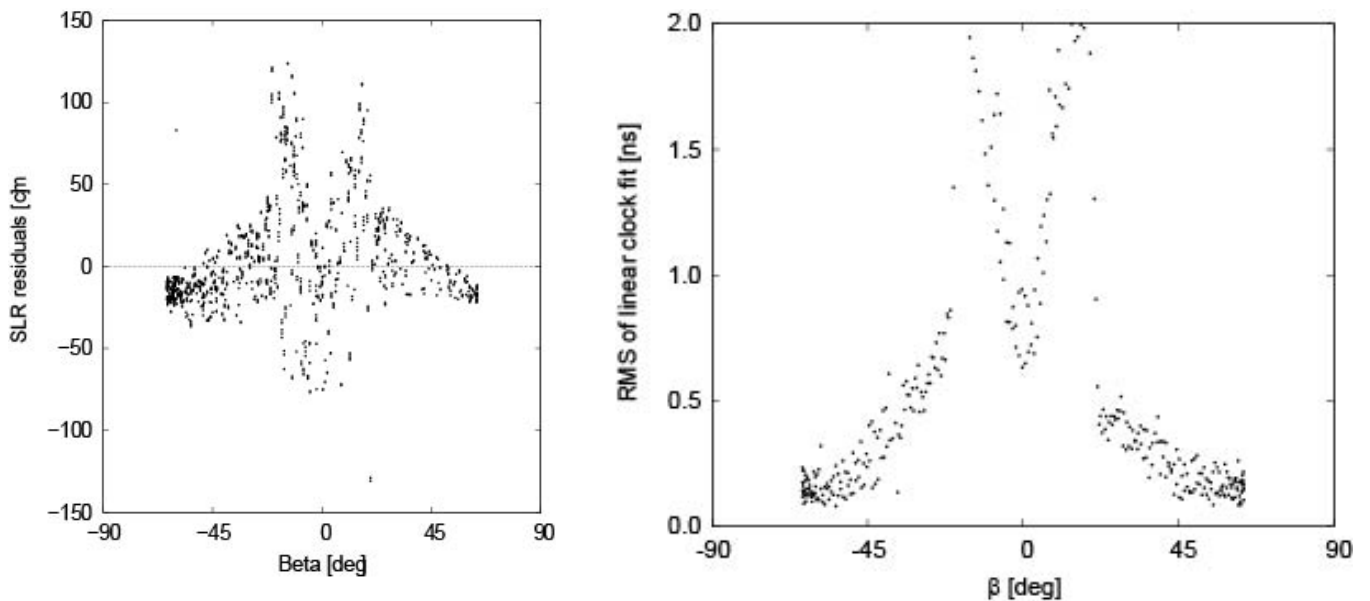


Figure 1.11: SLR residuals (left) and RMS of linear clock fit (right) of QZS-1 as a function of the elevation angle (Beta) of the Sun above the orbital plane.

AIUB contribution to the TGVF/OVF

L. Prange¹, E. Orliac¹, R. Dach¹

¹*Astronomical Institute, University of Bern*

TGVF/OVF is a project part of the Galileo program, the European Global Navigation Satellite System (GNSS). TGVF stands for “Time and Geodetic Validation Facility” and OVF for “Orbit Validation Facility”. TGVF is the continuation of the former GGSP project, namely the Galileo Geodetic Service Provider (GGSP). OVF is one out of two entities defining the TGVF together with TVF, the Time Validation Facility.

OVF’s main tasks are twofolds:

- To produce a set of reference products (such as orbits, Earth Rotation Parameters, satellite clocks mainly) that can be used as reference by the Galileo Mission Segment (GMS) to validate the navigation data it produces for uplink to the Galileo satellites
- To define, realize and provide access to the GTRF, the Galileo Terrestrial Reference Frame. The GTRF is the geodetical basis for all other Galileo products and services and is aligned to the ITRF.

The OVF is organized in a similar way to the International GNSS Service (IGS) in the sense that the delivered products are the results of the combination of several independent solutions. Those solutions are produced by three Processing Facilities (PF), the Astronomical Institute of the University of Bern (AIUB) hosting one of them. The PFs are in charge of estimating orbits, ERPs, satellite and receiver clocks, Differential Code Biases (DCBs), Inter-System Biases (ISB), ionosphere maps and troposphere delays. The three PFs use three different software packages, namely the Bernese GNSS Software [Dach et al., 2007], EPOS [Angermann et al., 1997] and NAPEOS [Springer, 2010], and each PF has its own analysis strategy. However, contrarily to the IGS, the PFs are requested to process the same dataset. The data is stemming from Galileo (Experimental) Sensor Stations (G(E)SS) and from selected stations of the IGS and IGS-MGEX networks (see Figure 1.12). Not all stations are providing Galileo data, but as shown in Figure 1.12 in Prange et al. (2015) the situation steadily improves over time. The data is post-processed in weekly batches. PFs’ individual products are then combined by the Combination Facility (CF) and later on verified by the Validation Facility (VF). The combined products have to be provided with a maximum latency of two weeks. In addition to these final products the OVF started to generate a full set of rapid products with a latency of 12 hours in late 2013.

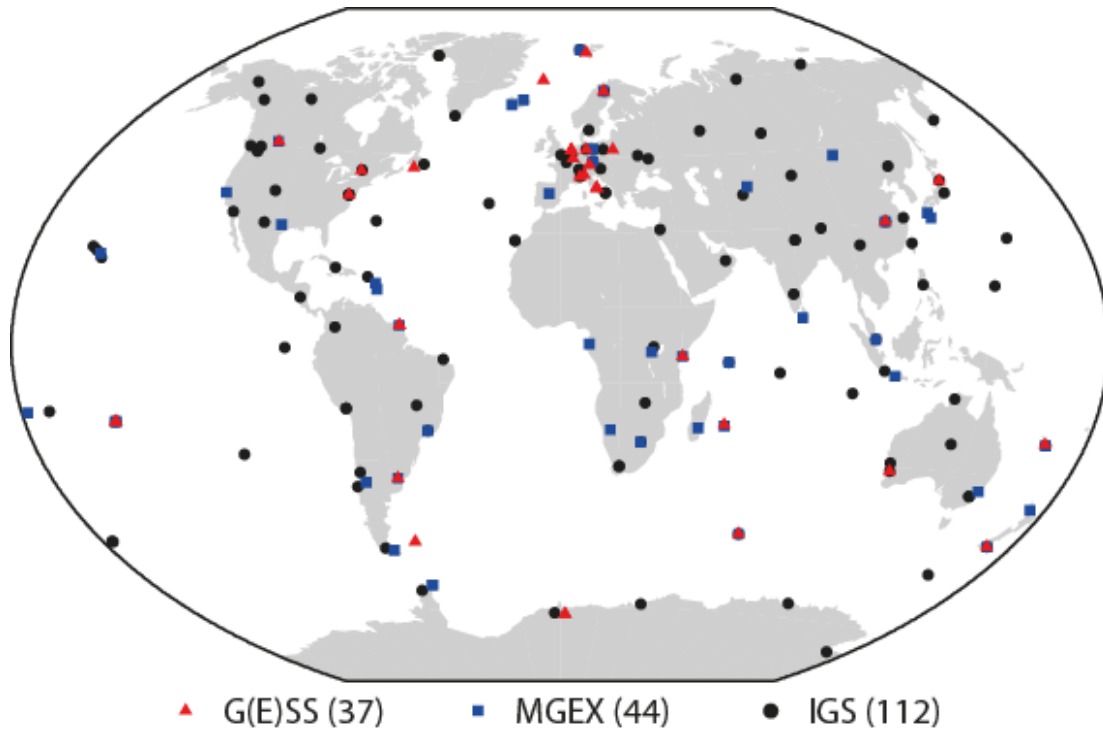


Figure 1.12: Distribution of G(E)SS/MGEX/IGS stations used by OVF.

The generation of the GTRF is based on the combination of long time series of weekly SINEX solutions and is updated regularly.

The OVF also had for mission to support the In-Orbit Test (IOT) activities, which started after the launch of the first two IOV spacecrafts in October 2011. Support activities naturally extended to the last phase of the project, namely the Full Operational Capability (FOC) phase, where the full Galileo constellation (30 satellites) shall be established. The estimation of satellite antenna Phase Center Variation (PCV) maps and the provision of an interface between TGVF and the space-geodetic community are additional tasks of the OVF.

The Swiss Optical Ground Station and Geodynamics Observatory Zimmerwald

T. Schildknecht¹, A. Jäggi¹, M. Ploner¹, E. Brockmann²

¹*Astronomical Institute, University of Bern*

²*Federal Office of Topography, swisstopo*

The main activities at the Zimmerwald Observatory are:

Satellite Laser Ranging (SLR)

The Zimmerwald SLR station is part of the global tracking network of the International Laser Ranging (ILRS) since the foundation of this service in 1998. The SLR observations acquired with the monostatic 1-m Zimmerwald Laser and Astrometry Telescope (ZIMLAT, see Fig. 1) are delivered in near real-time to the global ILRS data centers. The SLR activities at Zimmerwald are performed by the Astronomical Institute of the University of Bern (AIUB) and the Swiss Federal Office of Topography (swisstopo). Zimmerwald continues to be the most productive SLR station of the ILRS in the northern hemisphere second to Yarragadee only, a station in Australia.

Optical Observations of Space Debris

Space debris – man-made non-functional objects of all sizes in near-Earth space – has been recognized as an increasing threat for current and future space operations. AIUB uses optical techniques to detect, track and physically characterize space objects including small-size debris. The observations acquired with the ZIMLAT telescope are predominantly used to build-up and maintain orbit catalogues of small-size space debris and to characterize objects using light curves and color photometry. The project shares the ZIMLAT telescope with the SLR project during night-time. The 0.2-m ZIMmerwald SMall Aperture Robotic Telescope (ZimSMART) is used to maintain an orbit catalogue of space debris in the geostationary ring. Data is shared in the context of scientific collaborations with the European Space Agency ESA, the International Scientific Optical Network (ISON), and the Keldysh Institute of Applied Mathematics of the Russian Academy of Sciences (KIAM).

New 0.7m Sensor for Space Situational Awareness (SSA) and Optical Communication

The 6-m dome of the observatory has been refurbished in 2013 and will host a new 0.7m telescope to be installed in 2015. The project shall demonstrate the combined use of a single telescope and associated infrastructure for optical space debris observation and optical communication to spacecraft in Low Earth Orbits (LEO). Both applications require optical telescopes capable of precisely tracking LEO targets with similar sized apertures. Moreover, optical communication sessions will also be conducted during daytime, where no space debris observations take place. The optical communication experiment will be conducted by RUAG Space Switzerland. During night time this sensor will be used in particular to characterize space debris by means of spectroscopy and multi-color photometry.

Global Navigation Satellite Systems (GNSS)

GNSS receivers are operated at Zimmerwald by swisstopo and AIUB. Two permanent GNSS receivers mounted on 9-meter masts provide data to the data centers of the International GNSS Service (IGS), to the EUREF, and to the Automated GNSS Network for Switzerland (AGNES) of swisstopo.

Gravimetry

A permanent Earth tide gravimeter is operated at Zimmerwald by ETH Zurich. The instrument of the type ET-25 (LaCoste & Romberg) collected, with the exception of some short time periods, a continuous data set. Additionally twice a year, absolute gravity measurements using a FG5 (Micro-g LaCoste) instrument were performed by swisstopo in collaboration with the Federal Office of Metrology (METAS).



Figure 1.13: Swiss Optical Ground Station and Geodynamics Observatory Zimmerwald. The Zimmerwald 1-m Laser and Astrometry Telescope ZIMLAT is to the right, the Zimmerwald Small Aperture Robotic Telescope (ZimSMART) is housed in the small dome at the left, and the new 0.7-m telescope will be set up in the 6-m dome in the background. One of the two 9-meter masts of the permanent GNSS stations can be seen in the foreground.

Satellite Laser Ranging at Zimmerwald

M. Ploner¹, T. Schildknecht¹, A. Jäggi¹, P. Lauber¹, J. Utzinger¹, M. Prohaska¹, E. Brockmann²

¹Astronomical Institute, University of Bern

²Federal Office of Topography, swisstopo

Building on the high flexibility of the SLR station, three very different types of measurements were carried out: The standard SLR services, the Bistatic Experiment and the Time Transfer to a spacecraft.

GNSS Constellation

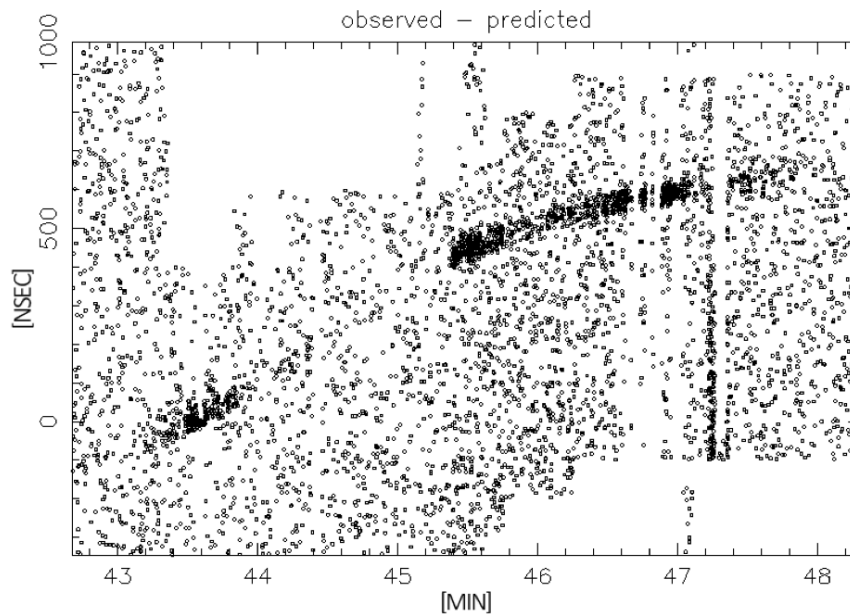
Since summer 2010 the complete Glonass constellation (currently 24 satellites) is ranged from Zimmerwald. The number of observations per normal point (#OBS/NP) is almost a factor of two higher for Glonass satellites equipped with uncoated reflectors than for those with coated reflectors. The difference in #OBS/NP is a result of the higher return rate for satellites with uncoated reflectors. The lower RMS of the normal points for uncoated reflectors can be explained by the higher #OBS/NP. No significant differences can be seen between different types of Glonass satellites (Glonass, Glonass-M and Glonass-K).

BISTATIC EXPERIMENT

In the so called ‘bistatic’ experiment the SLR station Graz is firing laser pulses to space debris objects using a powerful laser (200 mJ @ 532 nm, 3 ns pulse length, 80 Hz) provided by the Deutsches Zentrum für Luft- und Raumfahrt (DLR) Stuttgart. On March 28, 2012 the Zimmerwald SLR station for the very first time successfully detected and time-tagged photons diffusely reflected by the body of the European ENVISAT spacecraft.

Bistatic Experiment Graz-ENVISAT-Zimmerwald

Envisat 28 March 2012, 20:40 – 20:50 UT: Returns measured at Zimmerwald



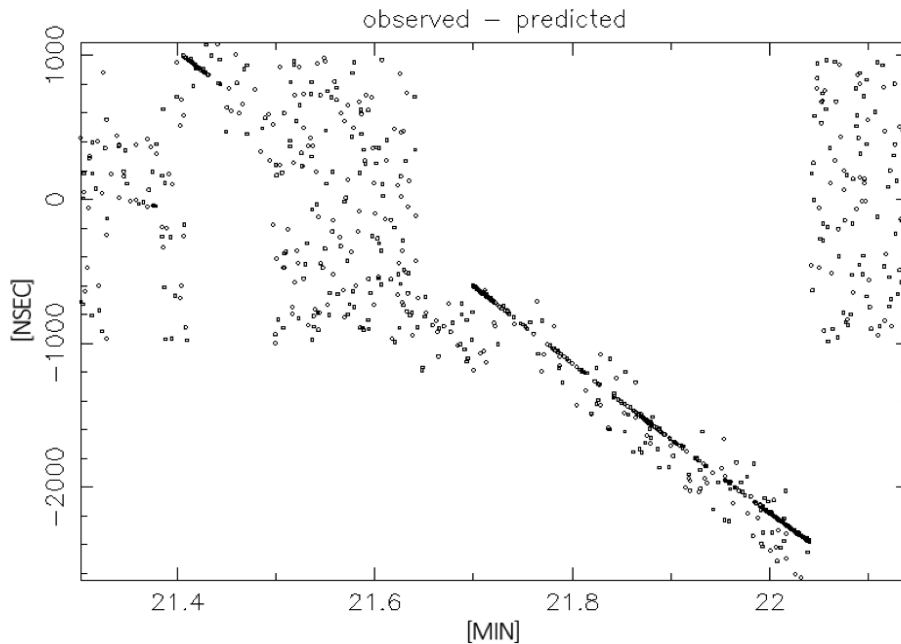
Georg Kirchner, Martin Ploner, Johannes Utzinger 28.03.2012

Figure 1.14: Bistatic Experiment Graz-ENVISAT-Zimmerwald (GR28MR12U-new.pdf).

About one year later (18th June 2013) photons reflected on a space debris object (upper stage CZ-2C) with a considerably smaller radar cross section than ENVISAT could be detected.

Bistatic Experiment Graz-"CZ-2C"-Zimmerwald

CZ-2C 18 June 2013, 21:17 - 21:25 UT: Returns measured at Zimmerwald



Georg Kirchner, Martin Ploner, Johannes Utzinger, Pierre Lauber 18.06.2013

Figure 1.15: Bistatic Experiment Graz-"CZ-2C"-Zimmerwald (D118JN13V-new.pdf).

For bistatic range measurements the receiving components have to be synchronized to the Graz firing times within a few microseconds. Knowing the exact firing times of the Graz laser in advance, the expected arrival times of the Graz photons in Zimmerwald are calculated and the detector is activated accordingly. The collected data can be used to calculate improved orbits of the tracked debris objects. But this would ask for measuring the time stamps of the stop pulses with an absolute accuracy below 1 nanosecond. This is not possible so far due to the following unsolved issues. On the one hand, the time synchronization of the event timer with UTC is done by a GPS receiver with an accuracy of 100 ns. On the other hand, the delay between the reference point of the telescope (intersection point of the telescope axis) and the event timer is only estimated with an accuracy of a few nanoseconds.

LRO

In case of range observations to the Lunar Reconnaissance Orbiter (LRO) the laser system has to operate in a special mode. At the spacecraft, the observation window has a width of 8 ms and a frequency of 28 Hz. The pump diodes of the amplifiers can be triggered with a variable time interval between approximately 9 and 11 ms in steps of 10 microseconds. By means of the pockels cell selecting the pulses to be amplified, the actual firing rate can be reduced by an additional integer factor. For the LRO one-way ranging experiment the laser fires at approximately 14 Hz, i.e. with a basic pump interval of 10.200 ms (corresponds to a frequency of 98 Hz) and a reduction factor of 7. The firing time can be empirically corrected in steps of 1 ms in case of unsuccessful observations. Especially during daytime operation the actual pointing offset of the telescope due to thermal effects is empirically estimated using GNSS

satellites passing nearby. On 20th July 2009 the SLR station Zimmerwald was the first European SLR station that successfully carried out observations to LRO. Since this success 3647 observations minutes were collected at Zimmerwald. Five years later another remarkable success was reported by the ILRS, namely the first simultaneous ranging to LRO between a European (Zimmerwald) and an U.S. station (Greenbelt) on September 15, 2014.

Year	Observation Minutes
2009 (from 20th July)	41
2010	164
2011	756
2012	399
2013	1159
2014 (until end of mission)	1128

Table 1.1: LRO Observation minutes per year.

Combination of SLR, GPS, and GLONASS observations using co-locations in space as a contribution to the ITRF

K. Sośnica^{1,2}, D. Thaller^{1,3}, R. Dach¹, A. Maier¹, A. Jäggi¹

¹*Astronomical Institute, University of Bern*

²*Now with Institute of Geodesy and Geoinformatics, Wrocław University of Environmental and Life Sciences*

³*Now with Federal Agency for Cartography and Geodesy, BKG*

In the framework of the realization of the International Terrestrial Reference Frame (ITRF), Satellite Laser Ranging (SLR) observations to LAGEOS and Etalon satellites are used for the definition of the origin (i.e., the center of mass of the planet Earth with its fluids) and for the definition of the scale (along with Very Long Baseline Interferometry, VLBI). The absolute orientation is provided by VLBI. The polar motion parameters derived from Global Navigation Satellite Systems (GNSS) as well as the horizontal components of station coordinates are of superior quality as compared to the SLR-derived values. GNSS solutions are crucial for the densification of the ITRF to regional and national reference frames. Moreover, the global distribution of the GNSS stations is nowadays homogeneous with a high density of observing stations, as opposed to the SLR network with merely seven observing stations in the southern hemisphere. The high consistency and a good connection between SLR and GNSS are thus indispensable.

Until now, the connection between SLR and GNSS solutions was realized by local ties from the fundamental geodetic stations providing observations from more than one space-geodetic technique. This connection, however, can also be realized in space using, for example, SLR observations to GPS and GLONASS satellites (e.g., Thaller et al., 2011) or SLR observations to LEO satellites equipped with GPS receivers. The call for participation for the upcoming ITRF2014 asked for the first time also for pre-combined solutions. Following this call the members of the Center for Orbit Determination (CODE) consortium, including the Astronomical Institute of the University of Bern (AIUB), the Federal Agency for Cartography and Geodesy (BKG) and the Technical University in Munich decided to provide pre-combined GNSS-SLR solutions, which are based on the CODE contribution to IGS-Repro2 campaign (Lutz et al., 2015b). The multi-technique pre-combined solution includes three different types of data:

1. microwave data to GPS and GLONASS satellites,
2. SLR data to LAGEOS and Etalon satellites,
3. SLR data to GPS and GLONASS satellites.

The satellite co-locations are independent of the local ties on ground, which are often affected by systematic errors (Altamimi et al. 2011). Moreover, the increasing number of SLR observations to GNSS satellites allows us to strengthen the determination of SLR station coordinates due to the improved observation geometry and a larger number of observations (see Figure 1.16 for an example). When analyzing GNSS microwave observations, the modeling of the uncalibrated satellite antenna phase center offsets is a major error source for the scale (Thaller et al. 2011; 2014). The estimation of satellite clocks and the orbit modeling issues, including the estimation of parameters designed for the absorption of the impact of solar radiation pressure, affect the GNSS-derived geocenter series, in particular the Z component (Meindl et al. 2013). Laser range observations are free of many propagation issues related for instance to ionosphere delays, microwave antenna phase center variations, or phase ambiguities. SLR in general can thus provide the scale for GNSS, SLR data to spherical satellites provides the geocenter unaffected from orbit modelling issues, whereas GNSS can contribute with better polar motion parameters and a denser network. Finally, the space co-locations strengthen the orbit determination of GNSS satellites, and allow to estimate the satellite microwave antenna offsets and values of the Laser Retroreflector Arrays (LRAs) offsets (see Figure 1.17).

All operational satellites of the GLONASS system are equipped with LRAs, whereas only two GPS satellites of Block-IIA were equipped with LRAs. Only three GLONASS satellites were, however, recommended by the ILRS for tracking between 2002 and 2010 (typically one satellite per plane). In 2010, the ILRS decided to increase the number of officially tracked GLONASS satellites to six (two satellites per plane). Exceeding the ILRS

recommendations, several SLR stations started tracking the full constellation of GLONASS in 2010 and 2011. In 2014-2015, a series of GNSS-dedicated tracking campaigns was carried out by SLR observatories in which a higher priority for GLONASS satellites was introduced during several months.

The SLR observations to GNSS satellites are subject to systematic effects related to the SLR detectors. These systematic effects are not well investigated in the SLR community. Thus, we analyzed SLR residuals to microwave-based GNSS orbits; in particular, we studied the dependency between SLR residuals and the incidence nadir angles for SLR stations equipped with different receiving systems. The laser range residuals for stations operating in the multi-photon mode with high detection energy, such as Yarragadee (7090) and Wettzell (8834), typically show a significant negative slope w.r.t. the nadir angle (see Fig. 3). The maximum slope of -1.1 mm/deg for Wettzell corresponds to a difference of the mean SLR offset of more than 15 mm between observations at nadir angles of 0° and at 14° . The residuals of stations with single-photon detectors with low return rates, such as Zimmerwald (7810) or Herstmonceux (7840), have a positive statistically insignificant slope of at maximum 0.09 mm/deg. This corresponds to a difference of 1 mm between the SLR observations at nadir angles of 0° and 14° . These results confirm that the satellite signature effect introduces nadir-dependent offsets in the SLR observations of up to 15 mm for high-detection-energy stations, whereas the single-photon stations are free of this effect. The laser ranges registered by multi-photon stations are thus shorter for high nadir angles as the pulses are reflected by the near edge of the array.

The mean SLR offsets to GLONASS-M at a level of 0.1-1.8 mm for single-photon stations imply that there is no need for estimating range biases for single-photon SLR stations tracking the satellites with uncoated corner cubes. For multi-photon stations, the offsets and the offset-dependency on the nadir angle have to be well understood and mitigated in the future. The mean SLR offset of the order of 0.1-1.8 mm implies that there is no scale difference between SLRF2008 and IGB08. Consequently, the microwave-based (GNSS) and laser-based (SLR) technique solutions of space geodesy are consistent at the 1 mm level and they are free from scale issues (Sośnica et al., 2015).

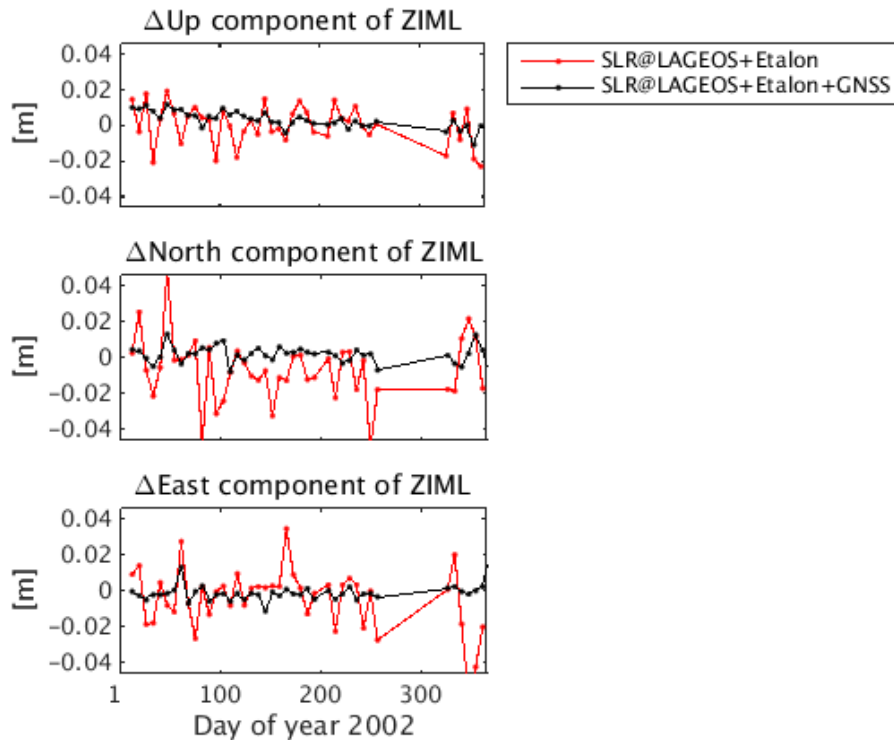


Figure 1.16: Weekly differences between a priori coordinates (SLRF2008) and estimated coordinates of the SLR station in Zimmerwald in the Up, North, and East component.

Microwave GNSS	SLR@LAGEOS+Etalon
GNSS Station Coordinates	SLR Station Coordinates
-	Geocenter coordinates
GPS and GLONASS orbits	LAGEOS and Etalon orbits
Earth Rotation Parameters (X pole, Y pole, Length-of-Day)	
Phase-code, Inter-system, Inter-frequency Biases	Range Biases (1-3 stations)
APL Scaling Factors	APL Scaling Factors
Troposphere Delays	-

Microwave GNSS	SLR@GNSS	SLR@LAGEOS+Etalon
GNSS Station Coordinates	SLR Station Coordinates	
Geocenter Coordinates		
GPS and GLONASS orbits		LAGEOS, Etalon orbits
Antenna Offset	LRA Offset	-
Earth Rotation Parameters (X pole, Y pole, Length-of-Day)		
Phase-code, Inter-system, Inter-frequency Biases	Range biases (all stations)	Range Biases (1-3 stations)
APL Scaling Factors	APL Scaling Factors	
Troposphere Delays	-	

Figure 1.17: Left: Parameters estimated from a solution co-locating GNSS and SLR techniques using local ties (nominal approach). Right: Parameters estimated from a solution co-locating GNSS and SLR techniques in space (co-location by commonly estimated parameters at GNSS satellites).

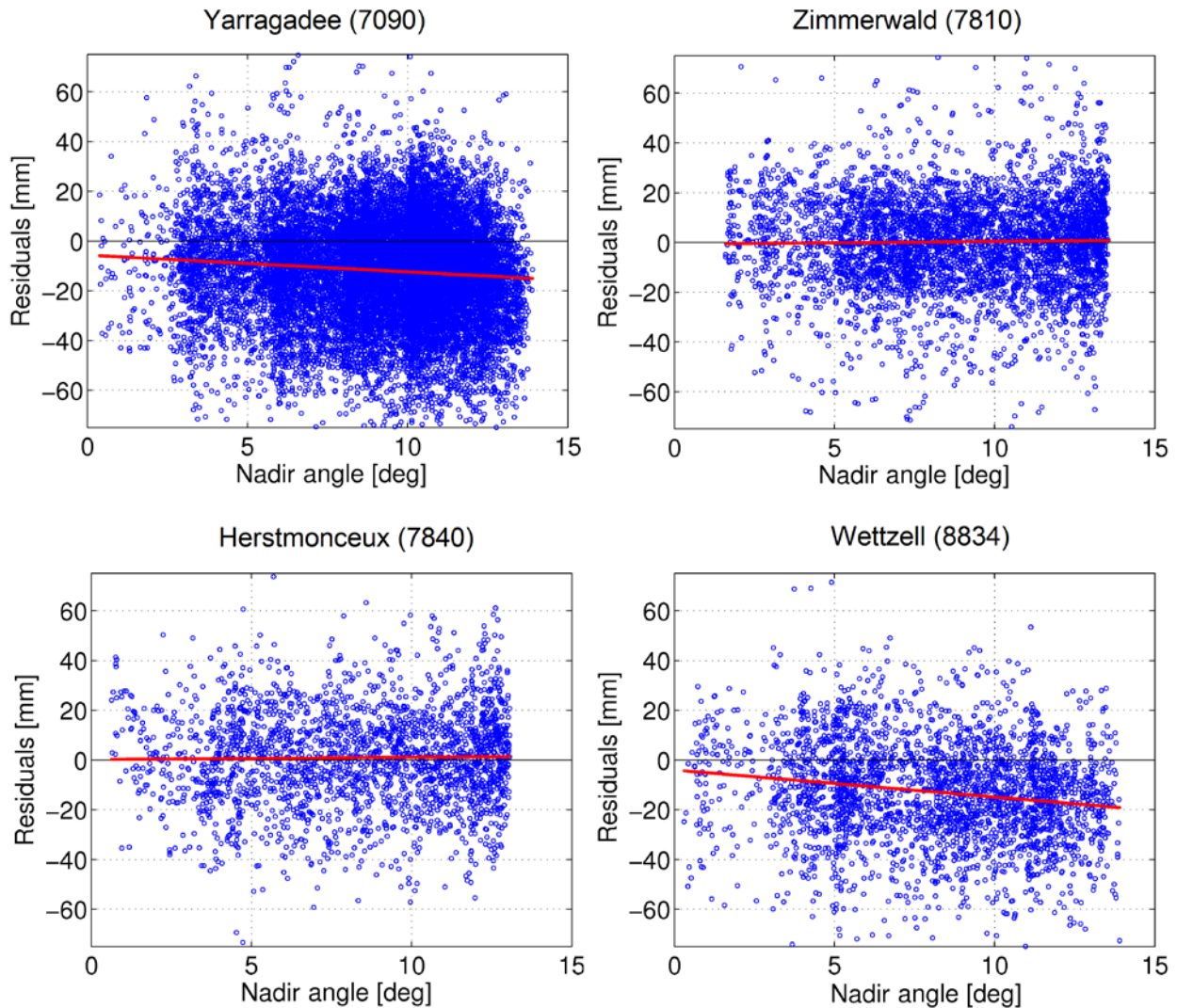


Figure 1.18: SLR residuals to GLONASS-M satellites with uncoated LRAs as a function of the nadir angle for 2012-2013, after Sošnica et al. (2015). The regression coefficient (a slope) is depicted in red color.

GNSS Clock Modelling and Estimation

K. Wang and M. Rothacher

Geodesy and Geodynamics Lab, Institute of Geodesy and Photogrammetry, ETH Zurich

In GNSS processing, the receiver clock error, which is highly correlated with the vertical component of the receiver coordinates and the troposphere Zenith Path Delay (ZPD) parameters, is typically estimated as random parameter at each epoch. However, for high-stability receiver clocks like Hydrogen-Masers (H-Masers), the good clock stability can be used. The receiver clock behavior of these high-performance clocks was thus modeled with appropriate deterministic and stochastic models to de-correlate the clock parameters and the vertical component of the receiver coordinates in the kinematic Precise Point Positioning (PPP) solutions within the project "Satellite and Station Clock Modelling for GNSS" funded by European Space Agency (ESA).

Figure 1.19 shows the change of the number of H-Maser, rubidium, cesium and quartz clocks connected to stations of the International GNSS Service (IGS) from January 1, 2000 to October 15, 2014 based on the daily updated summary file of the IGS site logs. The former stations that have been closed down and the stations connected with clocks that are only documented as "internal" were not counted in the plot. From Figure 1.19 we can observe a dramatic increase in the number of the H-Masers, and also the total number of atomic clocks in use in the IGS. With the increasing number of high-precision atomic clocks connected to GNSS receivers during these 15 years, receiver clock modelling becomes an important topic in GNSS processing.

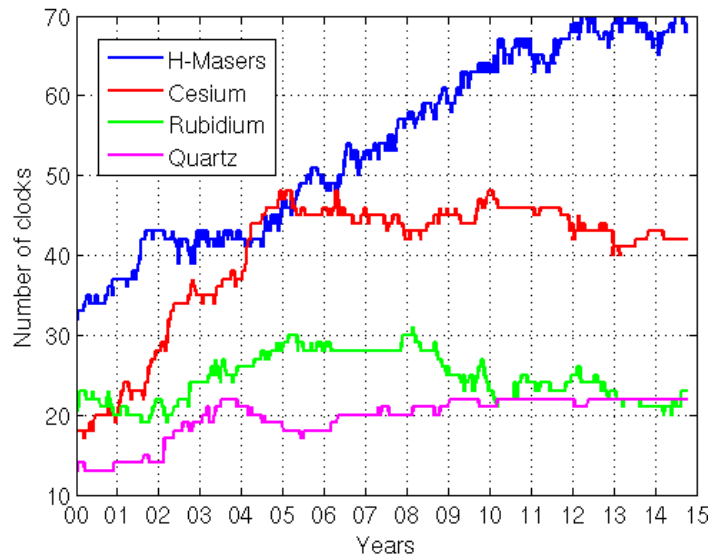


Figure 1.19 Number of different atomic clocks and quartz clocks connected to IGS stations from January 1, 2000 to October 15, 2014.

Based on the high stability of most of the H-Masers (in the range of 10^{-14} to 10^{-13} at an averaging time of 5 minutes), we modeled the clock errors of the receivers connected with H-Masers with a simple deterministic model, namely a low-order polynomial, and relative constraints between subsequent epochs with different weights (see Wang and Rothacher, 2013). Figure 1.20 shows the standard deviation (STD) of the kinematic heights of five static IGS stations connected to H-Masers on February 2, 2011. The x-axis represents the relative sigma of the epoch-to-epoch clock constraint, which determines the weight of the constraint. We see that, with decreasing relative sigma (increasing weight of the relative clock constraint) from the right to the left side of the figure, the estimated kinematic heights of the static stations are significantly stabilized until a very small relative sigma (smaller than 2 mm) is reached.

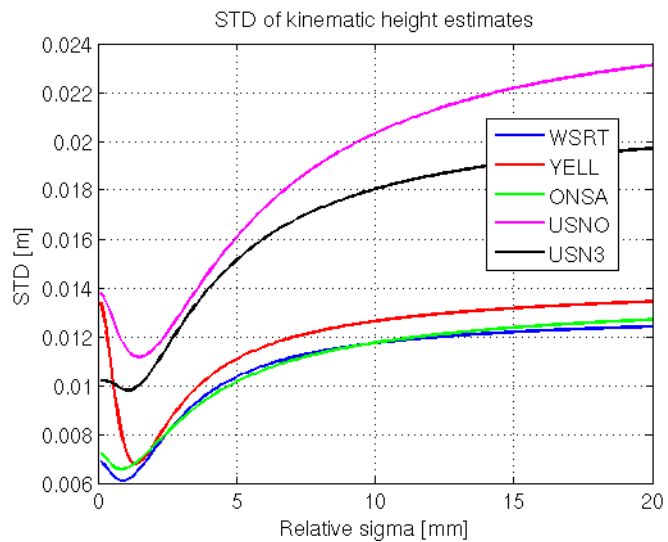


Figure 1.20: Standard deviations of the kinematic heights of different IGS stations connected to H-Masers on February 2, 2011 applying different relative clock constraints.

GNSS Reprocessing

K. Wang and M. Rothacher

Geodesy and Geodynamics Lab, Institute of Geodesy and Photogrammetry, ETH Zurich

During the last 15 years, the number of the GLONASS satellites available in GNSS processing has continuously increased, especially after 2002. In order to see the influence of the GLONASS satellites on the combined solutions of the GNSS analysis, a joint-reprocessing of GPS and GLONASS observations collected by more than 300 globally distributed GNSS stations from 1994 to 2011 was performed by Technical University of Dresden, Technical University of Munich, University of Bern and ETH Zurich within the project "Geodätische und geodynamische Nutzung reprozessierter GPS-, GLONASS- und SLR-Daten" funded by the Swiss National Science Foundation (SNF) and the Deutsche Forschungsgemeinschaft (DFG). Before 2002 only the GPS observations were included in the processing. Apart from that, Satellite Laser Ranging (SLR) observations were also used for the validation of the results.

Table 1.2 lists the results of the GPS-only, GLONASS-only and GPS/GLONASS-combined solutions from the combined reprocessing on the 1-day and the 3-day basis that are now available. GNSS-related parameters like station coordinates, orbits and Earth rotation parameters were analyzed and compared between solutions with and without including GLONASS observations. Apart from that, GPS/GLONASS combined satellite clocks were also estimated based on the orbit solutions (see Fritsche et al., 2014).

Parameter	Solution type
Orbits	Osculating orbit element
	Precise ephemerides
	Standard orbit
Earth rotation	Poles, Pole rates
	UT1-UTC, Length of Day (LOD)
	Geocenter coordinates
Coordinates	Station coordinates
Atmosphere	Troposphere zenith delays
	Troposphere gradients
Clocks	Satellite clock corrections
Biases	Differential Code Biases (DCB)

Table 1.2: Results of the homogeneous reprocessing of GPS and GLONASS observations.

Figure 1.21 shows, e.g., the mean orbit overlap differences for GPS (Figure 1.21, up) and GLONASS (Figure 1.21, bottom) daily orbit arcs from the GPS-only, the GLONASS-only and the GPS/GLONASS-combined solutions on the 1-day basis. The overlaps over 11 years (from January 2002 to March 2013) are shown in the figure. We see that the GLONASS orbits have been improved in the GPS/GLONASS-combined solutions compared to the GLONASS-only solutions. In contrast, significant differences cannot be observed in the GPS orbit overlaps by adding GLONASS observations.

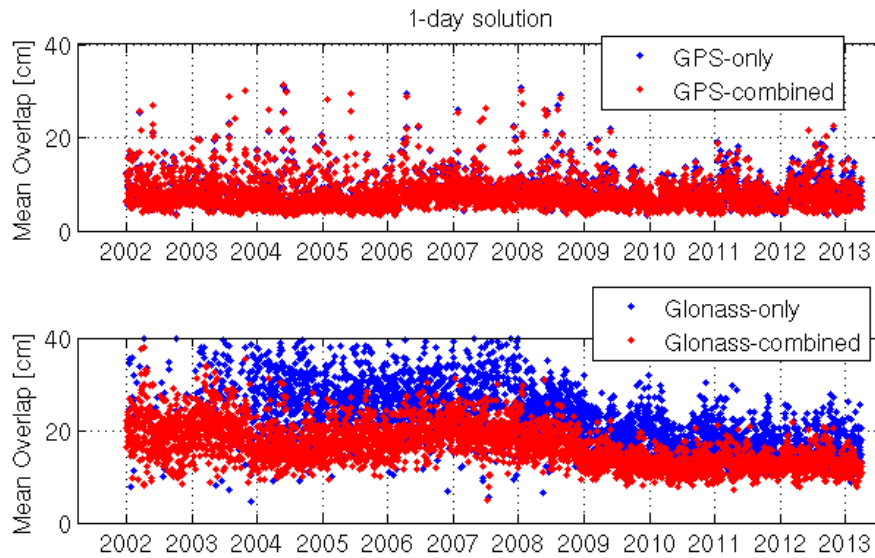


Figure 1.21: Mean orbit overlaps for GPS and GLONASS satellites using the GPS-only, the GLONASS-only and the GPS/GLONASS-combined solutions on the 1-day basis.

Co-location of Space Geodetic Techniques on Ground and in Space

B. Männel and M. Rothacher

Geodesy and Geodynamics Lab, Institute of Geodesy and Photogrammetry, ETH Zurich

Co-location in space, describing the ties between space geodetic techniques on-board satellites, allows new and innovative insights into individual techniques and their combination for the realization of the terrestrial reference frame. In recent years very promising results were presented concerning GNSS, SLR and DORIS combinations on-board existing GNSS and LEO satellites. Within the next decade co-location in space will become more and more important as dedicated missions will, hopefully, be launched (e.g. GRASP) and innovative observation scenarios are under development (tracking L-band signals with radio telescopes, quasi-simultaneous SLR, ...). In this project we studied, together with the project partner at Wetzell/Germany (TU Munich), selected aspects of both, co-location on-board LEOs and GNSS satellites, respectively, as they are available today. By a series of simulations also future developments were investigated.

As an initial, but essential activity, new subroutines and considerable source code changes were implemented into the Bernese GNSS software (Version 5.2). This modified version is now capable to simulate SLR observations to satellites, to process classical VLBI measurements of quasars and to simulate and to process VLBI observations of satellites. Furthermore, the software is now able to combine VLBI, SLR and GNSS data at the observation level. Some minor changes were also done to handle non-gravitational forces for orbit determination and to derive ionospheric delay corrections from GNSS observations (for the correction of VLBI observations of GNSS satellites).

A high-quality precise orbit determination (POD) is crucial for co-location in space. Therefore, much effort has been spent on orbit parametrization and modelling. Figure 1.22 shows the RMS difference of our reduced-dynamic GRACE-A orbits with the JPL solutions over 10 years (2003 to 2012). By using a box-wing model together with a model for non-gravitational forces on top of estimating stochastic pulses every 6 min, the RMS values are reaching a level of 2 cm. Apart from GRACE, also OSTM/Jason-2 and GOCE were processed, as these missions provide high-quality GPS data and accurate reference orbits are available. High-quality on-board sensor offset vectors and sensor characteristics are essential. Therefore, an extensive literature study was carried out and SLR range biases have been estimated and studied. By combining LEO and ground-based GPS observations in an undifferenced processing, geocenter coordinates have been estimated for the years 2010-2012. By including the two GRACE satellites, GOCE and OSTM/Jason-2 the geocenter coordinates are significantly improved w.r.t. a purely ground-based GPS network. Comparisons with SLR and geophysical solutions are envisaged. Concerning future LEO satellites for co-location in space a number of simulations were carried out. The main focus was on observation times for VLBI baselines and the achievable coordinate accuracy.

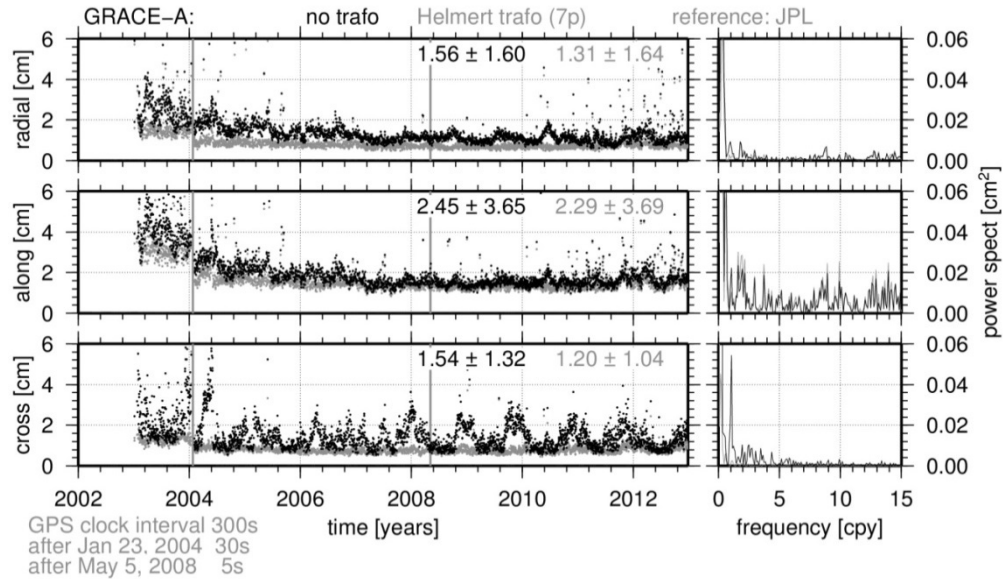


Figure 1.22: Daily RMS of the orbit comparison w.r.t. JPL orbit solutions for GRACE-A; vertical lines indicate a change of the GPS clock products

In recent years GLONASS L1 signals have been observed by a couple of radio telescopes in Europe (e.g. Kodet et al., 2014). Combining these measurements with simultaneous GNSS and SLR observations allows a co-location in space using currently available sensors and satellites. As G-VLBI (VLBI observation of GNSS satellites) might be restricted to L1 because of bandwidth limitations of some radio telescopes, correcting the ionospheric delay will be crucial. We studied the feasibility of introducing corrections derived from co-located GNSS L4 (=L1-L2) phase observations (Männel and Rothacher, 2015). Figure 1.23 shows an exemplary validation result, where the ionospheric delay corrections were applied to a GNSS L1 processing (V_{LAR}). The height coordinate repeatability improves significantly compared to an L1 solution, when corrections are taken from global ionospheric maps (V_M). Extensive simulation studies of VLBI tracking of GNSS satellites were carried out. These simulations show 3D station coordinate RMS values of 1 cm for a regional network observing a GLONASS constellation two hours per day for 15 days (observation interval of 1 min and white noise of 5 cm assumed). Also simulated and real data for SLR and GNSS were included within these studies (Männel et al., 2014).

In the following project phase we will study co-location on ground and in space by focusing on the unique instrumentation at Wettzell, where three radio telescopes, two SLR stations and a delay-compensated optical frequency and time distribution system are currently available or will become operational within the next months.

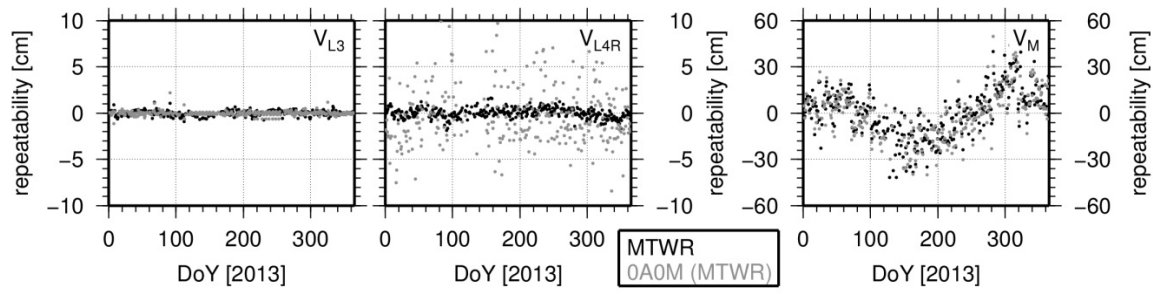


Figure 1.23: RMS of the height coordinate repeatability for Matera-Wetzell: baselines MATE-WTZR (black) and MAT1-WTZZ (grey); dual frequency solution (left), single frequency with ionospheric corrections derived from MATE-WTZR (middle) and taken from global ionospheric maps (right)

Analysis of Permanent GNSS Networks at swisstopo (PNAC)

E. Brockmann, D. Ineichen, S. Lutz, S. Schaer

Federal Office of Topography, swisstopo

The Automated GNSS Network of Switzerland (AGNES) is a multi-purpose reference network for national first order surveying, scientific research such as geodynamics and GNSS meteorology and serves as a base for the Swiss positioning service (swipos). 29 AGNES stations were set up from 1998 till 2001. AGNES reached its designated configuration of 31 stations by the end of 2006. After the enhancement of the network by GPS/GLONASS mid of 2007, totally 41 receivers are operating continuously to serve the various applications. In the first quarter of 2015 the network will be capable to support full Multi-GNSS functionality.

The characteristics of the permanent GNSS-networks analyzed at swisstopo are shown in the Table 1.3 and in Figure 1.24. The routine operation of the Permanent Network Analysis Center (PNAC) is divided into 3 sub-network solutions, which are generated on an hourly and daily basis. All analyses are done with the Bernese Software (BSW5.2 since beginning 2013). The use of synergies with the global analyses of the permanent network of the International GNSS Service (IGS) performed at the Astronomical Institute of the University of Berne (AIUB) which operates the Center for Orbit Determination in Europe (CODE) could be realized by several software modules which are absolutely identical at AIUB and swisstopo. Furthermore, improvements of the BSW were developed and the software developments can also be exchanged via the Concurrent Versions System (CVS).

Network solution	Stations (2010 → 2014)	Processing interval	Delay
1: EUREF (EPN) sub-network	50 -> 51	daily observations	14-21 days
2: AGNES + sub-net EUREF	118 -> 172 (41 AGNES)	daily observations	14-21 days
3: AGNES + sub-net EUREF	115 -> 176 (41 AGNES)	hourly observations	1:45 hour

Table 1.3: Network analyses of permanent GNSS data at swisstopo.

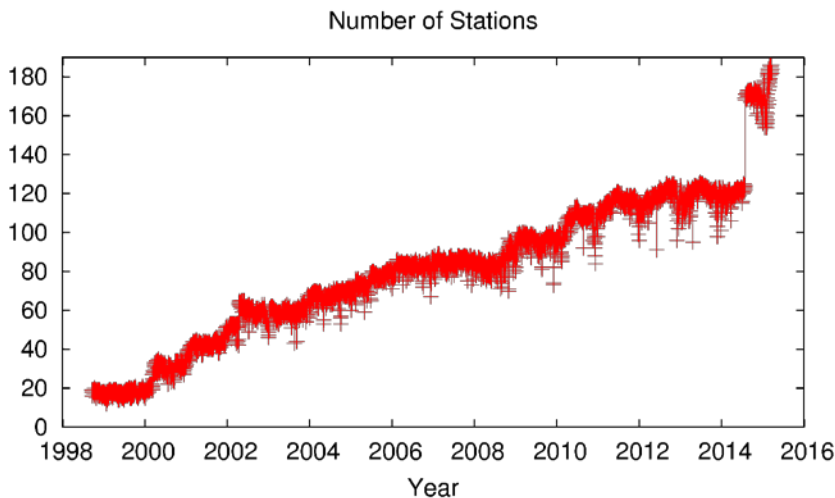


Figure 1.24: Number of sites processed operationally on a daily basis.

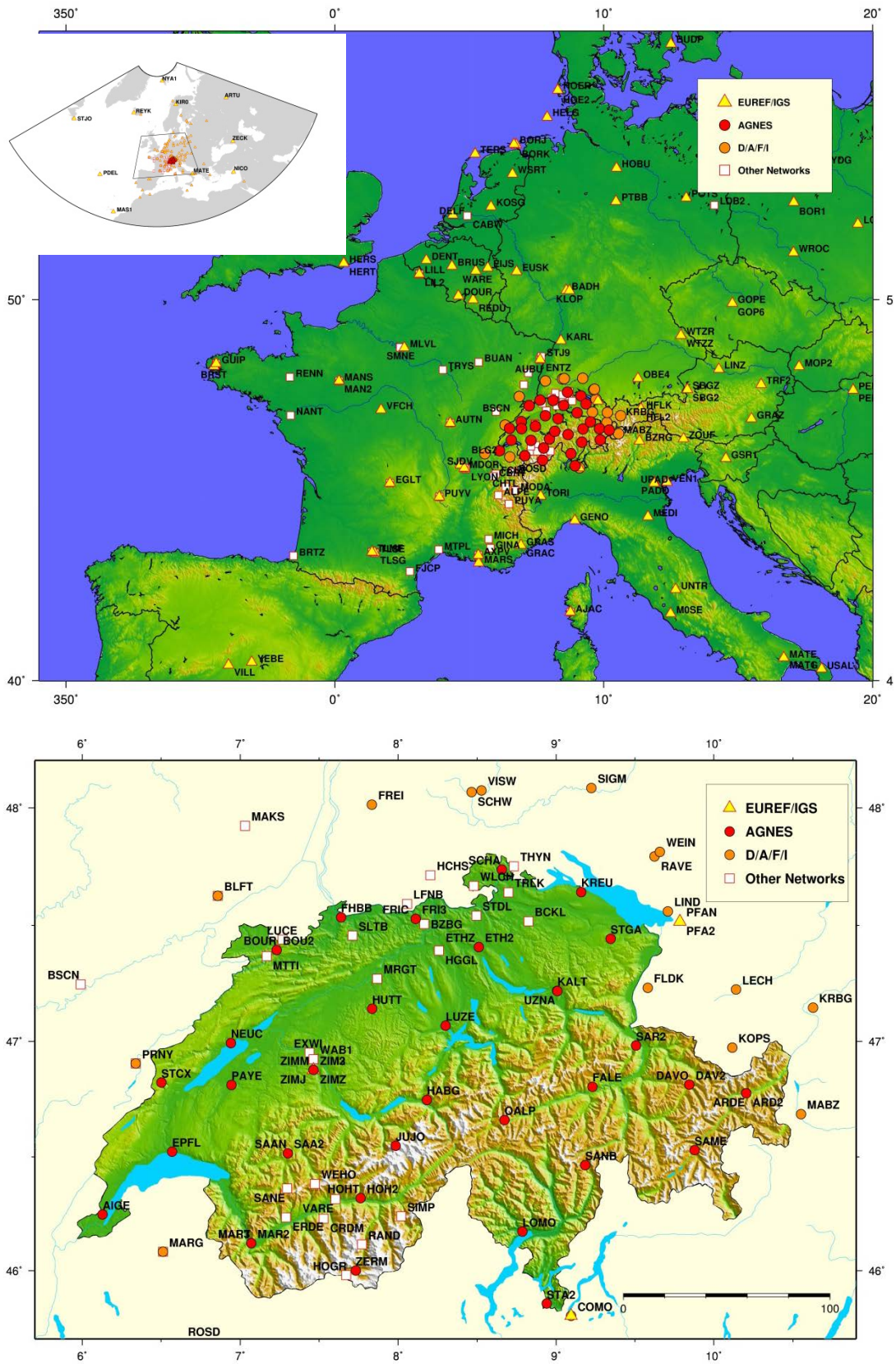


Figure 1.25: Overviews of the permanent GNSS stations processed at swisstopo.

The number of analyzed sites has continuously been increased including foreign stations close to the Swiss national border (partly delivering also data in real-time for the positioning service), third-party stations, and new EPN stations. Especially, double stations are important, because the L1-only solutions (daily as well as kinematic every epoch) enable a reference station monitoring of even better performance as possible on longer distances and ionosphere-free data analysis.

It's worth mentioning that the routine data processing is very similar (by processing options as well as by identical processing steps) to the performed re-processing. Due to the increased number of stations optimizations were important developments (unification of all daily processing jobs, clustering, hardware and operating system changes, etc.).

Figure 1.25 shows the processed networks in Europe and Switzerland.

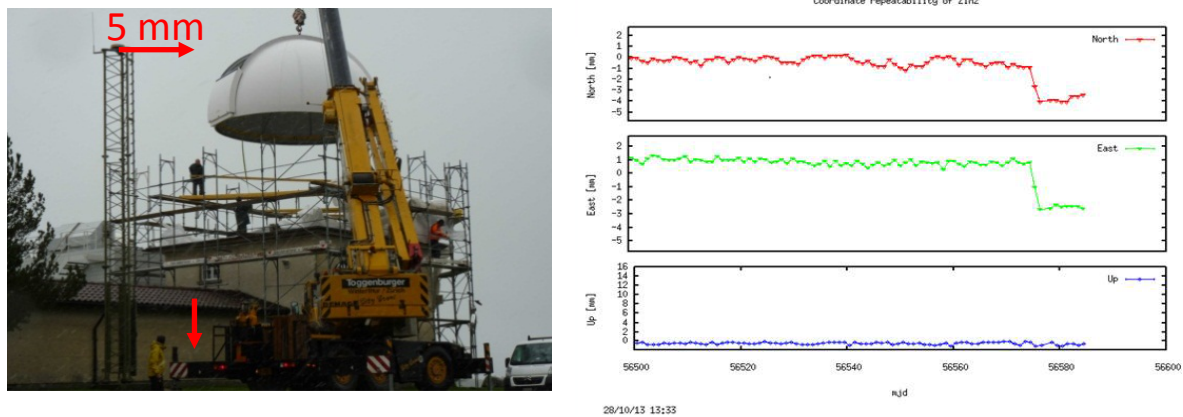
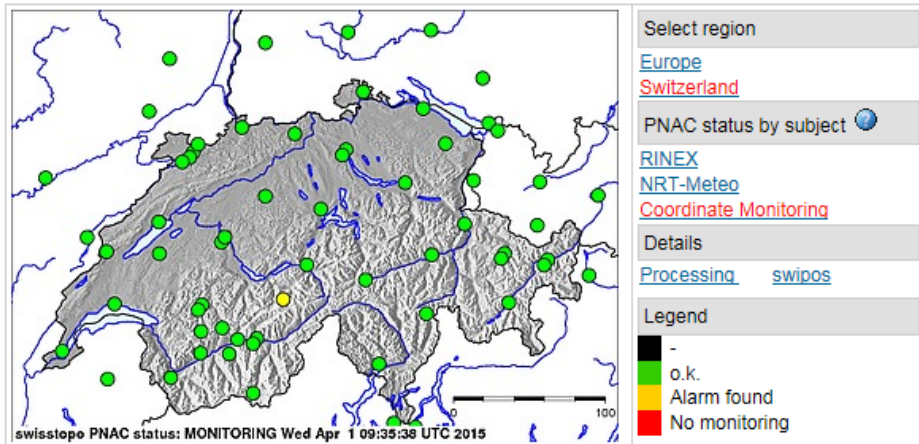


Figure 1.26: Crane “accident” 10.10.13 caused displacement for station ZIM2 of totally 5 mm (detected by short baseline analysis to ZIMM and ZIMJ).

Figure 1.26 shows an example of a short baseline analysis at geostation Zimmerwald. Due to a too closely operating 40-t crane a horizontal displacement of 5 mm took place. This was precisely monitored by the web-based monitoring system which releases additionally SMS messages in case of problems (see Figure 1.27).

The main processing products are coordinates for reference frame maintenance and zenith total delay estimates for numerical weather prediction and climate monitoring. From solution 1 of Table 1.3, swisstopo contributes, as one of several European processing centers of the European Permanent Network EPN, weekly (and daily) coordinate and troposphere parameters and also rapid and ultra rapid products for EUREF coordinate monitoring purposes. Solution 2 and 3 of Table 1.3 are used for monitoring the Swiss reference frame in near real-time and generating products used in federal surveying and for scientific applications (Tectonics, GNSS meteorology). Besides contributing with NRT troposphere estimates to the EGVAP project (EUMETNET), swisstopo contributes since 2014 also to the COST project GNSS4SWEC. The time series and the performed re-processing activities enable a first analysis of the development of troposphere estimates over longer time periods.



Coordinate Monitoring status by site

AIGE	ARD2	ARDE	BLFT	BOU2	BOUR	BSCN	COMO	GRDM	DAY2
DAVO	EPFL	ERDE	ETH2	ETH2	FALE	FHBB	FLDK	FREI	FRI3
HABG	HOH2	HOHT	HUTI	JUJO	KALT	KOPS	KRBB	KREU	LECH
LIND	LOMO	LUCE	LUZE	MABZ	MAKS	MAR2	MARG	MTT	NEUC
OALP	PAYE	PFA2	PRNY	SAA2	SAAN	SAME	SANB	SANE	SAR2
SCHA	SIGM	STA2	STCX	STGA	VARE	VISW	WEHO	WEIN	ZERM
ZIM2	ZIMM								

Available plots by site

Station	Network / Info	Quality Summary	Coord. repeat. daily	Short L1 basel. daily	Meteo	30 / 7 days 24 / 1h-Monitor	3 days 30s-Monitor
AIGE	Agnes	🚫	📶	🔴	☁️	📶	📶
ARD2	Agnes	🚫	📶	🔴	☁️	📶	📶
ARDE	Agnes	🚫	📶	🔴	☁️	📶	📶
BLFT	RGP	🚫	📶	🔴	☁️	📶	📶
BOU2	Agnes	🚫	📶	🔴	☁️	📶	📶
BOUR	Agnes	🚫	📶	🔴	☁️	📶	📶

Figure 1.27: web-based monitoring of the permanent network analysis.

Multi-GNSS activities at swisstopo

S. Lutz, E. Brockmann, D. Ineichen, S. Schaer

Federal Office of Topography, swisstopo

Global Navigation Satellite Systems (GNSS) are used for satellite-based positioning, navigation, and time transfer services. There are two established systems for geodetic two-frequency analysis: The Global Positioning System (GPS) from the United States of America and the Global Navigation Satellite System (GLONASS) from the Russian Federation. Four additional global or regional systems are currently under development: Galileo from the European Union, BeiDou from China, QZSS from Japan, and IRNSS from India. There will be more carrier frequencies as well as new and enhanced signals to be considered in satellite geodesy – also for GPS and GLONASS.

Many advantages of multi-GNSS compared to single- or dual-system processing for scientists and engineers can be identified:

- Improved visibility to the satellites.
- Augmented availability of the signals.
- Lower vulnerability due to erroneous satellites or systems.
- More possibilities of combinations (frequencies, systems) and thus better control of the background models by comparing different solutions.

With first tests in Zimmerwald swisstopo started in the new multi-GNSS era. Mid 2011 the ZIM2 receiver started to generate RINEX-3 data (but included only GPS and GLONASS, because the station is used in the positioning system swipos). The ZIM3 receiver was connected with an antenna splitter to the ZIM2 antenna. This receiver delivers the maximally available number of satellite systems and signals to the IGS MGEX project since beginning 2013 (Figure 1.28). Furthermore, a swisstopo collaborator is chairing the EUREF Multi-GNSS working group.

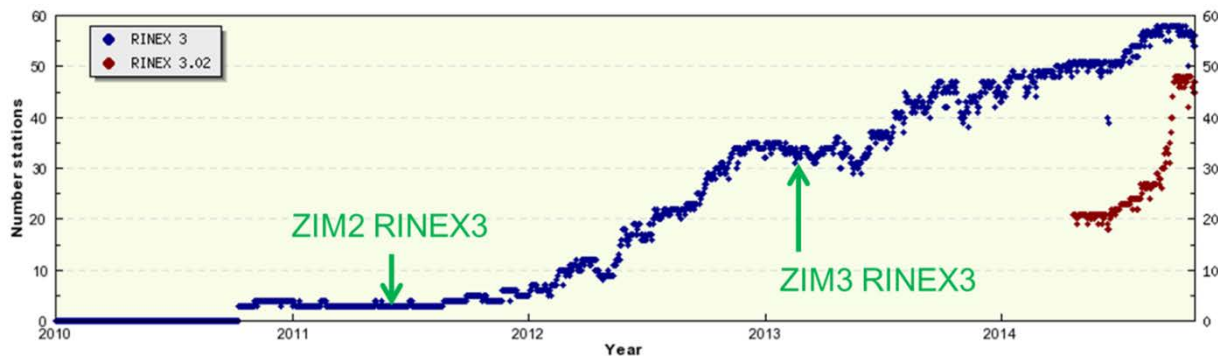


Figure 1.28: Contribution of swisstopo with multi-GNSS data to EUREF (and also IGS-MGEX).

A next step towards the integration of the new constellations and signals into the data analysis is the quality monitoring of the observation files. The International GNSS Service (www.igs.org) and its Multi-GNSS Experiment (MGEX) are important references concerning standards, conventions, and publicly available specifications of all systems. Precise satellite orbits and clocks, as well as further post-processing products are available through MGEX, too. Observation data in the dedicated RINEX-3 format can be downloaded from global or regional data centers. Using broadcast orbits with an accuracy of a few meters, a first availability and consistency check of the observations in near real-time is possible (Figure 1.29). This pre-analysis is done in a fully automated way. The results are updated once per day and made available on the PNAC website (PNAC monitoring → Data monitoring → swisstopo: Daily RINEX-2/3 monitor).

To analyze the data in post-processing mode and to integrate the new satellite systems for multi-GNSS solutions, the current development version of the Bernese GNSS Software (Dach et al. 2007) from the Astronomical Institute of the University of Bern is used. RINEX-3 observation files from the actual PNAC network and a few additional stations were downloaded and some general input files had to be updated. Precise satellite orbits and clocks are taken from IGS and the MGEX project. Preliminary results based on the standard procedure for daily solutions including Galileo are most promising (Figure 1.30), but it is obvious that inter-system biases and other issues are affecting the results. The higher complexity of the multiple observation types and the characteristics of the different constellations is a big challenge for multi-GNSS applications. With the project “AGNES-3” (see article in Commission 4, this volume) the Swiss national network will be enhanced in a way that all stations are capable to track and provide data including the new upcoming satellite systems.

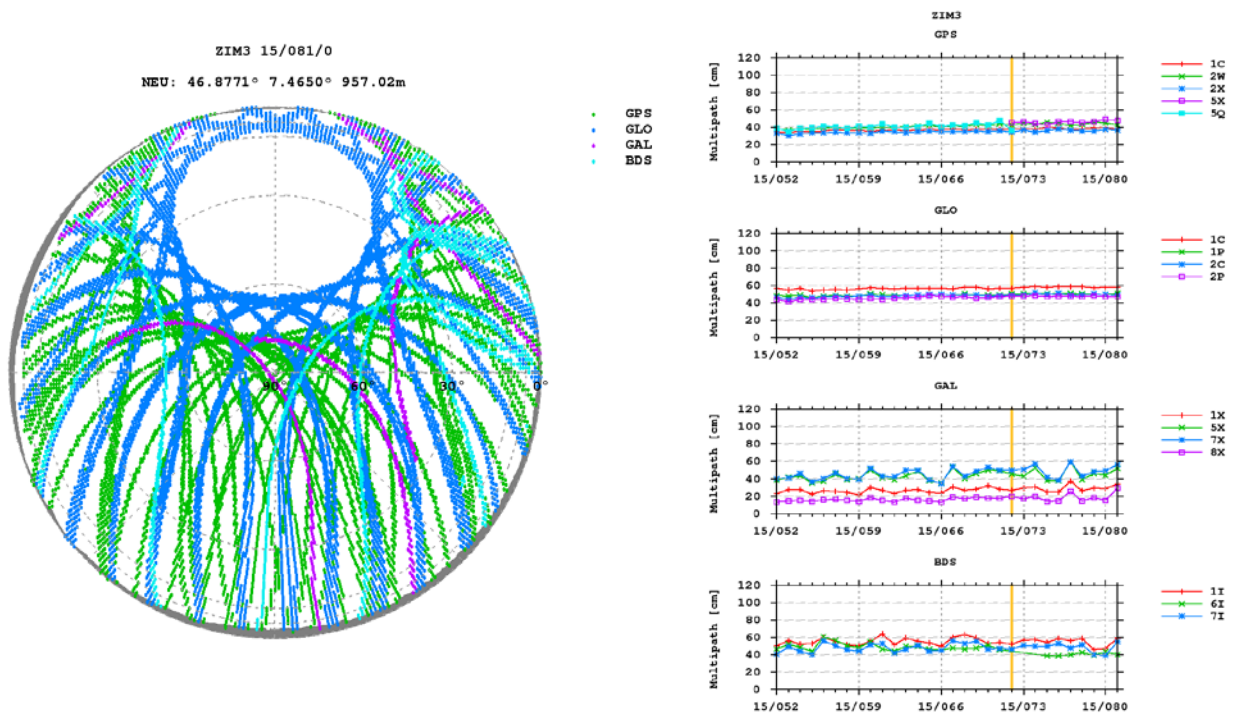


Figure 1.29: Examples from the RINEX-3 observation file monitoring at swisstopo. Left: Visibility of the satellites from the four constellations GPS, GLONASS, Galileo, and BeiDou at the Zimmerwald station ZIM3. Right: Mean code multipath of the multiple signals calculated with G-Nut/Anubis. The yellow vertical line indicates the day of a change in the firmware and tracking mode (GPS 5Q to 5X).

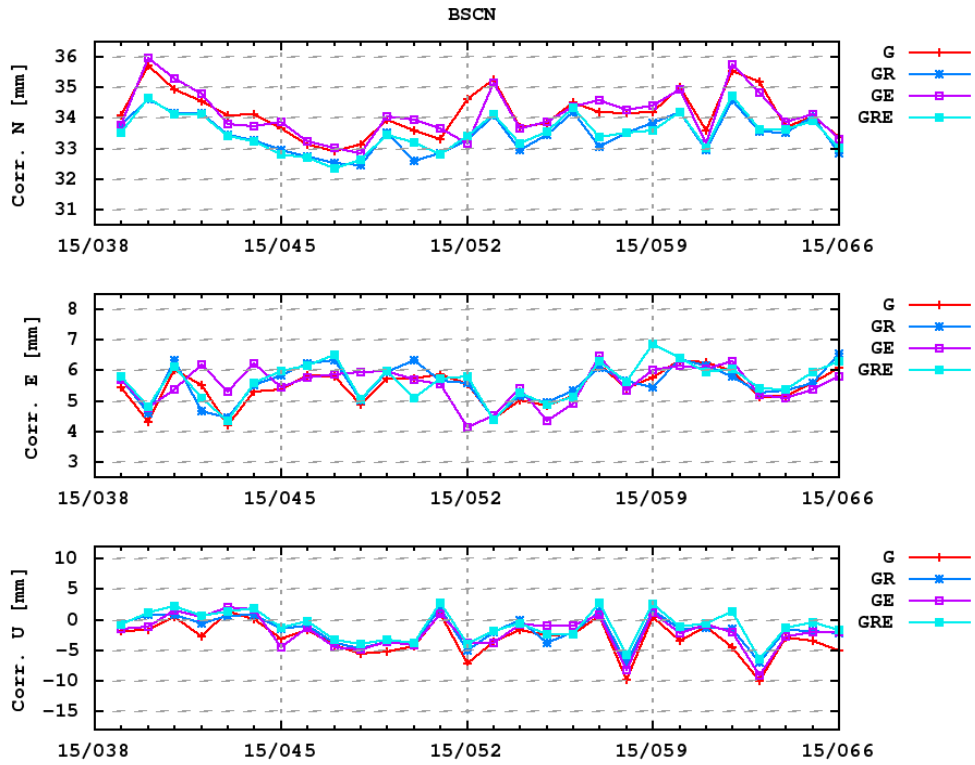


Figure 1.30: Coordinate differences in North, East, and Up of station BSCN (Besançon, FR) with respect to a linear a priori model. The results from a GPS-only (G), a combined GPS plus GLONASS (GR), a GPS plus Galileo (GE), as well as a GPS plus GLONASS plus Galileo (GRE) dual-frequency network solution are shown.

Reprocessing activities at swisstopo

D. Ineichen, E. Brockmann, S. Lutz, S. Schaer

Federal Office of Topography, swisstopo

The results of the reprocessing activities within the framework of the International GNSS Service (IGS) offer regional and local analysis centers the possibility to benefit from consistent input products for their own reprocessing activities. swisstopo decided to perform such a reprocessing using orbit and Earth rotation parameters stemming from the reprocessing series 2011 and 2013 of the Center for Orbit Determination in Europe (CODE).

The analysed network consists of stations from the Automated GNSS Network of Switzerland (AGNES), the EUREF Permanent Network (EPN), the International GNSS Service (IGS), as well as permanent stations from neighbouring countries (starting with a total of 20 stations in the daily solutions of 1996 and ending up with 170 stations in 2014).

The main motivation to perform the reprocessing was to achieve as homogenous time-series as possible for coordinate and troposphere estimates by applying consistent processing options over the whole time interval using the Bernese GNSS Software Version 5.2 (see Dach et al. 2007). Furthermore, the reprocessing allowed to make use of absolute antenna calibration values (specific for GLONASS also), Global Mapping Function (GMF) for troposphere parameter estimation, and higher order ionosphere terms. The results for the EPN and IGS sites were moreover provided to EUREF as swisstopo's contribution to the EPN-Repro2 reprocessing activity (solution identifier LP0 and LP1).

After having computed 6776 daily solutions (from DOY 007, 1996 to DOY 207, 2014), a multi-year solution was done by combining all these normal equation files with the Bernese program ADDNEQ2. A daily extending of these series by adding new solutions from our routine processing provides always up-to-date estimates of the station coordinates and steadily improves the velocity determinations. This multi-year solution replaces the so far official swisstopo time-series based on weekly solutions. For the sites of the Swiss permanent GNSS network (AGNES), the resulting coordinates of the multi-year reprocessing differ by a maximum of 5 mm in the horizontal components and 18 mm in the vertical component. These differences to the previous multi-year solution are mainly due to the transition from relative to absolute antenna calibration values (see Figure 1.31). The estimated velocities for Switzerland (relative to Geostation Zimmerwald) are in the range of ± 0.6 mm/y for the horizontal components and $+2.0/-1.7$ mm/y for the vertical component. The velocities of the new reprocessed solution and the previous multi-year solution show maximal differences of 0.3 mm/y (horizontally) and 0.5 mm/y (vertically).

Follow-up computations (e.g. with new modelling options) of the whole reprocessing time-series are easier and faster to do, starting from pre-processed single-difference files and having already solved most of the problems in the first run. Such a second reprocessing was performed investigating new processing options, such as individual antenna calibration values, Vienna Mapping Function (VMF) and atmospheric non-tidal pressure loading. Table 1.4 shows the corresponding improvements of the coordinate repeatabilities, especially for the height component.

Reprocessing is an ongoing task: New input products, new models and enhanced processing options will demand for new versions of reprocessed time-series also in the near future.

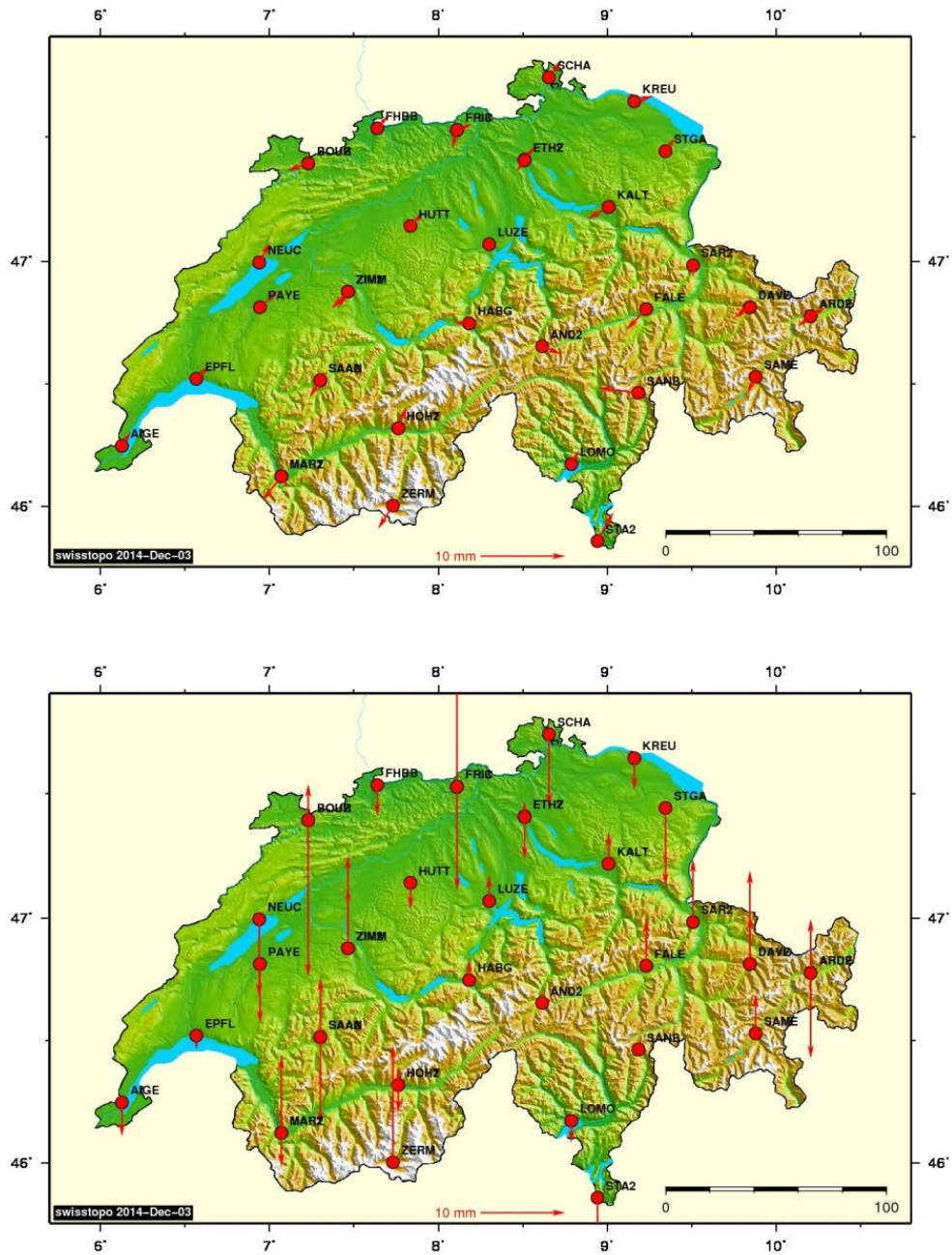


Figure 1.31: Coordinate differences between the new reprocessed multi-year solution and the previous official solution (horizontal components top, vertical component bottom). The main reason for these coordinate differences is the transition from relative to absolute antenna calibration values.

Solution Type	North [mm]	East [mm]	Up [mm]
GMF / I08	1.54	1.41	4.53
VMF / C08	1.54	1.40	4.30
VMF / APL / C08	1.51	1.37	4.08

Table 1.4: Coordinate repeatability values for different reprocessed multi-year solution: Global Mapping Function with calibrated antenna group values "GMF/I08", Vienna Mapping Function with individually calibrated antenna values "VMF/C08", and Vienna Mapping Function with atmospheric non-tidal pressure loading and individually calibrated antenna values "VMF/APL/C08".

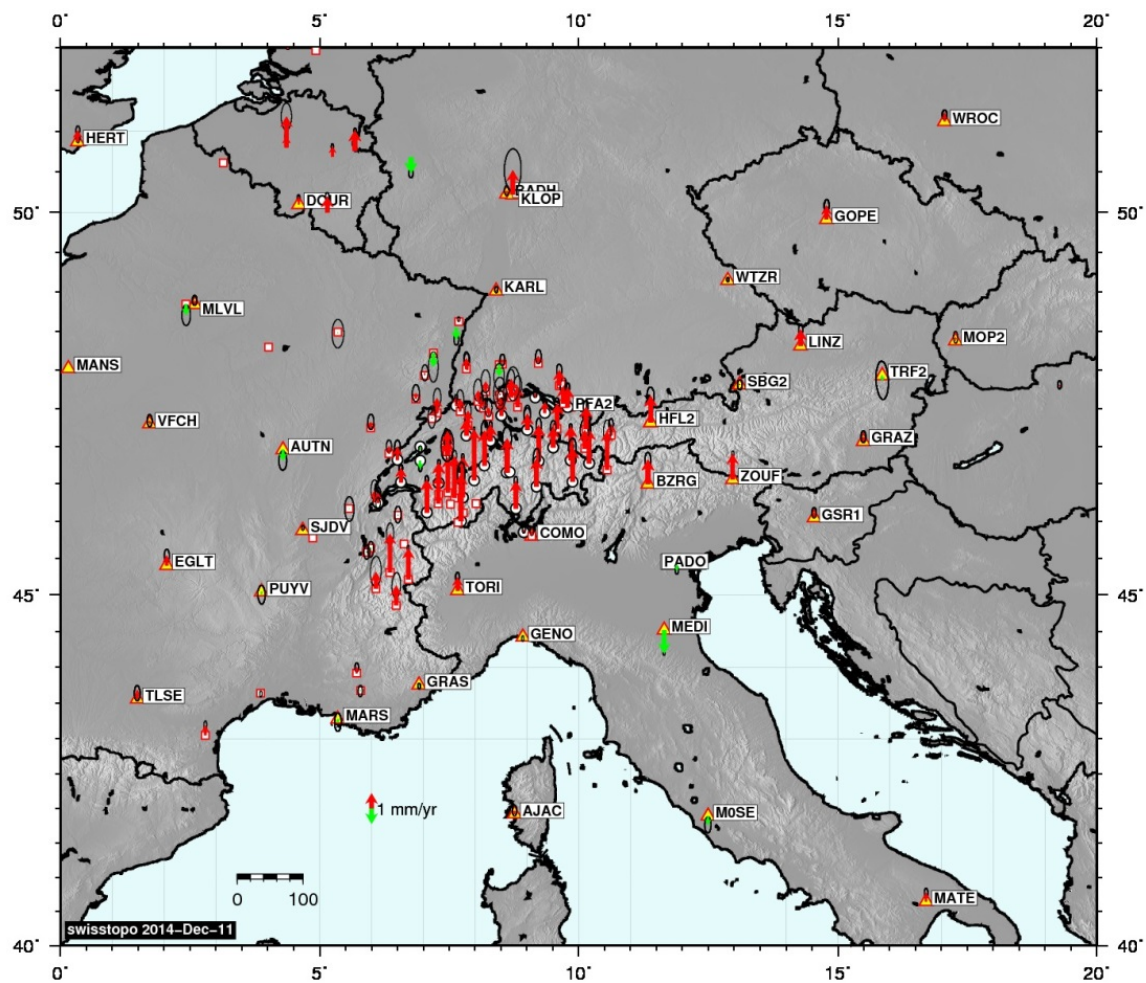


Figure 1.32: Vertical velocities from the multi-year combination of the reprocessed daily solutions with respect to the Igb08 reference frame.

Revision and Updates of the Networks of the National Geodetic Survey

A. Wiget

Federal Office of Topography, swisstopo

The concept and the various networks of the actual Swiss National Geodetic Survey (“Landesvermessungswerk LVW95”), including the continuously operating GNSS stations AGNES, the GPS network LV95 (control points), the national height network LHN95 and the national gravity network LSN2004 are described in (Wiget et al., 2011a). The Geodesy Division of the Federal Office of Topography swisstopo published different reports (in German and French) giving further details, for instance about the concepts of revisions and updates including general rules and update periods (Wiget et al., 2010). A separate public report defines the quality standards and threshold values to be followed for the national geodetic survey (Wiget et al., 2011c). These standards are monitored and documented annually. Furthermore, the data models of the geodata of the geodetic survey available in the spatial data infrastructure of Switzerland NSDI (<http://map.geo.admin.ch>) are described in the public report (Wiget et al., 2011b).

The backbone of the Swiss terrestrial reference frames LV95 and CHTRF95 are continuously operating GNSS stations AGNES in combination with the GPS network LV95. This network consists of 210 carefully selected control points which were established and measured from 1988 till 1995 completely using GPS observations. Following the above mentioned concept of revisions the stations of the LV95-network are periodically visited and maintained in a 6-years interval (see Figure 1.33 below). In the same year, selected points of the old reference frame LV03 are revised, including the renovation of one or two of the 21 historic, geodetic pyramids maintained by swisstopo. For quality checks the LV95-network was completely re-observed three times, in 1998, 2004 and 2010. The results of these re-observations, described in previous national reports of Switzerland, proved the stability of the stations (Schlatter 2011, Brockmann 2011 and Wiget et al., 2011d). The measurements and their results were also used for the geodetic analysis of geodynamic deformations in Switzerland (Villiger 2014 in Commission 3, this volume). The next re-observation of the complete LV95-network is planned for 2016.

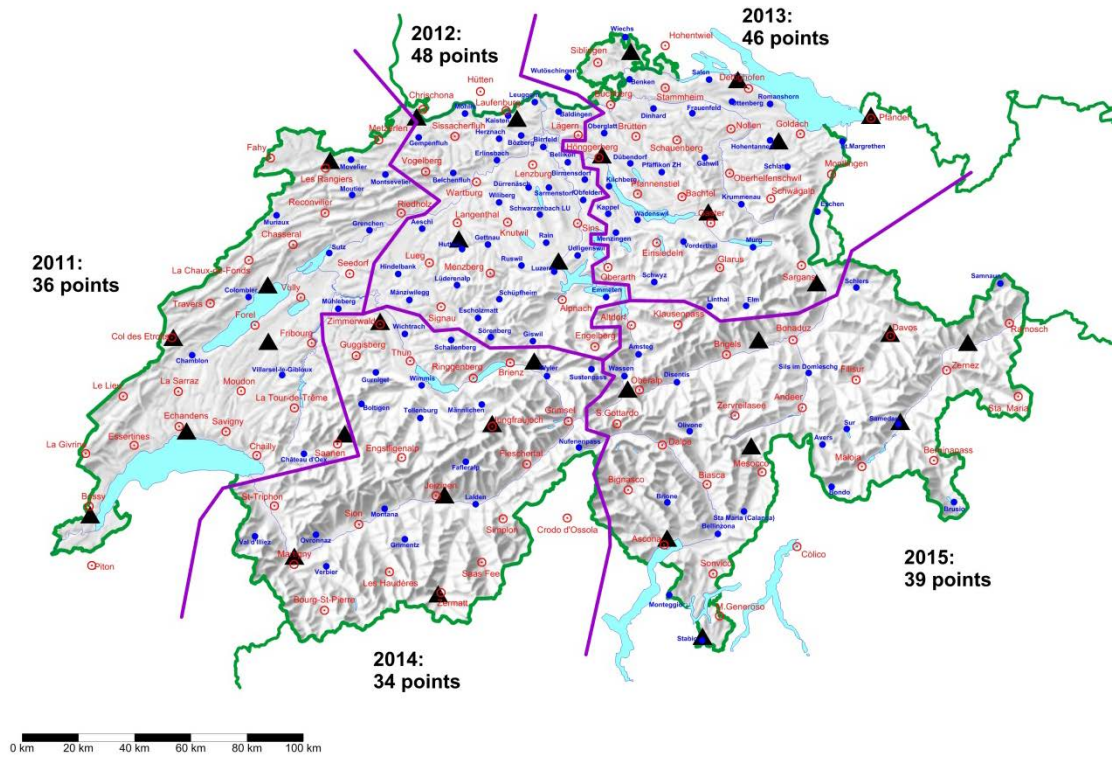


Figure 1.33: Periodic revisions of the LV95 control points (blue and red symbols) and AGNES-stations (black triangles) together with control points of the old national survey LV03 in the same regions (not shown on the map).

Measurements for the National Height System

A. Schlatter and A. Wiget

Federal Office of Topography, swisstopo

Between 2011 and 2014 a total of 520 km (around 130 km per year) of leveling observations have been performed within the National Height Network LHN95 (see red lines in Figure 1.34). This is exactly the same average of km per year as between 2007 and 2010. Usually, these measurements were carried out on lines that were leveled 40 to 50 years ago for the last time.

The main lines leveled in this epoch were the third observations of the north-south traverse from Olten to Chiasso/Como (Italy), not including the Gotthard railway tunnel: Olten – Aarburg – Sursee – Luzern – Oberarth – Altdorf – Amsteg – Wassen (North of Gotthard) and Airolo (South of Gotthard) – Biasca – Bellinzona – Lugano – Chiasso/Como.

These measurements can be combined with the first leveling through the new Gotthard railway base tunnel (57 km) from Erstfeld to Bodio, performed in 2013. This part is now integrated in the national height network LHN95. The Gotthard area with the leveling line over the pass as well as through tunnels on two different levels and various vertical shafts is now a very interesting test field to study effects of reductions-methods on measurements, gravity and density models, potential theory and differences of the geoid and the quasi-geoid, recent crustal movements and so one.

At the southern end of the north-south traverse the connection and link to the Italian leveling network was established and extended to Como because the reference marks in the Chiasso area show significant subsidence. Further local connections to height reference marks in Italy were measured in Castasegna (Val Bregaglia) and in Campocologno (Val Poschiavo). The connection to France was renewed in the area of Vallorbe.

Additional measurements carried out in the National Height Network during this epoch were:

Oberarth – Sattel – Pfäffikon; Bennau – Einsiedeln; Luzern – Lopper; St. Gallen – Rorschach; Bivio – Julierpass; and as reference for hydrological measurements of the Federal Office for the Environment (FOEN/BAFU): Interlaken – Zweilütschinen – Grindelwald.

In 2014 the seventh precision leveling through the Hauenstein railway base tunnel (length of the line 10.3 km) was measured since the installation of the special reference marks for deformation studies. Apart from some minor differences the results of the 2009 observations were confirmed.

Besides these line measurements, which principally serve for the realization of the two national vertical reference frames (LN02 and LHN95), geoid determination and the investigation of recent crustal movements, regular local maintenance works were performed. The national height network contains today around 4'500 km of leveling lines with approximately 8'500 benchmarks.

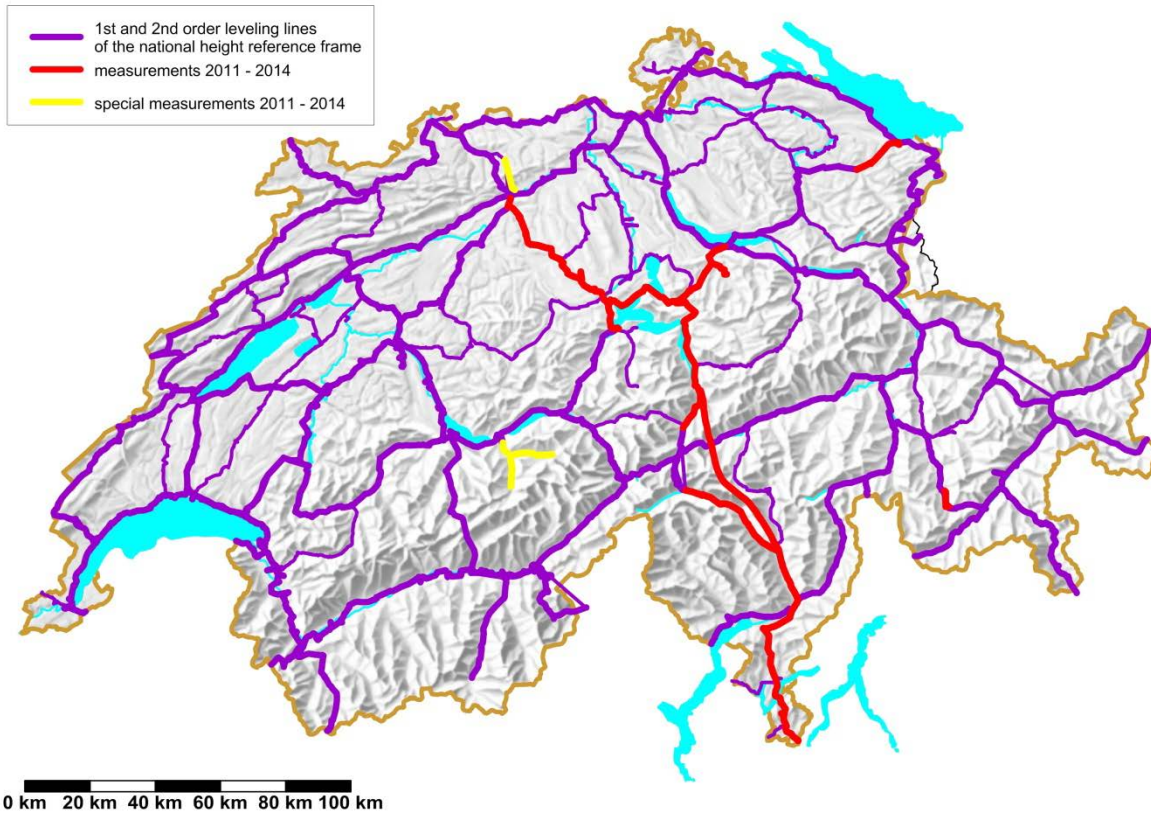


Figure 1.34: Measurements 2011 – 2014 for the National Height System LHN95

The Nationwide Change of the Reference Frame from LV03 to LV95

A. Wiget

Federal Office of Topography, swisstopo

The Ordinance on Geoinformation (GeoIO, SR 510.620) determines that the transition period from the old geodetic reference system and frame (CH1903/LV03) to the new one (CH1903+/LV95) has to be completed by Dec. 31, 2016 for reference data and by Dec. 31, 2020 for all the other official sets of geodata under federal legislation. Therefore, the cantons started to organize and realize the transformations using the so called Fineltra algorithm, a linear transformation by finite elements, and the respective software tools developed by swisstopo (see next article by Kistler et al., this volume). An important part of this transition is the information of the various actors as well as agencies and persons concerned – eventually every producer and user of geodata. For this, the Geodesy Division of the Federal Office of Topography swisstopo published an information- and communication-concept, including tools like designated web-pages (www.swisstopo.ch/lv95) or a short introductory movie (<http://www.swisstopo.admin.ch/internet/swisstopo/en/home/docu/video/lv95-vid.html>) (Wiget 2012a and Wiget 2012b). The communication-concept as well as other activities of federal institutions were presented and discussed in various conferences and presentations (e.g. Wiget 2014).



Figure 1.35: Short introductory movie about the new coordinates for Switzerland (in German, French, Italian and English) on the swisstopo website as well as on Youtube.

By end of 2014 the following seven cantons (state level) have realized the transition of their official cadastral surveying to LV95: Valais (VS), Geneva (GE), Appenzell Ausserrhoden (AR), Zug (ZG), Basel Stadt (BS), Basel Landschaft (BL), Thurgau (TG).

Towards a Distortion Free National Spatial Data Infrastructure in Switzerland: Approach, Developed Tools and Internet Services for the Change of the Reference Frame

M. Kistler, U. Marti, J. Ray, Ch. Baumann and A. Wiget

Federal Office of Topography swisstopo

According the federal law for geo information the complete Spatial Data Infrastructure SDI of Switzerland has to be transformed from the historical reference frame LV03 to the new one LV95 (related to ETRF93) in high accuracy. In doing so, the deadline for reference datasets is end of 2016 and for the other base data sets 2020.

Developed Software Tools, Libraries and Plugins

swisstopo developed in the last couple of years a variety of software tools, libraries and services for the reference frame change to support the different stakeholders best possible. In a first step, the client solution GeoSuite with the modules REFRAME and TRANSINT have been developed. This software is not only able to transform or to interpolate geo datasets into various formats (e.g. GIS or CAD quasi standard formats), it also provides direct access to all datasets in the SDI of Switzerland over an integrated application programming interface API as well as to any Web Map Service WMS available.

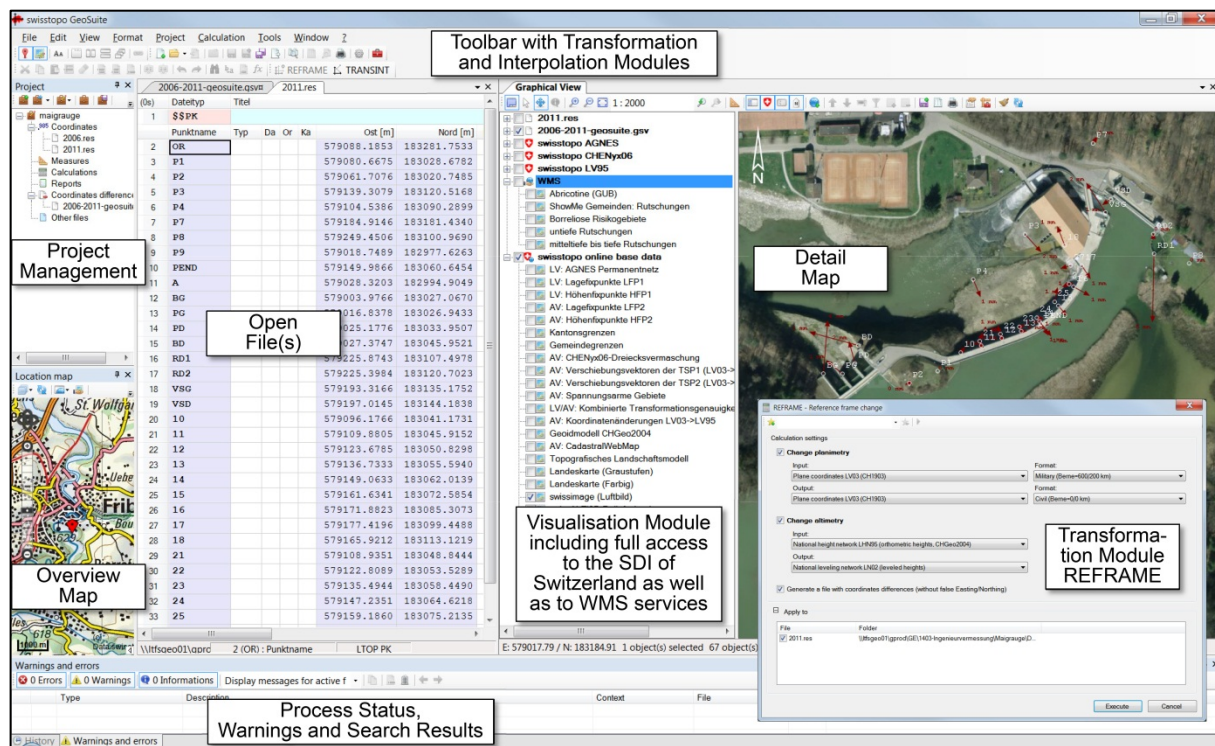


Figure 1.36: Graphic user interface GUI of the software GeoSuite with the different modules: REFRAME was designed to provide the official transformation algorithms for the reference frame change and TRANSINT for individual transformations or interpolations. The visualisation module includes full access to all datasets of the SDI of Switzerland (e.g. official site descriptions of all survey points of Switzerland) and any other dataset available as WMS services.

With this visualization module, the results of a transformation or interpolation can be easily analysed or documented. Furthermore, all the transformation and interpolation algorithms are available as dynamic link library DLL for the integration in third party products, e.g. in GIS extensions for cadastral works, or for the development of Plugins, e.g. realized for FME by swisstopo itself. With the REFRAME- and TRANSINT-Transformer for FME, transformations of any possible file format are supported.

Internet Services released

In a second step, a set of Internet services has been developed:

1. Transformation Services

Transformation services as Machine to Human (M2H) service for all the common geofomats and as Machine to Machine (M2M) service for real-time transformation in the federal geoportal > <http://map.geo.admin.ch> or for the Swiss positioning service swipos. In this way, swipos can offer GNSS corrections for both reference frames.

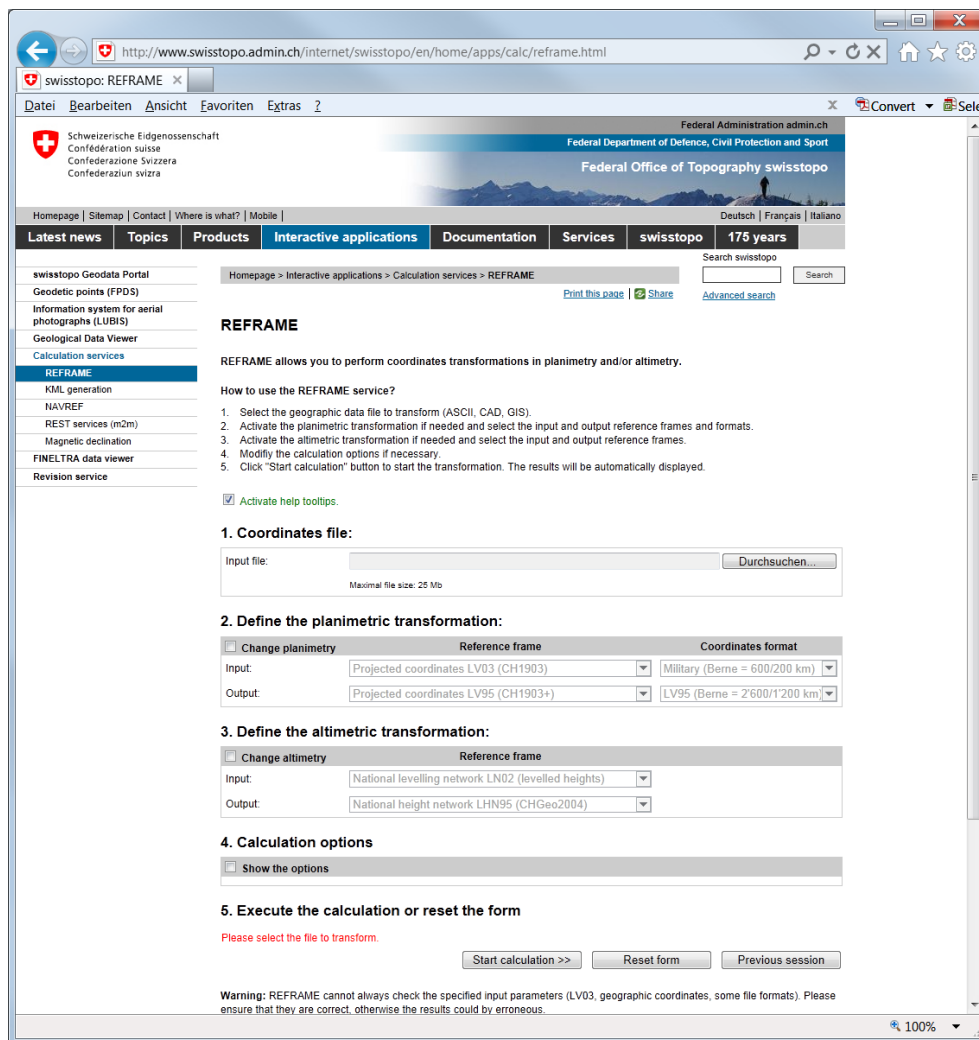


Figure 1.37: REFRAME transformation service.

2. Interpolation Services

Interpolation services for the conversion / rectification of geo datasets on the very local level with big distortions based on deformation grids, for instance for the transfer of all reference and base datasets of the canton of Basel-Stadt:

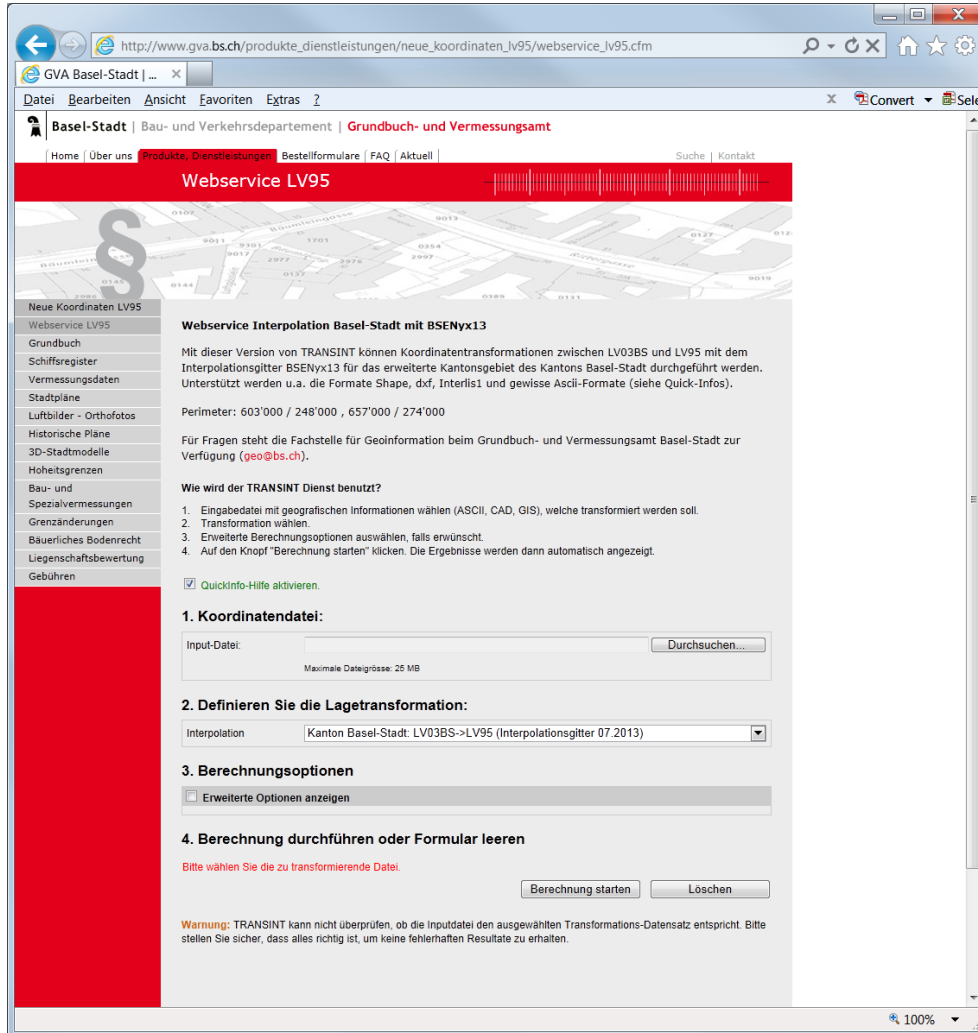


Figure 1.38: TRANSINT interpolation service.

3. Visualisation Services for Survey Points and the Transformation Accuracy

Visualisation services for desktop and mobile devices, e.g. all the survey point site descriptions with old and new coordinates and different metadata are available or a map with the expected transformation accuracy for the whole country.

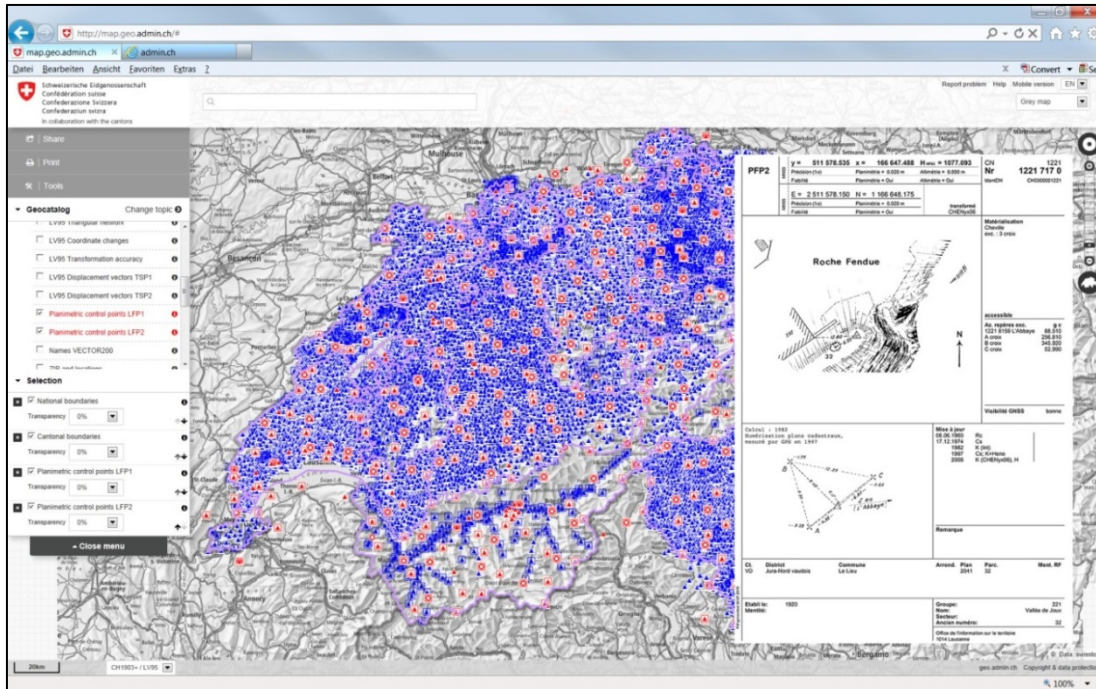


Figure 1.39: Visualisation service for survey points on national (red) and cantonal level (blue). In the site descriptions (see example right), coordinates of these points, which are distributed all over Switzerland, are always available in both reference frames together with many metadata information.

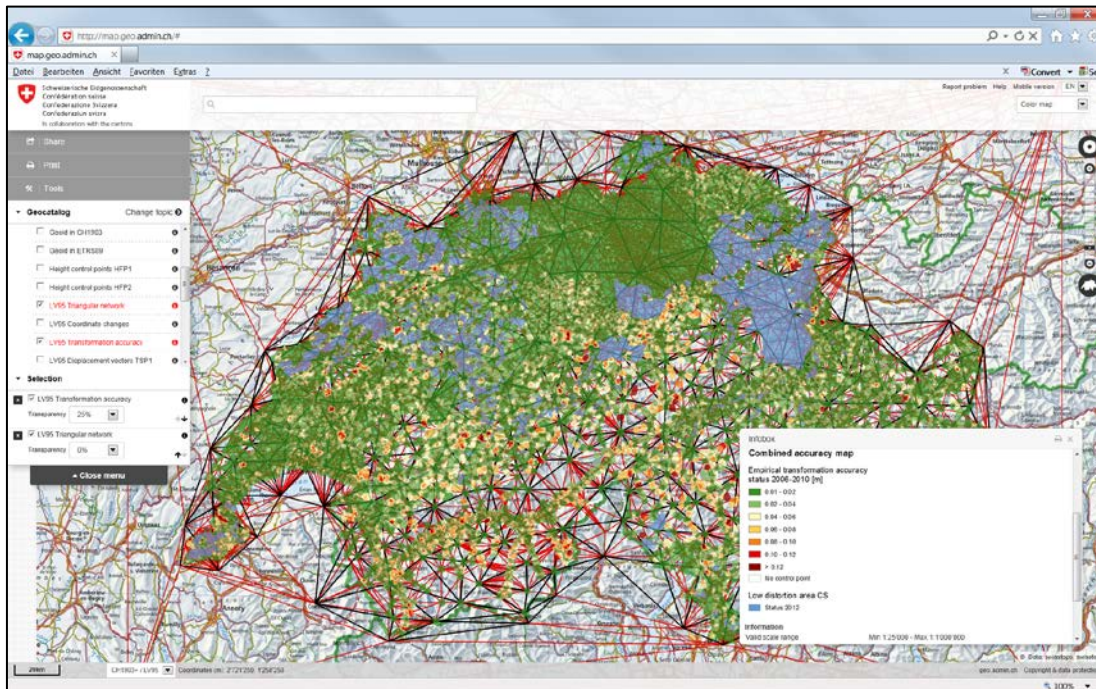


Figure 1.40: Visualisation service for the transformation accuracy based on a statistical method over control points distributed all over Switzerland (GNSS measured coordinates in comparison with transformed ones). Furthermore the cadastral authorities nominated so-called low distortion areas (blue surfaces): in these areas, cadastre survey fulfils the higher accuracy requirements related to the new global reference frame, so that measurements with GNSS sensors can be done in an absolute way without having to respect the local situation.

4. Download Services

Last but not least, different download services for DLLs and transformation datasets have also been realised.

As described in the article before (this volume) until today, about one third of 23 cantons (state level) have already transformed their SDIs successfully and for another third, the preparation work has already been started. Nevertheless it is assumed that both reference frames and therefore the tools to "switch" from one to the other have to be supported another decade until the last geo dataset in Switzerland is transformed.

Bibliography Commission 1

- Altamimi, Z., Collilieux, X., and Metivier, L. (2011): ITRF2008: an improved solution of the international terrestrial reference frame. *J Geod* 85(8):457-473, doi: 10.1007/s00190-011-0444-4.
- Angermann, D., Baustert, G., Galas, R., and Zhu, S.Y. (1997): EPOS.P.V3 (Earth Parameter & Orbit System): software user manual for GPS data processing; version September 1997, (Scientific Technical Report; 97/14).
- Arnold, D., Beutler, G., Sośnica, K., Meindl, M., Lutz, S., and Dach, R. (2015a): Updating the empirical CODE orbit model and validation of GPS and GLONASS orbits using Satellite Laser Ranging data. This volume.
- Arnold, D., Meindl, M., Beutler, G., Dach, R., Schaer, S., Lutz, S., Prange, L., Sosnica, K., Mervart, L., and Jäggi, A. (2015b): CODE's new solar radiation pressure model for GNSS orbit determination. *Journal of Geodesy*, DOI:10.1007/s00190-015-0814-4
- Arnold, D., Lutz, S., Beutler, G., Schaer, S., and Dach, R. (2015c): Impact of orbit modeling on GNSS-derived geodynamic parameters. This volume.
- Baumann C., Sośnica, K., Thaller, D., Jäggi, A., Dach, R., and Mareyen, M. (2012): LARES: Analysis of the first months of data. Proceedings of the International Technical Laser Workshop 2012 (ITLW-12), Frascati (Rome), Italy, November 5-9, 2012.
http://www.lnf.infn.it/conference/laser2012/2tuesday/3_4_6baumann/baumann_1.pdf
- Beutler, G., Brockmann, E., Gurtner, W., Hugentobler, U., Mervart, L., Rothacher, M., and Verdun, A. (1994): Extended orbit modeling techniques at the CODE processing center of the International GPS Service for geodynamics (IGS): theory and initial results. *Manuscr. Geod.* 19: 367–384.
- Brockmann, E. (2010): EUREF-TWG Project: Monitoring of official national ETRF coordinates on EPN web. In: *Bulletin of Geodesy and Geomatics BGG, LXIX, 2-3, 2010*, Instituto Geografico Militare, Firenze, pp 245-256.
- Brockmann, E., and Ineichen, D. (2010): Geostation Zimmerwald: Ablotung 2010. Messungen vom 21. Oktober und 4. November 2010. swisstopo Report 10-14. Bundesamt für Landestopografie, Wabern.
- Brockmann, E., and Ineichen, D. (2010): Auswertung der NaGNet-Stationen bei swisstopo: Datenfluss, Schnittstellen, Auswertungen und Monitoring. swisstopo Report 10-20. Bundesamt für Landestopografie, Wabern.
- Brockmann, E. (2011): Diverse EUREF-TWG Präsentationen zum Thema "National ETRF coordinates of EPN permanent stations", Validation ETRF08, Galileo/RINEX3 (Padua, 3.-4.03.2011, Chisinau 24.05.2011, Frankfurt 27.-28.10.2011).
- Brockmann, E. (2011): LV95 / CHTRF2010 (Swiss Terrestrial Reference Frame 2010): Teil 2: Auswertung der GPS-Messungen 2010 und Resultate der Gesamtausgleichung 1988-2010. swisstopo Report 10-25. Bundesamt für Landestopografie, Wabern.
- Brockmann, E. (2011): EUREF'11: Paper contributions to the EUREF-Symposium in Chisinau, May 25-28, 2011: «National Report of Switzerland», «20 years of maintaining the Swiss Terrestrial Reference Frame CHTRF», «Consideration of Station-Specific Intersystem Translation Parameters at CODE», and «EUREF-TWG Project: Monitoring of official national ETRF coordinates on EPN web». swisstopo Report 11-11. Bundesamt für Landestopografie, Wabern.

- Brockmann, E., and Schlatter, A. (2011): 20 years of maintaining the Swiss terrestrial reference frame CHTRF. Subcommission for the European Reference Frame (EUREF), Chisinau, 25.-28.05.2011.
- Brockmann, E., Ineichen, D., Kistler, M., Marti, U., Schaer, S., Schlatter, A., Vogel, B., Wiget, A., and Wild, U. (2011): Geodetic activities at swisstopo presented to the EUREF2011 Symposium. Subcommission for the European Reference Frame (EUREF), Chisinau, 25.-28.05.2011.
- Brockmann, E. (2011): swisstopo (LPT) E-GVAP Report. Expert group meeting in Toulouse, 20.-21.10.2011.
- Brockmann, E., Schlatter, A. (2011): Station velocities in Switzerland derived from 20 years of geodetic satellite navigation observations. Swiss Geoscience Meeting. Zürich, 12.11.2011.
- Brockmann, E., Andrey, D., Ineichen, D., Misslin, C., Schaer, S., and Wild, U. (2011): Automated GPS Network in Switzerland (AGNES), International Foundation HFSJG, Activity Report 2011, University of Bern, 2011.
- Brockmann, E. et al. (2012): EUREF'12: Paper contributions to the EUREF-Symposium in Paris, June 6-8, 2012: «National Report of Switzerland» and «Geodetic control surveys at the Geostation Zimmerwald». swisstopo Report 12-07. Bundesamt für Landestopografie, Wabern.
- Brockmann, E., Wiederkehr, M., and Misslin, C. (2012): AGNES-Ersatzstandort Andermatt: Beurteilung des Standortes Andermatt (Gütsch) und die Beurteilung von drei Alternativstandorten, swisstopo Report 12-16. Bundesamt für Landestopografie, Wabern.
- Brockmann, E., Andrey, D., Ineichen, D., Misslin, C., Schaer, S., and Wild, U. (2012): Automated GPS Network in Switzerland (AGNES), International Foundation HFSJG, Activity Report 2012, University of Bern, 2012.
- Brockmann, E., Ineichen, D., and Schaer, S. (2013): Benefits of double stations in permanent GNSS networks. EGU2013, Vienna, 7.-12.04.2013.
- Brockmann, E., Ineichen, D., Marti, U., Schaer, S., and Schlatter, A. (2013): Determination of the Swiss Alpine Uplift using GNSS and Levelling, Poster presentation at the IAG 2013 Scientific Assembly. Potsdam, Germany, 2.-6.09.2013.
- Brockmann, E., Andrey, D., Ineichen, D., Misslin, C., Schaer, S., and Wild, U. (2013): Automated GPS Network in Switzerland (AGNES), International Foundation HFSJG, Activity Report 2013, University of Bern, 2013.
- Brockmann, E., Bock, O., Dach, R., Dick, G., Dousa, J., Hugentobler, U., and Pacione, R. (2014): Reprocessing Activities as possible contribution to GNSS4SWEC. GNSS4SWEC workshop, Munich, 25.-28.02.2014.
- Brockmann, E. et al. (2014): National Report of Switzerland. EUREF-Symposium in Vilnius, 1.-7.06.2014.
- Brockmann, E. (2014): Intercomparison of ZTD solutions: operational – reprocessed (global, continental). GNSS4SWEC workshop, Varna, 09.-13.09.2014.
- Brockmann, E. (2014): Status of the working progress in Switzerland. GNSS4SWEC workshop, Varna, 9.-13.09.2014.
- Brockmann, E. (2014): swisstopo Report for EGVAP 2014. EGVAP expert meeting, Exeter, October 2014.
- Bruyninx, C. (2004): The EUREF Permanent Network: a multi-disciplinary network serving surveyors as well as scientists, *GeoInformatics*, Vol 7, pp. 32-35.
- Bruyninx C., Habrich, H., Söhne, W., Kenyeres, A., Stangl, G., and Volksen, C. (2012): Enhancement of the EUREF Permanent Network Services and Products, "Geodesy for Planet Earth", IAG Symposia Series, Vol 136, pp. 27-35, DOI 10.1007/978-3-642-20338-1_4.
- Burkard, M. (2013): Fixpunkt-Datenservice (FPDS): Erneuerung FPDS2, Entwicklung der neuen Interfaces Export und Import. swisstopo Report 13-04. Bundesamt für Landestopografie, Wabern.

- Burkard, M. (2013): Fixpunkt-Datenservice (FPDS): Erneuerung FPDS2, Entwicklung des neuen Interfaces Bezugsrahmenwechsel LV03 → LV95. swisstopo Report 13-06. Bundesamt für Landestopografie, Wabern.
- Dach, R., Hugentobler, U., Meindl, M., and Fridez, P. (2007): The Bernese GPS Software Version 5.0, Astronomical Institute, University of Bern.
- Dach, R., Beutler, G., Jäggi, A., and Schildknecht, T. (2011): GNSS-Forschungsarbeiten am Astronomischen Institut der Universität Bern . Geomatik Schweiz, vol. 109(6), pp. 280-283.
- Dach, R., Böhm, J., Lutz, S., Steigenberger, P., and Beutler, G. (2011): Evaluation of the impact of atmospheric pressure loading modeling on GNSS data analysis. *Journal of Geodesy*, vol. 85(2), pp. 75-91, DOI 10.1007/s00190-010-0417-z.
- Dach, R., Schaer, S., Lutz, S., Meindl, M., Bock, H., Orliac, E., Prange, L., Thaller, D., Mervart, L., Jäggi, A., Beutler, G., Brockmann, E., Ineichen, D., Wiget, A., Weber, G., Habrich, H., Ihde, J., Steigenberger, P., and Hugentobler, U. (2012): Center for Orbit Determination In Europe: International GNSS Service: Technical Report 2011; edited by M. Meindl, R. Dach, and Y. Jean (AIUB), IGS Central Bureau, pp. 29-40, July 2012.
- Dach, R., Schaer, S., Lutz, S., Meindl, M., Bock, H., Orliac, E., Prange, L., Thaller, D., Mervart, L., Jäggi, A., Beutler, G., Brockmann, E., Ineichen, D., Wiget, A., Weber, G., Habrich, H., Ihde, J., Steigenberger, P., Hugentobler, U. (2013): Center for Orbit Determination In Europe: International GNSS Service: Technical Report 2012; edited by R. Dach and Y. Jean (AIUB), IGS Central Bureau, pp. 35-46, April 2013.
- Dach, R., Schaer, S., Lutz, S., Baumann, C., Bock, H., Orliac, E., Prange, L., Thaller, D., Mervart, L., Jäggi, A., Beutler, G., Brockmann, E., Ineichen, D., Wiget, A., Weber, G., Habrich, H., Söhne, W., Ihde, J., Steigenberger, P., and Hugentobler, U. (2014): Center for Orbit Determination In Europe: International GNSS Service: Technical Report 2013; edited by R. Dach and Y. Jean (AIUB), IGS Central Bureau, pp. 21-34, May 2014.
- Dow, J.M., Neilan, R.E., and Rizos, C. (2009): The International GNSS Service in a Changing Landscape of Global Navigation Satellite Systems. *Journal of Geodesy*, 83(3-4), pp. 191-198, DOI 10.1007/s00190-008-0300-3, 2009.
- Emery, P., Ray, J., and Ulrich, D. (2013): GeoSuite - Modul TRANSINT und REFRAAME. swisstopo Manual 10-d, Bundesamt für Landestopographie, Wabern.
- Fritsche, M., Rodriguez-Solano, C., Steigenberger, P., Sośnica, K., Wang, K., Dietrich, R., Hugentobler, U., Dach, R., and Rothacher, M. (2012): Joint Reprocessing of GPS, GLONASS and SLR Observations: First Results, 2012 International GNSS Workshop.
- Fritsche, M., Rodriguez-Solano, C., Steigenberger, P., Sosnica, K., Wang, K., Dietrich, R., Hugentobler, U., Dach, R., and Rothacher, M. (2013a): Impact of GLONASS in a rigorous combination with GPS, International Association of Geodesy Scientific Assembly 2013.
- Fritsche, M., Rodriguez-Solano, C., Steigenberger, P., Sosnica, K., Wang, K., Dietrich, R., Hugentobler, U., Dach, R., and Rothacher, M. (2013b): Joint Reprocessing of GPS, GLONASS and SLR, European Geoscience Union General Assembly 2013. http://www.bernese.unibe.ch/publist/2011/artproc/DOI_10.1007_s00190-010-0417-z.pdf
- Fritsche, M., Sośnica, K., Rodriguez-Solano, C., Steigenberger, P., Dietrich, R., Dach, R., Wang, K., Hugentobler, U., and Rothacher, M. (2014): Homogeneous reprocessing of GPS, GLONASS and SLR observations. *Journal of Geodesy*, vol. 88(7), pp. 625-642. DOI 10.1007/s00190-014-0710-3.

- Fujimoto, K., Scheeres, D., Herzog, J., and Schildknecht, T. (2014): Association of optical tracklets from a geosynchronous belt survey via the direct Bayesian admissible region approach. *Advances in Space Research*, 53, 2014, pp. 295-308. http://www.bernese.unibe.ch/publist/2014/artproc/DOI_10.1007_s00190-014-0710-3.pdf
- Gazeaux, J., Williams, S., King, M., Bos, M., Dach, R., Deo, M., Moore, A.W., Ostini, L., Petrie, E., Roggero, M., Teferle, F.N., Olivares, G., and Webb, F.H. (2013): Detecting offsets in GPS time series: first results from the Detection of Offsets in GPS Experiment. *J. Geophys. Res. Solid Earth*, 118, L23602, DOI 10.1002/jgrb.50152.
- Geiger, A. (2011a): Geodätische Kommission: Seit 150 Jahren relevant, *SCNAT-Info*, 2011, 19–19.
- Geiger, A. (2011b): Mehr als das Ausmessen und Abbilden der Erdoberfläche, *Geosciences actuel*, 2011, 5–7.
- Geiger, A. (2011c): Schweizerische Geodätische Kommission: 150 Jahre für die Geodäsie: Editorial, *Geomatik Schweiz*, 109, 259–259.
- Geiger, A. (2011): Editorial zum 150 Jahr Jubiläum der SGK. *Geomatik Schweiz*, Vol. 109, Issue 6, ISSN 1660-4458
- Geiger, A. (2011): Geodätische Kommission: seit 150 Jahren relevant. *SCNATinfo*, p.19, 2011.
- Geiger, A. (2014): Gefragte Fragen gefragt?, *AVN : Allgemeine Vermessungs-Nachrichten*, 02/2014.
- Gendt, G., Altamimi, Z., Dach, R., Söhne, W., and Springer, T. (2011): GGSP: Realisation and maintenance of the Galileo Terrestrial Reference Frame. *Advances in Space Research*, vol. 47(2), pp. 174-185, DOI 10.1016/j.asr.2010.02.001.
- Herzog, J., Schildknecht, T., Hinze, A., Ploner, M., and Vananti, A. (2013): Space Surveillance Observations at the AIUB Zimmerwald Observatory. *Proceedings of 6th European Conference on Space Debris*, Darmstadt, Germany.
- Ihde, J., Altamimi, Z., Brockmann, E., Bruyninx, C., Caporali, A., Dousa, J., Fernandes, R., Habrich, H., Hornik, H., Kenyeres, A., Lidberg, M., Mäkinen, J., Poutanen, M., Sacher, M., Söhne, W., Stangl, G., Torres, J., and Völksen, C. (2011): EUREF's Contribution to a National, European and Global Geodetic Infrastructure. *Proceedings of the IUGG symposium in Melbourne*, 27.06.-08.07.2011.
- Ineichen, D., and Brockmann, E. (2011): Geostation Zimmerwald: Ablotungen 2011. Messungen vom 22. August zur Bestimmung der kurzperiodischen Mastdeformationen“, *swisstopo Report 11-13*. Bundesamt für Landestopografie, Wabern.
- Ineichen, D., and Brockmann, E. (2012): Geodetic control surveys at the Geostation Zimmerwald. *EUREF-Symposium in Saint Mande, Paris*, 6.-8.06.2012.
- Ineichen, D., Brockmann, E., and Schaer, S. (2013): LPT (swisstopo) EPN analysis center and the switch to Bernese GNSS Software V5.2. *7th LAC Workshop Brussels*, 15.-16.05.2013.
- Ineichen, D., Brockmann, E., and Schaer, S. (2014): Reprocessing activities at swisstopo. *EUREF-Symposium in Vilnius*, 3.-7.06.2014.
- Ineichen, D. (2014): Auswertung von Navigationssatellitendaten, Resultate aus dem Reprocessing von bald 20 Jahren Permanentnetzdaten. *swisstopo Kolloquium 12.12.2014*. Bundesamt für Landestopografie, Wabern.
- Ineichen, D., and Brockmann, E. (2015): Geostation Zimmerwald: Einmessung 2014: Messungen vom 10.-15. November 2014 und Multiepochen-Ausgleichung 1987 - 2014“, *swisstopo Report 14-21*. Bundesamt für Landestopografie, Wabern.

- Kirchner, G., Koidl, F., Ploner, M., Lauber, P., Eckl, J., Wilkinson, M., Sherwood, R., Giessen, A., and Weigel, M. (2013): Multi-Static Laser Ranging to Space Debris Targets: Tests and Results, 18th International Workshop on Laser Ranging, Japan.
- Kistler, M., Marti, U., Ray, J., and Condamin, S. (2014): Der neue geodätische Software-Werkzeugkasten GeoSuite für Monitoraufgaben in der Ingenieurvermessung. Poster für den 17. Internationalen Ingenieurvermessungskurs 2014 - ETH Zürich.
- Kistler, M., Marti, U., Ray, J., Baumann, C., and Wiget, A. (2015): Towards a Distortion Free National Spatial Data Infrastructure in Switzerland: Approach, Developed Tools and Internet Services for the Change of the Reference Frame. Paper presented at the FIG Working week 2015 "From the Wisdom of the Ages to the Challenges of the Modern World". Sofia, Bulgaria, 17.-21.05.2015.
- Kodet, J., Schreiber, U., Plötz, C., Neidhardt, A., Kronschnabl, G., Haas, R., Calvés, M., Pogrebenko, S., Rothacher, M., Männel, B., Plank, P., and Hellerschmied, A. (2014a): Colocations of Space Geodetic Techniques on Ground and in Space; In: Behrend, D.; Bayer, K.; Armstrong, K. (eds.) IVS 2014 General Meeting Proceedings - "VGOS: The New VLBI Network", Science Press, ISBN (Online) 978-7-03-042974-2.
- Kodet, J., Männel, B., Schreiber, U., Rothacher, M., Plötz, C., Neidhardt, A., Haas, R., and Hellerschmied, A. (2014b): Colocations of Space Geodetic Techniques on Ground and in Space, European Geosciences Union 2014, Vienna, Austria, 27.04.–02.05.2014.
- Lutz, S., Beutler, G., Schaer, S., Dach, R., and Jäggi, A. (2014): CODE's new ultra-rapid orbit and ERP products for the IGS. GPS Solutions, in print. DOI: 10.1007/s10291-014-0432-2.
- Lutz, S., Steigenberger, P., Meindl, M., Beutler, G., Sosnica, K., Schaer, S., Dach, R., Arnold, D., Thaller, D., and Jäggi, A. (2015a): Impact of the arc length on GNSS analysis results. Submitted to Journal of Geodesy.
- Lutz, S., Steigenberger, P., Dach, R., Schaer, S., and Sośnica, K. (2015b): Reprocessing Activities at CODE. Swiss National Report on the Geodetic Activities in the years 2011-2015, Section 1 (Reference Frames), Swiss Geodetic Commission. This volume.
- MacLeod, K., and Agrotis, L. (2013): IGS RINEX Working Group Report 2011. International GNSS Service. Technical Report 2012, edited by Dach R and Jean Y (AIUB), IGS Central Bureau, pp. 191–194, 2013.
- Männel, B., and Rothacher, M. (2012a): Co-location in space and its impact on the geodetic reference frame for Earth observation, 10th Swiss Geoscience Meeting, 16-17.11.2012.
- Männel, B., and Rothacher, M. (2012b): Co-location of GPS, SLR and VLBI in space and its impact on the TRF, AGU Fall Meeting, 09-13.12.2012.
- Männel, B., and Rothacher, M. (2012c): Co-location of VLBI with other techniques in space: a simulation study, 7th IVS General Meeting, 04-09.03.2012.
- Männel, B., and Rothacher, M. (2013): Aspekte der Ko-lokation geodätischer Raumtechniken im Weltraum, Geodätische Woche 2013, 08-10.10.2013.
- Männel, B., Rothacher, M., Schreiber, U., and Kodet, J. (2014): GLONASS satellites simultaneously observed by VLBI, GNSS and SLR; In: Behrend, D.; Bayer, K.; Armstrong, K. (eds.) IVS 2014 General Meeting Proceedings - "VGOS: The New VLBI Network", Science Press, ISBN (Online) 978-7-03-042974-2.
- Männel, B., and Rothacher, M. (2015): Ionospheric corrections for single-frequency VLBI observations by co-located GNSS measurements, J. Geod., submitted.
- Meindl, M., Schaer, S., Dach, R., and Beutler, G. (2011): Different Reference Frame Realizations Using Data From a Global Network of Multi-GNSS Receivers. Proceedings of the 3rd International Colloquium - Scientific and Fundamental Aspects of the Galileo Programme, August 31 - September 02, Copenhagen, Denmark, 2011.

- Meindl, M. (2011): Combined Analysis of Observations from Different Global Navigation Satellite Systems. Geodätisch-geophysikalische Arbeiten in der Schweiz, vol. 83.
- Meindl, M., Beutler, G., Thaller, D., Dach, R., and Jäggi, A. (2013): Geocenter coordinates estimated from GNSS data as viewed by perturbation theory. *Advances in Space Research*, vol. 51(7), pp. 1047-1064, DOI 10.1016/j.asr.2012.10.026.
http://www.bernese.unibe.ch/publist/2013/artproc/DOI_10.1016_j.asr.2012.10.026.pdf
- Meindl, M., Beutler, G., Thaller, D., Dach, R., Schaer, S., and Jäggi, A. (2014): A comment on the article "A collinearity diagnosis of the GNSS geocenter determination" by P. Rebischung, Z. Altamimi, and T. Springer. *Journal of Geodesy*. DOI 10.1007/s00190-014-0765-1.
- Montenbruck, O., Rizos, C., Weber, R., Weber, G., Neilan, R.E., and Hugentobler, U. (2013): Getting a Grip on Multi-GNSS: The International GNSS Service MGEX Campaign, *GPS World*, 24(7), pp. 44–49, 2013.
- Müller, H.-R., Brockmann, E., Schnellmann, M., Spillmann, T., and Studer, M. (2011): Nagra's Permanent GNSS Network (NaGNet) in Northern Switzerland - Presentation of the Project and First Measurements. Workshop: Stress and deformation in the very slow deformation zone of North - West Alpine arc, Mt Ste Odile / Strasbourg, 29.05.-01.06.2011. http://www.bernese.unibe.ch/publist/2014/artproc/DOI_10.1007_s00190-014-0765-1.pdf <http://www.sgc.ethz.ch/sgc-volumes/sgk-83.pdf>
- Orliac, E., Dach, R., Voithenleitner, D., Hugentobler, U., Wang, K., Rothacher, M., and Svehla, D. (2011): Clock modeling for GNSS applications, AGU Fall Meeting 2011.
- Orliac, E., Dach, R., Wang, K., Rothacher, M., Voithenleitner, D., Hugentobler, U., Heinze, M. and Svehla, D. (2012a): Biases and Clock Modelling in the Frame of Ambiguity Resolution, 2012 International GNSS Workshop.
- Orliac, E., Dach, R., Wang, K., Rothacher, M., Voithenleitner, D., Hugentobler, U., Heinze, M. and Svehla, D. (2012b): Impact of code and phase biases and clock modelling on ambiguity resolution, AGU Fall Meeting 2012.
- Orliac, E., Dach, R., Wang, K., Rothacher, M., Voithenleitner, D., Hugentobler, U., Heinze, M., and Svehla, D. (2012c): Deterministic and stochastic receiver clock modeling in precise point positioning, EGU General Assembly 2012.
- Orliac, E., Dach, R., Wang, K., Rothacher, M., Hugentobler, U., and Svehla, D. (2013): Satellite Clock Modelling
- Ostini, L. (2012): Analysis and Quality Assessment of GNSS-Derived Parameter Time Series. PhD thesis of the Philosophisch--naturwissenschaftlichen Fakultät of the University of Bern.
- Perler, D., Hurter, F., Brockmann, E., Leuenberger, D., Ruffieux, D., Geiger, A., and Rothacher, M. (2010): GNSS meteorology: Activities in Switzerland. Paper presented at the COST Action ES0702 EG-CLIMET meeting 16.-19.11.2010, Cologne, Germany.
- Petit, G., and Luzum B. (Eds) (2010): IERS Conventions 2010. IERS Technical Note 36, Bundesamt für Kartographie und Geodäsie, Frankfurt am Main.
- Plag, H.-P., Gross, R. S., Miller, N. L., Rothacher, M., Zerbini, S., and Rizos, C. (2011): IGCP 565 Project: Developing the Global Geodetic Observing System into a monitoring system for the global water cycle. In Fried, J. and Scherfig, J., International Conference on Water Scarcity, Global Changes, and Groundwater Management Responses, December 2008, University of California, Irvine, United States, Proceedings, 953-972. The Urban Water Research Center, University of Irvine, Irvine, CA, United States.
- Ploner, M., Jäggi, A., and Utzinger, J. (2012): Skyguide and Flarm - 2 in-sky-laser-safety systems used at Zimmerwald. *Mitteilungen des Bundesamtes fuer Kartographie und Geodäsie Band 48*, "Proceedings of the 17th International Workshop on Laser Ranging, Extending the Range", May 16-20, 2011 Bad Koetzing, Germany; vol. 48, pp. 245-247; ISSN 1436-3445; ISBN 978-3-89888-999-5.

- Ploner, M., Jäggi, A., Lauber, P., Prohaska, M., Schildknecht, T., and Utzinger, J. (2012): SLR Tracking of GNSS Constellations at Zimmerwald. Proceedings of the International Technical Laser Workshop 2012 (ITLW-12), Frascati (Rome), Italy, November 5-9, 2012.
- Ploner, M., Utzinger, J., Lauber, P., Prohaska, M., Schlatter, P., Ruzek, P., Schildknecht, T., Sosnica, K., and Jäggi, A. (2013): Status of the Zimmerwald SLR station, 18th International Workshop on Laser Ranging, Japan.
- Ploner, M., Utzinger, J., Lauber, P., Prohaska, M., Schlatter, P., Ruzek, P., Schildknecht, T., Sośnica, K., and Jäggi, A. (2014): Status of the Zimmerwald SLR station. Proceedings of the 18th International Workshop on Laser Ranging, 11-15 November 2013 Fujiyoshida, Japan.
<http://www.bernese.unibe.ch/publist/2014/artproc/13-Po43-Ploner.pdf>
- Ploner, M., Lauber, P., Prohaska, M., Schlatter, P., Utzinger, J., Schildknecht, T., Jäggi, A. (2014): The new CMOS Tracking Camera used at the Zimmerwald Observatory. Proceedings of the 18th International Workshop on Laser Ranging, 11.-15.11.2013 Fujiyoshida, Japan.
<http://www.bernese.unibe.ch/publist/2014/artproc/13-04-21-Ploner.pdf>
- Ploner, M., Utzinger, J., Lauber, P., Prohaska, M., Schlatter, P., Ruzek, P., Schildknecht, T., Sośnica, K., and Jäggi, A. (2014): Status of the Zimmerwald SLR station. Proceedings of the 18th International Workshop on Laser Ranging, 11.-15.11.2013 Fujiyoshida, Japan.
<http://www.bernese.unibe.ch/publist/2014/artproc/13-Po43-Ploner.pdf>
- Ploner, M., Lauber, P., Prohaska, M., Ruzek, P., Schildknecht, T., and Jäggi, A. (2015): History of the Laser Observations at Zimmerwald. Proceedings of the 19th International Workshop on Laser Ranging, Celebrating 50 Year of SLR: Remembering the Past and Planning for the Future, October 27-31, 2014, Annapolis, Maryland, USA.
- Prange L., Dach R, Lutz S, Schaer S, and Jäggi, A. (2014). The CODE MGEX orbit and clock solution. In: Willis, P. (Ed.), IAG Potsdam 2013 Proceedings. International Association of Geodesy Symposia. Springer, accepted for publication.
- Prange, L., Orliac, E., Dach, R., Schaer, S., Sośnica, K. (2015): CODE five system solution for IGS MGEX. This volume.
- Ray, J. (2012): REFRAME plug-in for FME 2.4. swisstopo Manual. Bundesamt für Landestopografie, Wabern.
- Ray, J. (2012): TRANSINT .NET / COM library - Developer's manual. swisstopo Report 12-15. Bundesamt für Landestopografie, Wabern. <http://www.bernese.unibe.ch/publist/2014/artproc/13-04-21-Ploner.pdf>
- Raziq, N., El-Mowafy, A., Teunissen, P.J.G., Nardo, A., and van der Marel, H. (2012): Curtin and Delft Multi-GNSS M-GEX Stations: Infrastructure and Analysis Tools, IGS Workshop, Olsztyn, Poland, July 23-27, 2012.
http://www.lnf.infn.it/conference/laser2012/3wednesday/6_ploner/ploner_1.pdf
- Rodriguez-Solano, C. J., Hugentobler, U., Steigenberger, P., and Lutz, S. (2012): Impact of Earth radiation pressure on GPS position estimates. Journal of Geodesy, DOI 10.1007/s00190-011-0517-4.
- Rodriguez-Solano, C.J., Hugentobler, U., and Steigenberger, P. (2012): Impact of albedo radiation on GPS satellites; in: Kenyon, S. C.; Pacino, M. C.; Marti, U. J. (Eds.) Geodesy for Planet Earth, IAG Symposia, Vol. 136, pp 113-119, Springer, ISBN (Print) 978-3-642-20337-4, ISBN (Online) 978-3-642-20338-1, ISSN 0939-9585, DOI 10.1007/978-3-642-20338-1_14.
- Rodriguez-Solano, C.J., Hugentobler, U., Steigenberger, P., Blossfeld, M., Fritsche, M. (2014): Reducing the draconitic errors in GNSS geodetic products. J Geod 88:559-574. DOI 10.1007/s00190-014-0704-1.

- Rothacher, M., Angermann, D., Artz, T., Bosch, W., Drewes, H., Böckmann, S., Gerstl, M., Kelm, R., König, D., König, R., Meisel, B., Müller, H., Nothnagel, A., Panafidina, N., Richter, B., Rudenko, S., Schwegmann, W., Seitz, M., Steigenberger, P., Tesmer, V., and Thaller, D. (2011): GGOS–D: Homogeneous Reprocessing and Rigorous Combination of Space Geodetic Observations, *Journal of Geodesy*, Volume 85, Issue 10, pp. 679-705, DOI: 10.1007/s00190-011-0475-x.
- Rothacher, M. (2011): Die Höhere Geodäsie am IGP ETHZ: Zukünftige Entwicklungen am GGL, *Geomatik Schweiz*, 2011, 290–292.
- Rothacher, M., Drewes, H., and Hornik, H. (2011a): Coordination of Space Techniques, IUGG General Assembly.
- Rothacher, M. et al. (2011b): GGOS-D: Homogeneous reprocessing and rigorous combination of space geodetic observations, *Journal of geodesy*, 50, 679–705, doi:10.1007/s00190-011-0475-x.
- Rothacher, M., Neilan, R., Plag, H.-P., Drewes, H., and Hornik, H. (2011c): Global Geodetic Observing System (GGOS), IUGG General Assembly.
- Rothacher, M. (2012a): GNSS – mehr als Navigation und Positionierung, European Satellite Navigation Competition (ESNC) 2012, Kick-Off Meeting.
- Rothacher, M. (2012c): The Interactions between IGS and GGOS, 2012 IGS Workshop.
- Rothacher, M. (2013): Globaler Wandel, GGOS und GEOSS, *zfv*, Vol. 138, Nr. 1, pp. 16-20, ISSN 1618-8950.
- Rothacher, M., and Geiger, A. (2013): Professur für Mathematische und Physikalische Geodäsie, *Geomatik Schweiz*, 01/2013, pp. 5-6.
- Rothacher, M., and Grêt-Regamey, A. (2013): Die Studiengänge im Bereich Geomatik und Planung, *Geomatik Schweiz*, 01/2013, pp. 18-20.
- Rothacher, M., and Grêt-Regamey, A. (2013): Les filières proposées en Géomatique et Aménagement, *Geomatik Schweiz*, 01/2013, pp. 22-23.
- Salvini, D., Studer, M., Müller, H., Spillmann, T., Schnellmann, M., and Brockmann, E. (2011): Ein permanentes GNSS-Netz zur Aufzeichnung tektonischer Bewegungen In der Nordschweiz. *Swiss Geoscience Meeting*, Zürich, 12.11.2011.
- Schaer, S., Brockmann, E., Meindl, M., and Beutler, G. (2010): Rapid Static Positioning Using GPS and GLONASS.. In: *Bulletin of Geodesy and Geomatics BGG*, LXIX, 2-3, 2010, Instituto Geografico Militare, Firenze, pp 179-193.
- Schaer, S., and Meindl, M. (2011): Consideration of Station-Specific Intersystem Translation Parameters at CODE. Subcommission for the European Reference Frame (EUREF), Chisinau, 25.-28.05.2011.
- Schaer, S. (2013): Activities of IGS and Bias Calibration Working Group. *International GNSS Service Technical Report 2012*; edited by R. Dach and Y. Jean (AIUB), IGS Central Bureau, pp. 149-152, April 2013.
- Schaer, S. (2015): Ambiguity Resolution for GLONASS. This volume.
- Schildknecht, T., Herzog, J., Vananti, A., Ploner, M., and Fletcher, E. (2013): Coordinated Optical GEO Survey for European SSA Precursor Services. *Proceedings of AMOS Conference*, Maui, Hawaii.
- Schlatter, A. (2011): LV95 / CHTRF2010 (Swiss Terrestrial Reference Frame 2010): Teil 1: Messkonzept und Messkampagnen April – Oktober 2010 im GPS-Landesnetz LV95. *swisstopo Report 10-24*. Bundesamt für Landestopografie, Wabern.
- Schlatter, A., Brockmann, E., Ineichen, D., and Schaer, S. (2011): Dritte Wiederholungsmessung im GNSS-Landesnetz LV95, Messkampagne und erste Resultate. *swisstopo Kolloquium 1*. April 2011. Bundesamt für Landestopografie, Wabern.
- Schlatter, A. (2013a): NEOTEKTONIK 2011: Neotektonische Untersuchungen in der Nordschweiz und in Südwestdeutschland aufgrund kinematischer Ausgleichungen wiederholter Präzisionsnivelements. *swisstopo Report 12-13*. Bundesamt für Landestopografie, Wabern.

- Schlatter, A. (2013b): NEOTEK2011: Zusätzliche Profile im Untersuchungsgebiet und Höhenänderungen im zentralen Alpenraum. swisstopo Report 13-17. Bundesamt für Landestopografie, Wabern.
- Schlatter, A., and Imboden, C. (2015): Hauenstein-Basistunnel: Präzisionsnivellement 2014 (Messung G) und Deformationsanalyse 1986 – 2014. swisstopo Report 14-22. Bundesamt für Landestopografie, Wabern.
- Silha, J., Schildknecht, T., Hinze, A., Ploner, M., and Vananti, A. (2014): Additional optical surveys for space debris on highly eccentric and inclined MEO orbits. Proceedings of 65th International Astronautical Congress, Toronto, Canada.
- Sośnica, K., Thaller, D., Dach, R., Jäggi, A., and Beutler, G. (2012): Availability of SLR Normal Points at ILRS Data Centers Mitteilungen des Bundesamtes fuer Kartographie und Geodäsie Band 48, "Proceedings of the 17th International Workshop on Laser Ranging, Extending the Range", May 16-20, 2011 Bad Koetzing, Germany; vol. 48, pp. 365-368; ISSN 1436-3445; ISBN 978-3-89888-999-5
http://www.bernese.unibe.ch/publist/2012/artproc/proceedings_sosnica.pdf.
- Sośnica, K., Thaller, D., Dach, R., Jäggi, A., and Beutler, G. (2013): Impact of loading displacements on SLR-derived parameters and on the consistency between GNSS and SLR results. Journal of Geodesy, vol. 87(8), pp. 751-769, ISSN 0949-7714, DOI 10.1007/s00190-013-0644-1.
http://www.bernese.unibe.ch/publist/2013/artproc/DOI_10.1007_s00190-013-0644-1.pdf
- Sośnica, K., Jäggi, A., Thaller, D., Dach, R., Beutler, G., and Baumann, C. (2014): SLR-derived terrestrial reference frame using the observations to LAGEOS-1/2, Starlette, Stella, and AJISAI. Proceedings of the 18th International Workshop on Laser Ranging, Fujiyoshida, Japan.
http://www.bernese.unibe.ch/publist/2014/artproc/13-01-14_Sosnica_Proceedings.pdf.
- Sośnica, K., Jäggi, A., Thaller, D., Dach, R., and Beutler, G. (2014): Contribution of Starlette, Stella, and AJISAI to the SLR-derived global reference frame. Journal of Geodesy, vol. 88(8), pp. 789-804. DOI 10.1007/s00190-014-0722-z.
- Sośnica, K., Baumann, C., Thaller, D., Jäggi, A., and Dach, R. (2014): Combined LARES-LAGEOS Solutions. Proceedings of the 18th International Workshop on Laser Ranging, Fujiyoshida, Japan.
http://www.bernese.unibe.ch/publist/2014/artproc/13-Po-57_Sosnica_Proceedings.pdf.
- Sośnica, K., Rodriguez-Solano, C.J., Thaller, D., Jäggi, A., Dach, R., Beutler, G. (2014): Impact of Earth Radiation Pressure on LAGEOS Orbits and on the Global Scale. Proceedings of the 18th International Workshop on Laser Ranging, Fujiyoshida, Japan.
- Sośnica, K., Jäggi, A., Thaller, D., Dach, R., and Meyer, U. (2015): Earth Rotation and Gravity Field Parameters from Satellite Laser Ranging. Proceedings of the 19th International Workshop on Laser Ranging, Celebrating 50 Year of SLR: Remembering the Past and Planning for the Future, October 27-31, 2014, Annapolis, Maryland, USA. http://www.bernese.unibe.ch/publist/2015/artproc/Sosnica_3072.pdf
- Sośnica, K., Dach, R., Thaller, D., Jäggi, A., Beutler, G., and Arnold, D. (2015): Processing 20 years of SLR observations to GNSS satellites. Proceedings of the 19th International Workshop on Laser Ranging, Celebrating 50 Year of SLR: Remembering the Past and Planning for the Future, October 27-31, 2014, Annapolis, Maryland, USA. http://www.bernese.unibe.ch/publist/2015/artproc/Sosnica_3070.pdf
- Sośnica, K. (2015): Determination of Precise Satellite Orbits and Geodetic Parameters using Satellite Laser Ranging. Geodätisch-geophysikalische Arbeiten in der Schweiz, vol. 93.
- Sośnica, K., Thaller, D., Dach, R., Steigenberger, P., Beutler, G., Arnold, D., and Jäggi, A. (2015): Satellite Laser Ranging to GPS and GLONASS. J Geod, accepted for publication.
- Springer, T.A., Beutler, G., and Rothacher, M. (1999): A new solar radiation pressure model for GPS satellites. GPS Sol 3(2): 50–62.

- Springer, T. (2010): <http://www.positum.com/napeos.html>.
- Steigenberger, P., Lutz, S., Dach, R., and Hugentobler, U. (2011): CODE Contribution to the First IGS Reprocessing Campaign. Technical Report, http://www.bernese.unibe.ch/publist/2011/artproc/CODE_Repro1.pdf.
- Steigenberger, P., Hugentobler, U., Loyer, S., Perosanz, F., Prange, L., Dach, R., Uhlemann, M., Gendt, and G., Montenbruck, O. (2014): Galileo Orbit and Clock Quality of the IGS Multi-GNSS Experiment. *Advances in Space Research*. DOI 10.1016/j.asr.2014.06.030.
- Thaller, D., Dach, R., Seitz, M., Beutler, G., Mareyen, M., and Richter, B. (2011): Combination of GNSS and SLR observations using satellite co-locations. *Journal of Geodesy*, vol. 85(5), pp. 257-272, DOI 10.1007/s00190-010-0433-z.
http://www.bernese.unibe.ch/publist/2014/artproc/DOI_10.1016_j.asr.2014.06.030.pdf
- Thaller D., Sošnica, K., Dach, R., Jäggi, A., and Beutler, G. (2012): LAGEOS-ETALON solutions using the Bernese Software Mitteilungen des Bundesamtes fuer Kartographie und Geodäsie Band 48, "Proceedings of the 17th International Workshop on Laser Ranging, Extending the Range", May 16-20, 2011 Bad Koetzing, Germany; vol. 48, pp. 333-336; ISSN 1436-3445; ISBN 978-3-89888-999-5.
http://www.bernese.unibe.ch/publist/2012/artproc/proceedings_thaller_lageos.pdf.
- Thaller D., Sošnica, K., Dach, R., Jäggi, A., Mareyen, M., Richter, B., and Beutler, G. (2012): GNSS satellites as co-locations for a combined GNSS and SLR analysis Mitteilungen des Bundesamtes fuer Kartographie und Geodäsie Band 48, "Proceedings of the 17th International Workshop on Laser Ranging, Extending the Range", May 16-20, 2011 Bad Koetzing, Germany; vol. 48, pp. 82-86; ISSN 1436-3445; ISBN 978-3-89888-999-5. http://www.bernese.unibe.ch/publist/2012/artproc/proceedings_thaller_slr-gnss.pdf.
- Thaller, D., Sošnica, K., Dach, R., Jäggi, A., Baumann, C. (2012): SLR residuals to GPS / GLONASS and combined GNSS-SLR analysis. Proceedings of the International Technical Laser Workshop 2012 (ITLW-12), Frascati (Rome), Italy, November 5-9, 2012.
http://www.lnf.infn.it/conference/laser2012/3wednesday/11_thaller/thaller_1.pdf
- Thaller, D., Sošnica, K., Dach, R., Jäggi, A., and Baumann, C. (2012): The space tie between GNSS and SLR. Proceedings of the International Technical Laser Workshop 2012 (ITLW-12), Frascati (Rome), Italy, November 5-9, 2012. http://www.lnf.infn.it/conference/laser2012/2tuesday/3_4_9thaller/thaller_1.pdf
- Thaller, D., Sošnica, K., Dach, R., Jäggi, A., Beutler, G., Mareyen, M., and Richter, B. (2014): Geocenter coordinates from GNSS and combined GNSS-SLR solutions using satellite co-locations. *Earth on the Edge: Science for a Sustainable Planet, International Association of Geodesy Symposia*, vol. 139, 2014, pp. 129-134, DOI 10.1007/978-3-642-37222-3_16.
http://www.bernese.unibe.ch/publist/2014/artproc/DOI_10.1007_978-3-642-37222-3_16.pdf
- Thaller, D., Roggenbuck, O., Sošnica, K., Steigenberger, P., Mareyen, M., Baumann, C., Dach, R., and Jäggi, A. (2014): SLR-GNSS analysis in the framework of the ITRF2013 computation. Proceedings of the 18th International Workshop on Laser Ranging, Fujiyoshida, Japan.
<http://www.bernese.unibe.ch/publist/2014/artproc/13-01-05-Thaller.pdf>.
- Villiger, A., Marti, U., Brockmann, E., and Geiger, A. (2011): SWISS 4D. Determination and modeling of the tectonic deformation field of Switzerland. Poster presentation on the IUGG symposium in Melbourne, 27.06.-08.07.2011.
- Vogel, B., and Gutknecht, D. (2013): Landesgrenze. Nachführungskonzept. swisstopo Report 13-03. Bundesamt für Landestopografie, Wabern.
- Vogel, B., Schlatter, A., Scherrer, M., and Wiget, A. (2014): Fixpunkte und ihre Bedeutung. swisstopo Kolloquium 10. Januar 2014. Bundesamt für Landestopografie, Wabern.

- Wang, K., and Rothacher, M. (2011a): GNSS Clock Modelling and Estimation, XXV General Assembly of the International Union of Geodesy and Geophysics.
- Wang, K., and Rothacher, M. (2011b): Positioning improvements with stochastic clock modelling, 9th Swiss Geoscience Meeting.
- Wang, K., Rothacher, M., and Svehla, D. (2012): Kinematic positioning improvements with stochastic clock modelling, European Frequency and Time Forum (EFTF 2012).
- Wang, K., and Rothacher, M. (2013c): Stochastic modeling of high-performance GNSS satellite clocks and its impact on kinematic GNSS orbits, International Association of Geodesy Scientific Assembly 2013.
- Wang, K., and Rothacher, M. (2013d): Stochastic modeling of high-stability ground clocks in GPS analysis, *Journal of Geodesy*, 87, 427–437, doi:10.1007/s00190-013-0616-5.
- Wiget, A., Brockmann, E., Kistler, M., Marti, U., Schlatter, A., Vogel, B., and Wild, U. (2010): Nachführungskonzept für die geodätische Landesvermessung (in German and French). swisstopo Report 09-14. Bundesamt für Landestopografie, Wabern.
- Wiget, A., Brockmann, E., Kistler, M., Marti, U., Schlatter, A., Vogel, B., and Wild, U. (2011a): Das Landesvermessungswerk 1995 (LVW95). *Geomatik Schweiz* 6/2011: 270-279.
- Wiget, A., Brockmann, E., Kistler, M., Marti, U., and Wild, U. (2011b): Minimale Geodatenmodelle der Geodäsie. Beschreibung der Geodatenmodelle für die Georeferenzdaten des Bereiches Geodäsie (in German and French). swisstopo Report 10-06. Bundesamt für Landestopografie, Wabern.
- Wiget, A., Brockmann, E., Vogel, B., Wild, U., and Kistler, M. (2011c): Qualitätsstandards der Landesvermessung: Indikatoren, Standards und Messgrößen für die Produkte der geodätischen Landesvermessung (in German and French). swisstopo Report 10-11. Bundesamt für Landestopografie, Wabern.
- Wiget, A., Brockmann, E., Ineichen, D., Kistler, M., and Marti, U. (2011d): Stability of the Swiss terrestrial reference frame CHTRF. Poster presentation on the IUGG Symposium in Melbourne, June 27 – July 08, 2011.
- Wiget, A. (2012a): Bezugsrahmenwechsel LV03 → LV95. Grundlagen für ein Kommunikationskonzept (in German and French). swisstopo Report 11-14. Bundesamt für Landestopografie, Wabern.
- Wiget, A. (2012b): Neue Koordinaten für die Schweiz. Der Bezugsrahmenwechsel: Was müssen Vermessungs- und GIS-Fachleute wissen? *Geomatik Schweiz* 8/2012: 405-406.
- Wiget, A. (2012c): Der Fundamentalpunkt der neuen Landesvermessung LV95. Fachtagung „200 Jahre Fundamentalpunkt Bern“. Astronomisches Institut der Universität Bern (AIUB), Bundesamt für Landestopografie swisstopo, Schweizerische Geodätische Kommission (SGK), Gesellschaft für die Geschichte der Geodäsie in der Schweiz (GGGS) und Schweizerische Gesellschaft für Kartografie (SGK). Universität Bern, 20. Oktober 2012.
- Wiget, A., and Wicht, A. (2012): Landesgrenze Schweiz – Deutschland im Hochrhein und Untersee: Bestimmung gemeinsamer Koordinaten in ETRS89. swisstopo Report 12-12. Bundesamt für Landestopografie, Wabern.
- Wiget, A. (2014): Neue Koordinaten für die Schweiz: Grundsätze der Kommunikation; Aktivitäten der Bundesstellen. Nationaler Erfahrungsaustausch zum Bezugsrahmenwechsel. Olten, 1. April 2014.
- Wiget, A., Brockmann, E., Kistler, M., Schlatter, A., and Wild, U. (2014): Strategie Geodäsie 2015 – 2019. Strategisches Management des Bereiches Geodäsie 2015 – 2019. swisstopo Report 14-04. Bundesamt für Landestopografie, Wabern.

http://www.bernese.unibe.ch/publist/2011/artproc/DOI_10.1007_s00190-010-0433-z.pdf

2 Gravity Field

Absolute and Relative Gravity Measurements

U. Marti¹, H. Baumann², B. Bürki³ and S. Guillaume³

¹ *Federal Office of Topography, swisstopo*

² *Federal Institute of Metrology METAS*

³ *Geodesy and Geodynamics Lab, Institute of Geodesy and Photogrammetry, ETH Zurich*

The national gravity network SG95 (Schweregrundnetz 1995) was established between 1992 and 1995 by the Geodesy and Geodynamics Lab (GGL) of the ETH Zurich on behalf of the Swiss Geodetic Commission (SGC) and the Swiss Geophysical Commission (SGPC). It was based on absolute measurements on five stations (Zurich, Pratteln, Chur, Lausanne, Monte Ceneri), which have been observed with the JILA-G 6 of the BEV (Vienna) in 1994. This zero-order network was densified by relative measurements on about 110 stations, which formed the first and second order network. Mostly, these relative stations are identical with the principal stations of the national GPS network (LV95). SG95 was connected to the gravity networks of neighbouring countries by a few relative measurements to their nearest absolute stations. The relative observations have been performed with three Lacoste&Romberg G instruments in parallel. The accuracy of the adjusted gravity values of SG95 was in the order of 0.02 mgal. The measurements of SG95 were the contribution of Switzerland to the Unified European Gravity Network (UEGN).

In 2003, the project LSN2004 (Landesschwerenetz 2004) was started to modernize the national gravity Network. In this project, some new absolute stations were established and the existing ones were re-measured with an FG5. These activities were jointly performed by swisstopo and METAS. Additional relative measurements were performed with a SCINTREX-CG5 in order to improve the accuracy and stability of the network. The stations of LSN2004 are mostly the same as the ones in SG95. Only some destroyed or unsuitable stations have been replaced.

Since 1999, the Federal Institute of Metrology (Metas) owns the only absolute gravimeter in Switzerland. This FG-5 free fall instrument was acquired for their Watt balance experiment (redefinition of the SI-unit 'kilogram') and is principally used in the laboratories of METAS, where about once per month absolute measurements are performed. This instrument participates regularly at the international comparison campaigns. The last of these comparisons were the European campaign ECAG-2011 and the International campaign with 27 gravimeters (ICAG 2013) which took place both in Walferdange (Luxemburg).

Since 2003, a yearly absolute measurement takes place at the ECGN station in Zimmerwald where a permanent Earth-tide gravimeter is installed as well and regular relative measurements take place. In addition to the measurements in Zimmerwald measurements for LSN2004 are performed on 1-2 additional stations per year. Due to several problems with the FG5 in the period of 2011 to 2014 only in 2013 measurements for the LSN could be performed in Zimmerwald (see Figure 2.1), Basel and Chur. The results of these measurements were all published in the AGRAV database of BGI and BKG and are freely accessible. It is foreseen to repeat the absolute measurements on all stations in an interval of 10 years. Further absolute measurements in Switzerland took place in October 2013 on the calibration line Interlaken - Jungfrauoch (see separate report).

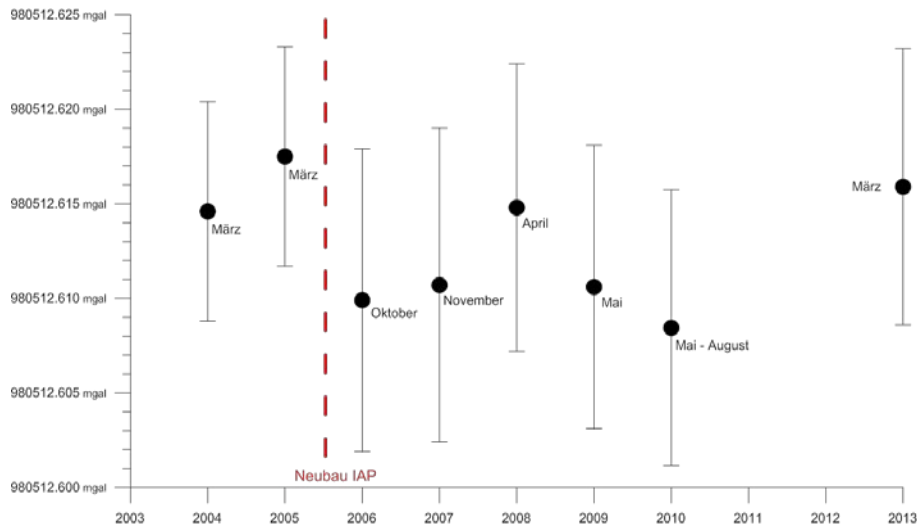


Figure 2.1: Repeatability of absolute gravity measurements in Zimmerwald

The absolute gravity network (0 order network) is densified by relative measurements (1st and 2nd order network). These stations - most of them are already included in SG95 - are observed regularly since 2005. The aim is to improve the accuracy and reliability of these stations. Per year, around 10 days of field measurements are carried out. All absolute and relative observations since 1992 are treated in one common adjustment. The resulting accuracy is usually better than 0.008 mGal.

National Gravity Network LSN2004

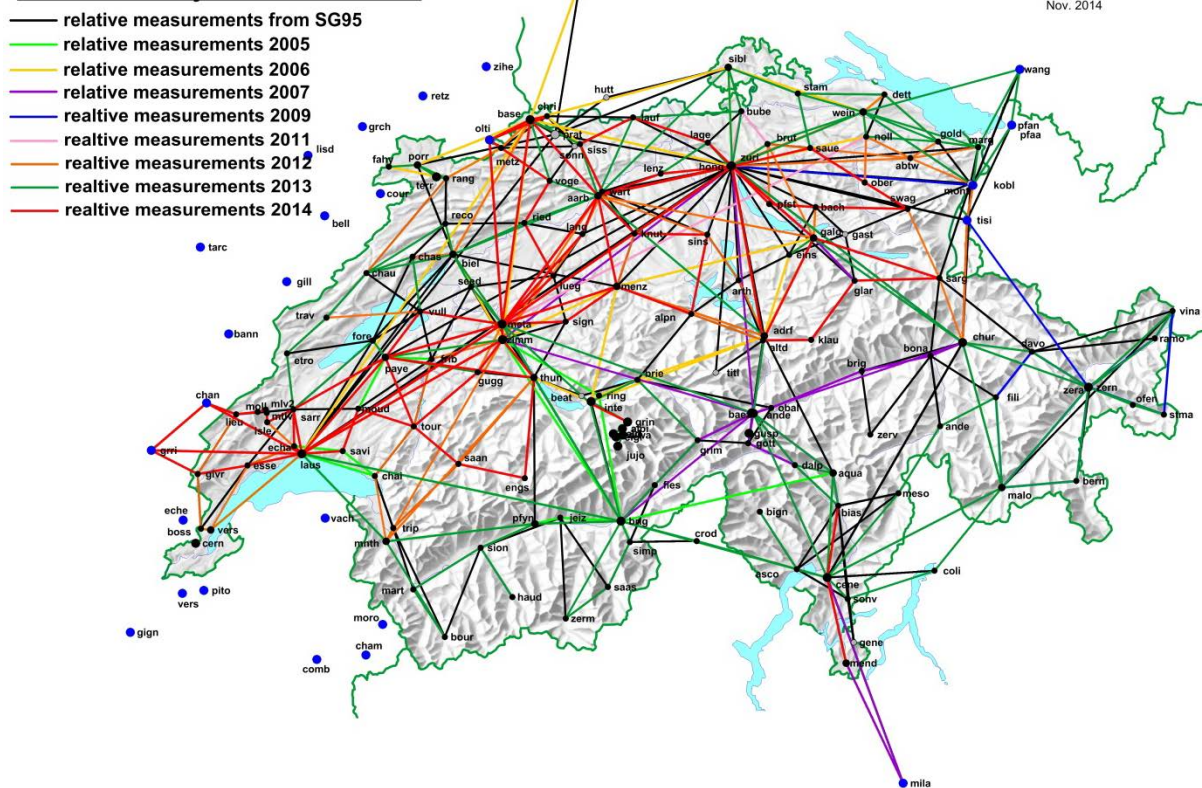


Figure 2.2: Relative Measurements for LSN2004

Gravimetric Calibration Line Interlaken-Jungfrauoch

U. Marti¹, B. Bürki² and H. Baumann³

¹ Federal Office of Topography, swisstopo

² Geodesy and Geodynamics Lab, Institute of Geodesy and Photogrammetry, ETH Zurich

³ Federal Institute of Metrology METAS

In order to determine scale factors of relative gravimeters it is usually necessary to calibrate these instruments regularly on points with known gravity values. Especially well suited are points with absolute measurements and with large gravity differences. Since 2009, the renewal of the existing calibration line from 1980 between Interlaken (altitude 570 m) and Jungfrauoch (altitude 3500 m) is under way. This line consists of 7 absolute stations and several eccentric points. The total gravity difference is more than 600 mGal. All absolute stations are easily accessible by car or are located in immediate vicinity of a station of the Jungfrau railway. Therefore, it is possible to measure the whole line with relative instruments in a closed loop in one day. The absolute stations have been chosen in a way that they are accessible during the whole year and that the gravity difference between two neighboring stations does not exceed 150 mGal. So, it is possible to calibrate as well gravimeters with a limited measuring range or with a non-linear scale factor. The expanded uncertainties ($k=2$) of the gravity values at the absolute stations are varying between 5 and 6 μGal . All vertical gravity gradients have been determined by relative measurements on three levels above the marker. The newly established calibration line is free to be used by the whole gravity community and we hope that many institutions will profit.

2 of the absolute stations (Grindelwald and Alpighen) have been observed already in 2010. 4 further stations (Kleine Scheidegg, Eigergletscher, Eigerwand and Jungfrauoch) have been observed in October 2013 with the upgraded FG5x of METAS. The foreseen station in Interlaken could, due to several problems with the site and the instrument, could not be observed until now. Besides of the absolute stations, some eccenters for relative measurements form part of the network. Whenever possible, the still existing points of the measurements of 1980 have been selected. All points are documented in the national database of geodetic reference markers.

On all absolute stations approximately 24 sets with 100 drops each were observed and corrected for the influence of the variable components such as Earth tides, ocean loading, atmospheric pressure and polar motion. On the occasion of the absolute measurements the VGG was determined by observations on 3 levels (about 40, 80 and 130 cm above the marker). The measurements and results are documented in the global database for absolute measurements AGrav (agrav.bkg.bund.de).

In parallel to the absolute measurements, a first campaign with relative gravimeters took place in October 2013. The following 3 instruments were used: A Scintrex CG-5 of swisstopo/ETHZ on all absolute and relative stations, the ZLS Burris B-78 from BAdW on the absolute stations and a few selected eccenters and a LCR type G meter (G-87) with a digital feedback system of DGFI who measured always in parallel with the ZLS instrument. Theoretically, the whole calibration line can be measured in one day, but in order to increase accuracy and reliability, it is better to invest at least 2 days. In our case we did the measurements in 3 days and each station has been visited at least on 2 days with each instrument.

The evaluation of the daily solutions of the relative measurements showed a repeatability of the CG-5 in the order of ± 0.03 mGal. This value seems to be a little higher than other measurements with this instrument but is explainable by some remaining hysteresis effects. The residuals of the ZLS Burris daily solutions are smaller (± 0.015 mGal) and the ones of the LCR are in the order of 0.03 mGal.

In a next step, the results of the complete solutions for each instrument were compared among each other and plotted with respect to the absolute measurements. For the LCR and ZLS two solutions from swisstopo and BAdW are available with independent software and different approaches for drift modeling. These 2 solutions agree in general better than 20 μGal . The result is shown in Figure 2.3. The large residuals of the LCR measurements are clearly visible. They go from -97 μGal in Alpighen to +125 μGal at Jungfrauoch and show a rather linear behavior with respect to the absolute gravity value. This indicates, that the scale factor of this instrument has to be improved. The results of the other 2 instruments (CG-5 and ZLS) are in rather good agreement of about ± 20 μGal with the absolute measurement. An obvious scale is not visible. There, the ZLS measurements show an offset of about -160 μGal towards the absolute and the CG-5 measurements, although their daily solutions are in good agreement. One possible explanation could eventually be found in a problem of the calibration table of the instrument.

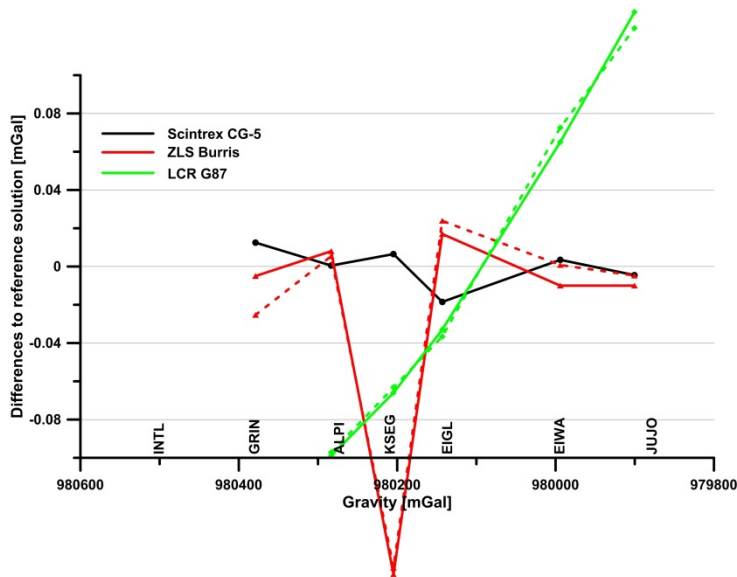


Figure 2.3: Comparison of the solutions of each instrument. Differences to the absolute measurements. Dashed lines indicate alternative evaluations by BADW

Finally, we computed an overall-adjustment of all absolute and relative measurements together and estimated one linear scale factor for each relative instrument. The found scale factors are -14 ± 10 ppm for the CG-5, -74 ± 23 ppm for the ZLS and $+568 \pm 61$ ppm for the LCR. Whereas for CG-5 and ZLS these factors are almost negligible, for the LCR it is highly significant and has to be considered. In this adjustment, the absolute measurements got some residuals as well (see Figure 2.4). They are in the range from $-10 \mu\text{Gal}$ (Grindelwald) to $+7 \mu\text{Gal}$ (Eigerletscher). This is significantly larger than the claimed accuracies and indicate some systematic differences between absolute and relative measurements.

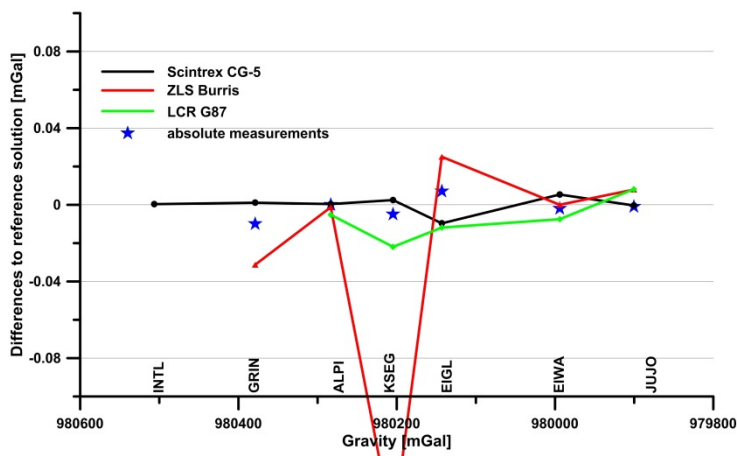


Figure 2.4: Comparison of the results of the relative measurements of each instrument and the absolute measurements after applying a constant scale factor for each relative gravimeter. Differences to the overall-adjustment.

Gravity Measurements for the Vertical Network

U. Marti¹ and A. Schlatter¹

¹ Federal Office of Topography, swisstopo

The gravity measurements for the vertical network along the first and second order leveling lines are usually performed in the same year as the leveling measurements. They are used for the calculation of geopotential numbers and orthometric heights and are only performed on a representative selection of all leveling points. For stations without measured gravity, the values are interpolated from the neighboring data on leveling lines or from the gravity data set of the Swiss Geophysical Commission and mass models with an accuracy of better than 1 mgal, which usually is enough for the correction of the leveling data.

Until 2007, a Lacoste&Romberg type G gravimeter was used for these observations. In 2008, ETH Zurich and swisstopo acquired a Scintrex CG-5 which had some problems in the beginning and could not be used until 2010 productively. The first gravity campaigns along the leveling lines could be performed in 2011, when a big part of the delay along the leveling lines of 2008-2010 could be caught up. Since then, the CG-5 is used routinely and more than 900 points have been measured between 2011 and 2014. All these measurements are documented in the national database of the reference benchmarks (FPDS).

It is to be mentioned that in the end of 2013 and in the beginning of 2014 it was possible to make gravity measurements on the whole length the new Gotthard base tunnel (57 km). Usually, the distance between the points was 900 meters. Only in the regions of the portals, the distance was reduced to 300 meters. It took 4 days on e-bikes to measure around 80 points.

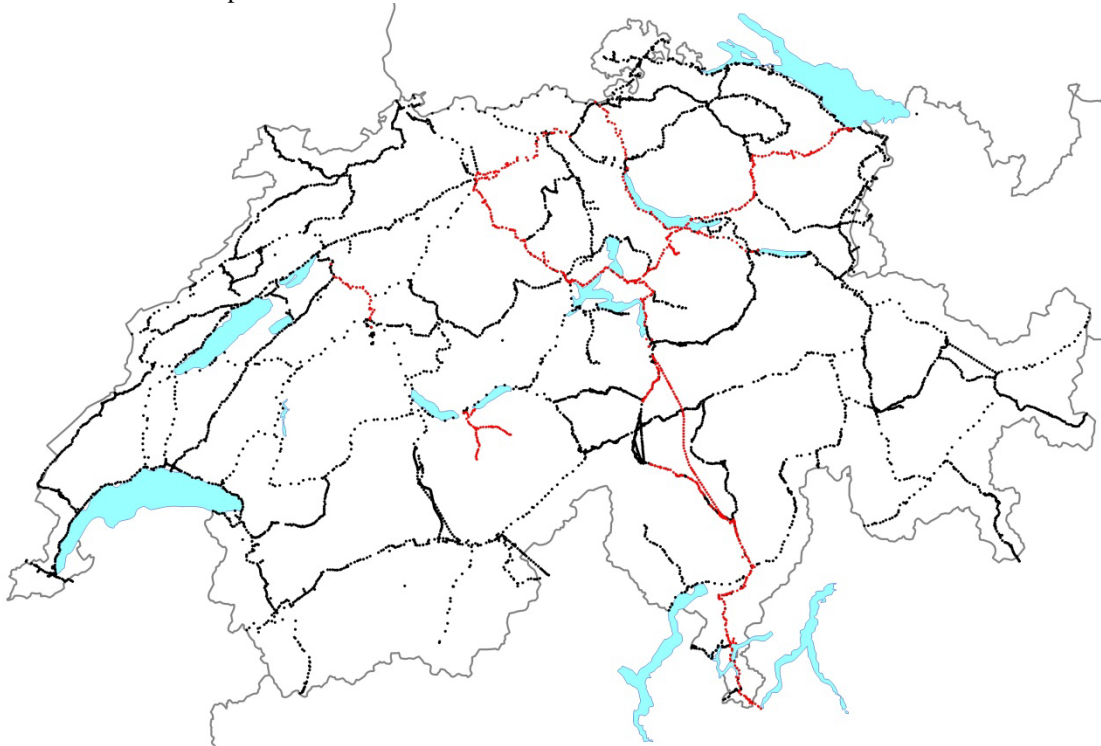


Figure 2.5: Available gravity measurements along the Swiss leveling lines. The red dots indicate the gravity measurements of 2011-2014.

Processing Facility for ESA's GOCE Gravity Field Explorer Mission

H. Bock^{1,2}, U. Meyer¹, A. Jäggi¹, R. Dach¹ and G. Beutler¹

¹*Astronomical Institute University of Berne*

²*Now with PosiTim UG*

The GOCE (Gravity field and steady-state Ocean Circulation Explorer) satellite was the first core mission of ESA's Earth Explorer programme (Drinkwater et al., 2003) and has been launched on March 17, 2009 from Plesetsk, Russia. The official end of the mission was declared on October 21, 2013 when the satellite ran out of fuel and the drag-free flight could no longer be realized. Three weeks later on November 11, 2013 the satellite re-entered the Earth's atmosphere. Figure 2.6 shows the orbit height of the satellite from October 17 to November 10, 2013. GPS measurements have been available until a few hours before the re-entry of the satellite and enabled precise orbit determination (POD) down to about 140 km altitude (Jäggi et al., 2014).

The Astronomical Institute of the University of Bern (AIUB) is member of the European GOCE Gravity Consortium (EGG-C), which was responsible for the GOCE Level 1b data processing and Level 2 product generation. This work was integrated in the GOCE High-level Processing Facility (HPF).

AIUB performed POD based on GPS measurements provided by an on-board 12-channel Lagrange receiver. The resulting Precise Science Orbit (PSO) consists of two different orbit types, a reduced-dynamic and a kinematic orbit. The procedure for generating the PSO was running automatically from October 31, 2009 until November 11, 2013 with a latency of 7-10 days. GOCE orbit results for the entire mission were presented by Bock et al. (2014).

The PSO products are validated by independent Satellite Laser Ranging (SLR) measurements. Figure 2.7 shows SLR residuals (mean: 0.18 cm, RMS: 1.84 cm) for the reduced-dynamic GOCE orbits for the time period from April 10, 2009 to October 21, 2013. The independent validation of the GPS-derived orbit results by the SLR tracking of the satellite was very helpful to achieve such a remarkable orbit quality.

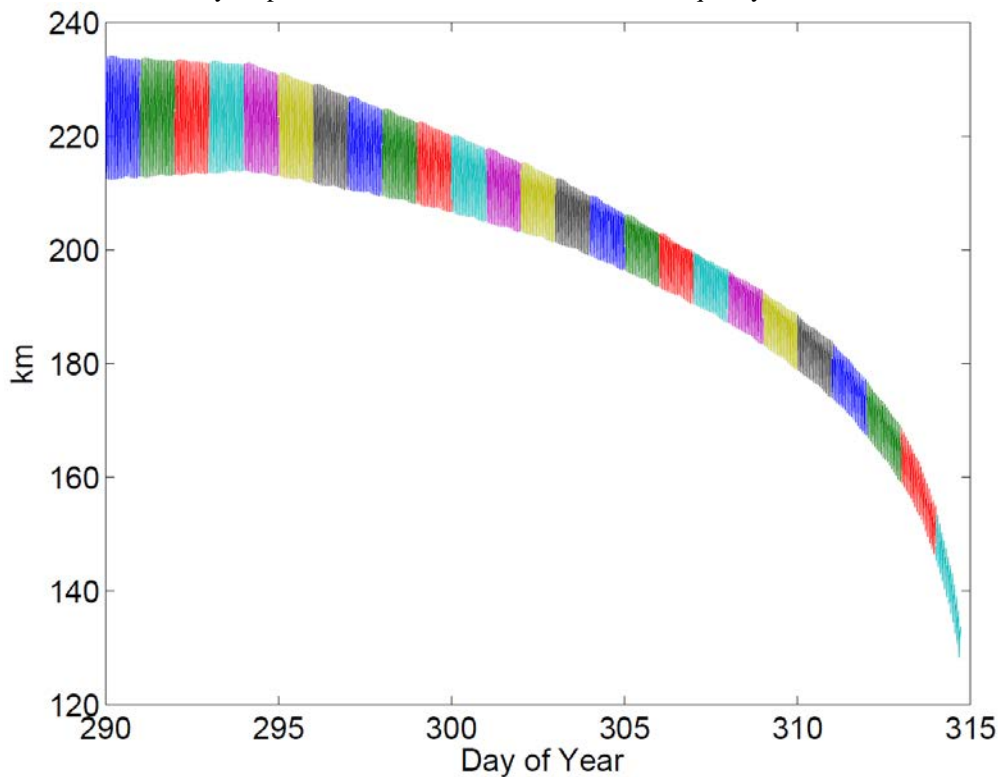


Figure 2.6: Orbit height for the last three weeks of the GOCE satellite

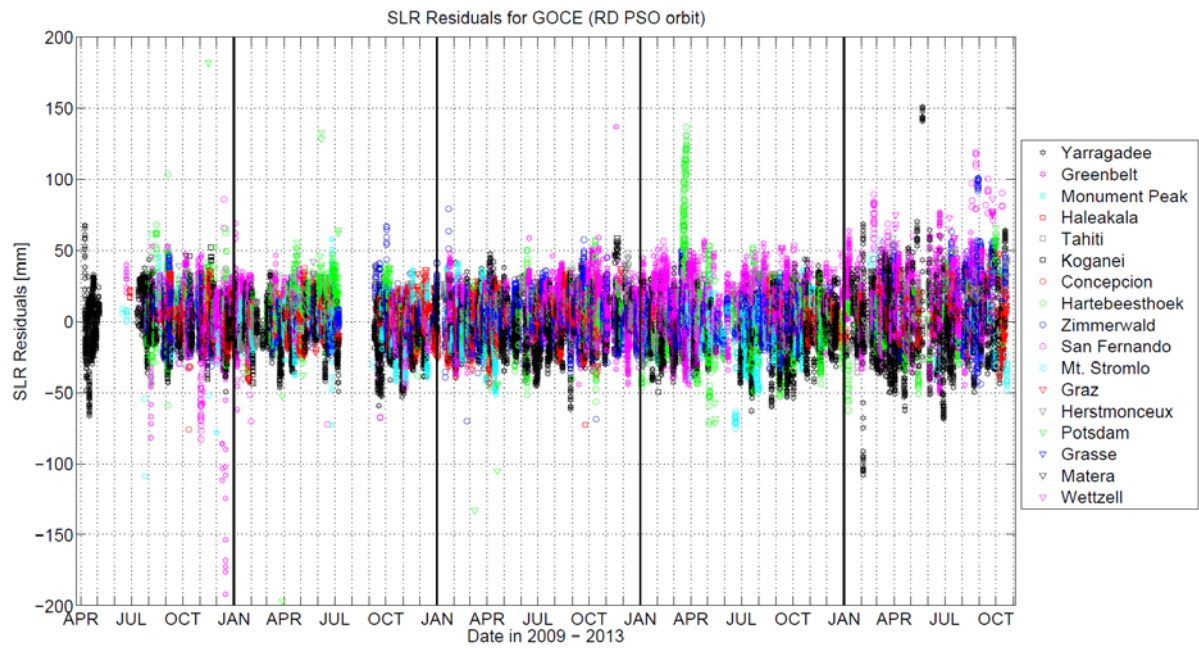


Figure 2.7: SLR validation for reduced-dynamic orbit from April 10, 2009 to October 21, 2013.

Combined Global Gravity Field Determination based on the GRACE-, GOCE-Missions

U. Meyer¹, A. Jäggi¹, G. Beutler¹ and L. Mervart^{1,2}

¹*Astronomical Institute University of Bern*

²*Institute of Geodesy, Czech Technical University Prague*

The determination of the gravity field of the Earth represents one of the three pillars of geodesy. Global gravity field solutions for the long and medium wavelengths are today derived from satellite observations, mainly of the three dedicated gravity field missions CHAMP, GRACE and GOCE. The estimation of gravity field parameters to model this major force acting on the satellites thereby is closely related to the determination of precise satellite orbits. Precise orbits are not only needed to geo-locate the observations of the instruments onboard the satellites dedicated to the gravity field determination, i.e., the K-Band microwave data in case of GRACE, or the gradiometer data in case of GOCE, but the GPS data themselves contain information about the long wavelength part of the gravity field. Despite the long history in precise orbit determination at AIUB as a member of the Center for Orbit Determination in Europe (CODE) the adaption of the orbit model for the GRACE satellites posed a special challenge due to the fact that the GRACE orbits are very actively controlled by a number of cold gas thrusters to maintain the fine pointing of the satellites that is a prerequisite for the flawless working of the microwave link. Meyer et al. (2012) studied the impact of the thruster pulses on the reduced dynamic satellite orbits of GRACE and confirmed the importance of the corresponding observed accelerations for gravity field determination.

Combined solutions from GRACE GPS and K-Band range-rate observations on the one hand, and from GOCE GPS and gradiometer data on the other hand, were determined at AIUB. For the GOCE gradiometer processing Jäggi et al. (2011) studied two-step procedures to take into account the colored noise of the gradiometer data for gravity field determination. In a first step normal equations based on each of the diagonal components of the gravity tensor were set up for the spherical harmonic (SH) coefficients. In addition also empirical piecewise linear parameters were set up for the gradiometer observables at one minute intervals. An inversion of the associated normal equations provided so-called “free solutions” for the SH coefficients and for the empirical parameters. In a second step either the gradiometer residuals or the estimated piecewise linear parameters from the first step were used to derive empirical covariances that were taken into account in the second step to further improve the gravity field estimates. Essentially the same performance could also be achieved within one step by constraining differences between consecutive parameters of the empirical piecewise linear gradiometer model. Irrespective of the actually used method, absorption of high frequency signal content of the gravity field by the piecewise linear parameters could be avoided.

The GOCE gradiometer observable is sensitive to the fine structure of the gravity field, but due to the band-limitation at low frequencies the coefficients of the gravity field at degrees smaller than about 30 are determined mostly from GPS (Figure 2.8, left). In Figure 2.9 (right) the combination of GRACE and GOCE gravity fields is illustrated with respect to the gravity field model GOCO03S. At low to medium degrees the GRACE solution is superior due to the high sensitivity of the K-Band observable even at low frequencies. Above degree 110 the combination is dominated by the GOCE gradiometer observable. The effect of the badly determined zonal coefficients is excluded in Figure 2.8, and Figure 2.9 by the use of degree medians instead of degree variances.

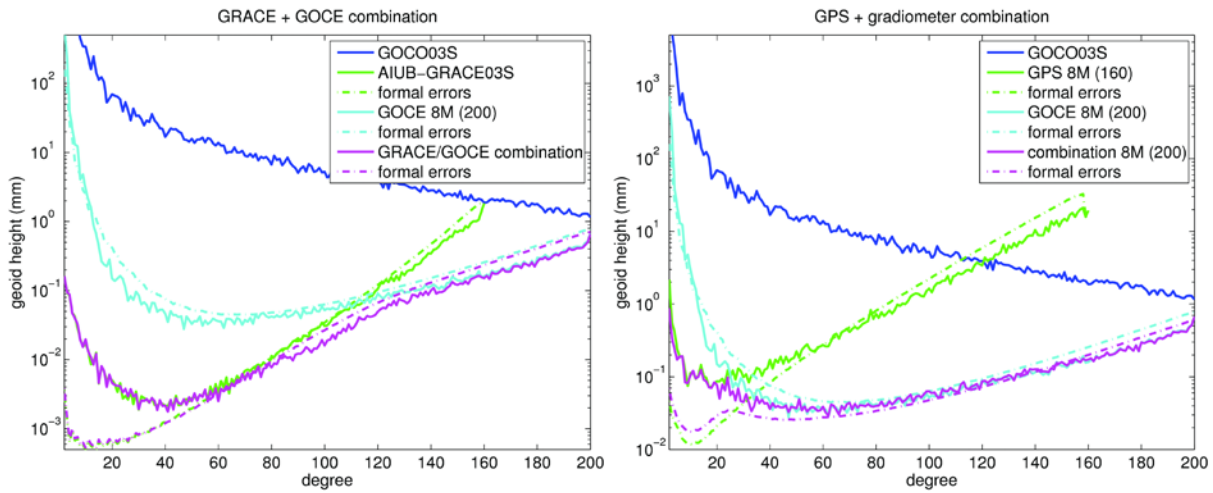


Figure 2.8, left: Difference degree medians between GOCE GPS-only, gradiometer-only, and combined GPS/gradiometer gravity field coefficients and the reference field GOCO03S.

Figure 2.9, right: Difference degree medians of GRACE-only, GOCE-only, and combined GRACE/GOCE gravity field coefficients relative to GOCO03S.

Apart from the improved sensitivity to small scale (high degree) features of the gravity field the combination of GRACE and GOCE observations has another major advantage compared to GRACE-only solutions. Due to the one-dimensional observation geometry of the GRACE K Band observable the spherical harmonic coefficients at certain orders suffer from aliasing of slowly varying gravitational signals, e.g., of tidal origin. In the triangle plot the concerned coefficients are visible as vertical stripes (Figure 2.10, left) afflicted from increased noise. By combination with GOCE data this problem is cured (Figure 2.11, right), even for medium degree coefficients that are still dominantly determined from the GRACE K-Band observations.

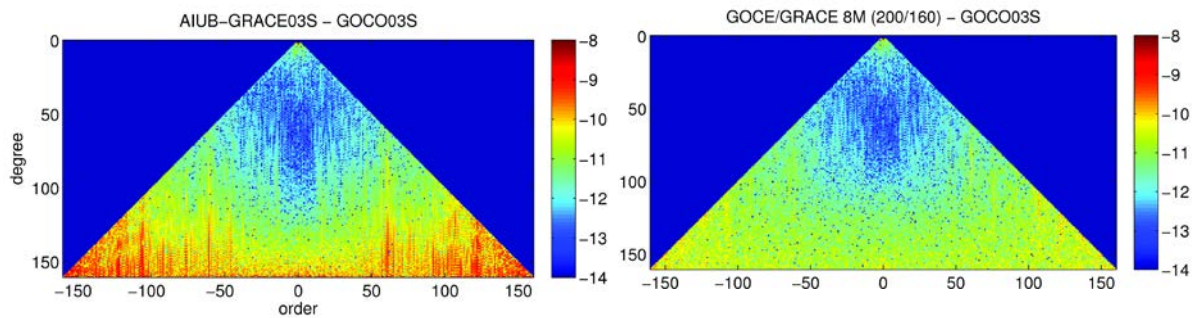


Figure 2.10, left: Triangle plot of the differences between sin- (left part of triangle) and cos-coefficients (right part of triangle) of the seven year GRACE gravity field solution AIUB-GRACE03S and GOCO03S.

Figure 2.11, right: Differences between the spherical harmonic sin- and cos-coefficients of a combined solution of AIUB-GRACE03S and eight months of GOCE gradiometer data compared to GOCO03S.

Time-variable Global Gravity Fields Derived from GRACE- and GOCE-Measurements

U. Meyer¹, A. Jäggi¹, G. Beutler¹ and L. Mervart^{1,2}

¹Astronomical Institute University of Bern

²Institute of Geodesy, Czech Technical University Prague

The main objective of the satellite mission GRACE is the determination of temporal variations in the Earth's gravity field, caused by mass transport on the Earth surface and in the oceans. The causes for the mass transport are the hydrological cycle with mainly seasonal variations in the tropic and subtropic zones (Figure 2.12, left) and the ice mass change and related glacial isostatic adjustment in the polar and subpolar zones (Figure 2.13, right). The former are an important input into hydrological models and are used for drought and flood monitoring, the latter play a major role in the study of climate change.

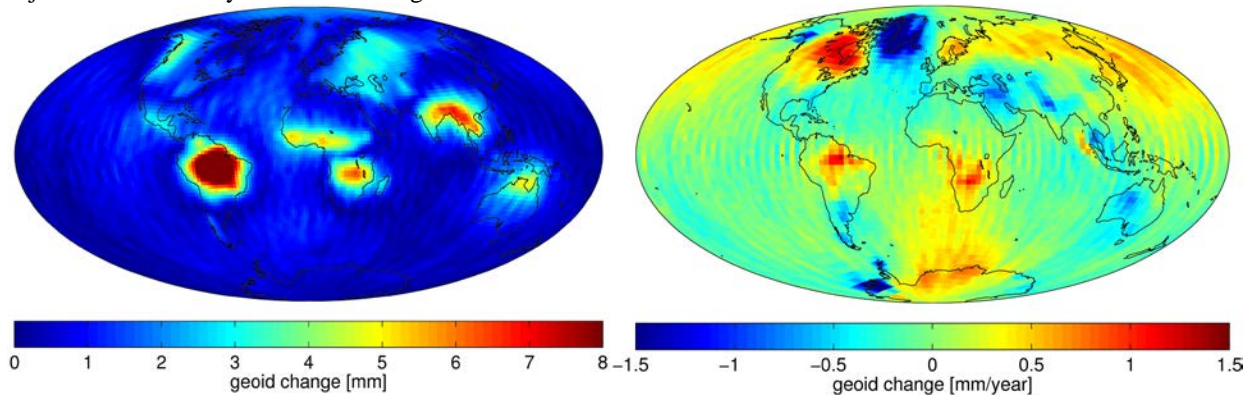


Figure 2.12, left: Amplitudes of seasonal variations derived from AIUB-RL2_60 monthly gravity field solutions. Only coefficients with significant contribution to the seasonal variations are considered. No smoothing was applied.

Figure 2.13, right: Significant trends in geoid height over the time span from 2004 to 2009, derived from AIUB-RL2_60 monthly gravity field solutions. Stripes over the ocean indicate the level of the remaining noise in the solutions. Again no smoothing was applied.

At AIUB two series of monthly gravity field solutions from GRACE GPS and K-Band data were released. The first one (Meyer et al., 2010) is based on RL01 of the GRACE L1B-data, the second one was presented at the GRACE Science Team Meeting in Potsdam in September 2014 and is based on the reprocessed RL02 of the L1B-data. Major improvements from AIUB-RL1 to RL2 where updates of background models for ocean tides and de-aliasing of short periodic atmosphere and ocean mass variations, and an improved parameterization of the accelerometer noise that significantly reduced aliasing with tidal signal at 161 day period. The short periodic gravity variations over the ocean that are mostly due to model errors and processing noise were reduced almost by a factor of two from AIUB-RL1 to RL2, which is competitive to the official state-of-the-art series of monthly gravity fields CSR-RL05 (Figure 2.14). Spells of increased variability over the oceans in Figure 2.14 correspond to periods of high solar activity and are the topic of current research. AIUB-RL2 is available in two versions, one resolved up to degree 60, the other up to degree 90.

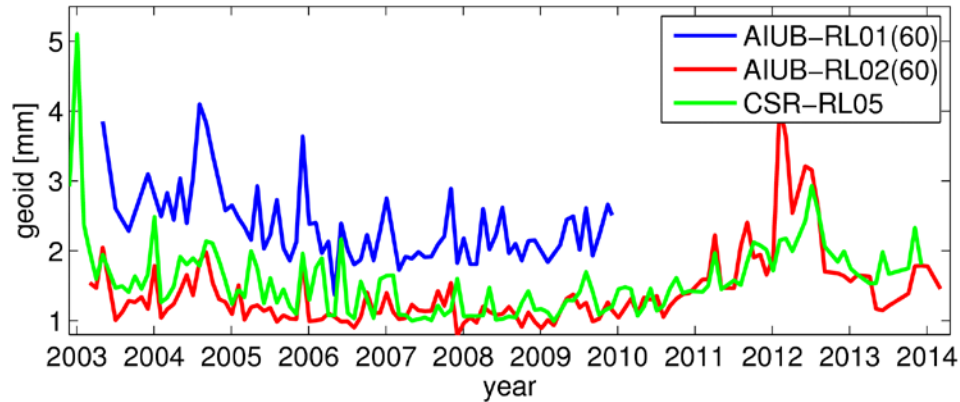


Figure 2.14: Noise of different series of monthly gravity field solutions in terms of standard deviations of short periodic variations over the oceans (weighted by the cosine of the latitude).

Special care has to be taken not to bias the monthly gravity field solutions towards models of the expected time variations that are used as part of the a priori force model in the orbit determination. Dampened signal observed in the original GFZ-RL05 time series triggered a dedicated study at AIUB to understand and illustrate the effect of regularization by separate estimation of arc-specific parameters designed to absorb instrument noise and gravity field parameters (Meyer et al., 2015a and 2015b).

The GRACE satellites are already far beyond their expected life time and may fail at every moment. The successor mission GRACE-FO is only due to for launch in 2017 and interest is high in possible gap filling scenarios. One idea is to use GPS observations to Low Earth Orbiting satellites (LEOs) and the AIUB supported a successful study at the university of Luxembourg with monthly gravity field solutions derived from kinematic orbits of the CHAMP satellites (Weigelt et al, 2013). Also the GOCE satellite with its very low orbit and consequently high sensitivity even of the GPS observations to the gravity field may contribute to the knowledge of temporal gravity variations. AIUB provided normal equations derived from GOCE kinematic orbits to IAPG at the Technical University of Munich where they were combined with GRACE normal equations derived from kinematic orbits and K-Band observations (Pail et al, 2011 and Rexer et al, 2015). But the contribution of GOCE remained small due to the slow orbit repeat ratio that is tailored to the solution of static high degree gravity fields and not well suited to resolve short term gravity variations.

Temporal Earth's Gravity Field Variations from SLR Observations.

K. Sośnica^{1,2}, A. Jäggi¹, U. Meyer¹, D. Thaller^{1,3}, A. Maier¹, G. Beutler¹ and R. Dach¹

¹*Astronomical Institute University of Bern*

²*Now with Institute of Geodesy and Geoinformatics, Wrocław University of Environmental and Life Sciences*

³*Now with Federal Agency for Cartography and Geodesy, BKG*

The temporal Earth's gravity field provides information about the mass transport in the system Earth, i.e., the relations between the mass redistribution in the atmosphere, oceans, land hydrology, and ice sheets. Satellite Laser Ranging (SLR) measurements to geodetic satellites have been delivering valuable information on the lowest-degree coefficients of the Earth's gravity field since 1975 and 1976, i.e., since the two SLR-dedicated spherical satellites Starlette and LAGEOS-1 were launched, respectively. Today, the Gravity Recovery And Climate Experiment (GRACE) mission is the key source of information for the temporal gravity field variations (Tapley et al., 2004). The tandem GRACE-A/B satellites allow defining the mass variations with high spatial resolution and accuracy. The lowest-degree coefficients of the gravity field are, however, still better defined by the geodetic SLR satellites, because the K-band GRACE observations are nearly insensitive to the geocenter variations, due to their interferometric measurement type; the coefficient C20 is degraded due to long-period signals such as the S2 and S1 tidal aliases with GRACE orbits. Therefore, the SLR satellites have still a non-negligible potential to determine the lowest-degree parameters of the Earth's gravity field.

The GRACE mission was initially designed for five years, but even today, after more than thirteen years of the mission, the GRACE satellites still provide precise data. There is, however, a serious risk that the mission may be decommissioned at any time. The GRACE Follow-On Mission (the successor of the GRACE mission) is planned to be launched in 2017, implying that most likely there will be a gap between the missions. Thus, the potential contribution of SLR in view of filling this gap in recovering the time variable low-degree coefficients shall also be assessed in this context.

We simultaneously estimate the gravity field up to degree/order 10/10, Earth rotation parameters (ERPs), station coordinates, satellite orbits, and range biases from combined SLR solutions incorporating nine geodetic satellites: LAGEOS-1/2, Starlette, Stella, AJISAI, Blits, Larets, and LARES as well as Beacon-C. The monthly gravity field solutions are based on 10-day arcs of LAGEOS satellites and 1-day arc of low orbiting SLR satellites. Estimating short arcs for low orbiting satellites avoids the accumulation of orbit errors and their propagation into the estimated gravity field parameters (Sośnica et al., 2015a). The gravity field parameters are obtained in a three-step procedure. In the first step, 1-day normal equations are generated individually for every low orbiting satellite and 10-day normal equations are generated for LAGEOS-1/2 using screened observation files. In the second step, 10-day solutions are generated by combining SLR observations to all satellites through stacking all common parameters except for the orbital parameters which are pre-eliminated before stacking, and thus, just implicitly contained in the resulting normal equation. At this stage, the continuity of ERPs is enforced at day boundaries, and the pseudo-stochastic pulses are constrained before stacking. Finally, monthly solutions are generated by stacking all parameters from three 10-day normal equations and by imposing minimum constraints on the core stations in the network, on ERPs, and on gravity field parameters.

Figure 2.15 shows that the strongest large-scale geoid deformations, e.g., in Greenland, Amazonia, North America, and Southeast Asia can be recovered by the SLR solutions. On the other hand, the smaller geoid deformations can be recovered by SLR only to a limited extent. The SLR solutions are noisy which is visible especially over the oceans, and the SLR-derived amplitudes of geoid deformations are typically smaller by 10% as compared to the GRACE results (Sośnica et al., 2014; 2015b). The most pronounced temporal geoid deformations in the Amazon Basin agree remarkably well between SLR and GRACE solutions (see Figure 2.16). SLR is also capable of recovering the secular gravity changes in Greenland caused by the accelerated ice mass depletion. SLR has, thus, a large potential in, on one hand, filling the gap between GRACE and GRACE Follow-On missions for studying large-scale gravity variations, and on the other hand, in multi-decadal studies of gravity change by incorporating historical SLR data. The consistent and homogeneous series of SLR observations seem to be indispensable in the studies of the temporal change of Earth's potential which may serve as an indication of the climate change.

Figure 2.17 compares the secular changes in the geoid height derived from GRACE (Meyer and Jäggi, 2014) and SLR for the same period. The comparison shows that the geoid changes in SLR solutions are 'spilled' over oceans as they are not limited to the areas of continents, because of the truncation of the spherical harmonic expansion. Some of the smaller geoid changes, e.g., the post-glacial rebound in Scandinavia could not be properly resolved by SLR, due to opposite trends in neighboring areas. On the other hand, not only the largest secular changes in Greenland and

Antarctica agree well between SLR and GRACE, but also some of the smaller deformations in Amazonia and Africa show similar trends in the SLR and the GRACE solutions. The signals related to, e.g., the Patagonian glaciers melting or to droughts in California can also be recovered by SLR, at least to some extent. We conclude that the agreement for secular geoid changes between SLR and GRACE solution is very good; however, SLR-derived gravity field models have a limited spatial resolution as compared to the GRACE solutions.

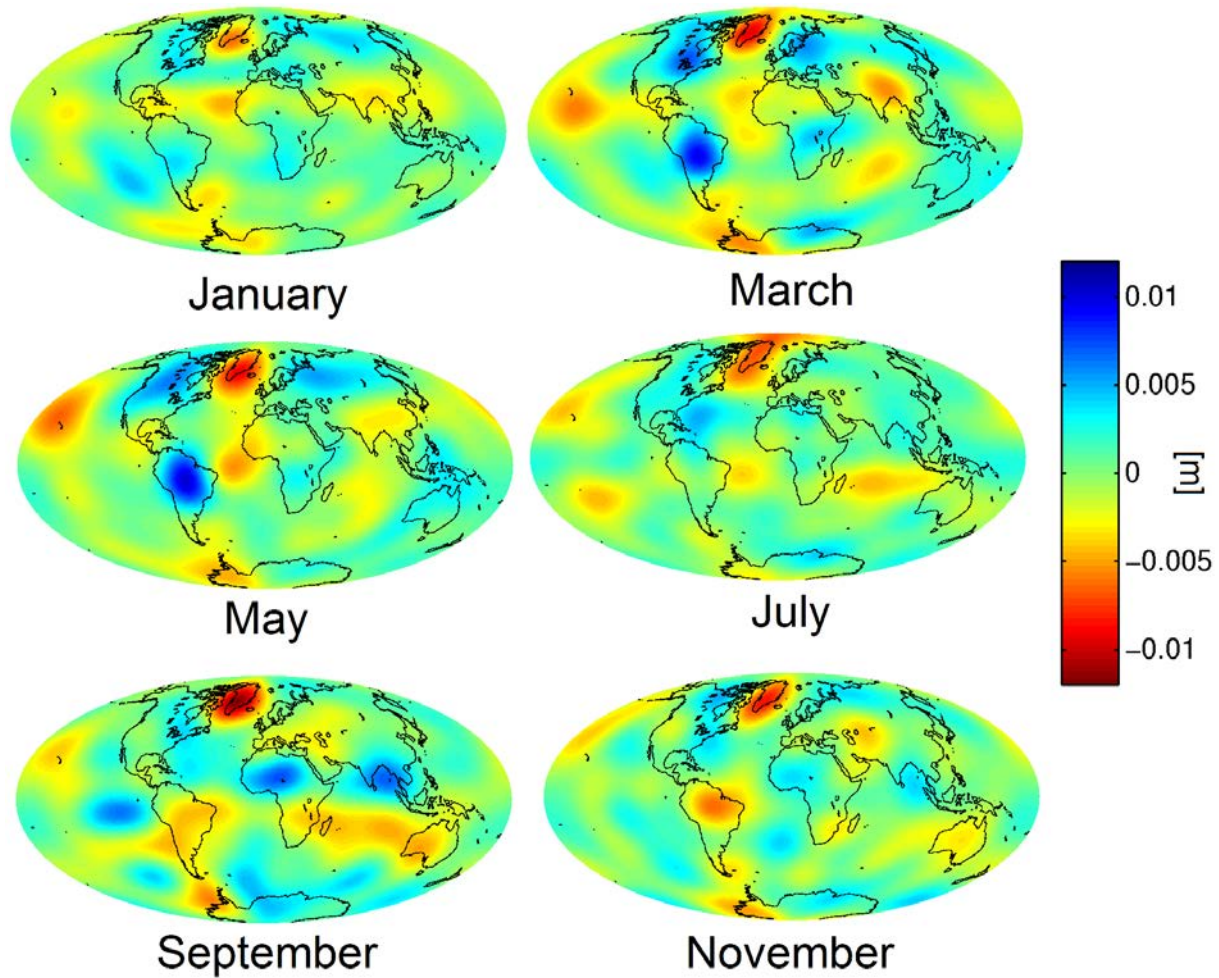


Figure 2.15: Mean monthly gravity field variations from SLR solutions up to d/o 10/10 w.r.t. EGM2008, no filtering applied from the period 2003-2014.

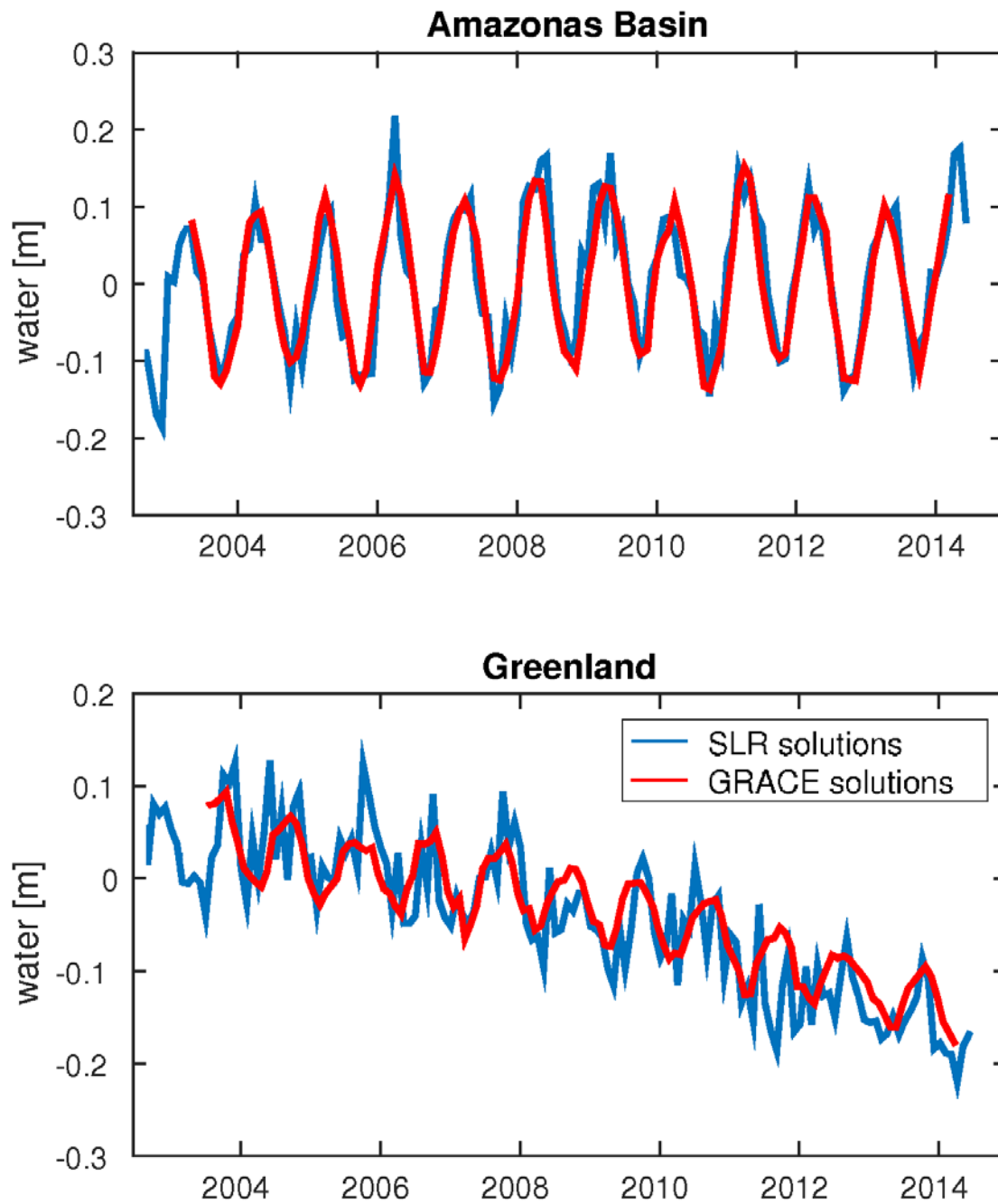


Figure 2.16: Temporal Earth's gravity field changes derived from SLR and GRACE for the Amazon Basin and Greenland using coefficients up to d/o 6/6.

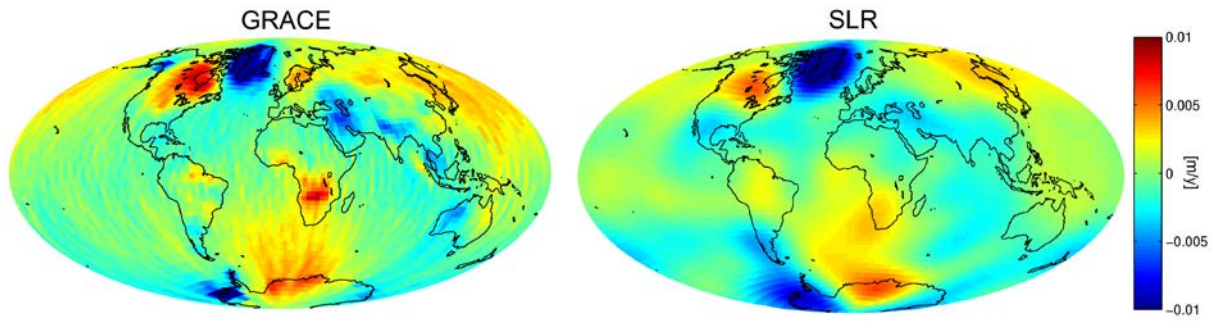


Figure 2.17: Secular changes in geoid heights from GRACE (up to d/o 60/60) and SLR (up to d/o 10/10) solutions in the period 2003-2013.

SWARM-Mission: Orbit Determination and Derived Gravity Field

D. Arnold¹, C. Dahle^{1,2}, H. Bock^{1,3}, A. Jäggi¹

¹Astronomical Institute University of Bern

²German Research Centre for Geosciences, Potsdam

³Now with PosiTim UG

ESA's Earth Explorer Mission Swarm consists of three identical satellites (launched on November 22, 2013) orbiting the Earth in nearly polar orbits at (initial) altitudes of about 460 km (Swarm-A and Swarm-C) and 530 km (Swarm-B), respectively. The main mission objective is to measure the magnetic field produced by the Earth's core, mantle, crust, oceans, ionosphere and magnetosphere. The Swarm mission may, however, also serve as a gravity field mission. Equipped with GPS receivers, accelerometers, star-tracker assemblies and laser retro-reflectors, the three Swarm satellites are capable to serve as a high-low satellite-to-satellite tracking (hl-SST) observing system, following the missions CHAMP (first single-satellite hl-SST mission), GRACE (twin-satellite mission with additional ultra-precise low-low SST) and GOCE (single-satellite mission in addition equipped with a gradiometer). GRACE, dedicated to measure the time-variability of the gravity field, is the only mission still in orbit, but its lifetime might end before launch of its follow-on mission GRACE-FO in August 2017, primarily due to aging of the onboard batteries after meanwhile more than 13 years of operation. Swarm is therefore a suitable candidate to provide time-variable gravity field solutions and to fill the gap between GRACE and GRACE-FO.

In the framework of the Swarm Quality Working Group (QWG), the Astronomical Institute of the University of Bern (AIUB) computes precise orbits for all three Swarm satellites based on GPS data, using the Bernese GNSS Software in its latest development status. Two types of orbits are determined. The first type is a reduced-dynamic orbit, parameterized by the six Keplerian elements, as well as empirical accelerations - in radial, along-track and cross-track directions - to absorb the non-gravitational accelerations like air drag and solar radiation pressure. The second orbit type is a kinematic orbit. This is a purely geometric orbit consisting of kinematic positions at every observation epoch. Both orbits are estimated from undifferenced ionosphere-free GPS observations, using empirical phase center variation maps established for the Swarm satellites. For the GPS satellites, the CODE final orbits and 5s clocks are introduced. The onboard laser retro-reflectors allow for an independent validation of the computed orbits by means of satellite laser ranging (SLR) observations. Figure 2.18 shows the SLR residuals (difference between range observed at SLR station and range computed from orbit) for the reduced-dynamic (left) and the kinematic (right) orbits of the three Swarm satellites over the entire year 2014. The numbers next to the figures indicate the mean values and standard deviations of the residuals.

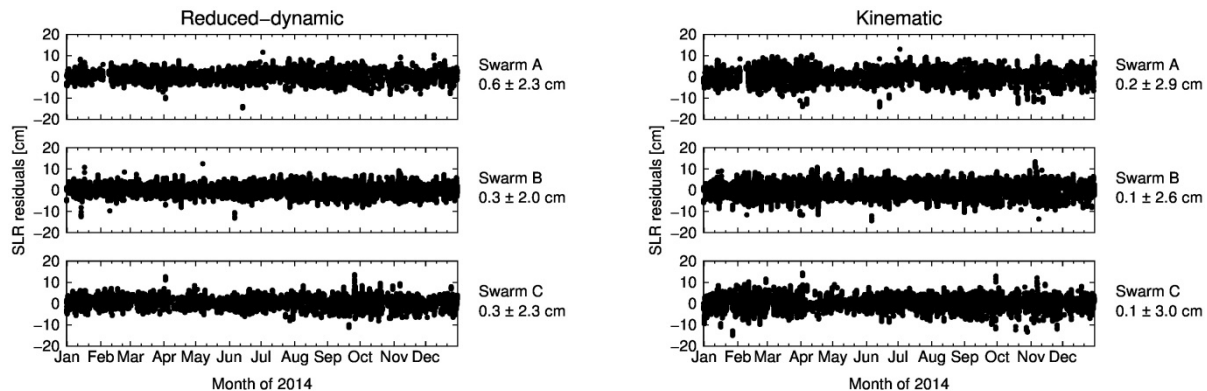


Figure 2.18: SLR residuals for reduced-dynamic (left) and kinematic (right) orbits of the three Swarm satellites for year 2014.

The GPS-derived positions of the kinematic Swarm orbits are subsequently used as pseudo-observations for a gravity field recovery using the Celestial Mechanics Approach (CMA) in which orbit and gravity field parameters are estimated simultaneously. Orbit parameters comprise the initial state vector at the beginning of each 24-hour arc, constant empirical accelerations over each arc, and piecewise constant empirical accelerations with a 15 minutes spacing. The gravity field is parameterized by setting up spherical harmonic coefficients up to degree and order 60,

while the coefficients of degree 61-120 are fixed to the gravity field model EGM2008. Long-term mean as well as monthly gravity field solutions can be generated from all three Swarm satellites individually, and these individual solutions can then be combined on the normal equation level to obtain the best solutions based on data from the Swarm mission. Figure 2 shows difference degree amplitudes w.r.t. EGM2008 and degree amplitudes of the formal errors for a combined Swarm solution over 2 months compared to a corresponding GRACE solution which is also based on hl-SST observations (from the same time interval) only. Up to degree and order 18 Swarm and GRACE solutions are of similar quality. The GRACE solution performs better for the higher degrees due to the lower orbital altitude of GRACE (about 420 km) compared to Swarm. It is thus promising to also study spatially large-scale time variations of the Earth's gravity field from Swarm as soon as longer time series can be processed.

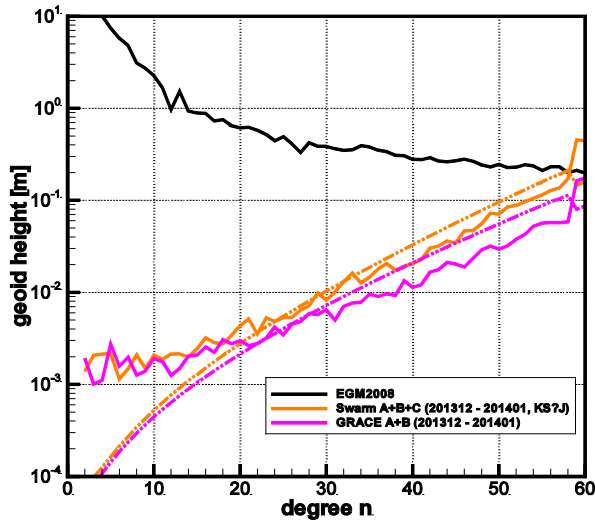


Figure 2.19: Difference degree amplitudes w.r.t. EGM2008 and formal errors of a combined Swarm-A, -B, -C and a combined GRACE-A, -B solution, both based on two months (12/2013 – 01/2014)

Analyzing GRAIL Data: First Lunar Gravity Field Solutions at AIUB

D. Arnold¹, S. Bertone¹, A. Jäggi¹, G. Beutler¹ and L. Mervart^{1,2,bernese}

¹*Astronomical Institute, University of Bern*

²*Institute of Geodesy, Czech Technical University Prague*

The NASA mission GRAIL (Gravity Recovery and Interior Laboratory, Zuber et al, 2013) inherited its concept from the GRACE (Gravity Recovery and Climate Experiment) mission to determine the gravity field of the Moon. The presence of Ka-band range measurements (Asmar et al, 2013) enables data acquisition even when the spacecraft are not Doppler-tracked from the Earth, thus allowing for the first time the accurate determination of the gravity field on both the near and far side of the Moon. Such knowledge is essential to improve the understanding of the Moon's internal structure and thermal evolution (Wieczorek et al, 2013). Currently, two official GRAIL gravity field models resolve the selenopotential up to degree and order 900: GL0900D (Konopliv et al, 2014) and GRGM900C (Lemoine et al, 2014). These solutions were obtained using the software packages MIRAGE, a gravity processing version of the JPL Orbit Determination Program, and GEODYN, respectively.

The first AIUB lunar gravity fields are based on data of the GRAIL primary mission phase, covering the period March to May 2012. Gravity field recovery is realized following the Celestial Mechanics Approach (CMA, Beutler et al, 2010), using a development version of the Bernese GNSS Software along with Ka-band range-rate (KBRR) data series as observations along with GRAIL-A/B dynamic positions (GNI1B, a by-product of NASA JPL processing) as pseudo-observations. All data are freely accessible via NASA's Planetary Data System (PDS). The usage of the GNI1B positions as pseudo-observations allows for a relatively straightforward adaption of our gravity field recovery procedures from GRACE (Meyer et al, 2012), where GPS-derived kinematic positions are available, to GRAIL without having first to implement Doppler data processing.

The Moon gravity field determination is performed in several steps. First, initial orbits are estimated based on a given a priori gravity field. We set up arc- and satellite-specific parameters (like initial state vectors and pseudo-stochastic pulses) as common parameters for all measurement types. Pseudo-stochastic pulses shall compensate for imperfect models of non-gravitational accelerations: indeed solar radiation pressure is not yet explicitly included in our force modeling.

Depending on the chosen a priori field, position and KBRR residuals space from around 1 m and 0.5 mm/s, respectively when using the old JGL165 gravity field (Konopliv et al, 2001), down to few cm and 1 $\mu\text{m/s}$, when consistently using the latest GRAIL gravity field. Apart from yielding sufficiently accurate a priori orbits for the gravity field determination, residuals from this step can also be efficiently used for the data screening.

The initial orbits are then used as a priori orbits for the actual gravity field recovery. The recovery is designed as a generalized orbit determination process, in which both the orbits and the gravity field are improved. A thorough analysis has been performed in order to choose an optimal spacing of the pseudo-stochastic pulses and to assess the performance of the CMA regarding the independence of the final gravity field solutions from the a priori gravity field.

Using an adequate parametrization (Arnold et al, 2015), we computed degree-200 solutions based on release 4 data of the primary mission phase. Figure 2.20 shows the difference degree amplitudes of the estimated degree-200 solutions w.r.t. GRGM660PRIM, a recent lunar gravity field (Lemoine et al, 2013). The red curve represents AIUB200a, the solution which was obtained using GRGM660PRIM up to degree and order (d/o) 200 as a priori field, i.e., by not making use of the American field beyond the maximum degree resolved. For reference, the difference degree amplitudes of the two pre-GRAIL gravity fields JGL165P1 and SGM150J are shown, as well. The dotted lines indicate the formal errors of the respective solutions.

To assess the importance of the KBRR data for gravity field solution, a position-only solution to d/o 200 was computed, using GRGM660PRIM up to d/o 200 as a priori field (see green curve in Figure 2.20). Its difference degree amplitude suggests that the solution is dominated by the dynamic GNI1B positions only at the lowest degrees. The inclusion of the KBRR data strongly improves the solution and reduces the formal errors over almost the entire spectral domain.

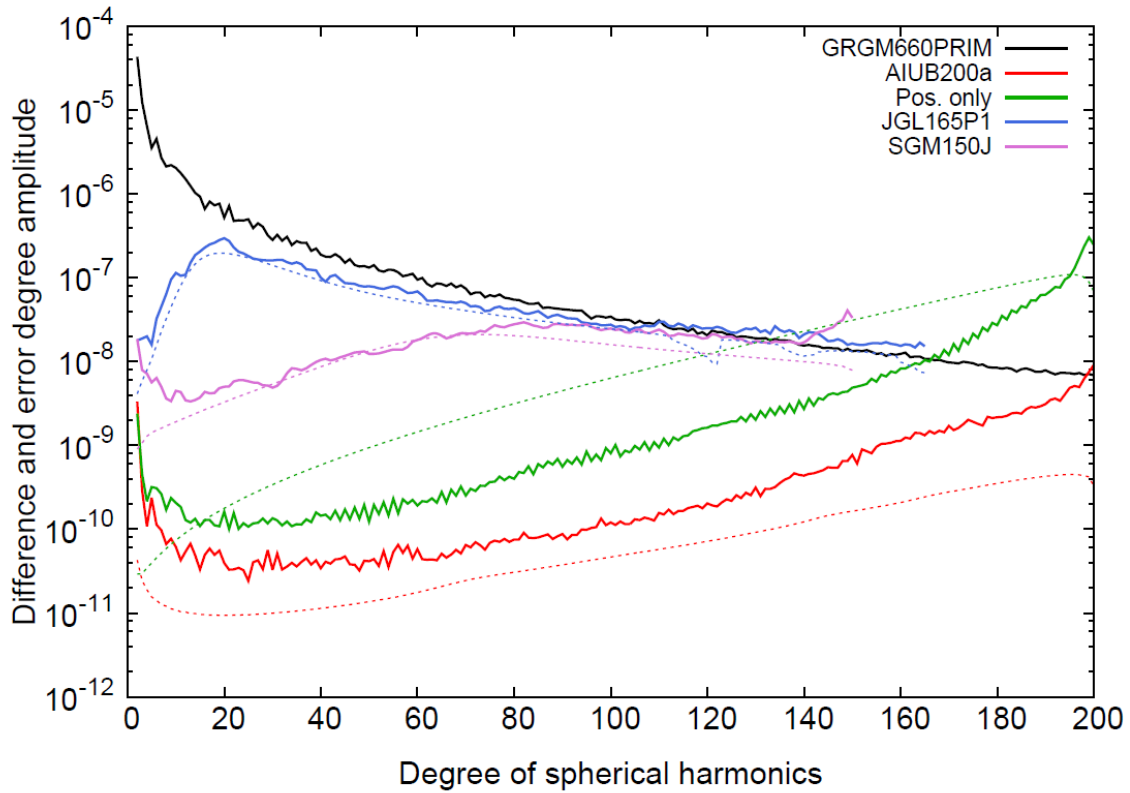


Figure 2.20: Difference degree amplitudes of estimated d/o -200 solutions and of two pre-GRAIL solutions. Red: the *a priori* field (GRGM660PRIM) was used up to d/o 200 as well. Green: a position-only solution, showing that KBRR observations improve the solution over nearly the full spectral domain. Dotted lines: formal errors.

Figure 2.21 shows the free-air gravity anomalies (Heiskanen & Moritz, 1967) derived from AIUB200a. It shows many details which can be correlated with surface features (a test w.r.t. LOLA topography-induced gravity fields showed a consistency above 0.98 up to degree 170) and it does not show the asymmetry in resolution between near- and far-side which was characteristic for all pre-GRAIL gravity field solutions.

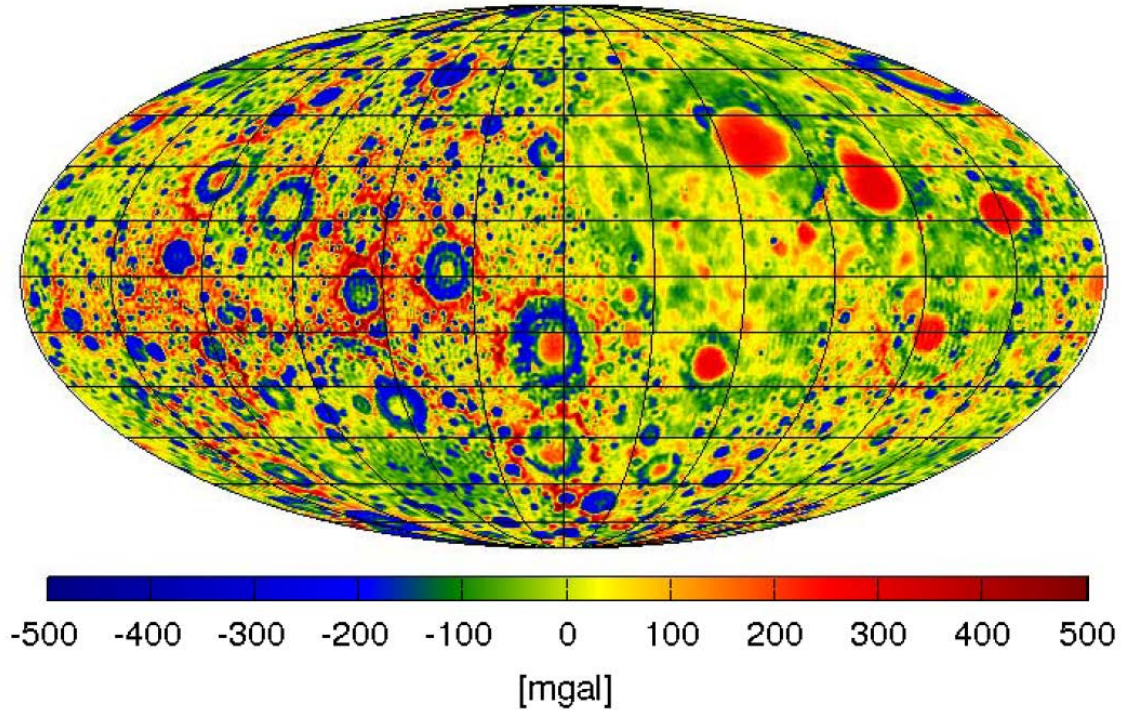


Figure 2.21: Free-air gravity anomalies on a $0.5^\circ \times 0.5^\circ$ grid (Mollweide projection centered around 270° , with the nearside of the Moon on the right).

In conclusion, AIUB200a represents an alternative solution for the lunar gravity field from GRAIL data obtained using an independent software. Although convenient for the initialization of GRAIL data processing, the use of the dynamic GNI1B positions is not entirely satisfactory. The ongoing implementation of DSN Doppler data processing into the Bernese GNSS Software, will allow us to contribute a fully independent solution. Moreover, to further improve our gravity field models, we intend to address the explicit modeling of direct and indirect solar radiation pressure and possibly other non-gravitational forces. Furthermore, the addition of the data at lower orbital altitude from the extended mission phase will strengthen our solutions.

GPS-only Gravity Field Recovery with GOCE, CHAMP, and GRACE

A. Jäggi¹, H. Bock^{1,2}, U. Meyer¹ and G. Beutler¹

¹Astronomical Institute University of Berne

²Now with PosiTim UG

Precise orbit determination (POD) of Low Earth Orbiters (LEOs) using GPS data is required to solve for the long-wavelength part of the Earth's gravity field. This is evident for missions uniquely relying on the GPS tracking technique such as the past gravity mission CHAMP. GPS-based POD is also important for the recently terminated gravity mission GOCE, where the low-degree coefficients of GOCE-only gravity field solutions are exclusively determined from GPS data, because the measurements of the core instrument, the three axis gravity gradiometer, are band-limited. As positions of low Earth orbiters (LEOs) may be determined from GPS measurements at each observation epoch by geometric means only, it is attractive to derive such kinematic positions in a first step and to use them in a second step as pseudo-observations for gravity field determination. The drawback of not directly using the original GPS measurements is, however, that kinematic positions are correlated due to the ambiguities in the GPS carrier phase observations, which in principle requires covariance information be taken into account over several epochs. The impact of covariance information on orbit reconstruction and gravity field recovery was studied by Jäggi et al. (2011a) to eventually compare GPS-only gravity field recovery from CHAMP, GRACE, and GOCE (Jäggi et al., 2011b).

The 1-sec kinematic positions of the GOCE satellite were used to generate gravity field solutions up to degree and order 120. Figure 2.22 shows geoid height differences of bi-monthly solutions covering November–December of the years 2009, 2010, 2011, 2012 with respect to ITG-GRACE2010. A Gaussian filter with a radius of 300km is adopted to focus on the long- to medium-wavelength part of the differences. Figure 2.22 clearly reveals that all four bi-monthly solutions are prone to systematic errors centered along the geomagnetic equator. Barely visible in 2009, the size of the systematic errors is increasing over the years with a maximum impact on the bi-monthly solution from 2011, where maximum geoid height differences reach peak values of 20 cm. Due to their systematic nature the errors are not reduced by accumulating longer data series but become more pronounced.

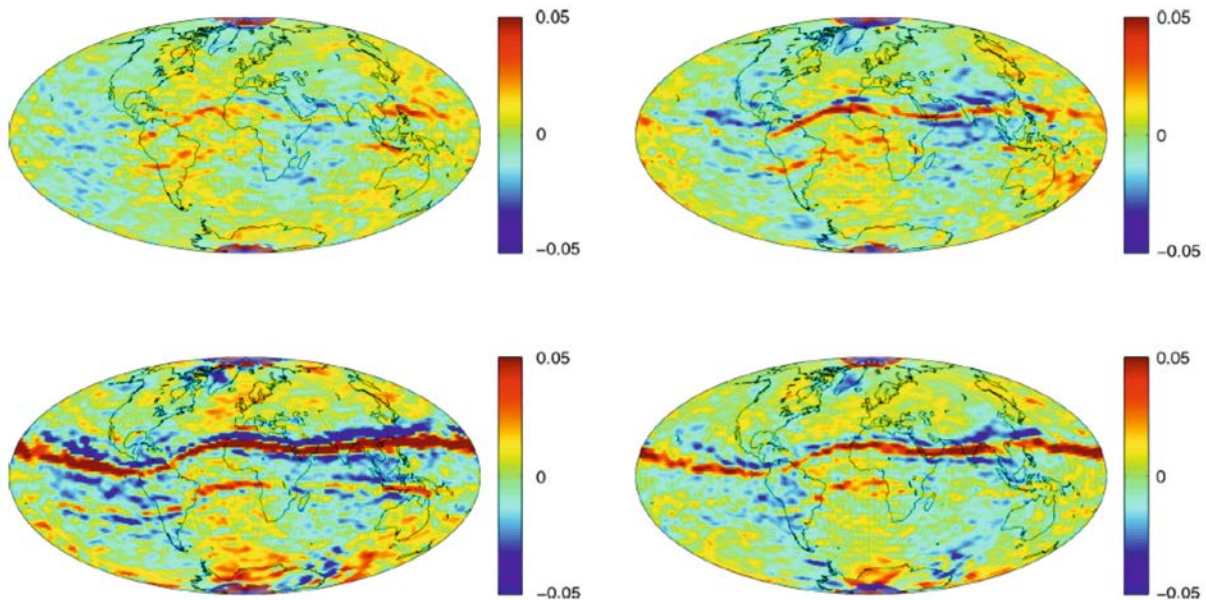


Figure 2.22: Filtered Geoid height differences (m) of based on GOCE kinematic positions wrt ITG-GRACE2010 for the Nov.-Dec. period of 2009 (top left), 2010 (top right), 2011 (bottom left), 2012 (bottom right).

In order to better confine the origin for the systematic errors around the geomagnetic equator the ionosphere-free GPS carrier phase residuals of the orbit determination may be averaged at the ionosphere piercing point of the

corresponding observation directions. Figure 2.23 (left) shows the averaged residuals for of the November–December period of the year 2011 when modeling the higher order ionospheric (HOI) correction terms as recommended by the IERS 2010 conventions. Since the systematics are still clearly visible, they are not caused by the HOI terms or, more precisely, that they cannot be eliminated or significantly reduced by the current HOI model implementation.

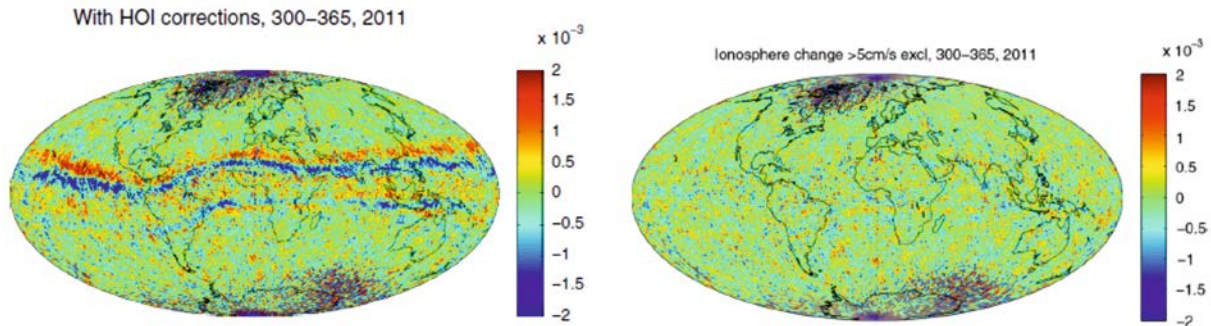


Figure 2.23: Mean (m) of phase observation residuals mapped to the ionosphere piercing point with without (left) and with (right) excluding data with ionosphere changes larger than 5 cm/s.

Jäggi et al. (2015) related the systematic errors to large ionosphere changes, which may be extracted by analyzing epoch differences of the geometry-free linear combination Figure 2 (right) shows for the November–December period of the year 2011 that the systematics can be largely eliminated by discarding measurements with ionosphere changes larger than 5 cm/s. Despite the exclusion of all observations related to large ionosphere changes, this merely corresponds to 94.4% of the total set of available GPS observations. On average 93.8% of the kinematic positions can still be determined, which implies a small reduction of about 6.2% for the set of kinematic positions used for gravity field recovery. For the time span of days 300–365 in the years 2009, 2010, and the 2012, the reduction is even significantly smaller, amounting to 0.1%, 0.2%, and, 3.7%, respectively. A clear reduction of the systematic errors was also observed in gravity field solutions by Jäggi et al. (2015) when using the improved set of kinematic positions.

TanDEM-X baseline solutions using differential GPS

A. Jäggi¹, O. Montenbruck², Y. Moon³ and D. Bodenmann¹

¹Astronomical Institute, University of Bern

²German Aerospace Center, German Space Operations Center

³German Research Centre for Geosciences, Potsdam

TanDEM-X (TerraSAR-X add-on for Digital Elevation Measurement) is the first Synthetic Aperture Radar (SAR) mission using close formation flying for bistatic SAR interferometry. The primary goal of the mission is to generate a global digital elevation model (DEM) with 2 m height precision and 10 m ground resolution from the configurable SAR interferometer with space baselines of a few hundred meters. As a key mission requirement for the interferometric SAR processing, the relative position, or baseline vector, of the two satellites must be determined with an accuracy of 1 mm from GPS measurements collected by the onboard receivers. Given the high importance of the accurate baseline solutions for the interferometric SAR processing, independent baseline solutions are routinely generated by both GFZ and the German Space Operations Center (DLR/GSOC) within the TanDEM-X project. For a further independent performance assessment, the TanDEM-X baselines were additionally computed by the Astronomical Institute of the University of Bern (AIUB) on a best effort basis to perform an inter-agency comparison of dual- and single-frequency baseline solutions (Jäggi et al., 2012).

Figure 2.24 shows the daily standard deviations (STDs) of the inter-agency baseline comparisons for January 2011 based on dual- and single-frequency GPS carrier phase observations, respectively. Empty bars indicate the statistics for entire 24 h arcs (including maneuver periods) and characterize the capability of the three agencies to handle the frequent TanDEM-X formation-keeping maneuvers. Filled bars, on the other hand, exclude time intervals for each day starting 20 min before the first maneuver and ending 20 min after the second maneuver, which allows to assess the consistency outside the maneuver periods.

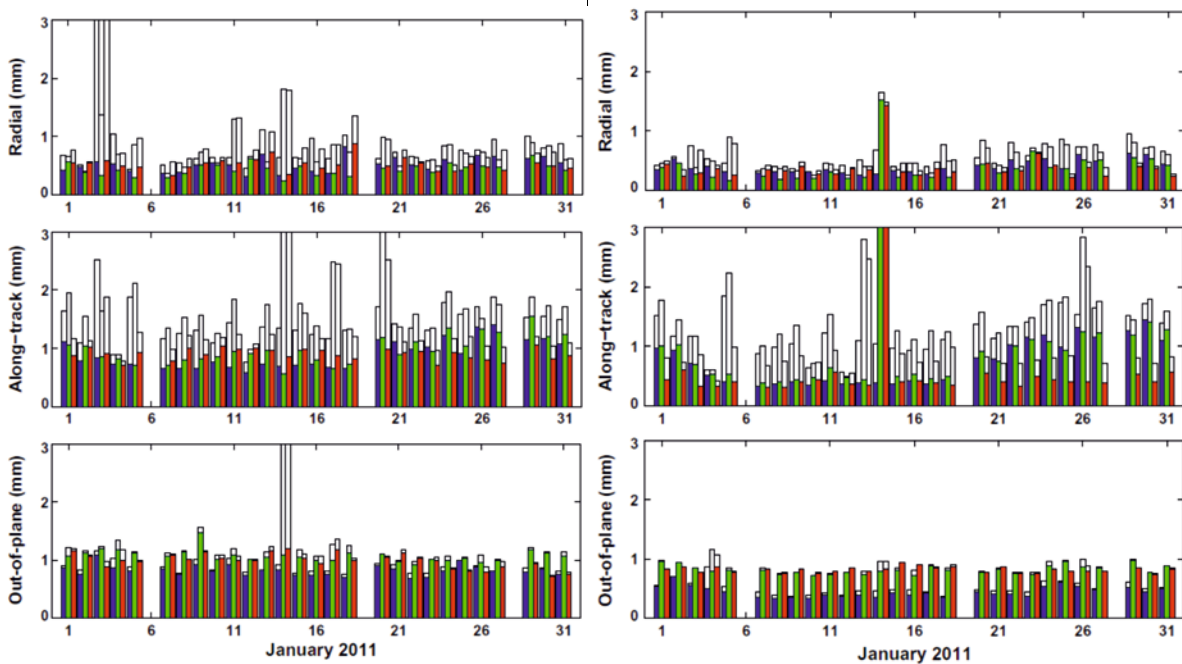


Figure 2.24: Daily standard deviations of inter-agency dual-frequency (left) and single-frequency (right) baseline comparisons (in blue: GFZ-DLR, in green: GFZ-AIUB, in red: AIUB-DLR).

Excluding maneuver time periods, Figure 2.24 (left) shows an almost constant consistency level between AIUB and DLR with STDs of about 0.5, 0.9, and 1.0 mm in the radial, along-track, and out-of-plane components, respectively. Apart from the out-of-plane component, the comparisons between GFZ and the other agencies reveal a slightly larger variability for the radial and along-track component, e.g., about 0.24 instead of 0.09 mm variability for the along-track component, but with almost identical overall STDs. Figure 2.24 (right) shows a further improvement when using single-frequency data, e.g., STDs of about 0.3, 0.4, and 0.8 mm in the radial, along-track, and out-of-plane

components between AIUB and DLR. When including maneuver time periods in the comparison of the solutions, a significant increase of the STD (up to a factor of two over 24 h) can be observed for the baseline difference in the radial and along-track direction.

Figure 2.25 show biases of about 1 mm at maximum between all agencies for dual-frequency solutions. Smallest biases of 0.1–0.2 mm occur for the radial direction. Tight relative constraints imposed on the empirical accelerations in the radial direction ensure a similar leveling for all baseline solutions. A consistent force modeling is more important to keep biases between the different solutions small than to significantly improve the STDs.

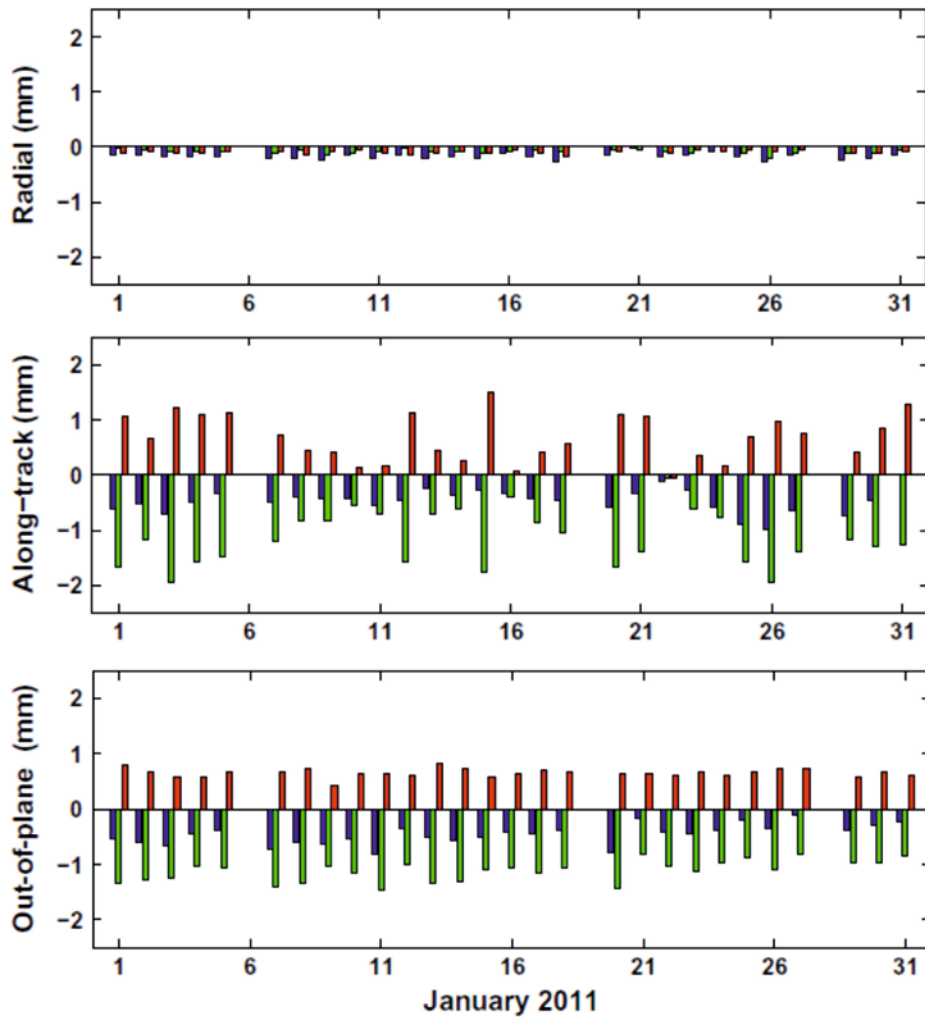


Figure 2.25: Daily mean biases of inter-agency dual-frequency baseline comparisons (in blue: GFZ-DLR, in green: GFZ-AIUB, in red: AIUB-DLR).

Geoid and Hydrography in Lacustrine Areas

A. Geiger¹, Ph. Limpach¹, M. Pozzi¹, M. Wessels², F. Anselmetti³

¹Institute of Geodesy and Photogrammetry, ETH Zurich, Switzerland

²Institut für Seenforschung, Germany.

³Institute of Geological Sciences and Oeschger Centre for Climate Change Research, University of Bern, Switzerland.

Challenges in hydrographic surveying are not only encountered during offshore operations, they also might be seen on pre-alpine lakes. An example is the Lake of Constance, the second large (pre) alpine lake, where the regional geoid has been determined by a highly dense survey of the lake's surface with an area of about 535 square km. The knowledge of the geoid is mandatory to relate levelled heights with ellipsoidal heights, e.g. determined by GPS. Also it is needed in hydrological calculation of the surface currents. Our project aimed at the determination of the geoid of the lake at an accuracy of a few centimeters. This has been achieved at least in most parts of the surveyed area where we reached an accuracy of about 3 cm after a cross-point analysis and a corresponding least square adjustment. The survey has been carried out during a larger campaign in the framework of European Interreg IV program. With the project called 'Tiefenschärfe' and the leading house being the 'Institut für Seenforschung' (Baden-Württemberg) a high precision bathymetry of the lake shall be determined. This gave the opportunity to measure the sea surface topography at the same instance as the bathymetric multibeam measurements were carried out by the University of Bern and the Institut für Seenforschung. From the geometry of the lake surface the geoid has been inferred. The basic principle of the used method is well established in geodesy and is sometimes referred to as 'direct determination of the Geoid', where the ellipsoidal height and the geoidal height of a point are determined and differenced yielding the so-called geoid undulation at that point (Figure 2.26). The uncontrolled outflow and inflow of the Lake of Constance leads to a mean seasonal variation of the sea level of approximately 1.5 m. During the campaign of a few months a rise and fall of the level of about 1.7 m has been observed. At the centimeter level inverse barometer and surface dynamics have to be considered.

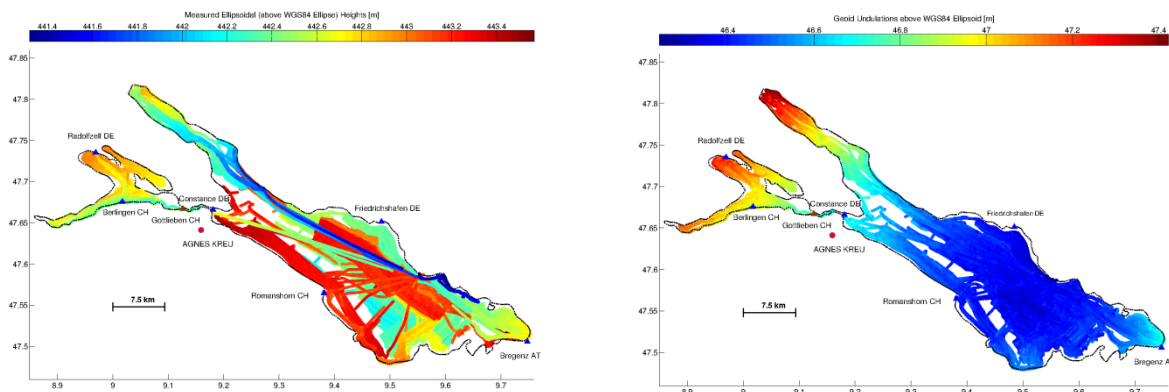


Figure 2.26: Instantaneous lake surface (5 months data) obtained by subtracting ultrasound distances from GPS heights, without time dependent height correction (left). The subtraction of tide gauges orthometric heights from ellipsoidal heights gives directly the searched geoid undulations. Blue triangles: tide gauges. Red dot: swisstopo's GNSS reference station 'Kreuzlingen'.

In our project we used gauge measurements which obviously contain these effects to a large extent. An additional challenge is given by the fact that the Lake of Constance is a tri-national region of Germany, Austria, and Switzerland and thus their coordinates are referred to their specific geodetic system. This is of special importance when using gauge measurements from different countries. In order to circumvent the difficult measurements of the ship's dynamics such as heave and roll we devised a simple and straight forward instrumental setup with the GPS antenna and the short range distance meter tightly collocated.

The described method has been extensively used in the Aegean and Ionian Sea as well as on further lakes in Switzerland. The aim of measuring in Switzerland is of interest for densifying geoid information and further analysis could also be helpful for hydrological calculations. Lakes surveyed are the Lake of Geneva and the Lake of Zurich. The Lake of Constance has been surveyed by a few airborne paths in 2005. This time, 2013, the described campaign was carried out on the sea surface (Figure 2.27).

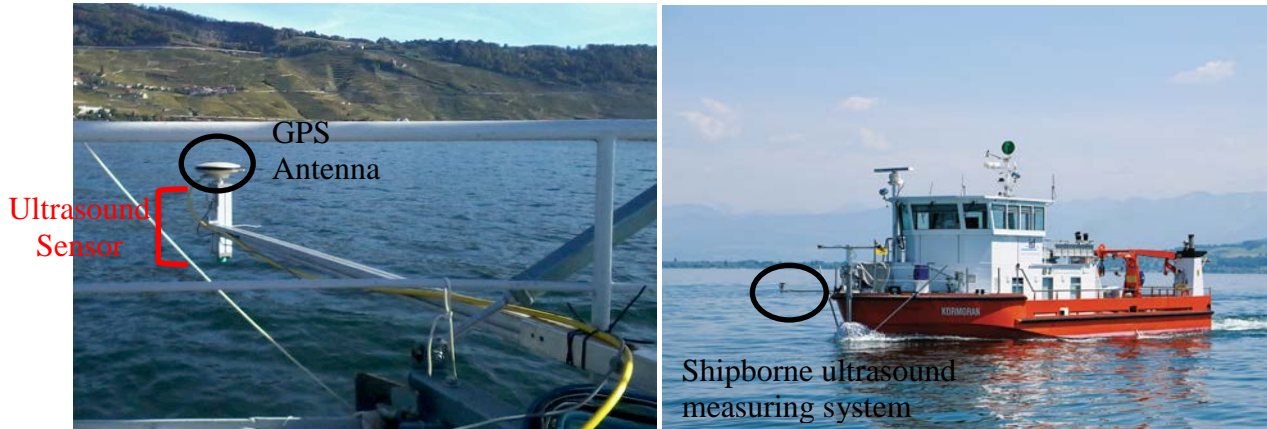


Figure 2.27: Shipborne ultrasound altimetry measuring the Lake Geneva (left)(credits: Institut F.-A. Forel, Uni Genève) and Lake Constance (right) on the survey vessel “Kormoran” of the Institut für Seenforschung (credits: “Tiefenschärfe hochauflösende Vermessung des Bodensees”).

Ultra precise geoid determination for a new generation of future linear collider: a feasibility study at CERN

S. Guillaume¹, A. Geiger¹, B. Bürki¹ and M. Jones²

¹*Geodesy and Geodynamics Lab, Institute of Geodesy and Photogrammetry, ETH Zurich.*

²*European Organization for Nuclear Research (CERN), Geneva, Switzerland.*

This work (Guillaume 2015) is part of the studies conducted by CERN as part of a project of a future electron-positron linear collider (CLIC) of 50 kilometers. In particular, it addresses a specific aspect related to its pre-alignment in the vertical dimension. In fact, in order to guaranty a high collision probability between incident particles (called luminosity), it is necessary that the diameter of the beams, at collision point, after 25 kilometers of continuous acceleration, do not exceed a few nanometers. This is only possible if some technical constraints are fulfilled. One of them concerns the accuracy constraints for the pre-alignment of quadrupoles along the whole machine. This alignment must be related to a straight line in Euclidean space with a precision of 10 microns over 200 meters sliding window. In practice, this can only be envisaged if a positioning system is capable of determining positions at this level of accuracy. In vertical, hydrostatic levelling systems (HLS) benefit of several advantages and represents serious candidates. In addition to their sub-micrometric resolution, HLS are robust and appear to be particularly reliable with respect to radiations. However, they are unable to realize a Euclidean straight line. Indeed, they are related to the surface of the fluid in hydrostatic equilibrium, connecting the different sensors, whose geometry is an equipotential of the Earth's gravity field.

The principal aim of this work is the study of the feasibility of the determination of underground gravity equipotential in a tunnel located at approximately 150 meters in depth. Moreover, a practical strategy which may be implemented is proposed. In a first step, after the rigorous definition of an operator which measures the misalignment, it is demonstrated that the Newtonian mechanic framework is precise enough in the frame of this project. Then, thanks to a rigorous formulation of forces contributing to the variations of the fluid-gaz interface in a 200 meters HLS system, it is shown that this interface can be approximated by equipotentials of the gravity field with a precision better than 1 micron.

The theoretical framework being fixed, the precision of astrogravimetric underground equipotential determinations is analyzed, on the one hand, by numerical Monte-Carlo simulations which model different kind of noise sources, and on the other hand, by several gravity field simulations generated by topography, near-field realistic geological anomalies and by surface variations of the Lake of Geneva. It appears that the principal source of uncertainty comes from the orthometric correction. In particular from the determination of the mean gravity acceleration along the plumbline. For the determination of the profile of CLIC, despite the fact that gravimetric measurements can be carried out on the surface of topography and in the tunnel, it is necessary to know the density of the masses between the surface and the tunnel with a precision between 100 and 200 kg/m³ for wavelengths between 200 to 3'000 meters. Concerning the pure astrogeodetic part, it is shown that the accuracy constraints can be reached within a reasonable time, less than one year, when five modern zenith cameras are deployed in parallel. In this regard, a new zenith camera system, called CODIAC (Compact Digital Astrometric Camera), entirely developed and manufactured at the Institute of Geodesy and Photogrammetry of ETH Zurich, is presented.

In order to validate the astrogravimetric method, the results of a campaign at CERN, along the tunnel TZ32, 850 meters in length, are presented (Figure 2.28 and Figure 2.29). The comparisons of the astrogravimetric determination with the predictions from a precise mass model integrating the topography, the near-field geology and the existing TZ32 and LHC tunnels, are in the order of 20 microns with respect to alignments over 200 meters, in agreement with predictions (Figure 2.30).

Finally, a direct and non-ambiguous method for the determination of underground equipotential is proposed. It is based on observations of underground deflections of the vertical variations. These observations are supposed to be carried out with a new instrument called, differential geodetic interferometric deflectometer, whose principle is simple and consists in measuring the tilt of a movable chariot, along a profile, by an interferometer and a tiltmeter (Figure 2.31). Because of atmospheric perturbations, the whole device must be placed in an appropriate vacuum tube. For a practical application, it is necessary to have a deflectometer of minimum 50 meters. Before that, in order to validate the feasibility of this new kind of instrument, a first prototype of 12 meters entirely developed in the

frame of this thesis, in collaboration with CERN. According to the first measurements showed that there are systematic effects which must be reduced at least of one order of magnitude before considering the construction of a longer range instrument (Figure 2.32).

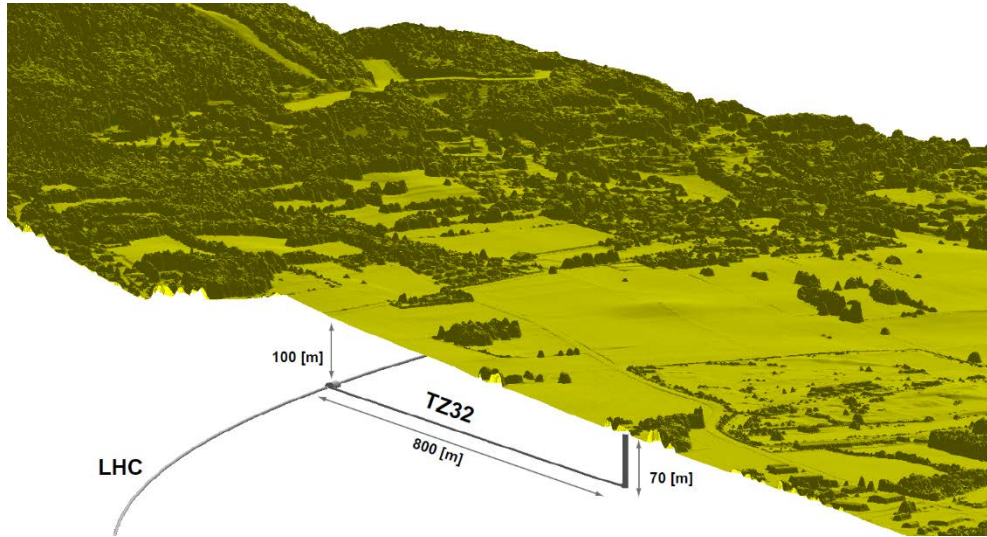


Figure 2.28: Perspective view of the tunnels TZ32 and LHC with topography. Source of digital surface model: système d'information du territoire à Genève (SITG).

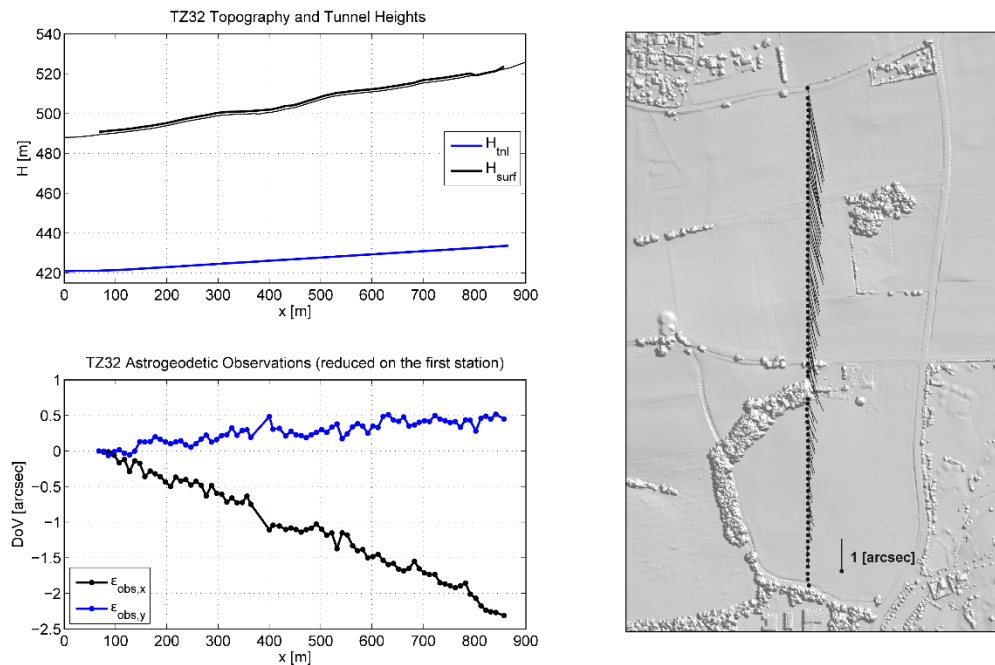


Figure 2.29: (upper, left) profile along the TZ32 of the topography and the tunnel. (Lower, left) deflection of the vertical observations projected along the TZ32 profile. (Right) map representation of the deflections of the vertical. The relief was computed from DSM data provided by SITG.

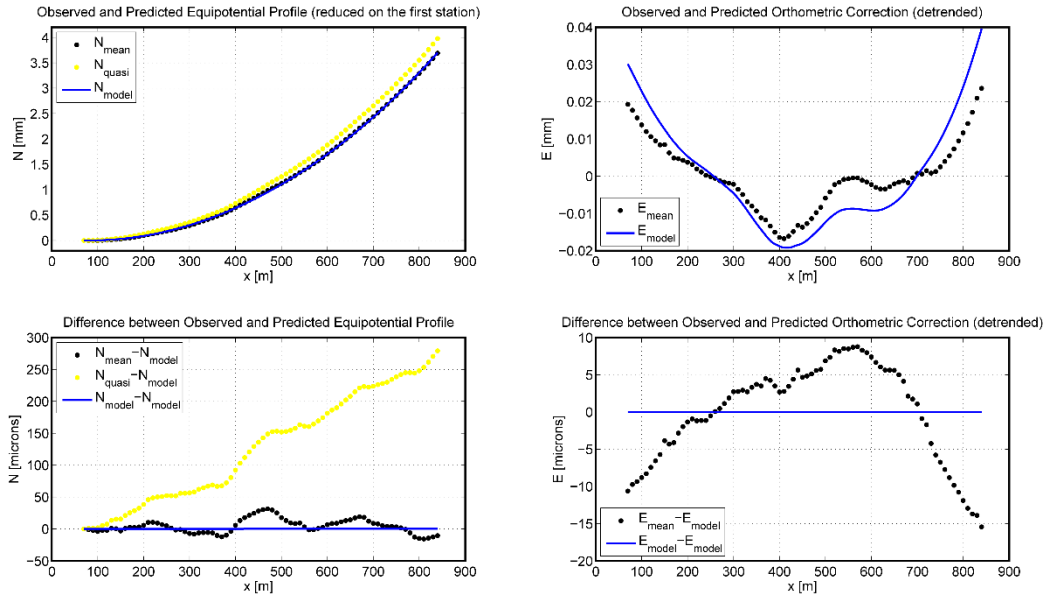


Figure 2.30: (upper, left) observed and predicted equipotential profile in TZ32. The deflection of the vertical are reduced on the first point. (Lower, left) difference between the observed and the predicted equipotential profiles. (Upper, right) detrended observed and predicted orthometric correction. (Lower, right) difference between the observed and the predicted orthometric correction.

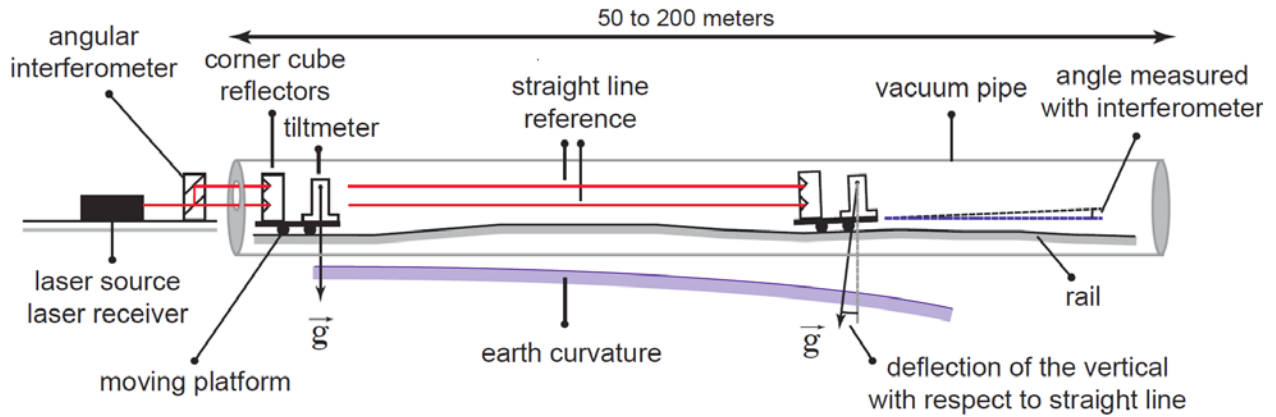


Figure 2.31: Functional sketch of the High Precision Interferometric Deflectometer.

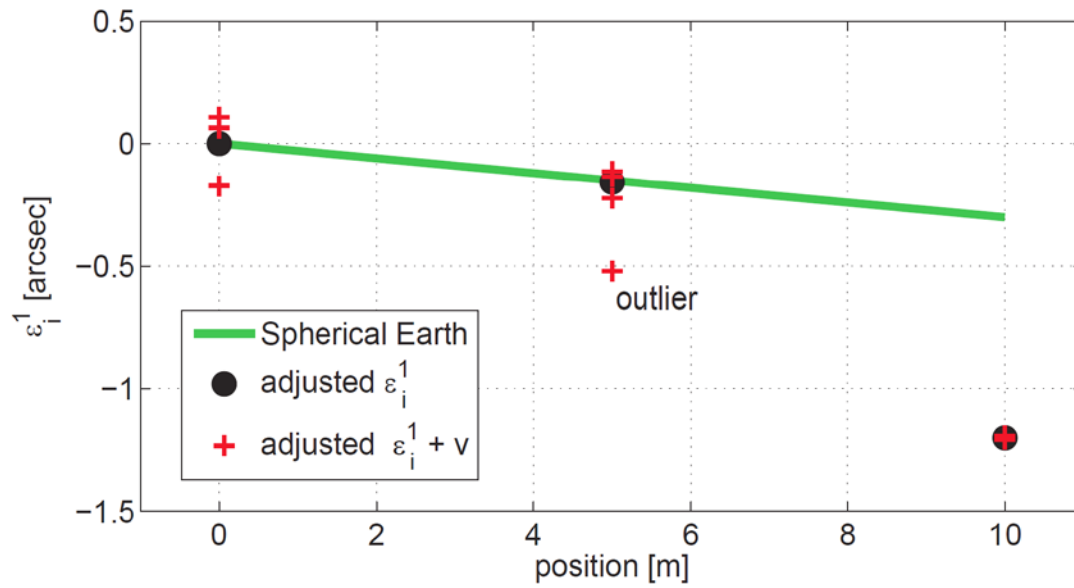


Figure 2.32: Adjusted deflections of the vertical and residuals compared to deflections from a spherical model of the Earth.

Digital Astronomical Deflection Measuring System CODIAC at ETH Zurich

B. Bürki, S. Guillaume, A. Wolf, P. Sorber, and H.P. Oesch

Geodesy and Geodynamics Lab, Institute of Geodesy and Photogrammetry, ETH Zurich

The Compact Digital Astrometric Camera (CODIAC) is a new zenith camera system entirely designed, developed and manufactured at the Institute of Geodesy and Photogrammetry of ETH Zurich (Guillaume 2015). The principal objective behind the development of a new system was to replace the 30 years old system DIADEM (Somieski 2008) with a system of reduced size and cost, based on commercial modern components that provide the same level of accuracy as DIADEM. In addition, it is designed with almost industrial standards in order to facilitate the use by non astrogeodetic experts, increase the performance in terms of productivity, and if necessary, provide the possibility to build additional instruments.

Instrumental Design

As it can be seen in Figure 2.33 and Figure 2.34, the design is similar to the system DIADEM. However, the interfaces of CODIAC are drastically improved and permit a complete steering by a single laptop connected to the instrument by only 2 USB-cables. The optical part consists of an astrograph telescope with a focal length of 600 mm and a focal ratio $f = 1:3$ and two (different) pairs of high resolution inclinometers. As a special feature, CODIAC is equipped with an internal micro controller enabling some basic operations such as automatic levelling using three lifting cylinders and rotation of the optical lenses without the need of an external computer.

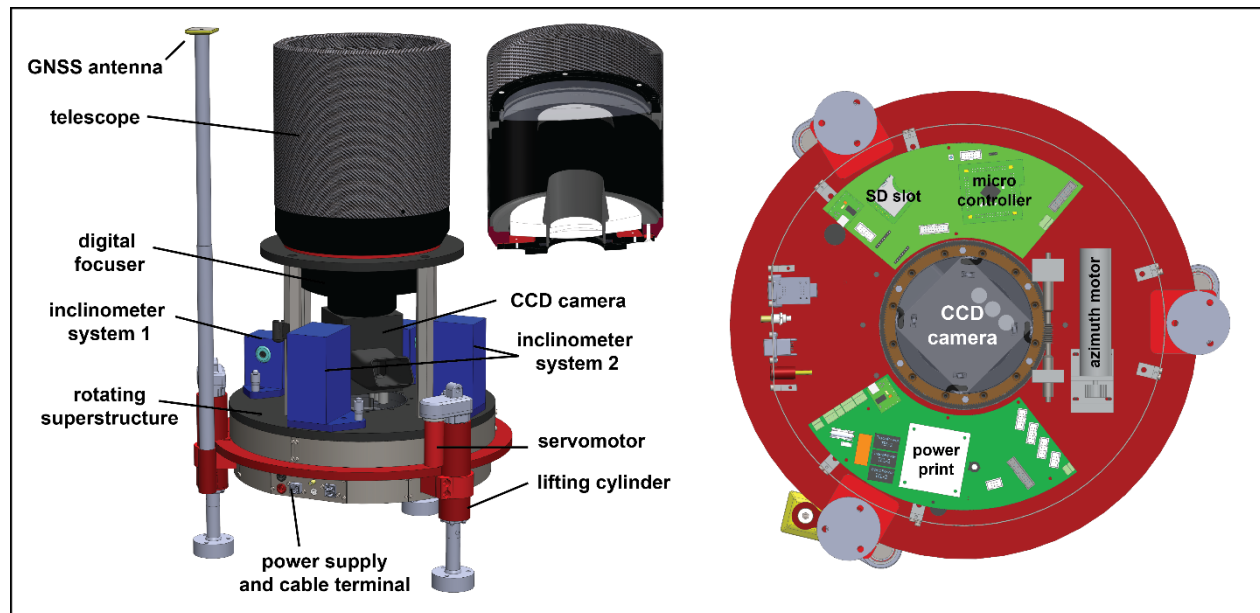


Figure 2.33: Main component of the Compact Digital Astrometric Camera CODIAC Optical System.

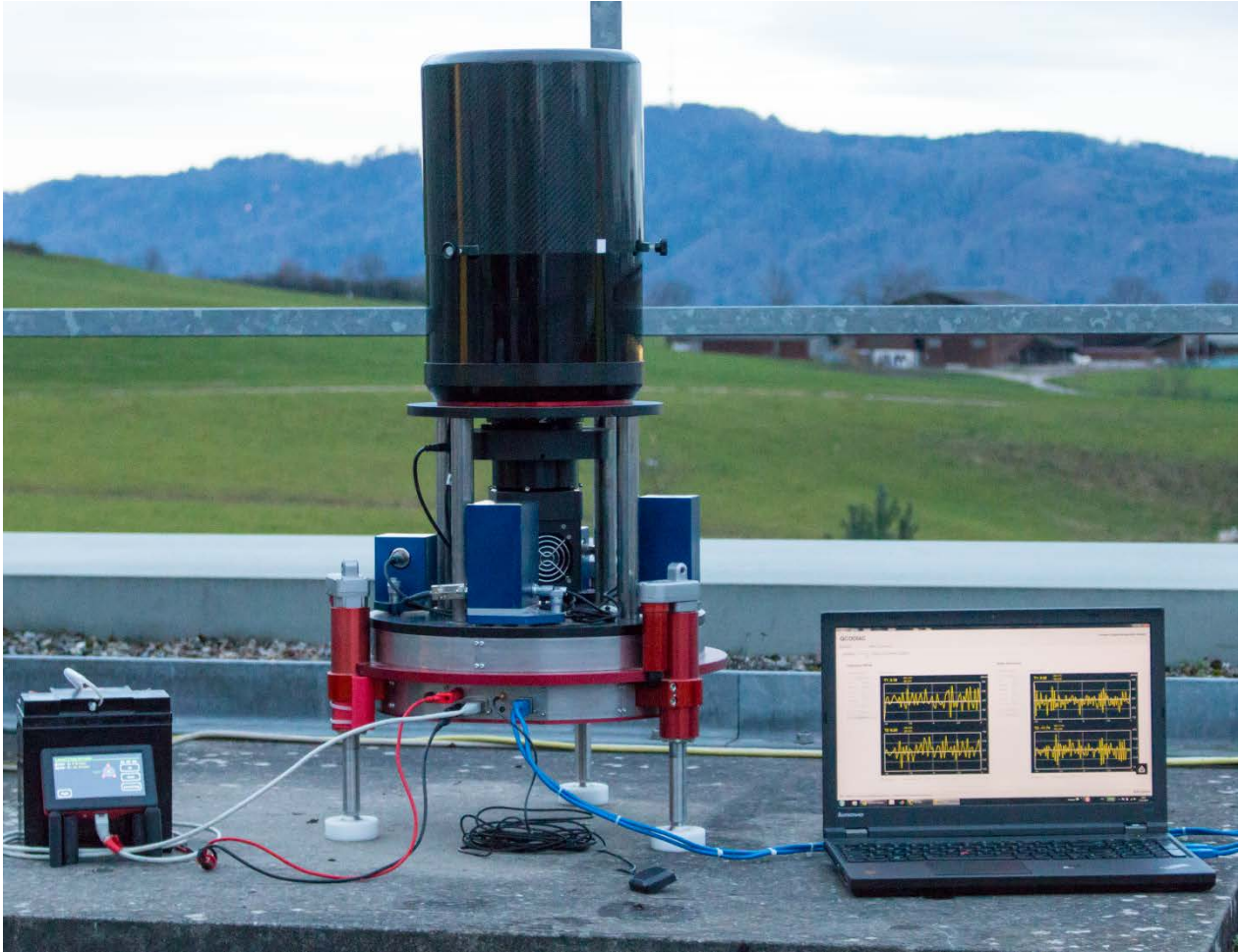


Figure 2.34: CODIAC deployed on the roof of the Geodesy and Geodynamics Lab of ETH Zurich.

First CODIAC Validation

The first validation of CODIAC was performed in summer 2014 in the training center of the NOAA's National Geodetic Survey (NGS) in Corbin USA. Standard measurements of approximately 30 minutes for each station were carried out by non-expert instructed surveyors at 6 stations separated by some 100 meters, during 4 different nights. In order to estimate the performance of the system in terms of precision and repeatability, each station was re-observed several times. The results are represented in Figure 2.35. Each station shows a very good repeatability, almost always better than 0.05 arcsec. To get a better idea of the performance of CODIAC at small scales, the lower plot in Figure 2.35, representing the deflections of the vertical reduced to the station center, shows significant signals with very low amplitudes of approximately 0.1 arcsec.

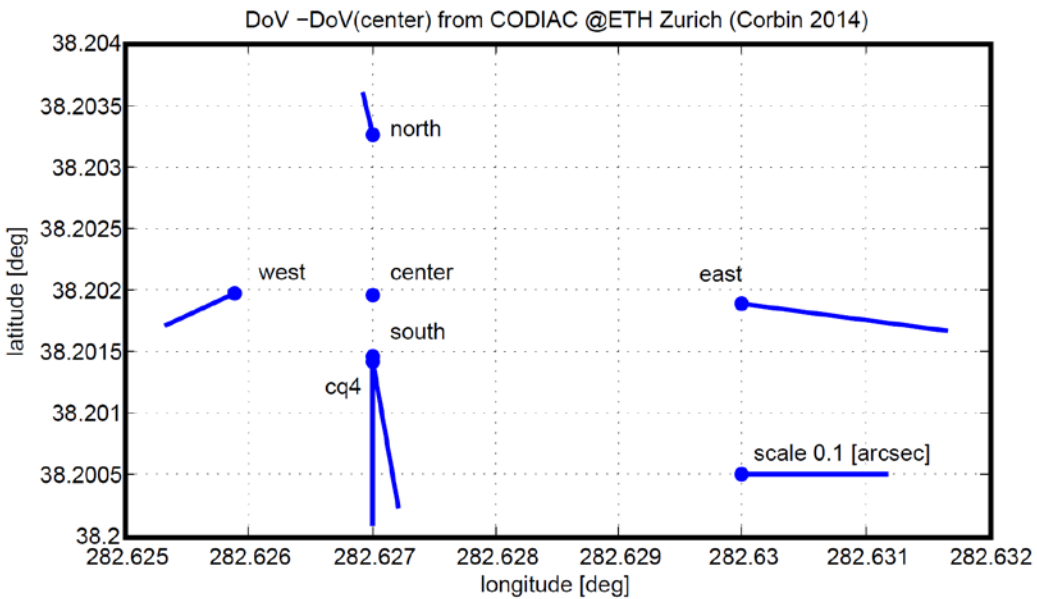
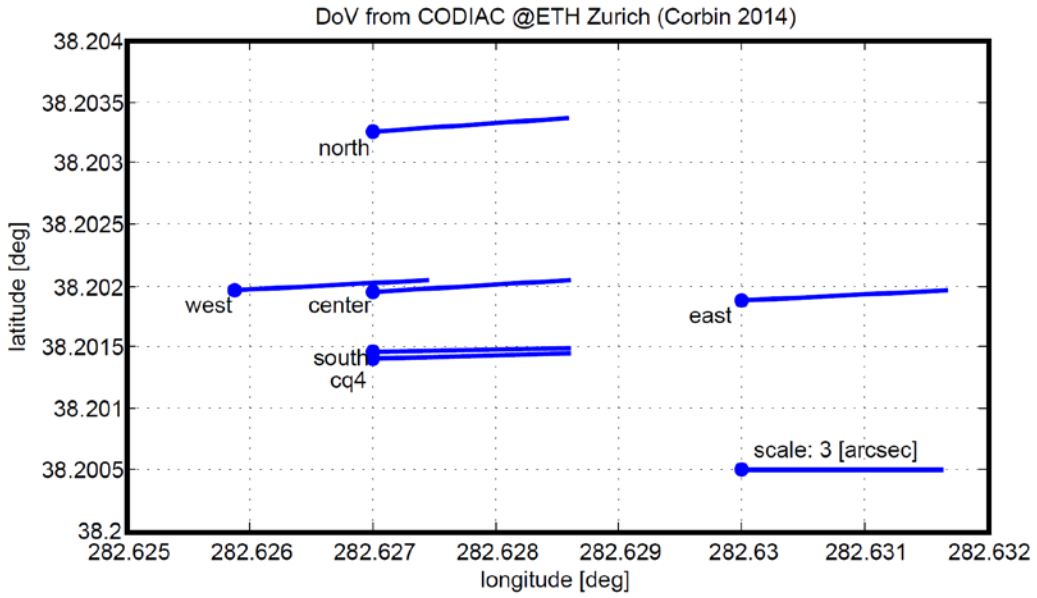


Figure 2.35: (upper) deflections of the vertical determined by CODIAC in Corbin (USA). (Lower) deflections of the vertical reduced to the station center.

SCIEX project REG for regional gravity field modelling

J. Kaminskis^{1,2}, M. Rothacher¹, A. Zarins², B. Bürki¹, S. Guillaume¹

¹Geodesy and Geodynamics Lab, Institute of Geodesy and Photogrammetry, ETH Zurich, Switzerland

²Institute of Geodesy and Geoinformation, University of Latvia, Latvia

At present, the Latvian quasi-geoid model LV98 developed by the author already in 1998 is still used and its accuracy is ~ 6 cm. The quality of model is limited mainly by the inadequate accuracy of the existing geodetic reference network at the given time. This also indicates that it is extremely important to implement a new 1-2 cm national-wide model for the rather flat territory of Latvia.

In order to achieve and verify the obtained results by several independent methods, we will use observations of zenith cameras to observe deflections of vertical (DoV). Results in this area are based on the knowledge of combined scientific methods such as geodesy, astrometry, and least squares adjustment theory. In order to make the development of model algorithms possible, the GGI of the University of Latvia constructs its own zenith camera. It also should be stated that such a new development of a rather well-known technique from the previous century is possible due to the progress of technologies of highly precise digital inclination-meters and CCD camera sensors, etc., allowing the determination of deflections of the vertical with an accuracy below a tenth of an arc second. Such a high accuracy makes observations very valuable for practical applications in gravity field research, civil engineering, and national economy, too.

After a series of first tests with the prototype camera starting in 2011 at the GGI, we recognized that some improvements are necessary. The following improvements are now in progress for the astrometric subsystem and the new camera (see Figure 2.36):

- 8 inch catadioptric telescope, F=2000 mm,
- CCD field of view 0.5 x 0.39 dg, 3300 x 2500 pixels,
- Star magnitude: up to 14m,
- Computer-controlled levelling, • Wireless data transmission.

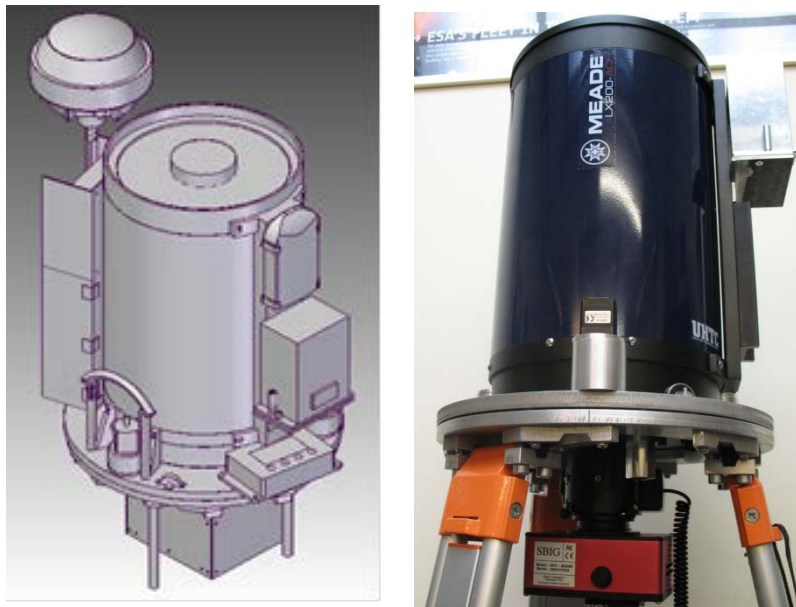


Figure 2.36: Latvian digital zenith camera design

Beside the transfer and exchange of experience and knowledge in the project REG (Research on Earth Gravity by zenith cameras) it is planned to perform test measurements in both countries and to establish a close cooperation between GGL and GGI in the field of geodesy and gravity field determination.

The realization of the project will lead to a much more accurate quasi-geoid model for Latvia based on the observed DoV. It will be possible to analyze and validate the proposed new model with the intermediate LV14 model in Latvia and to make comparisons with the official geoid models from neighboring countries.

For the implementation of new nation-wide geoid models and in case of serious internal discrepancies with other geoid models, the DoV measurements are essential. Since modern zenith cameras provide DoV values with an accuracy of about 0.1" over distances of several 100 km, centimeter level precision may be achieved in the geoid modelling using the method of astronomical levelling. It is also in our interest to support current NKG2015 geoid modelling and geoid computation activities around the Baltic Sea in the framework of a cooperation with the Nordic Geodetic Commission (NKG). In this case, independent observations of the vertical deflections should be used for quality control and to perform fine adjustments of the quasi-geoid model at short wavelengths.

Kinematic Gravity Determination by GNSS/INS Integration

J. Skaloud¹, E. Pares², M. Blazquez², I. Colomina²

¹ *Geodetic Engineering Laboratory, EPF Lausanne*

² *CTTC, Geomatics, Castelldefels, Spain*

Airborne gravimetry survey can determine nowadays, in areas with no ground infrastructures, the gravity with an uncertainty of 15 mGal, which in turn can provide at most a geoid with accuracy of 20 cm. It is expected that by utilizing phase observations from GALILEO an improvement factor of 3 could be achieved, even in areas with no ground support, while in infrastructured areas there is a hope to reach accuracy in the order of 0,1 mGal on spatial scales of ~ 10 km. These targets can be hit more easily with the availability of data from ESA mission "GOCE". This was the underlying ideal of the European Project (FP7) called GAL (Galileo for Gravity) that focused in the years 2011-2013 on the development of a state of the art methodology for determination of precise and high-resolution gravity field models through precise kinematic airborne gravimetry with GPS, EGNOS, GALILEO and strapdown Inertial Measurement Units (IMUs) and its further integration with GOCE global models. The GAL concept is based on the combination of satellite-derived global gravity models with airborne-derived local models. While GOCE measurements provide the global gravity model with 1-2 mgal accuracy (1-2 cm geoid accuracy) at 100 km wavelengths and longer, the airborne ranging and inertial measurements shall provide the local ones at comparable accuracy with resolutions ranging from 200 to 1 km. A multi-constellation data processing approach has been investigated that utilizes the combined exploitation of GPS and GALILEO data with strapdown inertial observations via new processing methodology. Once GALILEO reaches full constellation the processing strategy proposed by the GAL project shall enable gravity field measurements recovery at marginal cost in many non-surveyed areas in the world, in particular in developing countries.

The reported part of the GAL project revisited the concept of scalar gravity anomaly determination by an airborne strapdown INS/GNSS system. It stems from the previously investigated concepts (mainly within 1995-2005 period) with the goal to decrease the error spectrum of the system caused by accelerometer biases at lower frequencies and GNSS-position/velocity noise at shorter wavelengths. The determination of the random long-term accelerometer bias is indeed possible through combination of GRACE + GOCE data that provide an unbiased field with 80 km resolution while the decrease in velocity noise is expected by precise-point-positioning (PPP) method that merges satellite-phase observations from GPS and Galileo. In the absence of Galileo constellation the practical demonstration focused on the gravity-anomaly determination via INS/GNSS data filtering. The model is first incorporated into an extended Kalman filter/smoothing that determines the gravity anomaly together with the trajectory, which is a preferred method over the cascade determination (i.e. separate estimation of trajectory and specific forces, GNSS acceleration and low-pass filtering of the merged signal). Second processing methodology incorporates the same modeling within the concept of dynamic network. This approach allows imposing crossover conditions on the state of gravity anomaly at trajectory intersections while estimating the sensor and trajectory errors at the same time. This is indeed rigorous formulation of the problem that is expected to surpass the conditioning via crossover adjustment that in previous investigations followed the filtering/smoothing. Despite the remaining challenges of the method of dynamic network caused by large number of parameters (i.e. >106), first practical results are presented. The data comes from two flight campaigns in Spain (Pyrenees Mountains and Alicante-Griona region) where two navigation grade inertial systems were mounted together with multi GNSS receiver into an aircraft (Figure 2.38). Figure 2.37 presents the standard deviation of the free air anomaly for one of the flight. More details can be found in Skaloud et al. (2015).

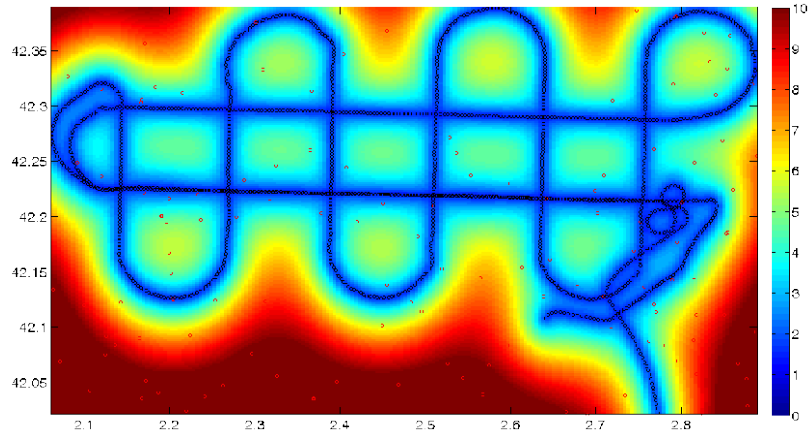


Figure 2.37: Predicted error standard deviation in terms of free air anomaly in the Pyrenees flight.



Figure 2.38: Kinematic airborne gravity sensor (two navigation-grade strapdown inertial sensors with geodetic-grade GNSS receivers) mounted in the plane.

Bibliography Commission 2

- Arnold, D., Bertone, S., Jäggi, A., Beutler, G., Mervart, L. (2015): GRAIL Gravity field determination using the Celestial Mechanics Approach. Submitted to Icarus, 2015.
- Asmar, S. W., Konopliv, A. S., Watkins, M. M., Williams, J. G., Park, R. S., Kruizinga, G., Paik, M., Yuan, D.-N., Fahnestock, E., Strelakov, D., Harvey, N., Lu, W., Kahan, D., Oudrhiri, K., Smith, D. E., and Zuber, M. T. (2013): The Scientific Measurement System of the Gravity Recovery and Interior Laboratory (GRAIL) Mission. *Space Science Reviews*, 2013, 178, 25-55.
- Baur, O., Bock, H., Höck, E., Jäggi, A., Krauss, S., Mayer-Gürr, T., Reubelt, T., Siemes, C., and Zehentner, N. (2014): Comparison of GOCE-GPS gravity fields derived by different approaches. *Journal of Geodesy*, vol. 88(10), pp. 959-973. DOI 10.1007/s00190-014-0736-6.
http://www.bernese.unibe.ch/publist/2014/artproc/DOI_10.1007_s00190-014-0736-6.pdf
- Beutler, G., Jäggi, A., Mervart, L., and Meyer, U. (2010): The celestial mechanics approach: theoretical foundations. *Journal of Geodesy*, 2010, 84, 605-624.
- Bock, H., Jäggi, A., Meyer, U., Visser, P., van den IJssel, J., van Helleputte, T., Heinze, M., and Hugentobler, U. (2011): GPS-derived orbits for the GOCE satellite. *Journal of Geodesy*, vol. 85(11), pp. 807-818, DOI 10.1007/s00190-011-0484-9. http://www.bernese.unibe.ch/publist/2011/artproc/DOI_10.1007_s00190-011-0484-9.pdf
- Bock, H., Jäggi, A., Meyer, U., Dach, R., and Beutler, G. (2011): Impact of GPS antenna phase center variations on precise orbits of the GOCE satellite. *Advances in Space Research*, vol. 47(11), pp. 1885-1893, DOI 10.1016/j.asr.2011.01.017.
http://www.bernese.unibe.ch/publist/2011/artproc/DOI_10.1016_j.asr.2011.01.017.pdf
- Bock, H., Jäggi, A., Beutler, G., and Meyer, U. (2014): GOCE: Precise orbit determination for the entire mission. *J Geod*, 88(11):1047-1060, doi 10.1007/s00190-014-0742-8.
- Dach, R., Beutler, G., Jäggi, A., and Schildknecht, T. (2011): GNSS-Forschungsarbeiten am Astronomischen Institut der Universität Bern . *Geomatik Schweiz*, vol. 109(6), pp. 280-283.
- Dahle, C., Bock, H., Jäggi, A., König, R., Michalak, G., and Flechtner, F. (2014): Orbit and Gravity Field Solutions from Swarm GPS Observations - First Results. 3rd Swarm Science Meeting, Copenhagen, Denmark, 19-20 June, 2014.
- Drinkwater, M.R., Floborghagen, R., Haagmans, R., Muzi, D., and Popescu, A.(2003): GOCE: ESA's first Earth Explorer core mission, *Space Science Reviews*, 108(1-2), 419-432,doi:10.1023/A:1026104216284.
- Heiskanen, W. A., and Moritz, H. (1967): *Physical geodesy*. San Francisco, W.-H.-Freeman [1967], San Francisco : W. H. Freeman, 1967
- Jäggi, A., Prange, L., and Hugentobler, U. (2011a): Impact of covariance information of kinematic positions on orbit reconstruction and gravity field recovery. *Advances in Space Research*, 47(9): 1472-1479, doi: 10.1016/j.asr.2010.12.009.
- Jäggi, A., Bock, H., Prange, L., Meyer, U., and Beutler, G. (2011b): GPS-only gravity field recovery with GOCE, CHAMP, and GRACE. *Advances in Space Research*, 47(6): 1020-1028, doi: 10.1016/j.asr.2010.11.008.
- Jäggi, A., Beutler, G., Meyer, U., Prange, L., Bock, H., Dach, R., Mervart, L. (2011): Gravity Field Determination at AIUB: From CHAMP and GRACE to GOCE. EGU General Assembly 2011, Vienna, Austria, April 3-8, 2011.
- Jäggi, A., Bock, H., Prange, L., Meyer, U., and Beutler, G. (2011): GPS-only gravity field recovery with GOCE, CHAMP, and GRACE. *Advances in Space Research*, vol.47(6), pp. 1020-1028, DOI 10.1016/j.asr.2010.11.008.
http://www.bernese.unibe.ch/publist/2011/artproc/DOI_10.1016_j.asr.2010.11.008.pdf
- Jäggi, A., Bock, H., and Floborghagen, R. (2011): GOCE orbit predictions for SLR tracking. *GPS Solutions*, vol. 15(2), pp. 129-137, DOI 10.1007/s10291-010-0176-6.
http://www.bernese.unibe.ch/publist/2011/artproc/DOI_10.1007_s10291-010-0176-6.pdf

- Jäggi, A., Montenbruck, O., Moon, Y., Wermuth, M., König, R., Michalak, G., Bock, H., and Bodenmann, D. (2012): Inter-agency comparison of TanDEM-X baseline solutions. *Advances in Space Research*, 50(2): 260-271, doi: 10.1016/j.asr.2012.03.027.
- Jäggi, A., Beutler, G., Meyer, U., Prange, L., Dach, R., and Mervart, L. (2012): AIUB-GRACE02S -- Status of GRACE Gravity Field Recovery using the Celestial Mechanics Approach. In: *Geodesy for Planet Earth*, edited by S. Kenyon, M.C. Pacino, and U. Marti, vol. 136, pp. 161-170, ISBN 978-3-642-20337-4, DOI 10.1007/978-3-642-20338-1_20.
- Jäggi, A., Sošnica, K., Thaller, D., and Beutler, G. (2012): Validation and estimation of low-degree gravity field coefficients using LAGEOS. *Mitteilungen des Bundesamtes fuer Kartographie und Geodäsie Band 48*, "Proceedings of the 17th International Workshop on Laser Ranging, Extending the Range", May 16-20, 2011 Bad Koetzing, Germany; vol. 48, pp. 302-304; ISSN 1436-3445; ISBN 978-3-89888-999-5 http://www.bernese.unibe.ch/publist/2012/artproc/proceedings_jaeggi.pdf.
- Jäggi, A., Bock, H., Thaller, D., Sošnica, K., Meyer, U., Baumann, C., and Dach, R. (2013): Precise Orbit Determination of Low Earth Satellites at AIUB using GPS and SLR data. *ESA Special Publications 722*, Papers from the ESA Living Planet Symposium 2013, Edinburgh, United Kingdom, December 2013. http://www.bernese.unibe.ch/publist/2013/artproc/ESA_LP_jaggi.pdf
- Jäggi, A., Beutler, G., Meyer, U., Bock, H., and Mervart, L. (2013): The role of position information for the analysis of K-Band data -- experiences from GRACE and GOCE for GRAIL gravity field recovery. *IAG Symposia proceedings Hotine-Marussi VIII in Rome*, June 17-21, 2013.
- Jäggi, A., Bock, H., and Meyer, U. (2014): GOCE Precise Orbit Determination for the entire mission – Challenges in the Final Mission Phase. In *Proceedings of the 5th International GOCE User Workshop*, Paris, France, November 25 - 28, 2014, ESA Publication SP-728.
- Jäggi, A., Dahle, C., Arnold, D., Meyer, U., Bock, H., Flechtner, F., and van den Ijssel, J. (2014): Orbit and Gravity Field Solutions from Swarm GPS Observations. *AGU Fall Meeting 2014*, San Francisco, California, 15-19 December, 2014.
- Jäggi, A., Bock, H., Meyer, U., Beutler, G., and van den Ijssel, J. (2015): GOCE: assessment of GPS-only gravity field determination. *Journal of Geodesy*, 89(1): 33-48, doi: 10.1007/s00190-014-0759-z.
- Kaminskis, J., Janpaule, I., Zarins, A., and Rothacher, M. (2014): LATVIAN DIGITAL ZENITH CAMERA IN TEST APPLICATIONS, *Proceedings of NKG General Assembly*, doi:10.13140/2.1.4621.4406.
- Konopliv, A. S., Asmar, S. W., Carranza, E., Sjogren, W. L., and Yuan, D. N. (2001): Recent Gravity Models as a Result of the Lunar Prospector Mission. *Icarus*, 2001, 150, 1-18
- Konopliv, A. S., Park, R. S., Yuan, D.-N., Asmar, S. W., Watkins, M. M., Williams, J. G., Fahnestock, E., Kruizinga, G., Paik, M., Strelakov, D., Harvey, N., Smith, D. E., and Zuber, M. T. (2014): High-resolution lunar gravity fields from the GRAIL Primary and Extended Missions. *Geophysical Research Letters*, 2014, 41, 1452-1458
- Lemoine, F. G., Goossens, S., Sabaka, T. J., Nicholas, J. B., Mazarico, E., Rowlands, D. D., Loomis, B. D., Chinn, D. S., Caprette, D. S., Neumann, G. A., Smith, D. E., and Zuber, M. T. (2013): High-degree gravity models from GRAIL primary mission data. *Journal of Geophysical Research (Planets)*, 2013, 118, 1676-1698
- Lemoine, F. G., Goossens, S., Sabaka, T. J., Nicholas, J. B., Mazarico, E., Rowlands, D. D., Loomis, B. D., Chinn, D. S., Neumann, G. A., Smith, D. E., and Zuber, M. T. (2014): GRGM900C: A degree 900 lunar gravity model from GRAIL primary and extended mission data. *Geophysical Research Letters*, 2014, 41, 3382-3389.
- Li, Y., Cheinway, H., Tzu-Pang, T., Cheng-Yung, H., and Bock, H. (2014): A Near-Real-Time Automatic Orbit Determination System for COSMIC and Its Follow-On Satellite Mission: Analysis of Orbit and Clock Errors on Radio Occultation. *IEEE TRANSACTIONS ON GEOSCIENCE AND REMOTE SENSING*, vol. 52(6), 2014, pp. 3192-3203, 10.1109/TGRS.2013.2271547. http://www.bernese.unibe.ch/publist/2014/artproc/HB_Proceedings.pdf

- Limpach, P., Kahle, H. –G., and Geiger, A. (2011a): Geoid Modeling in the Aegean Sea, XXV General Assembly of the International Union of Geodesy and Geophysics.
- Limpach, P., Kahle, H. –G., and Geiger, A. (2011b): Sea Surface Topography and Marine Geoid by Airborne Laser Altimetry and Shipborne Ultrasound Altimetry, XXV General Assembly of the International Union of Geodesy and Geophysics.
- Limpach, P., Pozzi, M., and Geiger, A. (2014): The Determination of the Geoid of Lake Constance, Proceedings of the ENC-GNSS 2014, European Navigation Conference - GNSS 2014, Rotterdam, The Netherlands, April 2014
- Lindegger, B. (2011): Zur Problematik der Geoidbestimmung im Unterengadin. Masterarbeit GEO 511. Universität Zürich.
- Marti, U., and Baumann, H. (2013): Absolute Schweremessungen in Zimmerwald und in Wabern bis 2010. swisstopo-Report 10-13.
- Marti, U., Baumann, H., Bürki, B., and Gerlach, C. (2015): A first traceable gravimetric calibration line in the Swiss Alps. IAG Symposia Series. Vol. 144
- Marti, U. (Editor) (2015): Gravity, Geoid and Height Systems. IAG Symposia Series Vol. 141.
- Meyer, U., Jäggi, A., and Beutler, G. (2012): The Impact of Attitude Control on GRACE Accelerometry and Orbits. In: Geodesy for Planet Earth, edited by S. Kenyon, M.C. Pacino, and U. Marti, 136: 139-146, ISBN 978-3-642-20337-4, doi: 10.1007/978-3-642-20338-1_17.
- Meyer, U., Jäggi, A., and Beutler, G. (2012): Monthly gravity field solutions based on GRACE observations generated with the Celestial Mechanics Approach. Earth and Planetary Science Letters, 345-348: 72-80, doi: 10.1016/j.epsl.2012.06.026.
- Meyer, U., Dahle, Ch., Sneeuw, N., Jäggi, A., Beutler, G., and Bock, H. (2013): The effect of stochastic orbit parameters on GRACE range-rate residuals and monthly gravity fields. IAG Symposia proceedings Hotine-Marussi VIII in Rome, June 17-21, 2013.
- Meyer, U., and Jäggi, A., (2014): AIUB-RL02 monthly gravity field solutions from GRACE kinematic orbits and range rate observations. GRACE Science Team Meeting 2014, GFZ Potsdam.
- Meyer, U., Dahle, C., Sneeuw, N., Jäggi, A., Beutler, G., and Bock, H. (2015a): The effect of stochastic orbit parameters on GRACE range-rate residuals and monthly gravity fields. In IAG Symposia proceedings Hotine-Marussi VIII, University of Rome La Sapienza, June 17-21, 2013.
- Meyer, U., Jäggi, A., Beutler, G., and Bock, H. (2015b). The impact of common versus separate estimation of orbit parameters on GRACE gravity field solutions. Journal of Geodesy, in press, doi: 10.1007/s00190-015-0807-3
- Moraes, T. A., Barlow, P.W., Klingelé, E., and Gallep, C.M. (2012): Spontaneous ultra-weak light emissions from wheat seedlings are rhythmic and synchronized with the time profile of the local gravimetric tide, *Naturwissenschaften*, 99, 465–472, doi:10.1007/s00114-012-0921-5.
- Pail, R., Fecher, T., Jäggi, A., and Goiginger, H. (2011): Can GOCE help to improve temporal gravity field estimates? In Proceedings of the 4th International GOCE User Workshop, Munich, Germany, March 31 - April 01, 2011, ESA Publication SP-696.
- Pail, R., Goiginger, H., Schuh, W.-D., Höck, E., Brockmann, J.M., Fecher, T., Mayer-Gürr, T., Kusche, J., Jäggi, A., Prange, L., Rieser, D., Hausleitner, W., Maier, A., Krauss, S., Baur, O., Krasbutter, I., and Gruber, T. (2011): Combination of GOCE data with complementary gravity field information. In Proceedings of the 4th International GOCE User Workshop, Munich, Germany, March 31 - April 01, 2011, ESA Publication SP-696. http://www.bernese.unibe.ch/publist/2011/artproc/p43_pail.pdf
- PDS, <http://pds-geosciences.wustl.edu/missions/grail/default.htm>
- Rexer, M., Pail, R., Fecher, T., and Meyer, U. (2015): Time Variable Gravity: Contributions of GOCE Satellite Data to Monthly and Bi-monthly GRACE Gravity Field Estimates. In Gravity, Geoid and Height Systems, edited by U. Marti, 141: 35-40, doi: 10.1007/978-3-319-10837-7_6.

- Skaloud, J., Colomina I., Pares E., and Blazquez M. (2015): Progress in airborne gravimetry by combining strapdown inertial and new satellite observations. Proceedings of IAG Symposia of IUGG General Assembly, Prague, Czech Republic, June 22-July.
- Somieski, A.E. (2008): Astrogeodetic geoid and isostatic considerations in the North Aegean Sea, Greece, Ph.D. thesis, ETH Zurich.
- Somieski, A.E., Bürki, B., and Kahle, H.-G. (2011): Astrogeodetic geoid and isostatic considerations in the North Aegean sea, Greece, 25th International Union of Geodesy and Geophysics General Assembly (IUGG 2011).
- Sośnica, K., Thaller, D., Jäggi, A., Dach, R., and Beutler, G. (2012): Sensitivity of Lageos Orbits to Global Gravity Field Models. *Artificial Satellites* Vol. 47(2), pp. 47-65, DOI 10.2478/v10018-012-0013-y.
- Sośnica, K., Jäggi, A., Thaller, D., Meyer, U., Baumann, C., Dach, R., and Beutler, G. (2014): Earth gravity field recovery using GPS, GLONASS, and SLR satellites. Proceedings of the 18th International Workshop on Laser Ranging, Fujiyoshida, Japan.
http://www.bernese.unibe.ch/publist/2014/artproc/13-01-08_Sosnica_Proceedings.pdf
- Sośnica, K., Jäggi, A., Thaller, D., Beutler G., and Dach, R. (2014): Contribution of Starlette, Stella, and AJISAI to the SLR-derived global reference frame. *J Geod*88(8): 789-804, doi: 10.1007/s00190-014-0722-z.
- Sośnica, K., Jäggi, A., Meyer, U., Thaller, D., Beutler G., Arnold, D., and Dach, R. (2015a): Time variable Earth's gravity field from SLR satellites. *J Geod*.
- Sośnica, K., Jäggi, A., Thaller, D., Dach, R., and Meyer, U., (2015b): Earth Rotation and Gravity Field Parameters from Satellite Laser Ranging. Proceedings of the 19th International Laser Ranging Workshop, NASA GSFC, October 27-31, 2014, Annapolis, US.
- Tapley, B., Bettadpur, S., Watkins, M., et al., (2004): The gravity recovery and climate experiment: mission overview and early results. *Geophys Res Lett* 31 (9) L09607 1-4.
- van Dam, T., Weigelt, M., and Jäggi, A. (2015): A Warmer World. *Science & Technology, Pan European Networks*, issue 14, pp. 58-59.
http://www.bernese.unibe.ch/publist/2015/artproc/EGSIEM_PanEuropeanNetworksLtd-1.pdf
- Van den IJssel, J., Visser, P., Doornbos, E., Meyer, U., Bock, H., and Jäggi, A. (2011): GOCE SSTI L2 tracking losses and their impact on POD performance. In Proceedings of the 4th International GOCE User Workshop, Munich, Germany, March 31 - April 1, 2011, ESA Publication SP-696.
http://www.bernese.unibe.ch/publist/2011/artproc/p4_vande.pdf
- Weigelt, M., van Dam, T., Jäggi, A., Prange, L., Tourian, M.J., Keller, W., and Sneeuw, N. (2013): Time-variable gravity signal in Greenland revealed by high-low satellite-to-satellite tracking. *Journal of Geophysical Research, Solid Earth*, 118: 3848-3859, doi: 10.1002/jgrb.50283.
- Wessels, M., Anselmetti, F., Artuso, R., Baran, R., Daut, G., Geiger, A., Gessler, S., Hilbe, M., Möst, K., Klauser, B., Niemann, S., Roschlaub, R., Steinbacher, F., Wintersteller, P., and Zahn, E. (2015): Bathymetry of Lake Constance: State-of-the-art in surveying a large lake. *Fachzeitschrift für Hydrographie*, Vol. 100, 02/2015, pp. 6-11.
- Wieczorek, M. A., Neumann, G. A., Nimmo, F., Kiefer, W. S., Taylor, G. J., Melosh, H. J., Phillips, R. J., Solomon, S. C., Andrews-Hanna, J. C., Asmar, S. W., Konopliv, A. S., Lemoine, F. G., Smith, D. E., Watkins, M. M., Williams, J. G., and Zuber, M. T. (2013): The Crust of the Moon as Seen by GRAIL. *Science*, 2013, 339, 671-675
- Zarins, A., Janpaule, I., and Kaminskis, J. (2014): On reference star recognition and identification, *Geodesy and Cartography*, 40, 143–147, doi:10.3846/20296991.2014.987456.
- Zenner, L., Gruber, T., Beutler, G., Jäggi, A., Flechtner, F., Schmidt, T., Wickert, J., Fagiolini, E., Schwarz, G., and Trautmann, T. (2012): Using Atmospheric Uncertainties for GRACE De-Aliasing -- First Results. In: *Geodesy for Planet Earth*, edited by S. Kenyon, M.C. Pacino, and U. Marti, vol. 136, pp. 147-152, ISBN 978-3-642-20337-4, DOI 10.1007/978-3-642-20338-1_18.
http://www.bernese.unibe.ch/publist/2012/artproc/zenner_iag09.pdf

Zuber, M. T., Smith, D. E., Watkins, M. M., Asmar, S. W., Konopliv, A. S., Lemoine, F. G., Melosh, H. J., Neumann, G. A., Phillips, R. J., Solomon, S. C., Wieczorek, M. A., Williams, J. G., Goossens, S. J., Kruizinga, G., Mazarico, E., Park, R. S., and Yuan, D.-N. (2013): Gravity Field of the Moon from the Gravity Recovery and Interior Laboratory (GRAIL) Mission. *Science*, 2013, 339, 668-671

3 Earth Rotation and Geodynamics Frames

CODE Contributions to Earth Rotation Monitoring

S. Schaer^{1,2}, R. Dach¹, S. Lutz^{1,3}, M. Meindl⁴, D. Thaller^{1,5}, G. Beutler¹

¹*Astronomical Institute, University of Bern*

²*Federal Office of Topography, swisstopo*

³*Now with Federal Office of Topography, swisstopo*

⁴*Institute of Geodesy and Photogrammetry, IGP, ETH Zurich*

⁵*Now with Federal Agency for Cartography and Geodesy, BKG*

The CODE stands for Center of Orbit Determination in Europe - a joint venture of Astronomical Institute, University of Bern, Switzerland, Bundesamt für Landestopografie (swisstopo), Wabern, Switzerland, Bundesamt für Kartographie und Geodäsie, Frankfurt a. Main, Germany, and Institut für Astronomische und Physikalische Geodäsie, Technische Universität München, Germany. CODE is one of the global Analysis Centers (AC) of the International GNSS Service (IGS). The activities of CODE as an IGS AC are described in Dach et al. (2009) or Schaer et al. (2015a).

The satellite orbits of Global Navigation Satellite Systems (GNSS) realize a quasi-inertial reference system, so that the analysis of tracking data from the global network of the IGS allows it to estimate Earth rotation parameters (ERPs). As a result x and y positions of the Earth's rotation axis in an Earth-fixed frame (polar motion) and rates thereof as well as excess length of day (LOD) are obtained.

Since April 1994 also daily values for drifts in nutation in longitude and obliquity are estimated at CODE.

Since week 1486 (June 29, 2008) CODE is internally using a 1-hour resolution for polar motion and LOD parameters. The ERPs are represented as a piece-wise linear polygon, so that continuity at the interval boundaries is automatically guaranteed. For the delivery to external sources (e.g., to the IGS via SINEX files) the representation of the parameters is transformed to offset and drift per 1-day interval applying some continuity conditions at the day boundaries. Separate time series are provided directly to the International Earth Rotation and Reference Systems Service (IERS) for further analysis.

In 2015, software and (final) processing was further developed and prepared for the capability to set up EOPs satellite wise. The same, by the way, applies also to the geocenter coordinate (GCC) parameters. By this expanded parameter setup, studies on the basis of NEQ results become feasible in assessing EOP (and GCC) differences specific to individual satellite systems, satellite planes, satellite groups (or blocks), etc. It is obvious that no (significant) differences (e.g. between GPS-derived and GLONASS-derived EOPs) should be present in the ideal case.

Today a time series of more than 21 years is available from CODE. Figure 3.1 shows the Chandler wander of the Earth's rotation axis starting with June 1993. The accuracy of the daily values as compared to other techniques is a few 0.1 mas. Figure 3.2 shows the variations of excess length of day for the time period of more than 21 years. In the frame work of the 2nd reprocessing campaign of the IGS, a time series of ERP based on homogeneous and most up-to-date models has been generated (Lutz et al. 2015).

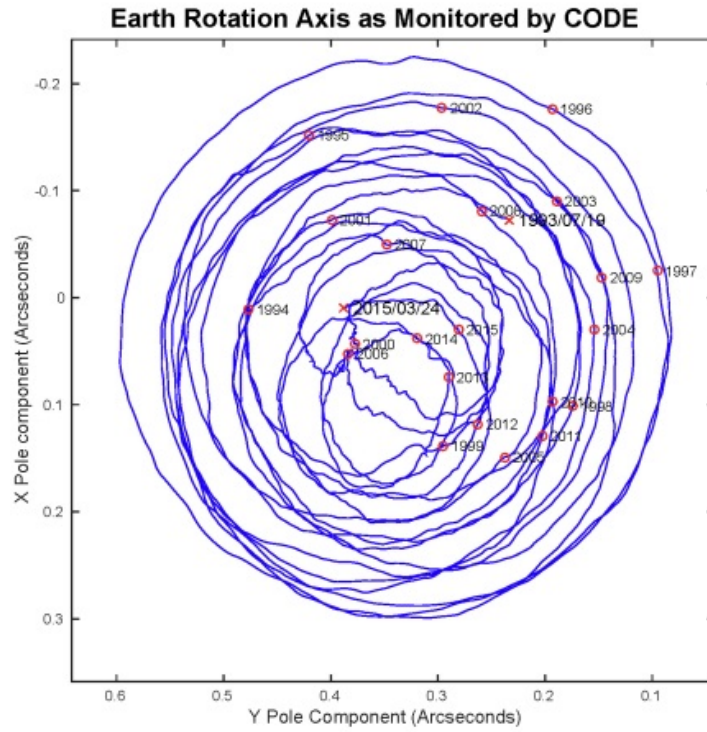


Figure 3.1: Polar motion derived from GNSS observations between July 1993 and March 2015.

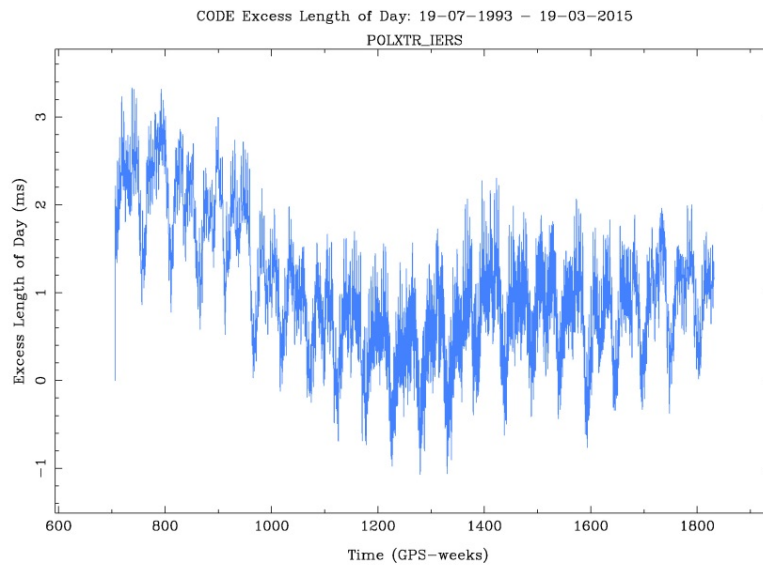


Figure 3.2: Excess length of day derived from GNSS observations between July 1993 and March 2015.

Impact of orbit modeling on GNSS-derived geodynamic parameters

D. Arnold¹, S. Lutz^{1,2}, G. Beutler¹, S. Schaer^{1,3}, R. Dach¹

¹Astronomical Institute, University of Bern

²Now with Federal Office of Topography, swisstopo

³Federal Office of Topography, swisstopo

The modifications of the empirical CODE orbit model to account better for the properties of non-GPS satellites, in particular of GLONASS satellites, are described in Arnold et al. (2015a) in this volume.

Orbit modeling, in particular modeling of solar radiation pressure (SRP) has a considerable impact on parameters of geophysical interest, in particular on the geocenter coordinates and on the Earth Orientation Parameters (EOPs) accessible to satellite geodetic methods. These are namely the x- and y-coordinates of the Earth's rotation axis, the so-called polar motion coordinates, and the angular velocity of Earth's rotation, expressed traditionally as excess day length, which is, apart from the sign, the first time derivative of *UT1-UTC*.

The variation of the GNSS-derived geocenter coordinates was studied in detail by Meindl et al. (2013a). It became in particular clear that GLONASS-only estimates resulted in heavily biased z-coordinates of the geocenter with amplitudes of more than 10 cm and periods of about 120 days. Figure 3.3 shows the spectra of the z-coordinates of the geocenter estimated using GPS-only, GLONASS-only, and combined observations of a global network of 92 combined GPS/GLONASS receivers in the years 2009-2011.

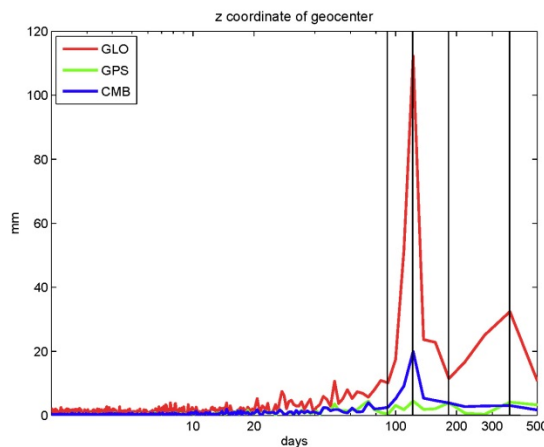


Figure 3.3: Amplitude spectra of geocenter *z* estimates in 2009-2012 using GLONASS-only, GPS-only, and combined solutions based on data of a global 92 receiver network

The amplitudes at 120 days (roughly three cycles per year, 3 cpy) for the GLONASS-only solution are truly remarkable – as documented by Meindl et al. (2013a). No trace of a 3 cpy term is present in the GPS-only solution. Unfortunately, a 20 mm amplitude still resides in the combined solution (blue curve in Figure 3.3).

Rodriguez-Solano et al. (2014) showed that the impact of the orbit model on the EOPs is significant, as well.

Let us focus now on the impact of SRP modeling on the EOPs. Whereas the physical effects are on the level of arc-seconds for polar motion and of milliseconds for the excess length of day (*lod*) – see Schaer et al. (2015b) in this volume - the impact of different SRP models is on the level of about 10-20 μ as for polar motion and of about 10 μ s for *lod*. These values are close to the noise level achievable by GNSS techniques, but as they are systematic in nature, they must be reduced to the extent possible.

Figure 3.4 shows the amplitude spectra of the differences of the x-coordinate of polar motion, as obtained from different orbit models, with respect to the corresponding values of the IERS 08 C04 series, which is in turn based on the contributions of all space geodetic techniques.

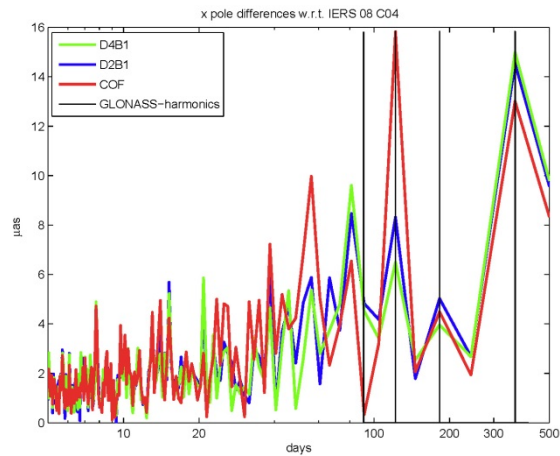


Figure 3.4: Amplitude spectra of differences of polar motion coordinate x obtained with different orbit models with respect to IERS 08 C04 (from Arnold et al (2015b)).

The COF series is based the old 5-parameter ECOM (section 1.4), the series D4B1 includes in addition to the parameters of the old ECOM the twice- and four-times-per-rev terms in the D-direction (direction Sun-satellite), and D2B1 represents a series, which includes only the twice-per-rev terms in D on top of the classic 5-parameter ECOM. The spurious term at 120 days in the x-coordinate of polar motion is clearly reduced by factors of about 2 and 3 for D2B1 and D4B1, respectively. The analysis performed by Arnold et al. (2015b), which led to the definition of the generalized ECOM, was based on the observations analyzed also in the frame of CODE REPRO-2. Figure 3.14 stems from Arnold et al. (2015b).

Two years of data are an absolute minimum to study orbit problems in GNSS analyses. It goes without saying that additional tests must be performed in the near future using the data of the year 2014. Also, the performance of the new ECOM in the IGS combination since January 4, 2015 must be monitored carefully.

Geocenter Estimation from GNSS data

S. Schaer^{1,2}, G. Beutler¹, R. Dach¹, M. Meindl³, S. Lutz^{1,4}

¹Astronomical Institute, University of Bern

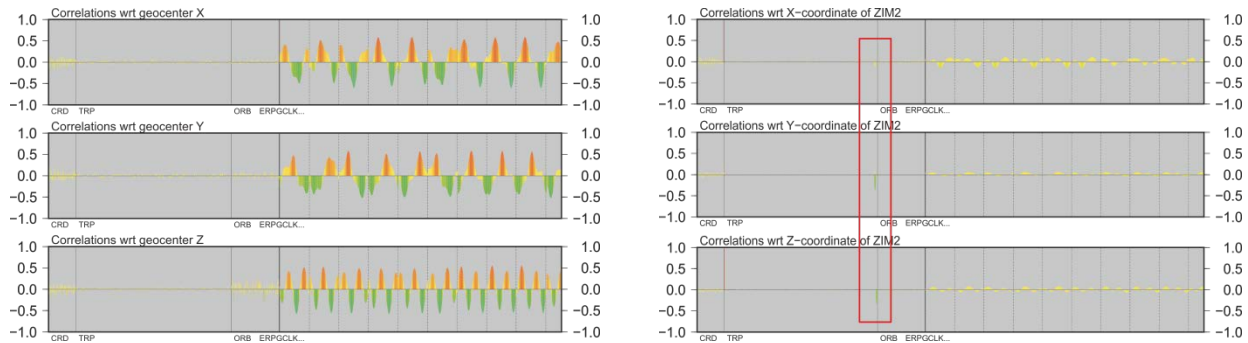
²Federal Office of Topography, swisstopo

³Institute of Geodesy and Photogrammetry, IGP, ETH Zurich

⁴Now with Federal Office of Topography, swisstopo

The satellites of the Global Navigation Satellite Systems (GNSS) are orbiting the Earth according to the laws of the celestial mechanics based on the gravitational law. As a consequence, the satellites are sensitive to the instantaneous center of the mass of the Earth. The coordinates of the (ground) tracking stations are referring to the center of figure as the conventional origin of the reference frame, which is supposed to be the long-term mean location of the center of mass. The difference between the center of mass and the center of figure is the instantaneous geocenter.

When estimating geocenter parameters from GNSS data in a IGS-style global solution (solving for GNSS satellite orbits, Earth rotation parameters, station coordinates, troposphere delays, receiver and satellite clock corrections) high correlations between geocenter parameters and satellite clock parameters result. They are, on the other hand, in the same order of magnitude like the correlations between station height and troposphere, compare both plots in Figure 3.5.



(note the correlation with the troposphere parameters, indicated with the red rectangle)

Figure 3.5: Correlations for selected parameters (top: geocenter parameters; bottom: station coordinates for ZIM2) extracted from the a posteriori covariance matrix; IGS-style GNSS solution with minimum constraint condition (no-net-translation and no-net-rotation) and geocenter parameters estimated.

To assess the sensitivity, the measurements for 90 globally distributed GNSS stations (GPS and GLONASS) are simulated without any observation noise. In this context the simulated phase measurements can serve for a solution where the ambiguities are freely estimated with real values. The code measurements may be used for a solution where all ambiguities are fixed to their correct integer values. An artificial geocenter shift of 10 cm towards the Z component is introduced when processing the simulated data. The results are summarized in Figure 3.6: If the shifted geocenter is forced to the origin of the reference frame (Datum: NNR+NNT; GCC: fixed) there is a discrepancy with respect to a “relaxed” solution (Datum: NNR+NNT; GCC: estimated). These differences underline the importance of the ambiguity resolution (otherwise the estimated real valued ambiguities may easily absorb a big amount of the geometric effects). The plots also illustrate, that the GLONASS orbits are much more sensitive to the geocenter discrepancy than the GPS orbits.

The simulation study has clearly shown that GNSS is sensitive to the geocenter as the deviation of the instantaneous center of mass from the origin of the reference frame. If the geocenter is not estimated, its influence propagates into

the other parameter (station coordinates, satellite orbits and clocks) of the GNSS analysis according to the error propagation laws of least squares adjustment. The geocenter parameters are highly correlated with other parameters in the GNSS data analysis – as for instance reported in Meindl et al. (2013a) - but the level of correlations is comparable with correlations between other parameters typically estimated in the GNSS data processing.

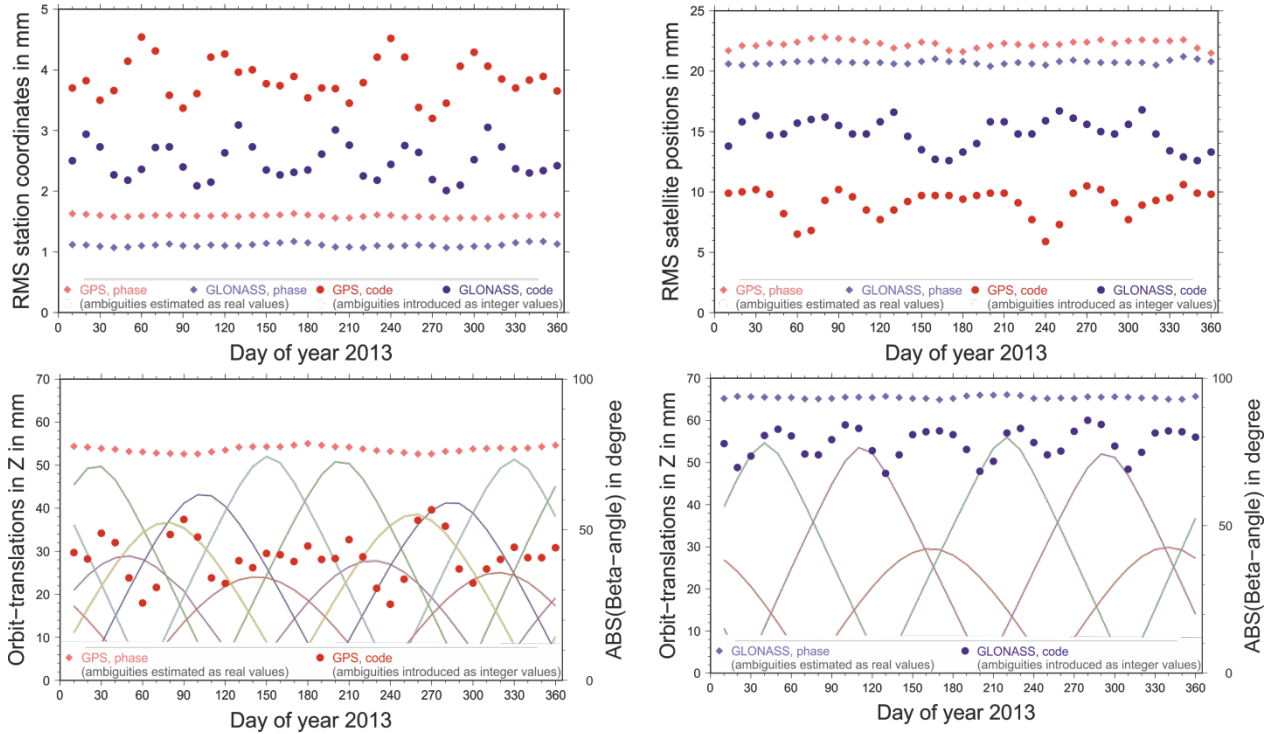


Figure 3.6: Comparison of the station coordinates (top left: RMS) and the satellite positions (top right: RMS; bottom translation in Z) using a Helmert-transformation between solutions from the simulated data once estimating with another one without estimating geocenter coordinates.

Geocenter coordinates and Earth rotation parameters from high and low orbiting SLR satellites

K. Sośnica^{1,2}, A. Jäggi¹, D. Thaller^{1,3}, R. Dach¹, A. Maier¹, G. Beutler¹

¹ *Astronomical Institute, University of Bern*

² *Now with Institute of Geodesy and Geoinformatics, Wrocław University of Environmental and Life Sciences*

³ *Now with Federal Agency for Cartography and Geodesy, BKG*

Geocenter motion can be defined as a motion of the center of mass of the entire Earth system, i.e., the solid Earth with oceans and the atmosphere, with respect to the origin of the reference frame. The reference frame is realized by long-term satellite observations provided by a network of ground stations. The artificial Earth satellites orbit around the instantaneous center of mass of the Earth in the inertial reference frame. Thus, a transformation between the inertial frame, defined by satellites, and the instantaneous Earth-fixed frame, realized by a global network of observing stations, provides the information about the geocenter motion. Geocenter is mathematically realized through the no-net-translation minimum constraint condition of the Helmert transformation imposed on a sub-set of stable fiducial stations that have well-established coordinates in the a priori reference frame.

In theory, all satellite geodetic techniques should be able to recover the geocenter coordinates. However, Global Navigation Satellite System (GNSS) and Doppler Orbitography and Radiopositioning Integrated by Satellite (DORIS) observations can be used for the determination of equatorial X and Y components of geocenter motion, but they are typically limited in the recovery of the Z-geocenter coordinate due to the correlation with orbit parameters related to the solar radiation pressure modelling (e.g., Meindl et al., 2013a, Kosek et al., 2014). SLR is nowadays the only technique that is fully capable of recovering the geocenter coordinates. The advantage of the SLR technique lies in the observation principle which applies very short and precise laser pulses, corresponding to a tracking accuracy at a level of a few millimeters. Moreover, SLR benefits from a simple construction of passive satellites, like LAGEOS. The geodetic SLR satellites are dense and spherical in shape and have greatly minimized area-to-mass ratios which also minimize the orbit perturbation related to non-gravitational forces, e.g., the atmospheric drag and solar radiation pressure.

Figure 3.7 shows the time series of geocenter coordinates derived from the 7-day SLR solutions using the observations to LAGEOS-1/2, Starlette, Stella, and AJISAI. The series is filtered using a 3-month sliding window of the Savitzky-Golay filter. The series shows seasonal variations with the mean amplitudes of 3, 2, and 4 mm for the X, Y, and Z components, however, the amplitudes vary for different periods. Until 2008 the mean offset of all geocenter components is below 1 mm and the slopes do not exceed 0.15 mm/year. This implies that the analysis is consistent with the a priori reference frame ITRF2008 that is based on the observations collected until 2008. In the period 2011-2013, the Y component shows a systematic shift of +4 mm and the Z component of -2 mm. Matsuo et al., (2014) associate these shifts with the accelerated ice mass depletion in Greenland and West Antarctica, which should introduce a slope of -0.17, +0.37, -0.56 mm/year for the X, Y, and Z component respectively. The origin of future reference frames should be aligned to the mean Earth's center-of-mass and thus it should be adapted to the processes related to the climate change.

The Earth rotation parameters (pole X and Y coordinates, and UT1-UTC or its first derivative in time denoted as Length-of-Day, LoD) define, along with the precession and nutation parameters, the transformation from the Earth-fixed to the inertial frame through a transformation matrix. Polar motion and LoD values can be derived from all space-geodetic techniques, whereas UT1-UTC can only be derived from VLBI or Lunar Laser Ranging observations, due to the direct correlation between UT1-UTC values with satellites' ascending nodes.

To assess the quality of SLR-derived Earth rotation parameters (ERPs), we generate three solutions using: (1) SLR observations to LAGEOS-1/2, (2) SLR observations to Starlette, Stella, and AJISAI (here called SLR-LEO), and (3) using all 5 satellites (here called multi-SLR). ERPs are mathematically computed through the no-net-rotation

minimum constraint condition of the Helmert transformation imposed on a sub-set of stable fiducial stations. We compare SLR-derived ERPs with the IERS-08-C04 series (Gambis, 2004) for the 7-day SLR solutions with and without co-estimating geopotential coefficients up to degree/order 4/4 (Sošnica et al., 2014). In the LAGEOS-1/2 solutions and in the multi-satellite SLR solutions without estimating the geopotential, the once-per-revolution empirical orbit parameters in the out-of-plane direction (WS/WC) are additionally estimated, because they are capable of absorbing large variations of C_{20} (Sošnica et al., 2012a). Omitting the estimation of WS/WC leads to inferior SLR solutions when C_{20} is not estimated.

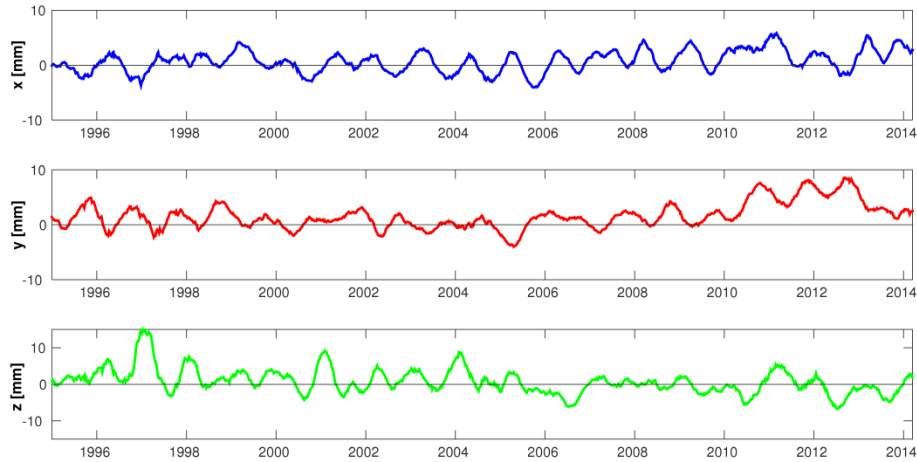


Figure 3.7: Geocenter coordinates derived from SLR observations filtered using a 3-month sliding window of the Savitzky-Golayfilter.

The current accuracy of SLR-derived polar motion, assessed using the WRMS w.r.t. the IERS-08-C04 series, is at a level of 118-149 μs , which corresponds to 4 to 5 mm on the Earth's surface. The WRMS of SLR-derived LoD, when the gravity field parameters are simultaneously estimated, is 56 $\mu\text{s}/\text{day}$, corresponding to about 26 mm on the Earth's surface, and the mean bias of SLR-derived LoD w.r.t. IERS-08-C04 is 6.3 $\mu\text{s}/\text{day}$, corresponding to 3 mm on the Earth's surface. In the LAGEOS solutions, the mean biases w.r.t. IERS-08-C04 for the X and Y pole coordinates are larger in the solution without estimating geopotential parameters. In the LAGEOS solutions with estimating geopotential the shift amounts to 4.1 and -8.0 μs for the X and Y pole coordinates, respectively. In the LAGEOS solutions without estimating geopotential parameters, these shifts are 45.8 and -54.1 μs . A particular degradation of LoD estimates is observed for the solution without estimating geopotential parameters, namely the WRMS grows from 57.0 to 120.5 μs . LoD absorbs the part of C_{20} that is not accounted for by a priori C_{20} values in the solution without estimating geopotential, which leads to a shift in LoD series (Sošnica 2014). As a result, the C_{20} estimates and the shift of LoD from the solution without estimating the geopotential are of the same order of magnitude. Thus, the estimation of C_{20} is beneficial for the LAGEOS solutions, when estimating LoD values.

The estimation of Earth's gravity field parameters is beneficial for low orbiting SLR satellites when a static a priori gravity field model is used. The degradation of pole coordinates is significant in the SLR-LEO solutions, which is reflected in WRMS of 267.9 and 437.5 μs for the X pole coordinate in the solutions with and without estimating the geopotential, respectively. Figure 3.8 (left) shows the X pole coordinates and Figure 3.8 (right) shows LoD estimates as differences w.r.t. the IERS-08-C04 series for different SLR solutions. The LAGEOS solution without estimating gravity field parameters is closest to the official ILRS solutions. Figure 3.8 clearly shows that including low orbiting satellites is beneficial for ERP estimation.

Both, the multi-SLR solutions with and without estimating the gravity field parameters, have a similar quality and a posteriori errors of pole coordinates at a similar level, which are much smaller as compared to LAGEOS-1/2 solutions. However, Figure 3.8 (left, middle) shows peaks of about 3.5, 7.0, and 14.0 days, which are related to the

lengths of the solution batches and its harmonics or to the orbit alias with tidal waves in the multi-SLR solutions with co-estimating geopotential. Figure 3.8 (left, middle) shows that all multi-SLR solutions (regardless whether estimating geopotential or not) do reduce the peaks in the X pole coordinate, which are apparent in the LAGEOS-1/2 solutions. These peaks are related to LAGEOS orbit modeling deficiencies or to the alias with tidal waves, e.g., the annual signal and an eclipsing period of LAGEOS-2 (about 111 days).

For LoD, the simultaneous estimation of the gravity field parameters reduces the offset of LoD estimates (Figure 3.8, right top), and reduces peaks in the spectrum analysis (Figure 3.8, right middle), which correspond, e.g., to orbit modeling deficiencies (peaks of 222 days - a draconitic year of LAGEOS-2, of 280 days - an eclipsing period of LAGEOS-1). The co-estimation of geopotential parameters substantially reduces the a posteriori error of estimated LoD (Figure 3.8, right bottom). The a posteriori error of LoD in the multi-SLR solutions (16.9 $\mu\text{s}/\text{day}$) is more than a factor of two higher than in the LAGEOS-1/2 solutions (7.1 $\mu\text{s}/\text{day}$) when the gravity field parameters are not estimated. This difference implies that the estimation of the gravity field parameters is essential for high-quality LoD estimates when using SLR data to low orbiting geodetic satellites.

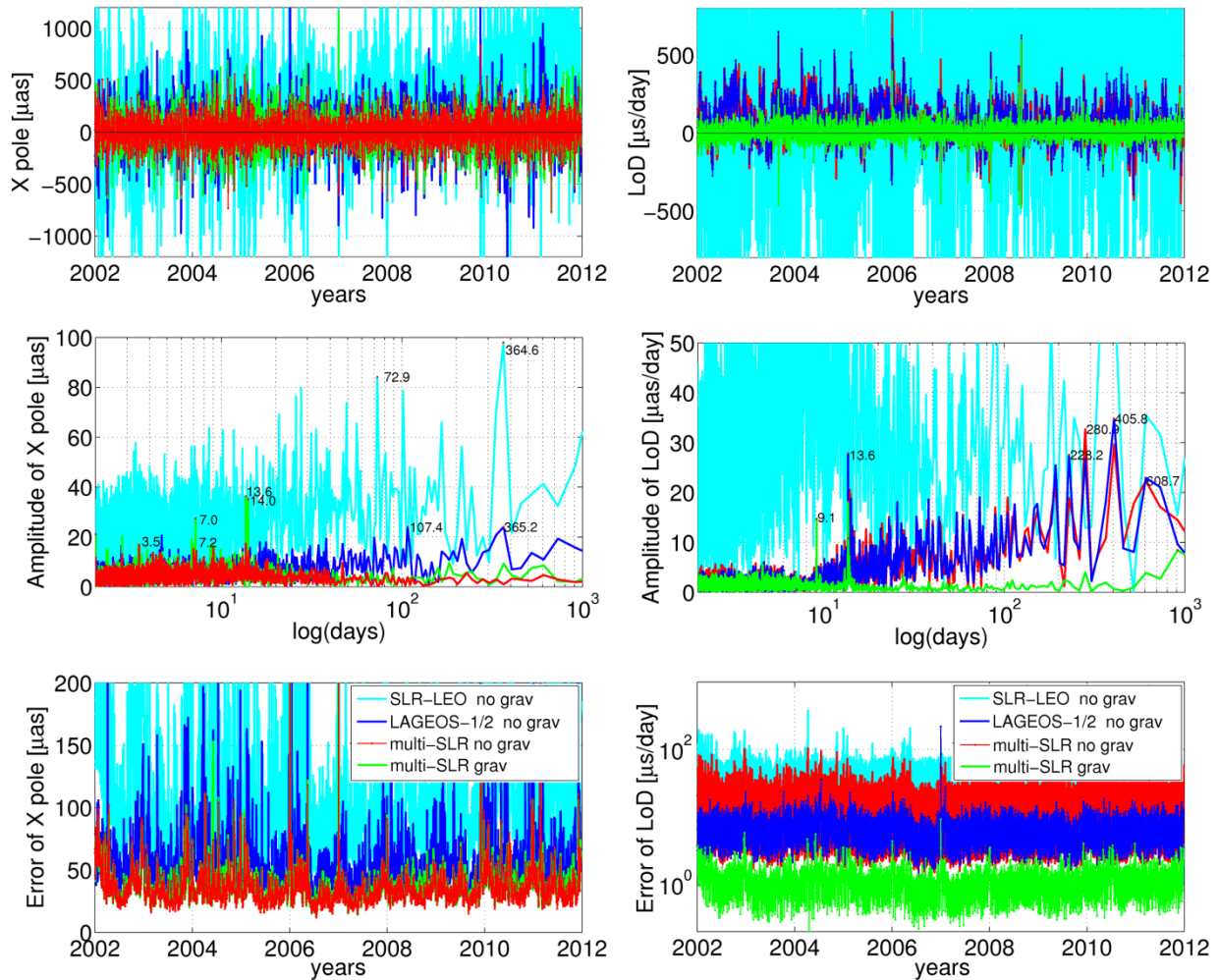


Figure 3.8: Left: Differences of the X pole coordinate w.r.t. IERS-08-C04 series (top), spectral analysis of the differences (middle), a posteriori errors of the X pole coordinates (bottom). The Y pole coordinate shows similar variations, thus, it is not shown here. Right: Differences of the LoD w.r.t. IERS-08-C04 series (top), spectral analysis of the differences (middle), a posteriori errors of LoD estimates (bottom). Note the logarithmic scale for the y axis in the bottom figure.

The Blue-Sky effect and the impact of the atmospheric pressure loading on SLR solutions

K. Sośnica^{1,2}, R. Dach¹, D. Thaller^{1,3}, A. Jäggi¹, G. Beutler¹

¹ *Astronomical Institute, University of Bern*

² *Now with Institute of Geodesy and Geoinformatics, Wrocław University of Environmental and Life Sciences*

³ *Now with Federal Agency for Cartography and Geodesy, BKG*

Displacements of the Earth's crust caused by tidal and non-tidal loading forces are of essential importance in space geodesy. Tidal corrections are commonly accepted by the international scientific community and applied at the observation level, whereas there is a still ongoing discussion on the way how to handle the non-tidal displacement corrections.

The combination of optical (SLR) and microwave (GNSS, VLBI, DORIS) observation techniques requires a special attention that has to be paid to atmospheric pressure loading corrections, because of the so-called Blue-Sky effect. The Blue-Sky effect is directly related to the weather-dependency of the SLR observations. SLR measurements can be performed only under almost cloudless sky conditions, typically during high air pressure conditions which deform the Earth crust downwards, and thus, introduce a systematic bias in all SLR-derived products. On the other hand the microwave techniques are weather-independent. Thus, applying the loading corrections reduces systematic effects from the SLR-derived parameters and enhances the consistency between SLR-based and microwave-based results through removing the impact of the Blue-Sky effect (Sośnica et al., 2013).

The impact of the Blue-Sky effect can be assessed as a difference between the mean atmospheric loading correction applied to SLR stations when an SLR station observes LAGEOS-1/2, and the mean correction to SLR stations for the entire time series (Sośnica et al., 2013). The effect assumes a value of 2.5 mm for many inland stations (note that there are no SLR stations in the region with the biggest atmospheric pressure loading deformation). The Blue-Sky effect reaches a maximum value of 4.4 mm for one SLR station located near Kiev in Ukraine. The largest effect yields for inland stations in central Asia and Eastern Europe, thus, for stations with largest impact of the atmospheric pressure loading.

Regarding the fact that some of the SLR stations are continuously improving their tracking capabilities the impact of the Blue-Sky effect becomes smaller for a few stations, e.g., the Blue-Sky effect was reduced for Zimmerwald from 1.8 mm in 1999 to 0.5 mm in 2010, for Greenbelt from 0.9 mm in 1999 to 0.3 mm in 2010, and for Katziwely from 3.1 mm in 1999 to 1.4 mm in 2010. The reduction of the Blue-Sky effect is especially visible for SLR stations which updated and automatized their laser systems or enabled day-time tracking capabilities. For the stations without significant tracking capability improvements, the Blue-Sky effect remains at the same level or even slightly increases.

Although the Blue-Sky effect is at the mm-level, it should be considered in SLR analyses, because all sources of errors leading to bigger discrepancies than 1 mm between space geodetic techniques should be taken into account in order to reach the goal of Global Geodetic Observing System (GGOS) for the precision of station positions of 1 mm. The Blue-Sky effect exceeds the goal of GGOS for about 57% of all SLR stations.

The mean Blue-Sky effect is 1.1 mm for all SLR stations. The systematic shift of the SLR station height due to the Blue-Sky effect has a non-negligible impact on the scale derived from SLR technique. The shift of 1.1 mm corresponds to a scale discrepancy of about 0.2 ppb w.r.t. the radius of the Earth. Therefore, the disagreement between the scale derived from SLR and VLBI, amounting 8 mm in ITRF2008, can be partly diminished when applying the atmospheric pressure loading corrections (Sośnica, 2014).

Applying atmospheric pressure loading corrections slightly improves the inner stability of SLR solutions and reduces the discrepancies between GNSS and SLR solutions. As a result, the estimated GNSS-SLR coordinate differences fit better at the 10% level to the local ties at the co-located stations (Sośnica et al., 2013). The impact of the atmospheric pressure loading is clearly detectable in the current high-quality SLR products, whereas, neglecting the loading corrections applied at the observation level introduces systematic effects in all SLR-derived parameters, i.e., in station coordinates, geocenter coordinates, satellites orbits, Earth rotation parameters, global scale, and gravity field parameters. The total impact of loading deformations cannot be fully accounted for when only the station coordinates are corrected in the a posteriori analysis, because all estimated parameters are affected. The impact of the atmospheric pressure loading on, e.g., the polar motion is systematic with a dominating annual signal of the amplitude of $45 \mu\text{as}$ and $42 \mu\text{as}$ for the X and Y pole coordinates, respectively (see Figure 3.10). Thus, the application of the loading corrections at the observation level is recommended for all space-geodetic solutions.

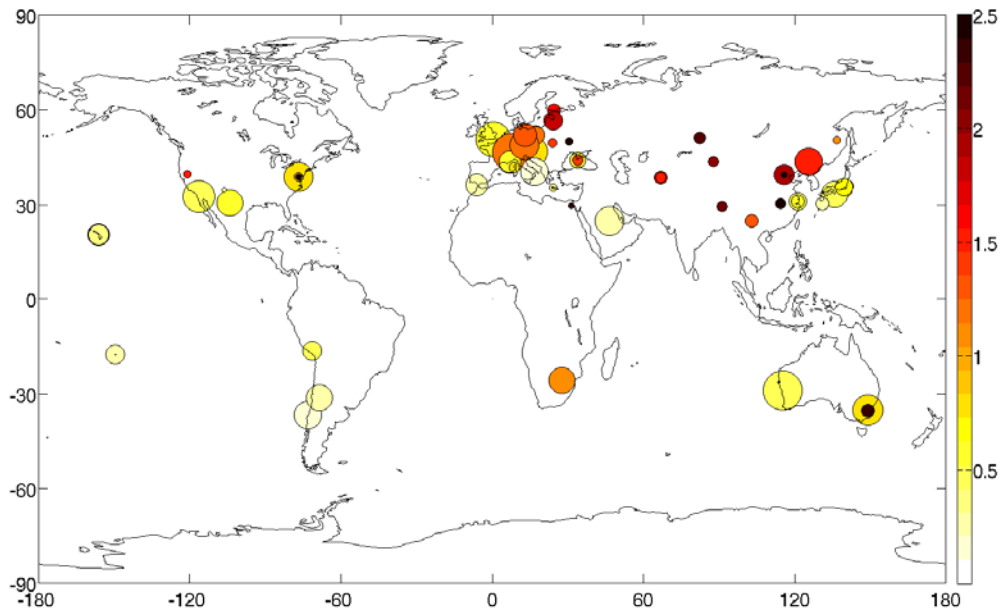


Figure 3.9: The Blue-Sky effect on SLR stations (units: mm). Area of the dots is proportional to number of normal points to LAGEOS satellites collected by stations.

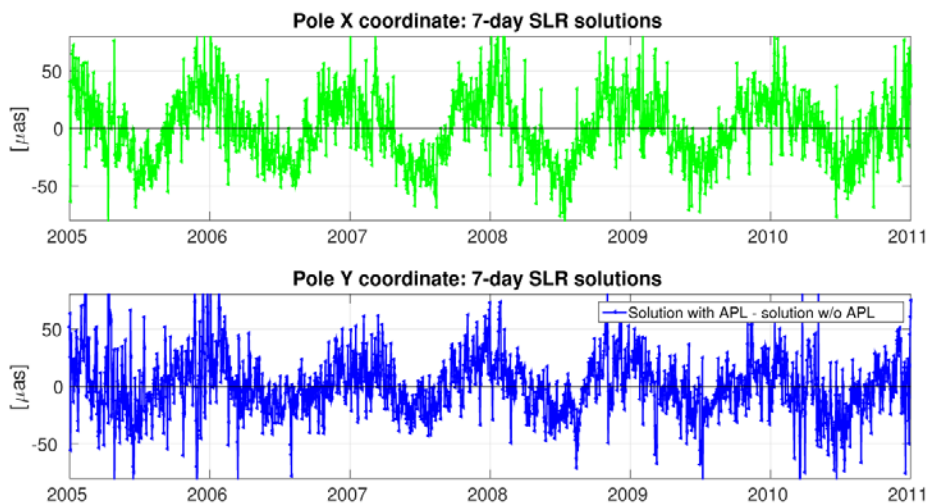


Figure 3.10: Differences of the pole coordinates derived from SLR solutions with and without applying atmospheric pressure loading (APL) corrections.

High-rate GPS for seismology

S. Hüberling and M. Rothacher

Geodesy and Geodynamics Lab, Institute of Geodesy and Photogrammetry, ETH Zurich

In recent years the development of GNSS receivers with sampling rates as high as 100Hz has sparked interest in capturing high-dynamic motions and has potentially enlarged the applicability in seismology.

The additional yield of information due to increased sampling rates, however, may be counteracted by a strong correlation of the measurements in time. Unfortunately, the tracking loop filters of the receivers produce correlations exactly in the frequency range (1-100Hz) of the expected benefit of high-rate receivers. The consequences of the correlations between subsequent epochs can be demonstrated by increased amplitude and phase retrieval errors during accelerated motions. The magnitude of these deviations directly depends on the bandwidth of the tracking loops used. A minimization of tracking loop-induced errors can be achieved in two ways: (1) by the optimization of the receiver tracking loop parameters (a larger bandwidth reduces the amplitude errors at high accelerations) and (2) by inverse filtering with a pre-estimated receiver transfer function. Especially for receivers with low and fixed tracking loop bandwidths the determination of a transfer function is crucial.

A lot of GPS coordinate time series with a broad variety of motions generated by a single-axis shake table have been produced. The discrepancies between the actual shake table motion (measured by inductive sensors) and the motions derived from the data of various GPS receivers are the basis for the determination of (receiver-specific) transfer functions. Based on sine oscillations with frequencies between 1-20Hz generated by the shake table, the relative amplitude and phase errors of 100Hz GPS measurements dependent on different loop bandwidths are shown in Figure 3.11 below. The solid lines denote the modeled receiver response based on the known receiver baseband parameters.

In contrary to seismological practice, using instruments already corrected by their response, the effect of the GPS receiver response was ignored up to now. However, the possible overestimation or reduction of the amplitudes and phase shifts are not insignificant for signals in the frequency range between 1 and 20Hz even with a wide loop bandwidth of 50Hz.

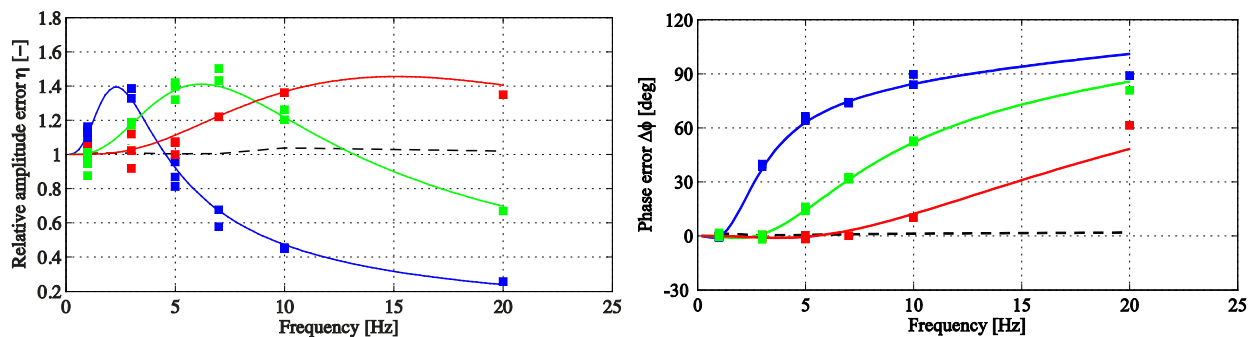


Figure 3.11: The squares represent the relative amplitude errors (left) and phase errors (right) between 100Hz GPS measurements by a Javad Sigma-G3TAJ receiver and the ground-truth. The measurements were performed with a loop bandwidth of 10Hz (blue), 25Hz (green), and 50Hz (red). The solid lines denote the modeled receiver response.

GNSS time series of the Tohoku earthquake

M. Meindl, P. Psimoulis, N. Houlié, M. Rothacher

Geodesy and Geodynamics Lab, Institute of Geodesy and Photogrammetry, ETH Zurich

Since 1994, the Geospatial Information Authority of Japan (GSI) operates a dense network of more than 1200 continuously observing GNSS receivers for crustal deformation monitoring as well as for surveying tasks. The stations of this so-called GNSS Earth Observation Network System (GEONET, Sagiya, 2004) cover Japan with a spatial distance of about 20 km.

Owing to GEONET, the Mw9.0 earthquake off the coast of Tohoku on March 11, 2011, is one of the best-observed seismic events ever. High-rate 1 Hz GPS observations recorded by 847 stations during the earthquake have been analyzed. The scientific Bernese GNSS Software 5.0 (Dach et al., 2007) was used to create high-quality coordinate time series based on a precise point positioning approach. The resulting displacement series show a formal accuracy of about 1 cm in North and East and about 2 cm in the vertical direction, respectively. Figure 3.12 shows the maximal horizontal and vertical displacements of the stations during the earthquake.

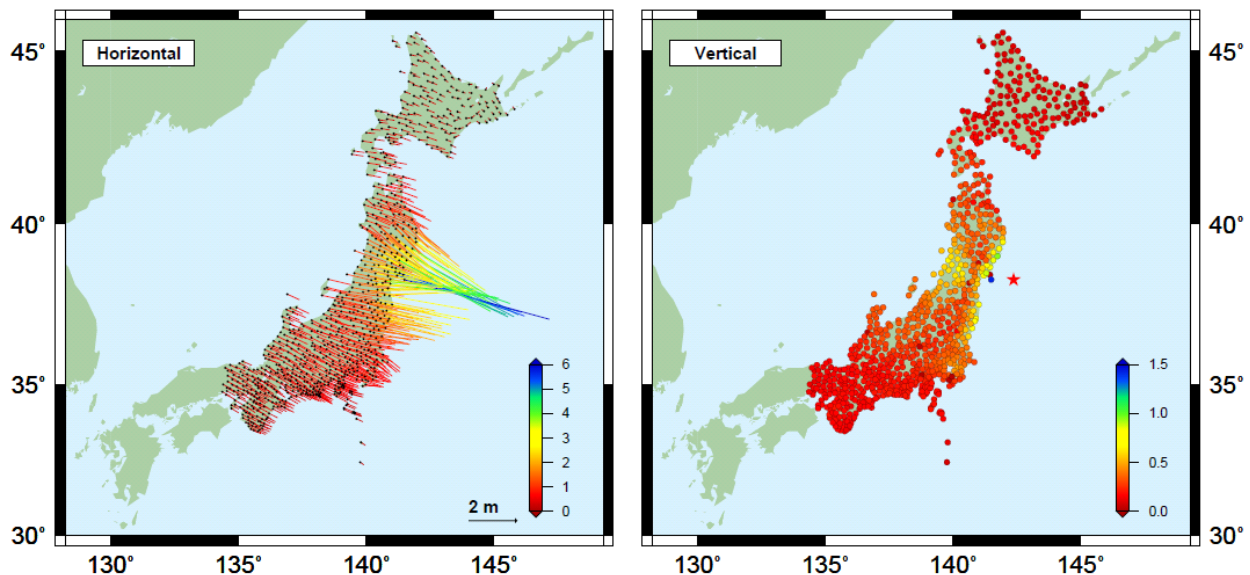


Figure 3.12: Maximum horizontal (left) and vertical (right) displacements as estimated from GEONET data (in m).

The displacement time series cannot only be used to visualize the earthquake (as in Figure 3.12) but they also contain valuable information for scientific research in the field of seismology and geophysics.

Psimoulis et al. (2015) used the series for comparisons with data from co-located strong-motion seismometers. They conclude that GPS and strong motion/accelerometer data can support and complement each other in certain frequency ranges. In another study (Psimoulis et al., 2014d), the displacements are successfully used to determine long-period oscillatory ground motions. These GPS-based motions are in good agreement with integrated accelerograms for the frequency range of 3-100 seconds.

GNSS reference stations for geodynamics and seismology in the Swiss Alps

P. Limpach, A. Villiger and A. Geiger

Geodesy and Geodynamics Lab, Institute of Geodesy and Photogrammetry, ETH Zurich

Five permanent GNSS reference stations were installed by the Geodesy and Geodynamics Lab (GGL) in canton Valais, Switzerland, from 2011 to 2014, in the frame of the COGEAR project. The stations are equipped with geodetic-grade Leica GRX1200+ GNSS receivers and Leica AR25 GNSS antennas (Figure 3.13). COGEAR (Coupled Seismogenic Geohazards in Alpine Regions) was a 4 years interdisciplinary project investigating the hazard chain induced by earthquakes. It was supported by the Competence Center for Environment and Sustainability (CCES) of the Swiss ETH Domain. The 5 GNSS stations are enlarging an existing network of 5 GNSS stations in Valais, already operated by GGL since 2005/2006. Between 2011 and 2014, these 5 stations were modernized, especially in terms of data transmission. To date, GGL operates 10 GNSS reference stations in Valais (Figure 3.14). The primary objective of these stations is the densification of the Swiss national GNSS network AGNES, operated by swisstopo, in a mountainous area with relatively high seismic activity compared to the rest of the Swiss territory. The major goals are long-term observations of tectonic crust deformations and observations of co-seismic deformations at small scales. Three of the stations are co-located with seismometer stations from the Swiss Seismological Service. In addition to a standard sampling interval of 30 s, all stations are collecting high-rate GNSS observations, locally stored in a ring-buffer, in order to support research in the field of GNSS seismology. The high-rate sampling frequencies are 20 Hz, 10 Hz or 1 Hz, depending on the receiver hardware. In cooperation with swisstopo, the COGEAR GNSS network is referenced to the national AGNES network. The data of the COGEAR network is operationally processed at GGL on a daily basis with Bernese GNSS software, together with a subset of AGNES stations. The COGEAR data is shared with swisstopo, where the data is integrated in the official processing of the AGNES network. The COGEAR GNSS stations (see Figure 3.13) are also used as a reference network for the monitoring of local deformations, slope instabilities and mass movements with low-cost single frequency GNSS receivers (see this Swiss National Report “GNSS for Deformation and Geohazard Monitoring in the Swiss Alps”).



Figure 3.13: Reference station RAND of the COGEAR GNSS network.

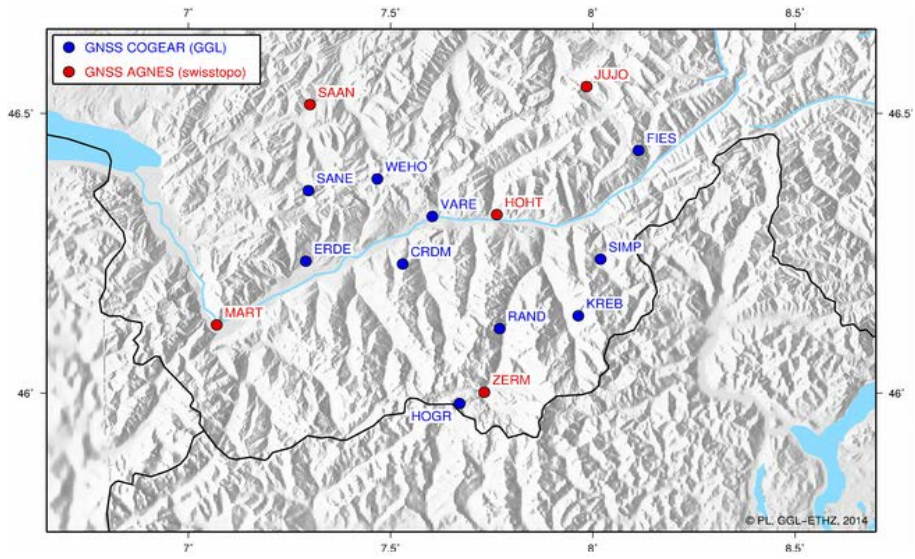


Figure 3.14: GNSS reference stations operated by GGL in the area of Valais, Switzerland (blue dots) and GNSS stations of the national AGNES network operated by swisstopo (red dots).

The Geodetic Three Dimensional Strain-Rate Field in Switzerland: New Methods and Results

A. Villiger¹, A. Geiger¹, E. Brockmann², A. Wiger², U. Marti²

¹Institute of Geodesy and Photogrammetry, ETH Zurich, Switzerland

²Federal Office of Topography swisstopo, Wabern-Bern, Switzerland

Compared to seismically active regions like Greece the seismogenic hazard in Switzerland is relatively small. Nevertheless, larger earthquakes can't be excluded also in Switzerland. In the regions of Valais and Basel seismic events with a magnitude above six have occurred.

The development of the geodetic metrology and satellite technology have made tools available to the researchers allowing for the precise determination of even small changes of any earth related parameters. Continental drift, crustal deformations and the strain accumulation can be determined and verified by geodetic means. However, this prove is not easy to be given in the region of Switzerland, because of the very small yearly movements generating equivalently small yearly distortions at a maximum of 25 nstrain per year corresponding to 2.5 mm on a baseline of 100 km.

Since many years the Swiss office of topography is carrying out repeated GNSS measurements on its first order network. The resulting time-series of coordinates together with the long-standing levelling time-series form the data base for the estimation of a coherent kinematic deformation field of Switzerland.

Thanks to further developments of the 'Adaptive Least-Square Collocation (ALSC)', which was devised at GGL, and the consideration of a physical crustal model it became possible to directly calculate a three dimensional strain tensor field from the combined surface measurements, e.g. GPS and levelling (Figure 3.15). Strain tensors thus obtained reveal a very high conformity with focal mechanisms determined from seismological data. For example the recently induced earthquake mechanism in the region of St. Gallen is in a complete agreement with the strain tensors determined by GPS-data (Figure 3.16).

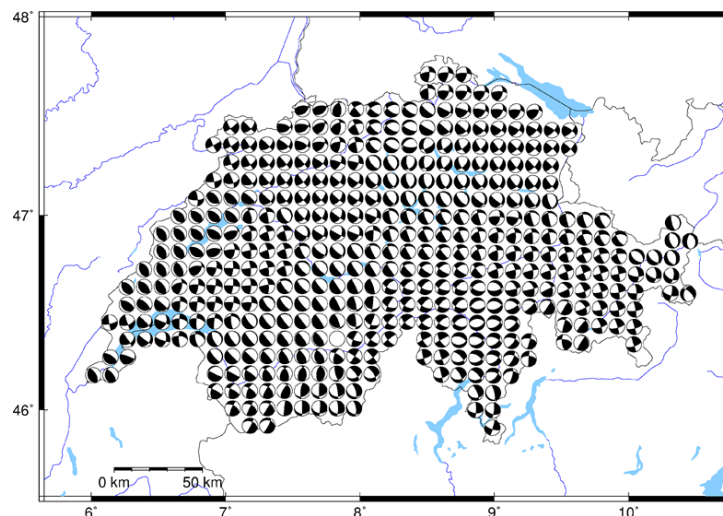


Figure 3.15: Three dimensional focal mechanisms ('Beachballs') derived from GNSS measurements. This data can be calculated from 3D crustal deformations determined by GNSS and levelling (Villiger, 2014).

The results represent an important step towards a deeper understanding of the processes underlying the crustal deformation in Switzerland. It is a novelty having shown the ability to predict focal mechanisms by GNSS data of very tiny long-term deformations.

The presented work is part of GGL's and SGC's activities in the domain of detection of recent crustal deformations and has been carried out in the frame of swisstopo's 'swiss 4D'-project.

The Swiss National Science Foundation and the Competence Center Environment and Sustainability of the ETH Domain (CCES) have partially funded the work in the frame of the project COGEAR.

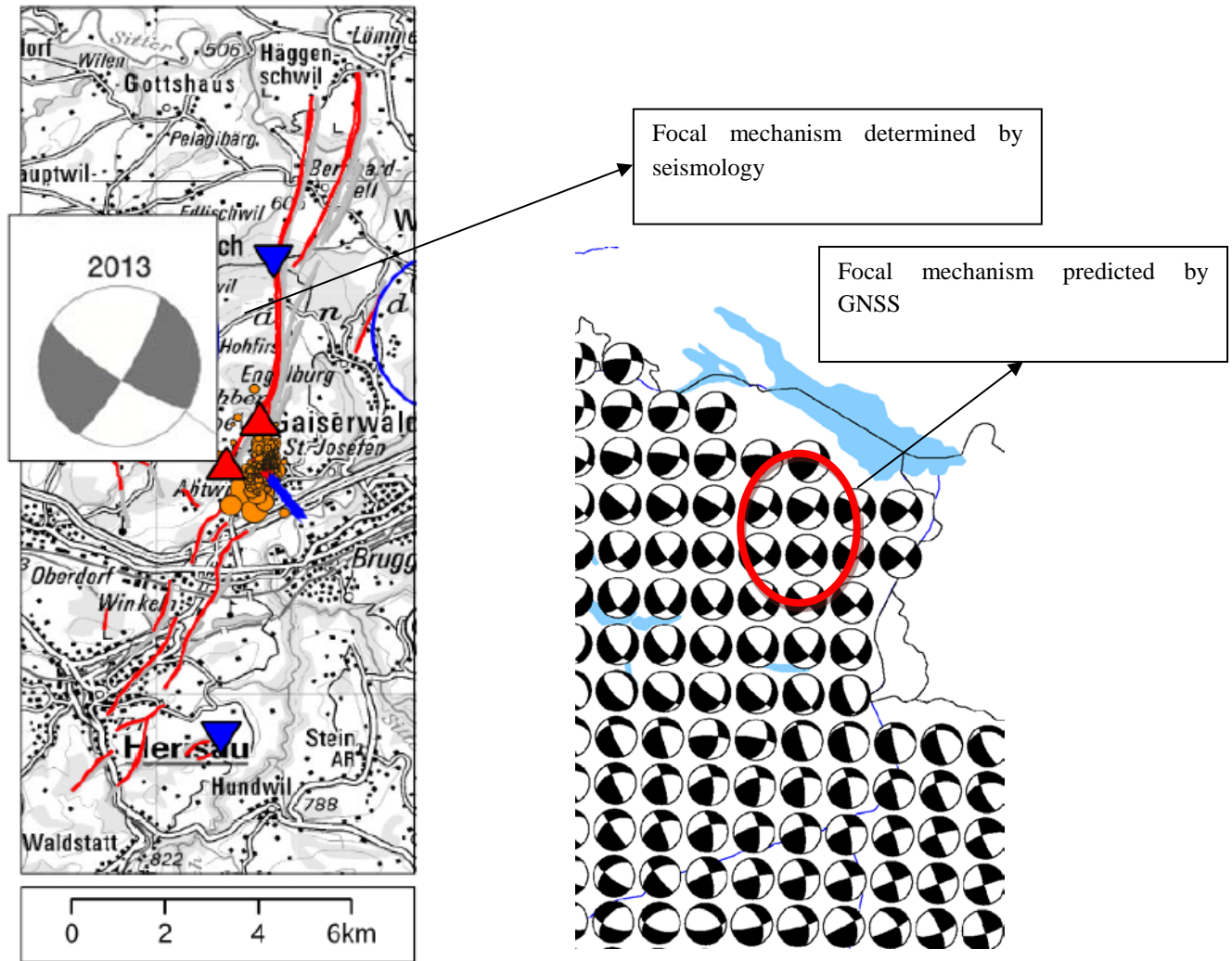


Figure 3.16: Detailed view of the region of St. Gallen. An earthquake triggered by geothermal experiments shows a seismologically determined shear mechanism which absolutely corresponds to the mechanism anticipated by geodetic measurements and our 3D predictor. (Villiger, 2014).

Strain rate and stress field of Switzerland

N. Houlié^{1,2}, J. Woessner³, M. Rothacher² and D. Giardini¹

¹ Seismology and Geodynamics, Institute of Geophysics, ETH Zurich

² Geodesy and Geodynamics Lab, Institute of Geodesy and Photogrammetry, ETH Zurich

³ Schweizerischer Erdbebendienst, ETH Zurich

We use geodetic and seismic datasets to check whether the surface deformation and the seismic activity are in agreement in terms of moment release and stress/strain orientations within the territory of Switzerland. We find that for most of the country, the stress released is consistent with the lithosphere deformation measured by the Global Positioning System (GPS). The surface strain rate ($< 5.0 \cdot 10^{-8}$ /yr) fits well with an average stress rate release of $\sim 2.0 \cdot 10^{11}$ Nm/yr, however, displays few agreement with long-term (and deep) deformation. For three regions, we find seismic activity and surface deformation not to be in agreement. In the Basel area, deep seismicity exists while surface deformation is absent.

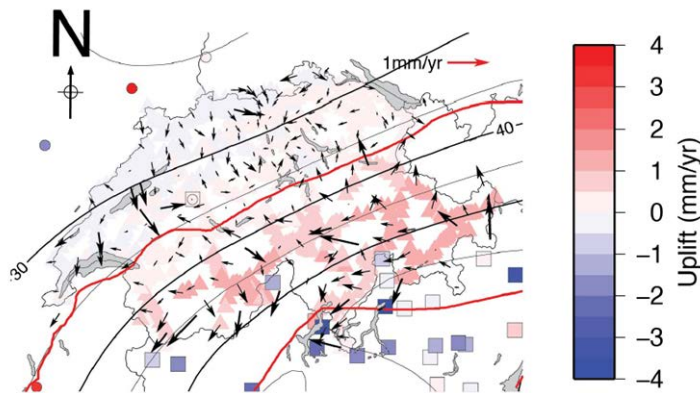


Figure 3.17: Horizontal relative (ZIMM fixed) and vertical rates computed from both, local and regional geodetic data in Switzerland and Europe (ITRF2008). Moho depths (km) (Spada et al., 2013; Wagner et al., 2012) are overlaid on uplift rates. A reasonable correlation between Moho depth and highest uplift rates (> 1 mm/yr) is visible. The ZIMM site is indicated by a circle inside a square.

This situation is in contrast to what is found in the Ticino and the Swiss Jura, where the seismic activity is absent, but surface deformation is detected ($\sim 2 \cdot 10^{-8}$ /yr). From surface strain rates, assuming that the entire accumulated strain over the last 120 yr is released seismically, we estimate the potential for a magnitude MW ~ 5.7 with very few seismicity detected in the Ticino while with the same strain rates in the Valais, seismic activity is abundant with historically documented destructive earthquakes.

Across plate boundaries (California, Northern Turkey, Iceland or New Zealand), where the seismic activity is important, measuring the surface strain rates is made easier, because their amplitudes are high ($> 10^{-7}$ /yr). In such areas, long-term strain rates are in agreement with seismic observations. There, higher strain rates also tend to shorten theoretical seismic cycle lengths (Houlié and Romanowicz, 2011b), enabling us to document larger portions of the seismic cycle. For slow deforming areas and intraplate regions, however, fewer seismic events are available to study and strain rates are of smaller amplitude, while seismic hazard may be significant, because fault systems, sometimes hidden under the surface, remain active and dangerous to populations. Studying these areas nonetheless allows us to understand, how small strain rates distribute across multiple fault systems and also, if stress can be stored without inducing rupture for long periods of time. In summary, studies focusing on tectonically quiet areas bridge the knowledge we gained on the dynamics of both plate boundaries and continental units. At the meeting point between the central European platform (Germany, Poland, Czech Republic), the Adria plate and the Alpine

orogen, Switzerland experiences little surface deformation with a strain rate $< 10^{-7}$ /yr (or less than 5 mm/yr over 50 km, the typical distance between two permanent GPS stations).

Strain accumulated in the Valais and the Ticino are, from a geodetic perspective, of similar size, however, the seismically released moment in the Ticino is by about a factor ten lower and may therefore 1) lead to an event of significant magnitude that is not present in today's historical catalogue for this area or 2) could be explained by the presence of crustal dislocation creep. The seismic hazard models for Switzerland report very small probabilities of moderate to large events in Ticino. From our observation and modelling results, we conclude that either the strain accumulated in Ticino is released through a different process within the lithosphere (deformation creep or distributed over several small fault systems) or that the seismic energy is not dissipated, implying a possible moderate to large event in future.

Assessment of high-rate GPS time series at long periods

K. Kelevitz¹, N. Houlié^{1,2}, D. Giardini¹ and M. Rothacher²

¹ Seismology and Geodynamics, Institute of Geophysics, ETH Zurich

² Geodesy and Geodynamics Lab, Institute of Geodesy and Photogrammetry, ETH Zurich

We present the comparison of 1 Hz GPS waveforms, very broadband seismograms and superconductivity gravimeter time series recorded during and after three mega-thrust earthquakes (2003 Hokkaido, 2004 Sumatra and 2011 Tohoku-Oki) for various period bands ($T > 30$ s). With this study we aim at filling the data availability gap that exists between periods of 300 s and 1200 s, corresponding to long period surface waves and the first normal mode of the free oscillation of the Earth, respectively. We assess the performance of each dataset at the light of comparisons with synthetic displacement waveforms. We find that GPS is well capable of recovering millimeter ground motion oscillations in a wide range of periods (30 to 1300 s), potentially providing valuable information on the lithosphere and upper-mantle heterogeneities on a scale of 300 to 3000 km.

Long-period surface motions play an essential role in the completion of Earth velocity models. These signals that participate in constraining the rheology of the crust and the upper mantle, are truly the backbone of large scale tomography. Both phases and arrival times of principal seismic waveforms are essential to the global consistency of the models, to the mapping of velocity anomalies on various scales and to the refining of 1D Earth models that are often used as a-priori models by inversion algorithms. Today, long-period data are provided by the very broadband seismometers operated by large regional (e.g., Berkeley Seismological network, USArray) or global (e.g., GEOSCOPE, Global Seismic Network) initiatives. The installation and maintenance costs of such instruments being very high, make these data very precious and the networks difficult to expand. Nevertheless, the quality of Earth velocity tomography depends on the location of instruments, on the quality of data available and on our capability to invert these data with precision. Thanks to both, the large amount of data collected by dense seismic networks and the increasing computational resources, global Earth velocity models are continuously improving. For regions located beneath the crust and down to depths of 400 km, most models are in agreement.

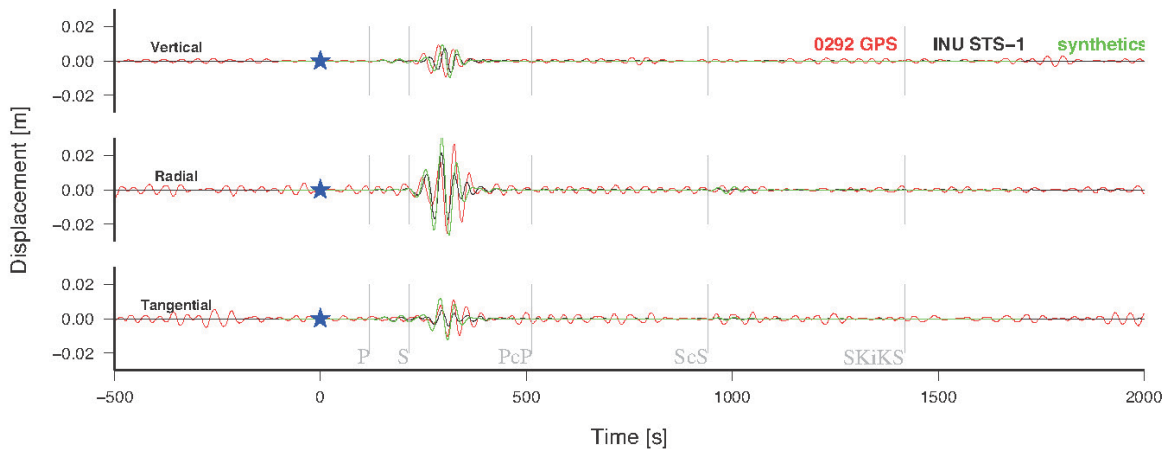


Figure 3.18: Vertical, and horizontal (radial and tangential) displacement series of GPS station 0292 (red), co-located INU STS-1 seismic station (blue) and synthetic data (green) of the Hokkaido earthquake with a 30 to 50 s Butterworth filter applied. The blue star indicates the origin time of the earthquake.

We compare high-rate GPS, broadband seismometer and superconducting gravimeter waveforms with 3D synthetic waveforms computed with SPEC-FEM 3D GLOBE (Komatitsch and Tromp, 2002) and AXISEM (Nissen-Meyer et al., 2014) codes. We determine displacement waveforms of periods ranging from 30 s to 1300 s for a selection of

high-rate GPS sites. By computing long-period waveforms, we supplement data gaps limited by the periods sampled by the surface wave ($T < 60$ s) and the first normal modes ($T \sim 1200$ s) period ranges. Evidence from processed high-rate GPS data of the 2003 Hokkaido, 2004 Sumatra and 2011 Tohoku-Oki earthquakes shows that the long-period GPS waveforms are in agreement with the synthetic seismograms and therefore that GPS is reliable to map seismic velocity heterogeneities. We conclude that GPS instruments have the potential to supplement networks of broadband seismometers and to enhance large-scale structures in the upper- and mid-mantle in the next generation of seismic tomography. The differences between the long-period GPS waveforms and the synthetic seismograms can be interpreted as deviation from the IASP91 or the S362ANI reference models used for generating the synthetic seismograms. These differences in surface wave propagation translate to lateral variations in the properties of the upper mantle, typically variations in density.

Lithosphere-asthenosphere interactions near the San Andreas fault

N. Houlié^{1,2}, Chamberlain³, C. and T. Stern³

¹ Seismology and Geodynamics, Institute of Geophysics, ETH Zurich

² Geodesy and Geodynamics Lab, Institute of Geodesy and Photogrammetry, ETH Zurich

³ Victoria University, Wellington, New Zealand

We decipher the strain history of the upper mantle in California through the comparison of the long-term finite strain field in the mantle and the surface strain-rate field, respectively, inferred from fast polarization directions of seismic phases (SKS and SKKS), and Global Positioning System (GPS) surface velocity fields. We show that mantle strain and surface strain rate fields are consistent in the vicinity of San Andreas Fault (SAF) in California. Such an agreement suggests that the lithosphere and strong asthenosphere have been deformed coherently and steadily since $> 1\text{Ma}$. We find that the crustal stress field rotates (up to 40° of rotation across a 50 km distance from 50° relative to the strike of the SAF, in the near-field of SAF) from San Francisco to the Central Valley. Both observations suggest that the SAF extends to depth, likely through the entire lithosphere. From Central Valley towards the Basin and Range, the orientation of GPS strain-rates, shear wave splitting measurements and seismic stress fields diverge indicating reduced coupling or/and shallow crustal extension and/or presence of frozen anisotropy.

In this study we assess the suitability of these end members to the San Andreas Fault zone in California, applying the techniques outlined by Houlié & Stern (2012e) and applied similarly to the Alpine Fault of New Zealand. Houlié & Stern used the GPS velocity field to compute strain rate fields of New Zealand and compare the maximal strain rate component ($\dot{\epsilon}_1$) field to the orientation of the fast axis of shear wave splitting based on the measurements of the SKS and SKKS seismic phases.

In contrast to the recent case study of New Zealand, where (Houlié and Stern, 2012e) were able to discern three distinct zones between pure, simple shear and volcanic stresses, in California the context is different. The pure shear zone following the extent of the fault is interrupted by significant deviations as discussed around the Clear Lakes volcanic centre, San Jose and the Big Bend region. The lack of diversity in the pattern of shear around the SAF is remarkably low considering the complexity, large lateral extent and total deformation of the area.

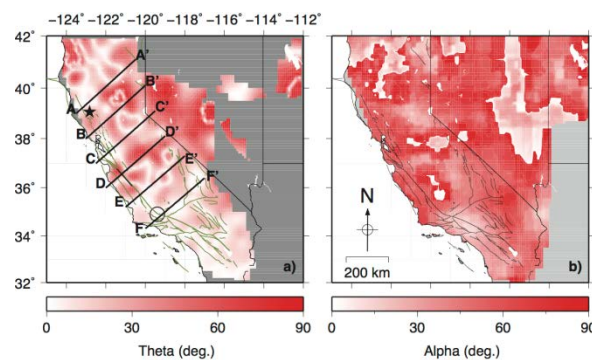


Figure 3.19: (a) θ as calculated from the difference between the SKS fast direction and the maximum extension direction derived from GPS. Both the GPS strain-rate field directions and shear wave splitting fast directions have been interpolated using the GMT surface algorithm. Both grid schemes use a node interval of 0.1° in both latitude and longitude. (b) α , the angle between GPS maximum shortening strain rate direction and average fault strike of 145° , interpolated using GMT surface algorithm with a 0.1° node interval. In panel a, the closed star locates Clear Lake, thick black section of SAF locates the approximate extent of the creeping section and the open circle gives the approximate location of the big bend region.

The similar stress orientations in both the crust and the mantle around the SAF zone are indicative of strain and stress transfer throughout the lithosphere. Therefore, it would hold that the San Andreas is a deep, pervasive fault structure as suggested by the recent documentation of non-volcanic tremor beneath the seismogenic extent (at around 30 km) of the SAF. The consideration that Northern California is thought to be underlain by partially subducted Pacific lithosphere is important, hence the accumulated stress is likely distributed throughout the Pacific lithosphere, which would suggest that some shear would occur on the near-horizontal interface between the crustal blocks at depth.

Long-period surface motion of the multi-patch Mw9.0 Tohoku-Oki earthquake

P. Psimoulis, N. Houlié, M. Meindl and M. Rothacher

Geodesy and Geodynamics Lab, Institute of Geodesy and Photogrammetry, ETH Zurich

We show that it is possible to capture the oscillatory ground motion induced by the Tohoku-Oki event for periods ranging from 3 s to 100 s using precise point positioning. We find that the ground motions of the sedimentary basins of Japan were large (> 0.15 m/s and > 0.15 m/s² for velocity and acceleration, respectively) even for periods larger than 3 s. We compare geodetic observables with a ground motion prediction equation designed for Japan's seismicity and find that the spectral acceleration is well estimated for periods larger than 3 s and distances ranging from 100 to 500 km. At last, through the analysis of the displacement attenuation plots, we show that the 2011 Tohoku-Oki event is likely composed of multiple rupture patches as suggested before by time-reversal inversions of seismic data.

The Mw9.0 earthquake off the Pacific coast of Tohoku-Oki on 2011 March 11 was fully recorded by the GEONET network, operated by the Geospatial Information Authority of Japan (GSI). The GEONET network is composed of over 1200 continuously observing GPS receivers (with an average spacing of 20 km). We processed 1 Hz GPS records from 847 GEONET stations of 15-hr duration, fully covering the earthquake period. The data was analyzed with the Bernese GNSS Software Version 5.0. The data were post-processed in a PPP mode using state-of-the-art models and a-priori information of highest quality from the Center for Orbit Determination in Europe (CODE). The displacement time-series in North, East, and vertical components were established separately for each station. The GPS displacement time-series show an a posteriori formal accuracy of about 1 cm in the horizontal and 2 cm in the vertical component, respectively.

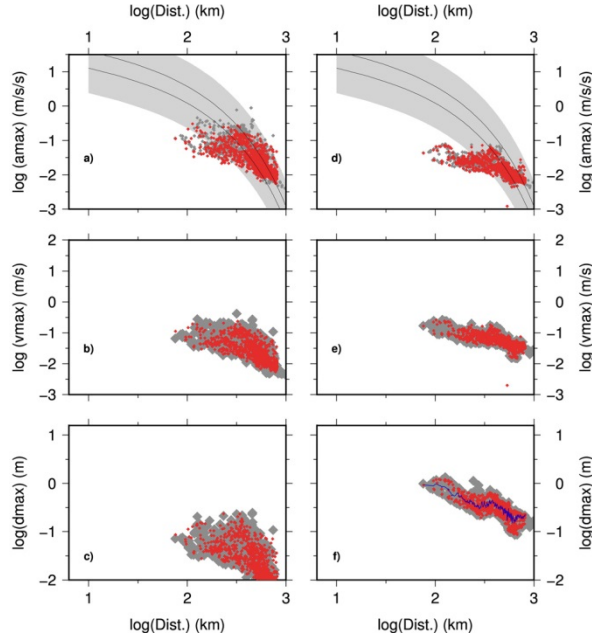


Figure 3.20: GPS (red) and strong-motion (grey) Maximum Ground Acceleration (MGA) velocity (MGV) and displacement (MGD) for the 3–10 s (left-hand panel) and 10–100 s (right-hand panel) period bands. The blue curve shows the average GPS MGA/MGV/MGD values.

The first conclusion of our work is that both, GPS displacement histories and integrated accelerograms are in agreement for the frequency range they have in common (3–100 s). We find that long-period oscillatory ground motions are accurately determined when based on GPS data. The double integration of accelerograms does not impact the precise resolution of the derived displacement data for periods less than 100 s for a large earthquake such as the Tohoku-Oki event. In future, the PPP GPS data will be processed in near real-time or even real-time (temporal point positioning), allowing the computation of maximum ground motion to supplement other seismic monitoring systems. Considering that the ground acceleration is expected to be more than five times higher at a period of 1 s than the signal at a period of 10 s, the reliability of the GPS for higher sampling rates (>1 Hz) will mostly depend on our capability to maintain the noise of the time-series at a level close to cm. We propose that the future generations of Ground Motion Prediction Equations (GMPEs) should include more long-period data such as GPS displacement time series, in order to better estimate effects of large magnitude ($M_w > 7$) events. Furthermore, we highlight the response of major sedimentary basins of Japan to the shake that followed the Mw9.0 Tohoku-Oki 2011 earthquake, for periods ranging from 3 to 10 s. The increase in oscillatory displacement at ~ 250 km distance from the epicenter can be interpreted as a second source of displacement along the fault generated by a second asperity as proposed by the source models of Maercklin et al. (2012). Long-period maximum oscillatory displacement can therefore be used as a constraint for source inversions, providing additional constraints on spatial pattern of rupture at depth.

Recent Crustal Vertical Movements from levelling and GNSS permanent networks

E. Brockmann, A. Schlatter

Federal Office of Topography swisstopo, Wabern, Bern

The analysis of more than 15 years of permanent AGNES and EPN/IGS data allow an estimation of vertical rates for the station coordinates. Additionally, vertical uplift rates can also be estimated using 100 years of repeated levelling for the Swiss levelling benchmarks which were observed at least 3 times.

In 2014 a new adjustment of the levelling network was performed, adding eight additional years to the previous adjustment where data till 2004 (RCM0406) were used. These results are labeled CHVTRF12 in Figure 3.21, RCM12 in Figure 3.22. In total, the impact of the additional observations on the levelling-derived velocities is extremely small.

A comparison of both methods, shown in Figure 3.22, impressively shows a general Alpine uplift. Nevertheless, the GNSS-derived vertical rates seem to be significantly higher especially in the northern region of Switzerland.

Due to the fact that the analysis of the Swiss permanent network AGNES is embedded in the European EPN/IGS network, the movements with respect to the stable part of the Eurasian plate can be determined. The results show that Switzerland is rising in average by 1.2 mm/year.

The GNSS results were recently updated by using the results of the reprocessing (1994-2014) and by using daily instead of weekly normal equations to estimate the velocities. The impact of switching to the consistently processed data is according to Figure 3.23 quite small (standard deviation of ± 0.25 mm/yr for the Swiss sites). Positive is also the availability of reliable velocities of an increased number of stations in Europe.

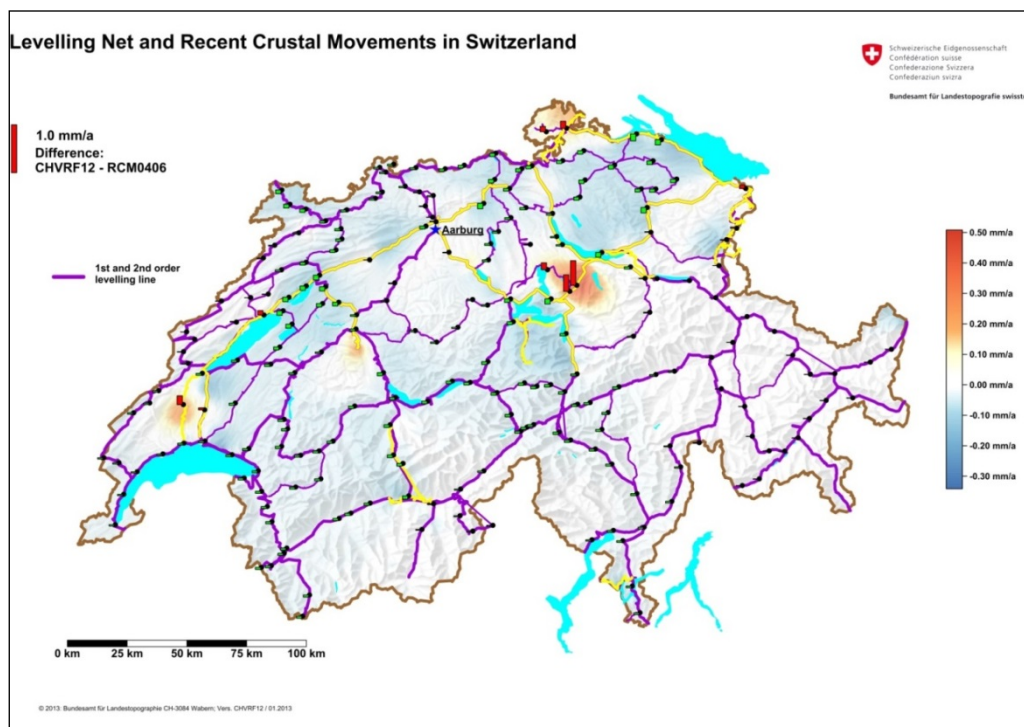


Figure 3.21: Impact of the vertical velocities derived from levelling adding measurements 2004 – 2012.

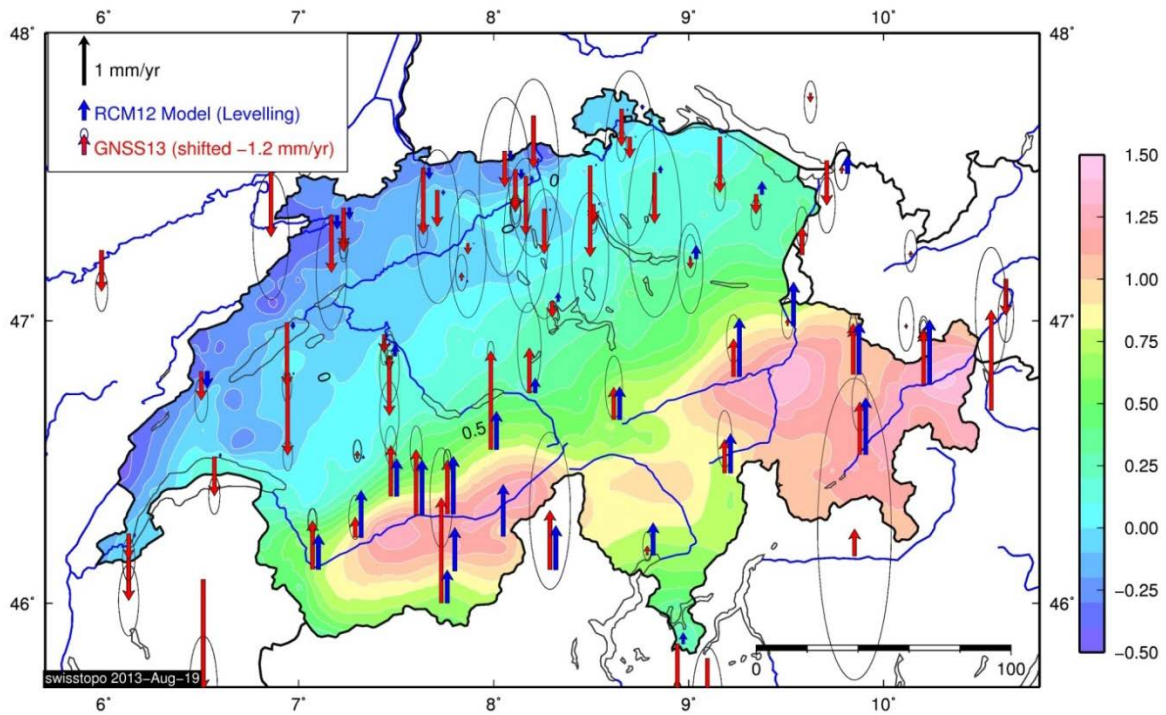
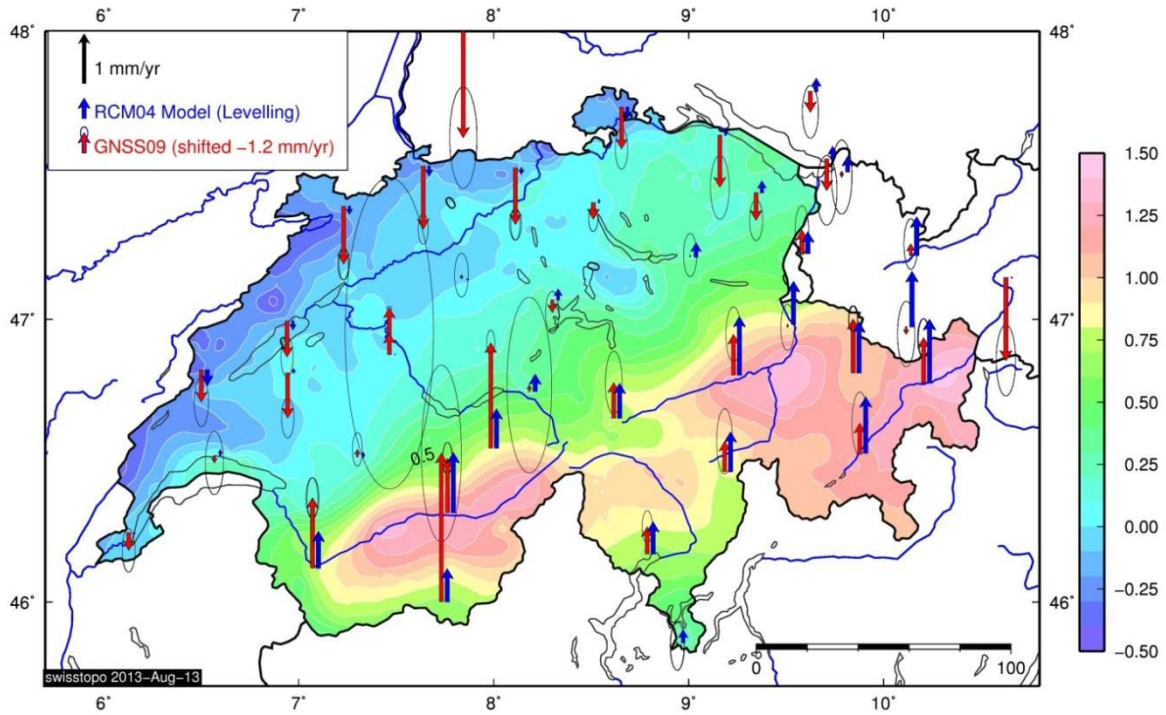


Figure 3.22: Comparison of vertical velocities between GNSS and the levelling-derived model expressed in the Swiss system (Aarburg zero vertical velocity). Upper diagram: Status Levelling 2004 (RCM04) and GNSS 2009. Lower diagram: Status Levelling 2012 (RCM12) and GNSS 2013. Red arrows indicate GNSS rates, blue arrows indicate RCM model values at the AGNES sites. The background contour surface shows the RCM model.

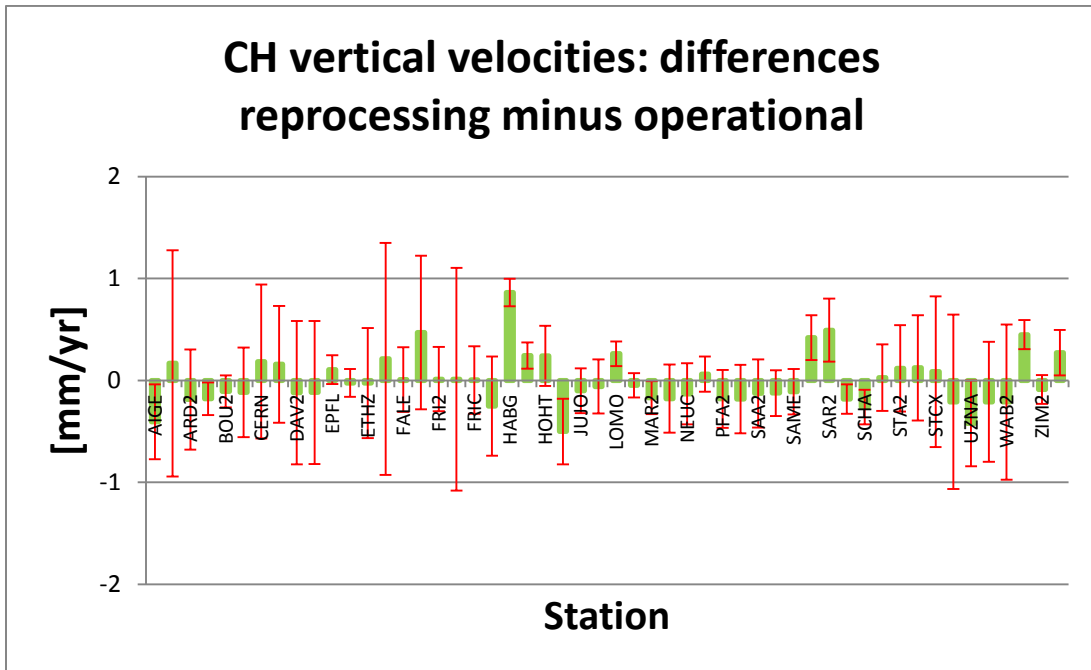


Figure 3.23: Differences of the vertical velocities between the operational analysis (weekly normal equations) and the reprocessing with an increased set of stations (based on daily normal equations).

Bibliography Commission 3

- Arnold, D., Beutler, G., Sośnica, K., Meindl, M., Lutz, S., and Dach, R. (2015a): Updating the empirical CODE orbit model and validation of GPS and GLONASS orbits using Satellite Laser Ranging data, this volume.
- Arnold, D., Meindl, M., Beutler, G., Dach, R., Schaer, S., Lutz, S., Prange, L., Sośnica, K., Mervart, L., and Jäggi, A. (2015b): CODE's new solar radiation pressure model for GNSS orbit determination. *Journal of Geodesy*, doi:10.1007/s00190-015-0814-4.
- Brockmann, E., Ineichen, D., Marti, U., Schaer, S., Schlatter, A., and Villiger, A. (2009): Determination of Tectonic Movements in the Swiss Alps using GNSS and Levelling. In: Kenyon S.C., Pacino M.C., Marti U.J. (Eds), *Geodesy for Planet Earth, Proceedings of the 2009 IAG Symposium*, Buenos Aires, Argentina, August 31 – September 4, 2009.
- Brockmann, E., Ineichen, D., Marti, U., Schaer, S., and Schlatter, A. (2013): Determination of the Swiss Alpine Uplift using GNSS and Levelling, Poster presentation at the IAG 2013 Scientific Assembly; 2-6 September 2013, Potsdam, Germany.
- Chamberlain, C., Houlié, N., Bentham, H.L.M., and Stern, T. (2014): Lithosphere–asthenosphere interactions near the San Andreas fault, *Earth and planetary science letters*, 399, 14–20, doi:10.1016/j.epsl.2014.04.048.
- Dach, R., Hugentobler, U., Meindl, M., and Fridez, P. (2007): The Bernese GPS Software Version 5.0, *Astronomical Institute, University of Bern*.
- Dach, R., Brockmann, E., Schaer, S., Beutler, G., Meindl, M., Prange, L., Bock, H., Jäggi, A., and Ostini, L. (2009): GNSS Processing at CODE: status report. *Journal of Geodesy* (special Issue: The International GNSS Service (IGS) in a Changing Landscape of Global Navigation Satellite Systems, guest editor C. Rizos), vol. 83(3-4), pp. 353-366, DOI 10.1007/s00190-008-0281-2.
- Dach, R., Beutler, G., Jäggi, A., and Schildknecht, T. (2011a): GNSS-Forschungsarbeiten am Astronomischen Institut der Universität Bern, *Geomatik Schweiz*, vol. 109(6), pp. 280-283.
- Dach, R., Böhm, J., Lutz, S., Steigenberger, P., Beutler, G. (2011b): Evaluation of the impact of atmospheric pressure loading modeling on GNSS data analysis. *Journal of Geodesy*, vol. 85(2), pp. 75-91, DOI 10.1007/s00190-010-0417-z.
http://www.bernese.unibe.ch/publist/2011/artproc/DOI_10.1007_s00190-010-0417-z.pdf
- Dach, R., Schaer, S., Hugentobler, U., Rodriguez Solano, C., Lutz, S., Steigenberger, P., Sośnica, K., Meindl, M., Beutler, G., and Jäggi, A. (2014a): Estimating the geocenter from GNSS data, *IGS Workshop 2014*.
- Dach, R., Meindl, M., Beutler, G., Schaer, S., Lutz, S., and Jäggi, A. (2014b): Estimating the Geocenter from GNSS Observations, *General Assembly of the European Geosciences Union (EGU 2014)*.
- Fäh, D., Moore, J.R., Burjanek, J., Iosifescu, I., Dalguer, L., Dupray, F., Michel, C., Woessner, J., Villiger, A., Laue, J., Marschall, I., Gischig, V., Loew, S., Alvarez, S., Balderer, W., Kästli, P., Giardini, D., Iosifescu, C., Hurni, L., Lestuzzi, P., Karbassi, A., Baumann, C., Geiger, A., Ferrari, A., Lalou, L., Clinton, J., and Deichmann, N. (2012): Coupled seismogenic geohazards in alpine regions, *Bollettino di Geofisica Teorica ed Applicata*, Vol. 53, n. 4, pp.485-508, December 2012, DOI 10.4430/bgta0048.
- Gambis, D. (2004): Monitoring Earth orientation using space-geodetic techniques: state-of-the-art and prospective. *J Geod*78(4-5): 295-303, doi: 10.1007/s00190-004-0394-1.
- Geiger, A., Villiger, A., and Fäh, D. (2011a): COGEAR Coupled seismogenic Geohazards in Alpine Regions (COGEAR), *25th International Union of Geodesy and Geophysics General Assembly (IUGG 2011)*.
- Geiger, A., Müller, M., Rothacher, M., Scheinert, M. (2011b): GeoHALO: Geoscientific Research with the New German “High Altitude and Long Range Research Aircraft” (HALO), *25th International Union of Geodesy and Geophysics General Assembly (IUGG 2011)*.
- Geiger, A., Villiger, A., and Limpach, P. (2011c): Status of module 2b: Geodetic measurements and kinematic modeling. *Third annual meeting of COGEAR, Visp, January 26-28, 2011*.

- Geiger, A., Rothacher, M., Villiger, A., Limpach, P., and Häberling, S. (2012a): Alpentektonik und Klimaerwärmung sichtbar im GNSS-Geomonitring ?. AHORN 2012, Davos, Switzerland, 30. Nov. 2012.
- Geiger, A., Villiger, A., and Limpach, P. (2012b): Status of module 2b: Geodetic measurements and kinematic modeling. Fourth annual meeting of COGEAR, Visp, January 25-27 2012.
- Geiger, A., Villiger, A., Limpach, P., Rothacher, M., Häberling, S., Kretz, A., and Müller, M.D. (2012c): Verschiebt es oder verschiebt es nicht?. Kolloquium Swiss4D, swisstopo, Bern, Schweiz, 25.01.2012.
- Häberling, S., Rothacher, M., and Zhang, Y. (2011a): Assessment of Shake Table Generated Earthquake Ground Motions Recorded Using High-Rate GPS, 25th International Union of Geodesy and Geophysics General Assembly (IUGG 2011).
- Häberling, S., and Rothacher, M. (2011b): GNSS Seismology, 25th International Union of Geodesy and Geophysics General Assembly (IUGG 2011).
- Häberling, S., Zhang, Y., Rothacher, M., Geiger, A., and Clinton, J.F. (2011c): Using a 1D Shake Table to Evaluate the Potential Contribution of High-Rate GPS to Seismology, AGU Fall Meeting 2011.
- Häberling, S., Rothacher, M., and Geiger, A. (2012): Assessment of high-rate GPS using a single-axis shake table, European Geosciences Union General Assembly 2012.
- Häberling, S., Rothacher, M., and Geiger, A. (2014): Transfer functions for high-rate GNSS receivers, EGU General Assembly 2014, Vienna, Austria, 27 April – 02 May.
- Häberling, S., Rothacher, M., Zhang, Y., Clinton, J.F., and Geiger, A. (2015): Assessment of high-rate GPS using a single-axis shake table. *Journal of Geodesy*. doi:10.1007/s00190-015-0808-2.
- Hildyard, M. W., Wright, T., Houlie, N., and Iwabuchi, T. (2012): Advances and New Insights into Real-time Magnitude Estimation for Earthquake and Tsunami Early Warning, 45th Annual Fall Meeting of the American Geophysical Union.
- Houlie, N., Occhipinti, G., Blanchard, T., Shapiro, N., Lognonne, P., and Murakami, M. (2011a): New approach to detect seismic surface waves in 1Hz-sampled GPS time series, *Scientific Reports*, 1, 44–, doi:10.1038/srep00044.
- Houlie, N., and Romanowicz, B. (2011b): Asymmetric deformation across the San Francisco Bay Area faults from GPS observations in Northern California, *Physics of the earth and planetary interiors*, 184, 143–153, doi:10.1016/j.pepi.2010.11.003.
- Houlie, N., Dreger, D., and Kim, A. (2012a): High-rate gps source solution of the 2004 Parkfield earthquake, ESC 2012- European Seismological Commission- 33rd General Assembly.
- Houlie, N., Wilson, M., Lithgow-Bertelloni, C., and Khan, A. (2012b): Understanding the geodynamic setting of Sao Miguel, Azores: A peculiar bit of mantle in the Central Atlantic, 45th Annual Fall Meeting of the American Geophysical Union.
- Houlie, N., Wilson, M., Lithgow-Bertelloni, C., and Khan, A. (2012c): Understanding the geodynamic setting of Sao Miguel, Azores: A peculiar bit of mantle in the Central Atlantic, SEDI 2012, Study of the Earth's Deep Interior.
- Houlie, N., and Stern, T. (2012d): A comparison of GPS solutions for strain and SKS fast directions: Implications for modes of shear in the mantle of a plate boundary zone, First International Conference on “Moldavian Risks - From Global to Local Scale.”
- Houlié, N., and Stern, T. (2012e): A comparison of GPS solutions for strain and SKS fast directions: Implications for modes of shear in the mantle of a plate boundary zone, *Earth and planetary science letters*, 345–348, 117–125, doi:10.1016/j.epsl.2012.06.029.
- Houlie, N., Cornwell, D.G., and Green, C. (2013a): State of the lithosphere-asthenosphere coupling beneath the United Kingdom, American Geophysical Union Fall meeting 2013.
- Houlié, N., Woessner, J., Villiger, A., Deichmann, N., Rothacher, M., Giardini, D., and Geiger, A. (2013b): Strain, Stress and Seismicity pattern in Switzerland. Vol. 15, EGU2013-7402-1, 2013. EGU General Assembly 2013.

- Houlié, N., and Stern, T. (2013c): A comparison of GPS solutions for strain and SKS fast directions: implications for modes of shear in the mantle of a plate boundary zone, 11th Swiss Geoscience Meeting 2013.
- Houlié, N., and Phillips, R.J. (2013d): Quaternary rupture behavior of the Karakoram Fault and its relation to the dynamics of the continental lithosphere, NW Himalaya–western Tibet, *Tectonophysics*, 599, 1–7, doi:10.1016/j.tecto.2013.03.029.
- Houlié, N., and Stern, T. (2014a): A comparison of GPS solutions for strain and SKS fast directions: Implications for modes of shear in the mantle of a plate boundary zone, EGU General Assembly 2014.
- Houlié, N., Dreger, D., and Kim, A. (2014b): GPS source solution of the 2004 Parkfield earthquake, *Scientific reports*, 4, doi:10.1038/srep03646.
- Houlié, N., Dreger, D.S., and Kim, A. (2014c): GPS source solution of the 2004 Parkfield earthquake, EGU General Assembly 2014.
- Houlié, N., Dreger, D.S., and Kim, A. (2014d): GPS source solution of the 2004 Parkfield earthquake, *Wegener 2014: Measuring and Modelling our Dynamic Planet*.
- Houlié, N., Dreger, D.S., and Kim, A. (2014e): GPS Source Solution of the 2004 Parkfield Earthquake, AGU 2014 Fall meeting.
- Houlié, N., Dreger, D.S., Kim, A., Kelevitz, K., Boschi, L., Nissen-Meyer, T., Giardini, D., and Rothacher, M. (2014f): Long-period GPS waveforms: What can GPS bring to Earth seismic velocity models?, *Advances in Earthquake Source Physics Workshop*.
- Houlié, N., Woessner, J., Rothacher, M., and Giardini, D. (2015): Strain rate and stress field of Switzerland, *Tectonophysics* (submitted).
- Ineichen, D., Brockmann, E., and Schaer, S. (2014): Reprocessing activities at swisstopo, EUREF-Symposium in Villnius, June 1-7, 2014. http://www.bernese.unibe.ch/publist/2014/artproc/DOI_10.1007_978-3-642-37222-3_16.pdf
- Kelevitz, K., Houlié, N., Rothacher, M., and Giardini, D. (2013): Mapping Earth's interiors with GPS records: The first steps, 11th Swiss Geoscience Meeting 2013.
- Kelevitz, K., Houlié, N., Boschi, L., Nissen-Meyer, T., and Giardini, D. (2014a): Long-period GPS waveforms: What can GPS bring to Earth seismic velocity models?, *European Geosciences Union General Assembly 2014*.
- Kelevitz, K., Houlié, N., Boschi, L., Nissen-Meyer, T., Giardini, D., and Rothacher, M. (2014b): Long-period GPS waveforms: What can GPS bring to Earth seismic velocity models? *The 14th Symposium of SEDI, Study of the Earth's Deep Interior*.
- Kelevitz, N. Houlié, Giardini, D., and Rothacher, M. (2015): Assessment of high-rate GPS time series at long periods, *GJL* (submitted).
- Komatitsch, D., and Tromp, J. (2002): Spectral-element simulations of global seismic wave propagation - II. Three-dimensional models, oceans, rotation and self-gravitation, *Geophysical Journal International*, 150(1):303–318.
- Kosek, W., Wnęk, A., Zbylut-Górska, M., and Popiński, W. (2014): Wavelet analysis of the Earth center of mass time series determined by satellite techniques. *J Geodyn* 80: 58-65.
- Lutz, S., Meindl, M., Beutler, G., Thaller, D., Springer, T., Dach, R., Schaer, S., and Jäggi, A. (2013): Orbit and ERP modeling issues of a multi-GNSS analysis, *IAG Scientific Assembly 2013*.
- Lutz, S., Schaer, S., Steigenberger, P., Dach, R., Beutler, G., Meindl, M., and Jäggi, A. (2014): Earth rotation and GNSS orbits from one-day and three-day arcs, *EGU General Assembly 2014*.
- Lutz, S., Steigenberger, P., Dach, R., Schaer, S., and Sośnica, K. (2015): Reprocessing activities at CODE. This volume.
- Maercklin, N., Festa, G., Colombelli, S., and Zollo, A. (2012): Twin ruptures grew to built up the giant 2011 Tohoku, Japan, earthquake, *Sci. Rep.*, 709(2), 1–7.

- Matsuo, K., Otsubo, T., Munekane, H., and Fukuda, Y. (2013): Geocenter motion excited by large-scale mass redistribution. Proc. of the 19th International Workshop on Laser Ranging, Annapolis, Oct 27-31, 2014.
- Meindl, M. (2011): Combined Analysis of Observations from Different Global Navigation Satellite Systems. Geodätisch-geophysikalische Arbeiten in der Schweiz, vol. 83. <http://www.sgc.ethz.ch/sgc-volumes/sgk-83.pdf>
- Meindl, M., Beutler, G., Thaller, D., Dach, R., and Jäggi, A. (2013a): Geocenter coordinates estimated from GNSS data as viewed by perturbation theory. Advances in Space Research, vol. 51(7), pp. 1047-1064, DOI [10.1016/j.asr.2012.10.026](https://doi.org/10.1016/j.asr.2012.10.026). http://www.bernese.unibe.ch/publist/2013/artproc/DOI_10.1016_j.asr.2012.10.026.pdf
- Meindl, M., Beutler, G., Thaller, D., Dach, R., Jäggi, A., and Rothacher, M. (2013b): GNSS-derived Geocenter Coordinates Viewed by Perturbation Theory, EGU General Assembly 2013.
- Meindl, M., Beutler, G., Thaller, D., Dach, R., Schaer, S., and Jäggi, A. (2015): A comment on the article “A collinearity diagnosis of the GNSS geocenter determination” by P. Rebischung, Z. Altamimi, and T. Springer, Journal of geodesy, 89, 189–194, doi:10.1007/s00190-014-0765-1.
- Müller, M.D., Geiger, A., and Kahle, H.-G. (2011a): Analysis of long-term GPS observations in Greece and geodynamic implications, 25th International Union of Geodesy and Geophysics General Assembly (IUGG 2011).
- Müller, M.D., Hollenstein, C., Geiger, A., and Kahle, H.-G. (2011b): Crustal deformation field in Greece determined from GPS measurements, 25th International Union of Geodesy and Geophysics General Assembly (IUGG 2011).
- Müller, M.D., Geiger, A., Kahle H.-G., Veis, G., Billiris, H., Paradissis, D., and Felekis, S. (2013): Velocity and deformation fields in the North Aegean domain, Greece, and implications for fault kinematics, derived from GPS data 1993–2009, Tectonophysics, 597-598, 34–49, doi:10.1016/j.tecto.2012.08.003.
- Newman, A.V., Stiros, S.C., Moschas, F., Saltogianni, V., Feng, L., Psimoulis, P., Karakas, O., Polster, S., and Jiang, Y. (2012a): Geodetic Observations of Ongoing Unrest at Santorini Caldera, Greece, AGU Fall Meeting 2012.
- Newman, A.V., Stiros, S., Feng, L., Psimoulis, P., Moschas, F., Saltogianni, V., Jiang, Y., Papazachos, C., Panagiotopoulos, D., Karagianni, E., and Vamvakaris, D. (2012b): Recent geodetic unrest at Santorini Caldera, Greece, Geophysical research letters, 39, L06309–, doi:10.1029/2012GL051286.
- Nissen-Meyer, T., van Driel, M., Stähler, S.C., Hosseini, K., Hempel, S., Auer, L., Colombi, A., and Fournier, A. (2014): AxiSEM: broadband 3-D seismic wavefields in axisymmetric media. Solid Earth, 5(1):425– 445.
- Panafidina, N., and Rothacher, M. (2011a): Impact of orbit modelling and the reference frame on subdaily variations in Earth rotation, EGU General Assembly 2011.
- Panafidina, N., Kurdubov, S., and Rothacher, M. (2011b): Empirical model of subdaily variations in the Earth rotation from GPS and its stability, Journées 2011 “Systèmes de référence spatio-temporels.”
- Panafidina, N., and Rothacher, M. (2011c): Subdaily variations in the Earth rotation, 25th International Union of Geodesy and Geophysics General Assembly (IUGG 2011).
- Panafidina, N., and Rothacher, M. (2012): Reliability of empirical tidal models from GPS observations, European Geosciences Union General Assembly 2012.
- Papazachos, C.B., Panagiotopoulos, D., Newman, A.V., Stiros, S., Vougioukalakis, G., Fytikas, M., Laopoulos, T., Albanakis, K., Vamvakaris, V., Karagianni, E., Feng, L., Psimoulis, P., and Moschas, F. (2012): Quantifying the current unrest of the Santorini volcano: Evidence from a multiparametric dataset, involving seismological, geodetic, geochemical and other geophysical data, European Geosciences Union General Assembly 2012.
- Psimoulis, P., Rothacher, M., Dalguer, L., and Zhang, Y. (2012): Development of a method for the detection of seismic events based on high-rate GNSS network measurements, 10th Swiss Geoscience Meeting.
- Psimoulis, P., Meindl, M., Houlié, N., and Rothacher, M. (2013): Development of an algorithm for the detection of seismic events based on GPS records: Case study Tohoku-Oki earthquake, EGU General Assembly 2013.

- Psimoulis, P., Houlié, N., Meindl, M., and Rothacher, M. (2014a): Consistency of PPP GPS and strong-motion records: case study of Mw9.0 Tohoku-Oki 2011 earthquake, arXiv preprint.
- Psimoulis, P., Houlié, N., Michel, C., Meindl, M., and Rothacher, M. (2014b): Consistency of GPS and strong-motion records: Case study of Mw9.0 Tohoku-Oki 2011 earthquake, EGU General Assembly 2014.
- Psimoulis, P., Houlié, N., Michel, C., Meindl, M., and Rothacher, M. (2014c): Long-period surface motion of the multipatch Mw9.0 Tohoku-Oki earthquake, AGU 2014 Fall meeting.
- Psimoulis, P., Houlié, N., Michel, C., Meindl, M., and Rothacher, M. (2014d): Long-period surface motion of the multi-patch Mw9.0 Tohoku-Oki earthquake, *Geophysical journal international*, 199, 968–980, doi:10.1093/gji/ggu302.
- Psimoulis, P., Houlié, N., Meindl, M. and Rothacher, M. (2015): Consistency of GPS and strong-motion records: case study of Mw9.0 Tohoku-Oki 2011 earthquake, *Smart Structures and Systems*, 26, 2.
- Rodriguez-Solano, C.J., Hugentobler, U., Steigenberger, P., Blossfeld, M., and Fritsche, M. (2014): Reducing the draconitic errors in GNSS geodetic products. *J Geod* 88:559-574. doi:10.1007/s00190-014-0704-1.
- Sagiya, T. (2004): A decade of GEONET: 1994–2003—the continuous GPS observation in Japan and its impact on earthquake studies, *Earth Planet Space*, 56, xxix–xli.
- Schaer, S., Arnold, D., Bock, H., Dach, R., Lutz, S., Orliac, E., Thaller, D., and Villiger, A. (2015a): CODE Contributions to the IGS, this volume.
- Schaer, S., Dach, R., Lutz, S., Meindl, M., Thaller, D., Beutler, G. (2015b): CODE contributions to Earth rotation parameters, this volume
- Seiler, R., Sonzogni, E., Houlié, N., Kirchner, J., Egli, M., and Cherubini, P. (2014): Increased tree-ring growth close to eruptive fissures prior to volcanic flank eruptions on Mount Etna (Sicily, Italy), *Tree Rings in Archaeology, Climatology and Ecology (TRACE 2014)*.
- Seiler, R., Houlié, N., Kirchner, J. W., Egli, M., Cullotta, S., Sonzogni, E., Andronico, D., and Cherubini, P. (2015): Increased tree-ring growth close to eruptive fissures prior to volcanic flank eruptions on Mount Etna (Sicily, Italy), *ADA 2015 The 4th International Asian Dendrochronological Ecology*.
- Sośnica, K., Thaller, D., Dach, R., Jäggi, A., and Beutler, G. (2012a): Sensitivity of Lageos Orbits to Global Gravity Field Models. *Artificial Satellites* 47(2): 47-65, doi: 10.2478/v10018-012-0013-y.
- Sośnica, K., Thaller, D., Dach, R., Ostini, L., Jäggi, A., Beutler, G., Rodriguez-Solano, C., Steigenberger, P., Hugentobler, U., Fritsche, M., Dietrich, R., Wang, K., and Rothacher, M. (2012b): Time Series Analysis of GNSS-SLR Co-located Stations, 2012 International GNSS Workshop.
- Sośnica, K., Thaller, D., Dach, R., Jäggi, A., Baumann, C., and Beutler, G. (2012c): The Blue-Sky effect. *Proceedings of the International Technical Laser Workshop 2012 (ITLW-12)*, Frascati (Rome), Italy, November 5-9, 2012. http://www.lnf.infn.it/conference/laser2012/4thursday/7_7sosnica/article_sosnika.pdf
- Sośnica, K., Thaller, D., Dach, R., Jäggi, A., and Beutler, G. (2013): Impact of loading displacements on SLR-derived parameters and on the consistency between GNSS and SLR results. *Journal of Geodesy*, vol. 87(8), pp. 751-769, ISSN 0949-7714, DOI 10.1007/s00190-013-0644-1. http://www.bernese.unibe.ch/publist/2013/artproc/DOI_10.1007_s00190-013-0644-1.pdf
- Sośnica, K. (2014): Determination of Precise Satellite Orbits and Geodetic Parameters using Satellite Laser Ranging. PhD thesis of the Faculty of Science of the University of Bern.
- Sośnica, K., Jäggi, A., Thaller, D., Dach, R., and Beutler G. (2014): Contribution of Starlette, Stella, and AJISAI to the SLR-derived global reference frame. *J Geod* 88(8): 789-804,doi 10.1007/s00190-014-0722-z.
- Sośnica, K., Jäggi, A., Thaller, D., Dach, R., and Meyer, U. (2015): Earth Rotation and Gravity Field Parameters from Satellite Laser Ranging. *Proceedings of the 19th International Workshop on Laser Ranging, Celebrating 50 Year of SLR: Remembering the Past and Planning for the Future*, October 27-31, 2014, Annapolis, Maryland, USA. http://www.bernese.unibe.ch/publist/2015/artproc/Sosnica_3072.pdf

- Thaller, D., Beutler, G., Jäggi, A., Meindl, M., Dach, R., Sošnica, K., and Baumann, C. (2013): Earth rotation parameters from satellite techniques, EGU General Assembly 2013.
- Thaller, D., Sošnica, K., Dach, R., Jäggi, A., Beutler, G., Mareyen, M., and Richter, B. (2014): Geocenter coordinates from GNSS and combined GNSS-SLR solutions using satellite co-locations. *Earth on the Edge: Science for a Sustainable Planet, International Association of Geodesy Symposia*, vol. 139, 2014, pp. 129-134, DOI 10.1007/978-3-642-37222-3_16.
- Varga, P., Krumm, F., Riguzzi, F., Doglioni, C., Süle, B., Wang, K., and Panza, G.F. (2012): Global pattern of earthquakes and seismic energy distributions: Insights for the mechanisms of plate tectonics, *Tectonophysics*, 530-531, 80–86, doi:10.1016/j.tecto.2011.10.014.
- Villiger, A., Marti, U., Brockmann, E., and Geiger, A. (2011a): SWISS 4D: Determination and modeling of the tectonic deformation field of Switzerland, 25th International Union of Geodesy and Geophysics General Assembly (IUGG 2011).
- Villiger, A., Geiger, A., Marti, U., Brockmann, E. (2011b): SWISS 4D: Estimation of the tectonic deformation field of Switzerland based on GPS measurements, pp. 375–375, Platform Geosciences, Swiss Academy of Science (SCNAT).
- Villiger, A., Geiger, A., Wiget, A., and Marti, U. (2011c): SWISS-4D II: Geodetic analysis of geodynamic deformations in Switzerland, 25th International Union of Geodesy and Geophysics General Assembly (IUGG 2011).
- Villiger, A., and Geiger, A. (2012a): Tektonische Deformationen innerhalb der Schweiz, Kolloquium der swisstopo.
- Villiger, A., Geiger, A., Marti, U., Brockmann, E., and Schlatter, A. (2012b): Swiss 4D: Determination of strain rates from GNSS campaign and levelling data, 10th Swiss Geoscience Meeting.
- Villiger, A., and Geiger, A. (2012c): Tektonische Deformationen innerhalb der Schweiz. Kolloquium der swisstopo, Bern, Schweiz, 25.01.2012.
- Villiger, A., Geiger, A., Marti, U., and Brockmann, E. (2013a): Extraction of a kinematic model for Switzerland based on GNSS and levelling data. *Geophysical Research Abstracts*. Vol. 15, EGU2013-PREVIEW, 2013. EGU General Assembly 2013
- Villiger, A., Geiger, A., Marti, U., and Brockmann, E. (2013b): Switzerland's strain field based on the swiss terrestrial reference frame 2010, International Association of Geodesy Scientific Assembly 2013.
- Villiger, A. (2014): Improvement of the kinematic model of Switzerland (Swiss 4D II), ETH-Zürich.
- Wright, T. J., Houlié, N., Hildyard, M., and Iwabuchi, T. (2012): Real-time, reliable magnitudes for large earthquakes from 1 Hz GPS precise point positioning: The 2011 Tohoku-Oki (Japan) earthquake, *Geophysical research letters*, 39, L12302, doi:10.1029/2012GL051894.

4 Positioning and Applications

Micro Aerial Vehicle, Advanced sensor orientation

J. Skaloud, M. Rehak, R. Mabillard

Ecole Polytechnique Fédérale de Lausanne

Low-cost and low-weight Unmanned Aerial Vehicle (UAV) systems with imaging capability have enjoyed a rapid development over the past years and are increasingly deployed as carriers for mapping purposes. They present a well-established tool for local-area remote sensing in the fields of agriculture, forestry, mining and hydrology as well as in the scientific research. Although these systems allow a new way of data collection in the field of geomatics engineering, they inherit an old (i.e. indirect) approach to sensor/image orientation. That is indeed insufficient for large scale mapping projects and cadastral surveying for which mapping accuracy at a 2-5 cm-level is needed. Furthermore, the quality of the employed inertial sensor (often part of a low-cost autopilot unit) is not sufficient for accurate attitude determination at a level of $\sigma_{att} = 0.01-0.1$ deg. We propose a GNSS/INS sensor payload for the sake of obtaining precise sensor orientation on a fix-wing and/or multi-rotor micro UAV from which either direct or integrated sensor orientation can benefit.

For the multi-rotor platform the optical sensor, the GNSS antenna and the in-house developed board with redundant inertial measurement units are all rigidly mounted on a gimbal (Figure 4.1) while on the fix-wing platform these are connected to aircraft chassis (Figure 4.2). The quality of position determination of the camera perspective-centre is shown in Table 4.1.

The developed orientation techniques focus on including absolute and relative aerial control. We confirm practically that both approaches are very effective: the absolute control allows omission of ground control points while the relative requires only a minimum number of control points. Indeed, the latter method represents an attractive alternative in the context of MAVs for two reasons: First, the procedure is somewhat simplified (e.g. the lever-arm between the camera perspective and antenna phase centers does not need to be determined) and, second, its principle allows employing a single-frequency antenna and carrier-phase GNSS receiver. This reduces the cost of the system as well as the payload, which in turn increases the flying time. The contribution of this approach to mapping accuracy is shown in .

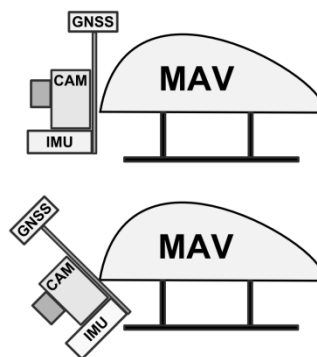


Figure 4.1 : Schematic sketch of the stabilized sensor mount for two distinct tilting angles.



Figure 4.2: Fixed-wing micro UAV platform in a mapping flight with precise orientation sensors.

	Horizontal [m]	Vertical [m]
Mean estimated accuracy of on-board positions	0.016	0.023
RMS of EO residuals w.r.t. AT positions using 25 GCPs	0.020	0.039
RMS GNSS residual	0.022	0.099

Table 4.1: Quality of the on-board position determination for Exterior Orientation (EO).

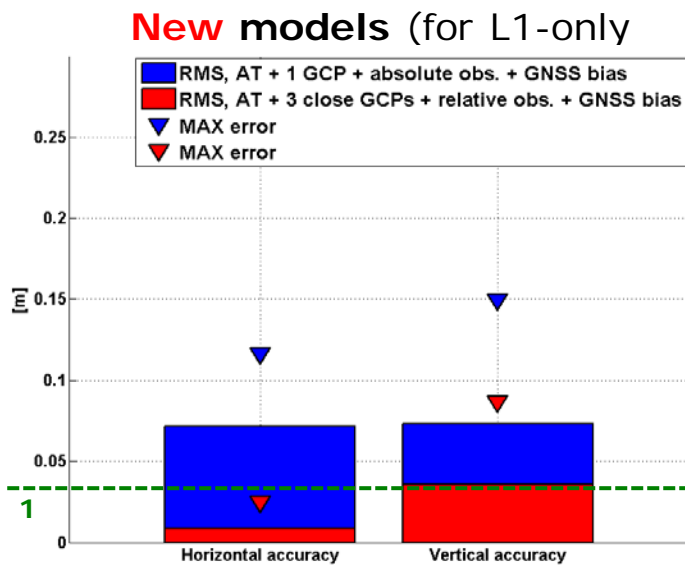


Figure 4.3: Precise mapping with L1-only GNSS receiver using relative sensor orientation.

Stochastic modeling of inertial sensors

Y. Stebler, S. Guerrier, J. Skaloud

Ecole Polytechnique Fédérale de Lausanne

The integration of observations issued from a satellite-based system (GNSS) with an inertial navigation system (INS) is usually performed through a Bayesian filter such as the extended Kalman filter (EKF). The task of designing the navigation EKF is strongly related to the inertial sensor error-modeling problem. Accelerometers and gyroscopes may be corrupted by random errors of complex spectral structure. Consequently, identifying correct error-state parameters in the INS/GNSS EKF becomes difficult when several stochastic processes are superposed. In such situations, classical approaches like the Allan variance (AV) or power spectral density (PSD) analysis fail due to the difficulty of separating the error processes in the spectral domain. Moreover, The conventional AV methodology is limited to models composed of processes characterized by linear regions in a Allan variance log-log plot and therefore this approach is far from being general.

For this purpose, we propose a new estimator based on the generalized method of wavelet moments (GMWM). The GMWM estimator matches theoretical and sample-based wavelet variances (WVs), and can be computed using the method of indirect inference (Figure 4.4). We show that that this estimator is consistent for the class made of the sum of independent white noise, drift, quantization noise, random walk, and Auto-Regressive models of order 1. Indeed, the GMWM has many advantages over existing alternative methods for applications in engineering or natural sciences.

To illustrate the impact of the importance of model structure and estimation precision in device positioning, we performed a test on the trajectory of a helicopter performing airborne laser scanning. Using extremely reliable equipment as a reference we emulated the noise low-cost (MEMS) IMU and study the impact of stochastic error models during different duration of GNSS-signal outages. The two first estimated models are based on the AV and on the KF-Self-Tuning approach. The GMWM was also used as an alternative estimator and model building approach. The trajectories are depicted in Figure 4.5 along with the “true” trajectory. It can be seen that the GMWM-based model (black-dashed line) limits significantly the error growth during the GPS-signal outage compared with the other two benchmark methods which diverged from the “true” trajectory by several thousand of meters! The poor performances of the standard methods explain the recent explosion of the research conducted to determine the stochastic modeling of MEMS-type inertial sensors.

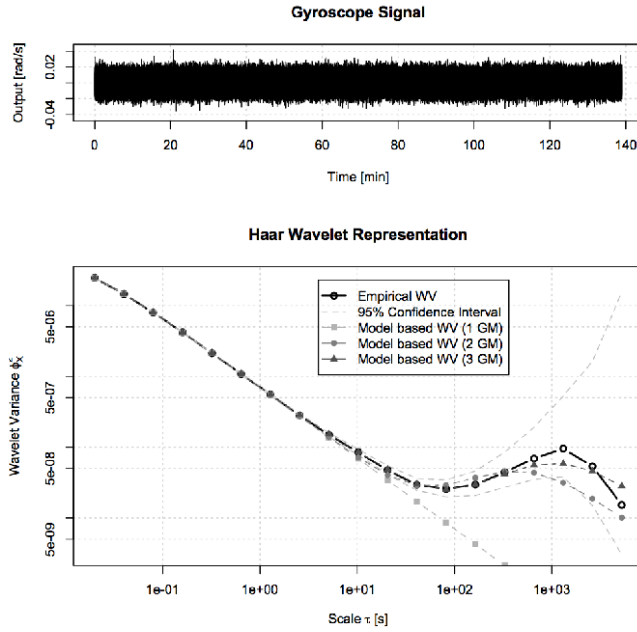


Figure 4.4: Gyroscope observed error process (top panel) and graphical comparison (log-log scale) between the Haar Wavelet Variance (line “o”) computed from the observed signal and the analytical signal using the estimated parameters of respectively the sum of 3 GM processes (line “dark triangle”), the sum of 2 GM processes (line •) and one GM process (line ■).

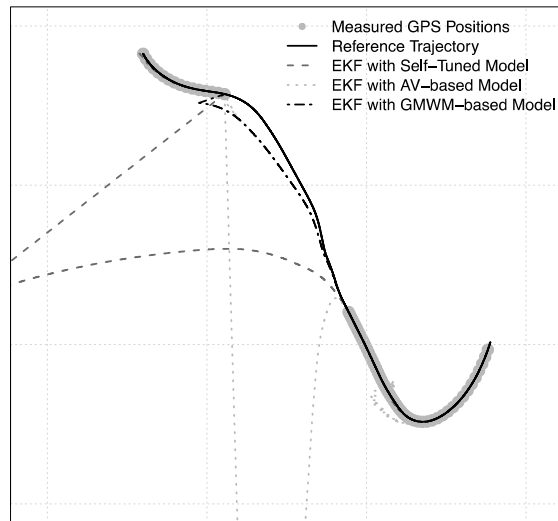


Figure 4.5: Comparison between a reference trajectory (black dotted line) issued from a mapping flight in which a GPS outage was introduced, with estimated error models based on the AV (light-grey line), the KF-Self-Tuning (dark-grey line) and the GMWM (black dashed line).

Vehicle trajectory analysis based on inertial techniques

Y. Stebler, J. Skaloud

Ecole Polytechnique Fédérale de Lausanne

Although well established in the aviation community, low-cost and vehicle-independent “black-box” technology for accident analysis, adapted to mass-market ground-based vehicles, is an emerging technology with growing importance. Whilst several products suited for cars are available on the market, almost no devices adapted for motorcycles exist. Due mainly to their particular dynamics and lack of space for installing any external device, the design of a data-recorder technology for a motorcycle is nontrivial. This becomes even more challenging if the technology has to be independent of the motorcycle type, low-cost, easy and fast to mount, and not based on GNSS technology (for autonomy and privacy issues). Motorcycle speed is essential information for analyzing the driver’s behavior at pre-crash phase. Based on inertial data delivered from an autarkic low-cost, MEMS- based inertial measurement unit (IMU) and voltage ripple signals taken from the motorcycles battery, we reconstruct forward velocity of a motorcycle respecting 5% error bars over a wide velocity range. The off-line reconstruction is based on a strapdown navigation algorithm combined with an autonomous (i.e. *without GNSS*) aiding via an extended Kalman filter. To stabilize the growth of inertial error the filter uses as the external measurements the residual periodic voltage fluctuations of the motorcycle’s generator – the residual AC ripple – together with available information on vehicle transmission and its geometry. Despite the structural simplicity of the algorithm and the relatively low performance of the IMU, we experimentally demonstrate that the proposed off-line estimator delivers accurate autarkic speed estimates for a large class of motorcycles.

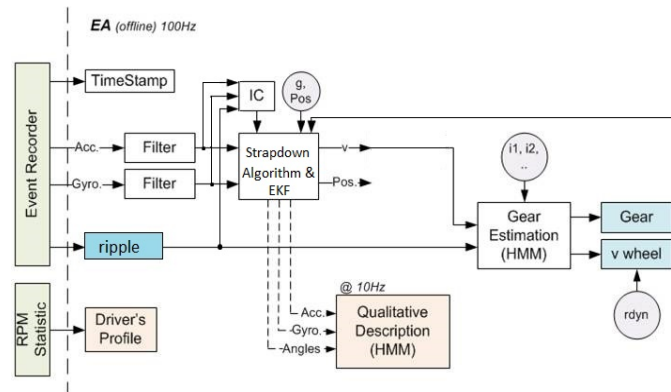


Figure 4.6: Inertial gyro- and acceleration inputs, together with the generators’ AC ripple, are post-processed and deliver objective output sequences including vehicle speed (forward speed) and qualitative description of driver behaviors (not discussed here). The set of needed external parameters is reduced to transmission ratios i_p , i_d and the dynamic radius r_{dyn} of the rear wheel. Initial conditions are estimated from a short static dataset.

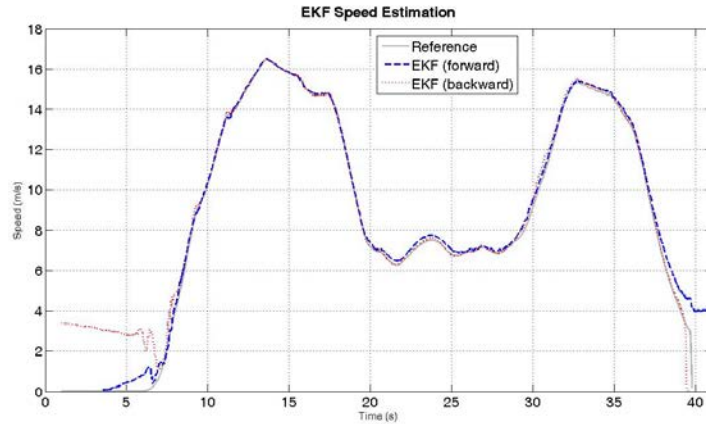


Figure 4.7: Vehicle Speed reconstruction for the roundabout maneuver using forward (blue) and backward (red) filtering. The gear speed is estimated using Hidden Markov-Modeling. The reference speed (gray) is based on GPS measurements and Hall-sensor based wheel speed measurements.

Drones for search and rescue

J. Skaloud, Y. Stebler.

Ecole Polytechnique Fédérale de Lausanne

The use of Unmanned Aerial Vehicles (UAVs) —more in general, Unmanned Aerial Systems (UASs)— for search and rescue (SAR) operations has been traditionally fed by developments made in other fields (e.g. military). The key system requirements for a UAV to be used for SAR for civilian application, is the degree of safety in navigation. Within the FP7 project named CLOSE-SEARCH, which stands for 'Accurate and safe EGNOS-SoL Navigation for UAV-based low-cost Search-And-Rescue (SAR) operations, a hybrid multi-sensor navigation system has been developed (Figure 4.8), benefitting from the European EGNOS system performance and exploring the use of redundant inertial measurement units (RIMU) and barometer to assess the potential of lower-cost, highly-redundant, ultra-safe systems.

The reported part of the project focuses on demonstrating that EGNOS-based UAV control is feasible by using a closely coupled EGNOS/RINS/BA concept and assessing the safety degree offered by such a solution, in terms of navigation integrity. Indeed, the use of redundant sensor configurations paves the way to achieving robust navigation. By providing redundant observations, the precision and reliability of the navigation parameters' estimation is significantly improved. Redundancy also enables detection and exclusion of eventual faulty measurements and therefore guarantees a higher continuity of operations in the presence of a fault. In short, the operational risk is evaluated with respect to n sensors. In CLOSE-SEARCH $n > 7$ as the navigation system is made of up of one GNSS receiver, four IMUs, one baro-altimeter, one magnetometer and several close-range sensors. Definition of *integrity risks* (IR) enables computation of protection thresholds in position, so called *protection levels* (PL), in the horizontal and vertical subspaces. These are compared against a set of "tolerable" thresholds called *horizontal* and *vertical alert limits* (HALs, VALs). By this mean the achieved navigation "safety" can be evaluated by the user. Although this concept is well established for highly demanding applications such as civil aviation, the "integrity risk" requirements for other applications have not been fully developed. We propose a strategy that outlines a set of integrity requirements adapted to the needs of two flight phases in SAR missions employing UAVs (Table 4.2).

During the test campaign, protection levels were derived from the EGNOS-GNSS/INS/BA solution. The results showed that choosing an IR of 10^{-3} and HAL, VAL of 10 meters, the availability (that is, the percentage of time that PLs are below ALs) is around 95 percent (Figure 4.9). That is to say, a UAV can safely fly down to 10 meters above ground, with the risk of "something goes wrong and undetected" remaining lower than 1 over 1000 during the 95 percent of the time. In different content these results may need further improvement, and the proposed integrity values may be re-evaluated.

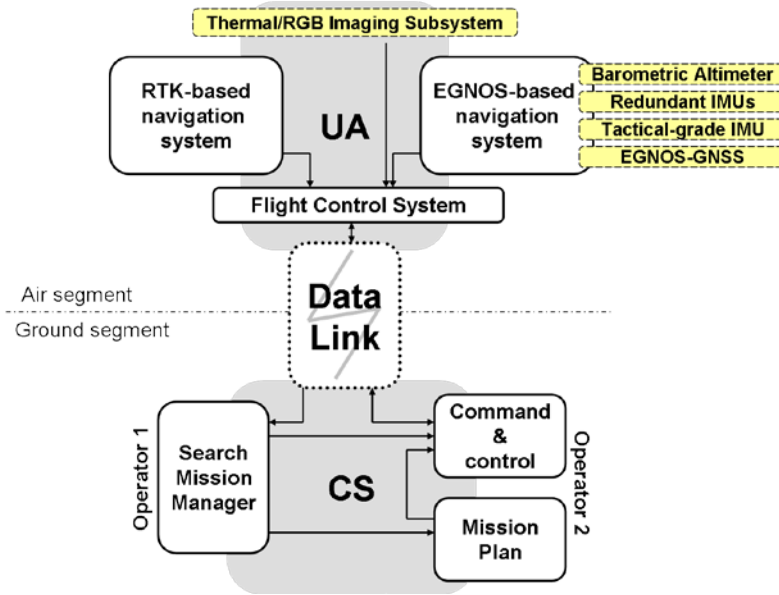


Figure 4.8: CLOSE-SEARCH system architecture

	IR (- / approach)	HAL, VAL (m)
APV-I (EGNOS certification)	2×10^{-7}	40, 50
W2W (waypoint-to-waypoint)	2×10^{-6}	4, 7.5
GA/S (ground approach/separation)	2×10^{-6}	2.5, 4

Table 4.2: Integrity Risk and Alert Limits defined in CLOSE-SEARCH for two UAV flight phases, waypoint-to-waypoint (W2W) and ground approach/separation (GA/S). Civil aviation APV-I values are stated for comparison.

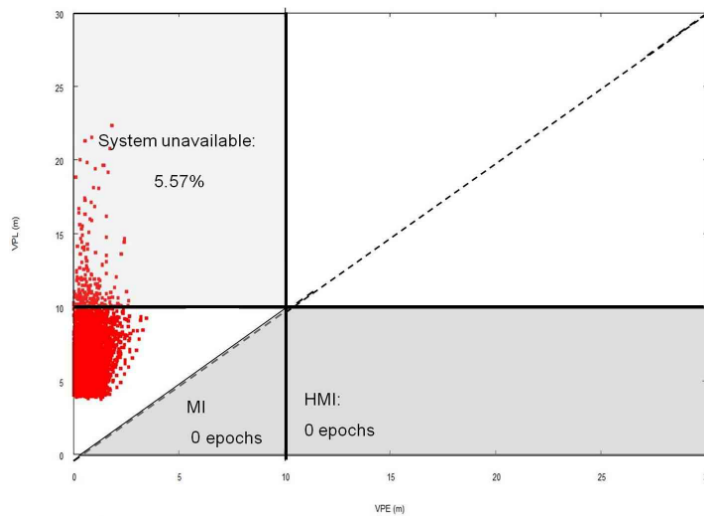


Figure 4.9: Stanford diagram comparing the true error and the protection level on the vertical subspace.

Fault detection and isolation in multiple MEMS-IMUs configurations

J. Skaloud, A. Waegli, S. Guerrier

Ecole Polytechnique Fédérale de Lausanne

The use of redundant Micro-Electro-Mechanical System (MEMS)-type sensors is an economically and ergonomically viable solution to improve navigation performance while enhancing sensor performance monitoring. The quality improvement of integrated trajectory determination comes on several levels: Firstly, the noise levels of the gyros and accelerometers can be estimated directly from the data and are therefore represent correct reflection of the reality. Indeed, the realistic estimation of the noise parameters in the inertial sensors is important for correct tuning of the Kalman Filter (KF) used in the GPS/INS integration. Secondly, the noise level of the overall system can be a reduced and defective sensor; spurious signals or sensor malfunctioning can be detected and isolated. This improves the accuracy of autonomous navigation and therefore a system utilizing redundant IMUs bridges the gaps in the GPS signals more effectively. Finally, more accurate orientation determination can be achieved with redundant IMU configurations. This represents an interesting alternative for reaching good orientation estimation with low-quality sensors yet in abundant manner.

In our investigations we will first consider the somewhat trivial (and less likely) case where the sensors of the same type (i.e. the gyroscopes or the accelerometers) have equal and time invariant noise level within a system (Figure 4.10: Norm of the angular rate measurement of 4 MEMS-IMUs in comparison to the reference measurement (tactical grade IMU).). Then, we allow variations to occur between sensors and in time. For such scenario our estimation will be based on a tool called Generalized Auto-Regressive Conditional Heteroskedasticity (GARCH) which is a widespread approach dealing with heteroskedastic time series. We will show that this method offers an interesting tool to model the magnitude of the noise in the residuals of multi-IMUs systems (Figure 4.11). Finally, we verify the theoretical reduction of the noise level by comparing the differences between the MEMS-IMU measurements and their best estimate to the reference values (Figure 4.12). The experimental noise reduction is approximately 48.6 % and 56% for simple averaging and GARCH, which is close to theoretical value (50%). Nevertheless, the methodology of fusion may introduce a bias when combining the IMU observations into one when considering their precision as equivalent. Further studies revealed that the relatively small differences between both methods could be considerably larger (up to 100%) when the noise level of one of the IMU differs substantially from the others, which highlights the importance of the proposed methodology.

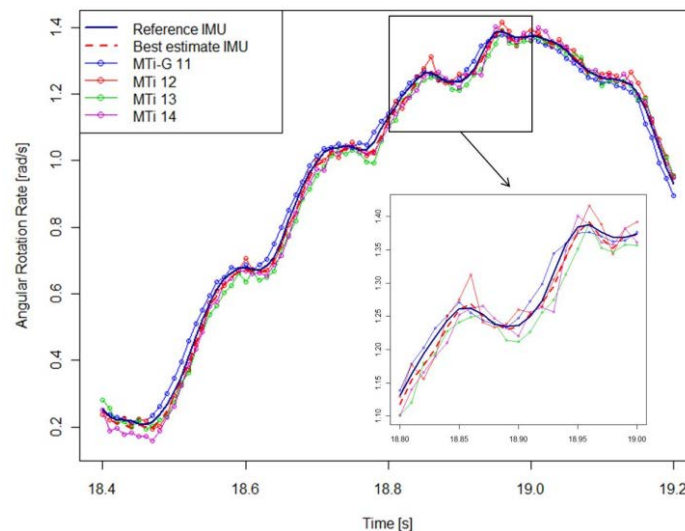


Figure 4.10: Norm of the angular rate measurement of 4 MEMS-IMUs in comparison to the reference measurement (tactical grade IMU).

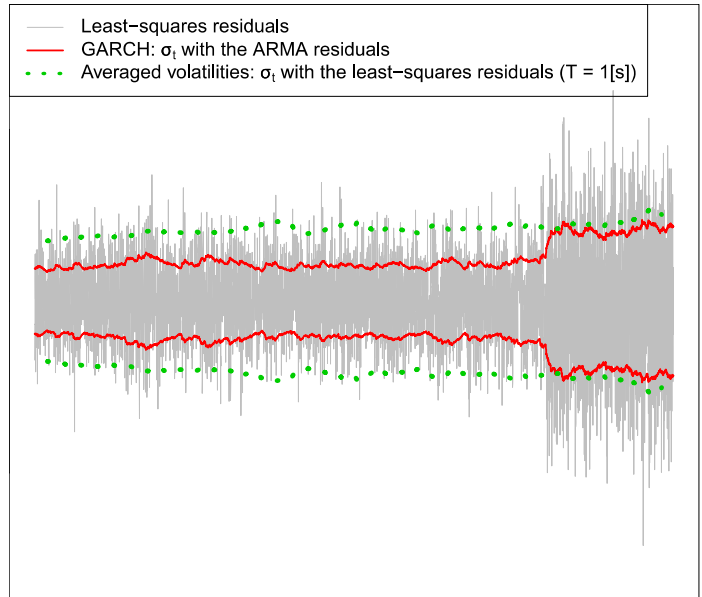


Figure 4.11: Comparison between the noise-level of a gyrosopic signal estimated with the “averaged volatilities” and with the GARCH methodology.

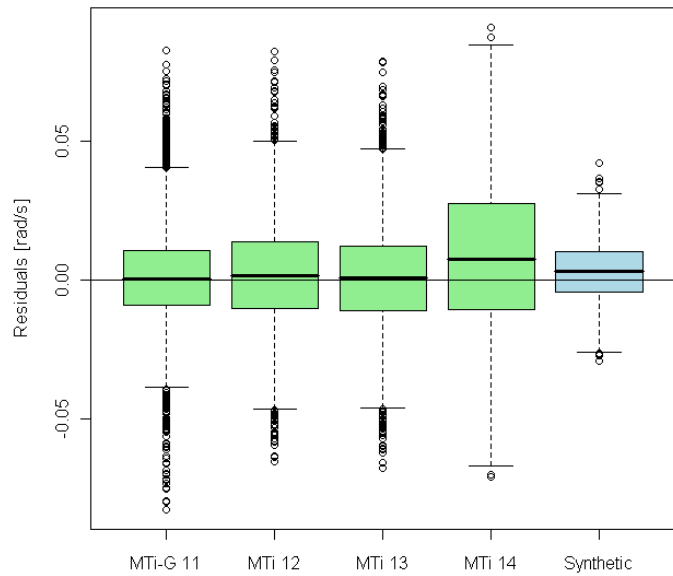


Figure 4.12: Boxplots of the residuals of the norm of the 4 MEMS-IMU and of the synthetic IMU (evaluated by simple averaging).

Automated assessment of digital terrain models from airborne laser scanning

Ph. Schaer, J. Skaloud

Ecole Polytechnique Fédérale de Lausanne

The goal of this project is to develop surface-related quality indicators as confidence-metrics of the final geoproducts derived from airborne laser scanning (ALS). Actually, number of factors is influencing the quality of the digital terrain models (DTM). Optimally, a DTM quality analysis should take into account the precision, absolute and relative accuracy of the initial sampling points. However, such quality measure should also consider the surface sampling variations (point density) as well as the spatial distribution of the point accuracies. In this research we present a novel procedure that enables the computation of height reliability indexes for each elevation of a DTM and the subsequent generation of a DTM quality map that encapsulates all such important factors. The method requires that two following conditions be met:

- Accuracy information for each ground point (represented by σ_x , σ_y , σ_z) involved in DTM generation is correctly determined and available. For a point-cloud generated by airborne laser scanning (ALS) the proposed procedure stems from our previous investigations that account for the quality of the trajectory, that of laser instrument as well as the system calibration and the relative geometry between the scanned ranges and the terrain.
- The DTM is represented as a regular raster with the elevation values calculated by projecting the cell-center coordinates on the corresponding facet of the triangular irregular network (TIN) whose nodes are the irregular sampled ground points as depicted.

The proposed methodology considers on one side the quality of point-cloud creation on the other hand its classification as well as density and interpolation (Figure 4.13). In short, each laser point related to ground have its own accuracy indicators σ_x , σ_y , σ_z that depend mainly on the reliability of trajectory estimation with GNSS/INS observation. The latter is strongly influenced by the (lack of) redundancy in satellite constellation (e.g. number of used satellite system, visible satellite vehicles and their geometry, recorded frequencies), number of base-stations and their separation as well as in inertial observation (e.g. redundant IMUs). These serve as a prerequisite for an estimation procedure that transforms the accuracy of individual targets within a laser point-cloud to a height reliability index of a DTM-raster. Within this mechanism the confidence levels of points representing TIN surface patch are propagated to DTM height-accuracy parameter (Figure 4.14) This parameter is then transformed to “height reliability index” according to the particular sampling density in the region (e.g. interpolation vs. extrapolations). Regrouping all raster cells with height reliability indexes forms the desired DTM quality map (Figure 4.15) that can be associated (i.e. as meta data) to the DTM. The quality map indicates areas where the height values are reliable and areas where they should be considered with a precaution. It reflects the dynamic nature of the data-acquisition process and can be a valuable asset when estimating the accuracy of DTM derived quantities (i.e. slope, aspects). Moreover, the availability of such cell-wise quality indicators allows constructing weighting schemes also for DTM's generated by merging data from different sources and estimating the accuracies of the results.

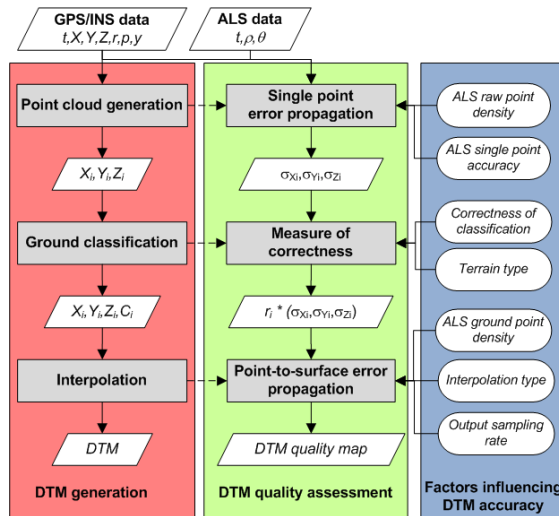


Figure 4.13: General workflow for DTM production from airborne laser scanning with suggested quality indicators.

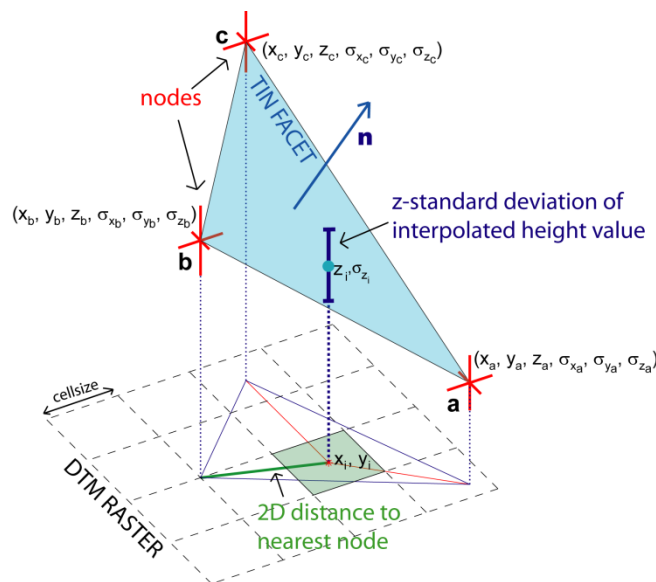


Figure 4.14: Propagation of individual point errors to DTM height by TIN interpolation.

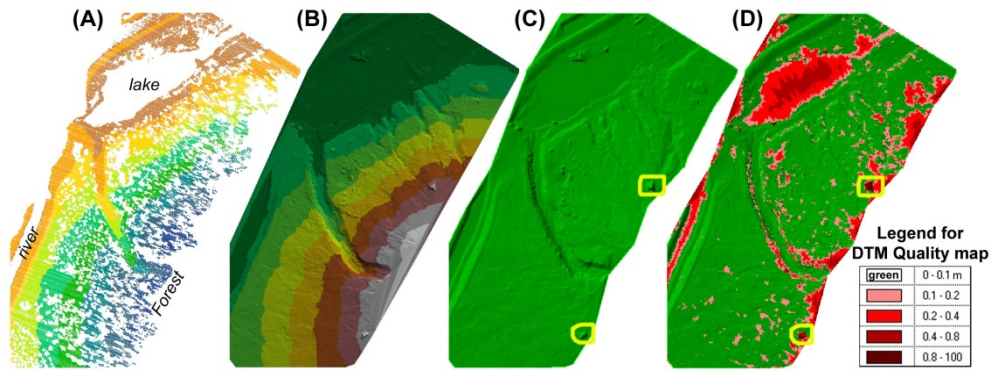


Figure 4.15: (A) Automatically classified ground points color-coded by elevation, (B) DTM-TIN, (C) DTM raster interpolated from TIN, (D) DTM quality map superposed on DTM color-coded by index r_z (cells with $r_z < 0.1$ are transparent, i.e. correspond to the green-shaded surface).

Snow moisture & snow properties determination with GNSS in alpine environment

J. Skaloud, C. Botteron

Ecole Polytechnique Fédérale de Lausanne

Moisture content in the soil and snow in the alpine environment is an important factor, not only for environmentally oriented research, but also for decision making in agriculture and hazard management. Current observation techniques quantifying soil moisture or characterizing a snow pack often require dedicated instrumentation that measures either at point scale or at very large (satellite pixel) scale. Given the heterogeneity of both snow cover and soil moisture in alpine terrain, observations of the spatial distribution of moisture and snow-cover are lacking at spatial scales relevant for alpine hydrometeorology.

We investigate the challenges of the determination of soil moisture and snow properties in alpine environments with respect to future perspective of retrieving such information via the reception of reflected Global Navigation Satellite Signals. This method, called GNSS-Reflectometry (GNSS-R), uses indirect (i.e., reflected) signals for remote sensing of the Earth's surface (Figure 4.16). While observations of the delays of the direct signal allow estimation of the water-vapor in the lower layers of atmosphere and could be conducted with existing instrumentation, processing of the reflected signals (normally considered as a noise in a GNSS-receiver) typically requires the construction of new instruments and new signal processing algorithms. Remarkably, relevant geophysical properties of the surface (e.g., soil moisture, water-body roughness and/or salinity retrieval, snow/ice cover determination, etc.) can potentially be retrieved by this approach. We study the option of receiving the direct & reflected signal simultaneously (i.e. via single antenna) or separately (i.e. dual antenna setup) with respect to different signal processing techniques while considering various combinations of signal-in-space signals. We show that the use of multiple constellation and new signals (i.e. as Galileo E5 and GPS L5) have a high positive impact on the resolution and accuracy of GNSS-R measurements for soil parameter extraction. Furthermore, when combined with other observations techniques as airborne laser scanning, this technology is a very good candidate for filling up the gap on the instrumentation level, thereby opening the use of this technology to observations over more difficult terrain such as the alpine environment.

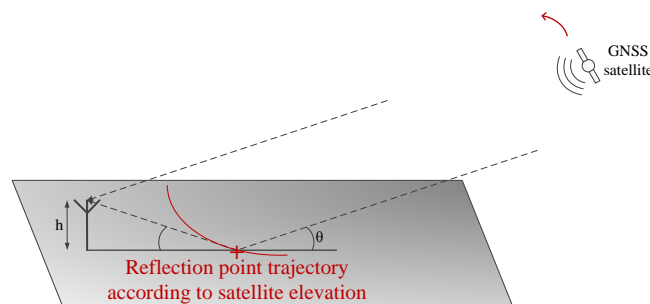


Figure 4.16: Example of a local-scale static GNSS-R experiment.

Prediction of phase ambiguity resolution

J. Skaloud, D. Willi

Ecole Polytechnique Fédérale de Lausanne

In kinematic Global Positioning System (GPS) applications, centimeter to decimeter level positioning accuracy can only be achieved by solving phase ambiguities in differential mode. Without a communication link between the rover and the reference receiver, the success of ambiguity resolution cannot be checked in real time and this fact can be problematic for some airborne mapping applications. As the success of kinematic ambiguity resolution depends mainly on the actual signal quality and on the geometry and the redundancy of the satellite constellation, we propose a quality indicator, applicable in real time and without a communication link to the reference station, which takes into account both aspects, the signal quality as well as the receiver to satellite geometry. The concept is general relies on a strict mathematical definition.

Two common existing GPS quality measures are combined to form one “phase-ambiguity-resolution predictor”: firstly the SIGMA- ε model, which is a signal intensity based weighing scheme reflecting the actual signal quality, secondly the Ambiguity Dilution of Precision (ADOP), which is an indicator of the geometric strength of a constellation. The parameters of the SIGMA- ε model are determined for different type of airborne antennas and signals (i.e. C/A code, P2 code L1 phase, L2 phase) by means of calibration. This model is validated for different level of antenna tilting up to 40 degrees to mimic the changing orientation in airborne environment. The model performances for code measurements are extremely high with coefficients of determination up to 98 % (Figure 4.17). The model is also calibrated for carrier phase observations. There the confidence in coefficient determination decreases to 70 %.

This stochastic model is then employed in the concept of ADOP developed by P. Teunissen in 1997. The value of the ADOP is dependent on the number of satellites and, if a geometry-based functional model is chosen, dependent on the satellite constellation. As the value ADOP depends on the relative and absolute weights attributed to each observation, the employment of correct stochastic model is a prerequisite for its application. The validation is conducted on a platform of a motorcycle on baselines-length limited to 15 km. There it is shown that the suggested indicator is able to correctly predict the success rate of ambiguity resolution in the majority of cases, but only as long as the ADOP is associated with a correct stochastic model (Figure 4.18).

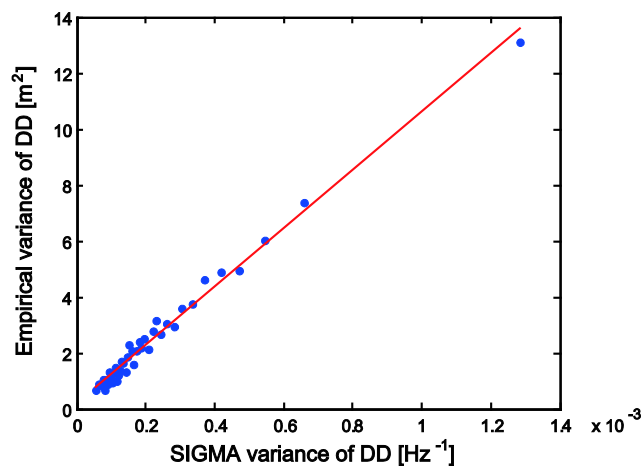


Figure 4.17: Calibration of SIGMA model parameters via linear regression for C/A code measurements with the Antcom G5 antenna.

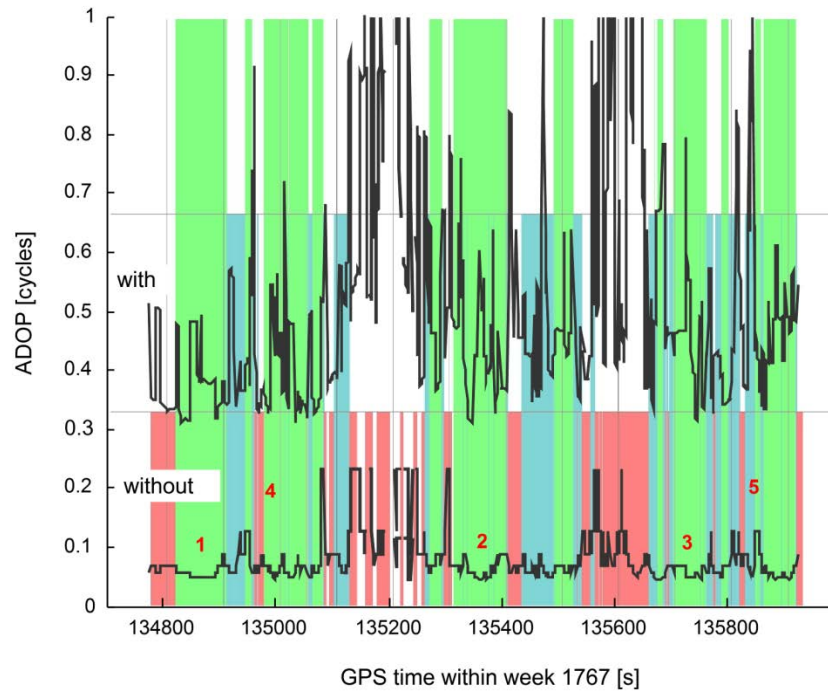


Figure 4.18: Comparison of ADOP computation with and without stochastic modelling. Green and blue: ambiguities resolved successfully in both and one processing direction during post-processing. Red: floating ambiguities. White: < 5 satellites in view (i.e. insufficient data coverage). Black lines: prediction of ambiguity resolution via ADOP with (upper) and without (lower) calibrated stochastic model.

Hyperspectral remote sensing of crop properties with Unmanned Aerial Vehicles

Y. Akhtman, D. Constantin, M. Rehak

Ecole Polytechnique Fédérale de Lausanne

A case study was conducted over the Field Phenotyping Platform (FIP) at the ETH Zürich research station for plant sciences at Eschikon, Lindau as collaboration between EPFL TOPO laboratory, Gamaya company and the ETHZ Crop Science Laboratory. The aim of this case study was the determination of crop properties and phenotypes as related to spectral characteristics by using a novel Hyperspectral Imaging (HSI) snapshot camera developed by Gamaya. We extracted the spectral data from a set of 34 plots (4 m²) including a range of different crops (soybean, sunflower, maize and buckwheat) were plant properties were determined. We calculated nine spectral indices reported for visible range. The spectral indices were related to leaf nitrogen, chlorophyll and total pigment concentration (in mg g⁻¹), canopy cover (fraction of plant per area %), leaf area index (m² m⁻²) and spad (leaf greenness). For each of the mentioned traits good to very good relationships were identified. Further we show the applicability of the camera and UAV setup for identification of phenotypic differences in winter wheat trial with more than 200 genotypes (Figure 4.19). The results were reported at the EARSel 2015 workshop in Luxembourg, April 2015.



Figure 4.19: HSI mapping with the help of UAV on crop field (left); mapping of phenotypes based on HIS (right)

UAV based multispectral imaging over a coral reef lagoon in Reunion Island

Y. Akhtman, D. Constantin, M. Rehak

Ecole Polytechnique Fédérale de Lausanne

A field campaign was conducted in September 2014 over the fringing reef of l'Ermitage, Saint Gilles, Reunion Island. This site is of particular interest because it shows signs of major erosion and is subject to sudden flooding occurring during heavy swells associated with storms and cyclones. Human impacts growing on the shoreline and on river basin in the recent decades have also affected coastal sedimentation (Figure 4.20). Preliminary analysis of the dataset, presented at EARSel 2015 workshop in Luxembourg, shows good discrepancy between corals and sands. Specifically, differences in bottom types are detected with an automated processing algorithm. We are still extending the image processing using several other processing techniques, both supervised and unsupervised.



Figure 4.20: UAV mapping on the Lagoon (left); HIS mapping of corals area (right)

Investigation of heavy metals distribution in suspended matter and macrophytes of the Selenga river delta using airborne hyperspectral remote sensing

Y. Akhtman, D. Constantin, M. Rehak

Ecole Polytechnique Fédérale de Lausanne

The Lemna-Baikal project is an international Swiss-Russian research initiative in the fields of physical limnology, geochemistry and hydrology of aquatic geosystems. The main methodological principle of the project is constituted by simultaneous collection of airborne wide-area Hyperspectral Imaging (HSI) and ground point-based data. In particular, a specially developed remote sensing platform based on the Headwall Photonics Micro Hyperspec VNIR sensor (250 bands, 400-1000 nm) was utilised as the main instrument. The platform was deployed using an Air Creation Tanarg 912S ultralight aircraft. Ground-truthing team collected water samples at 52 points, filtered it using Millipore Vacuum Pump through 0,45 mic filters to determine total suspended matter (TSM) concentration. Also samples of macrophytes were collected. In this study the distribution of heavy metals in the Selenga river delta was quantified and mapped (Table 4.3).

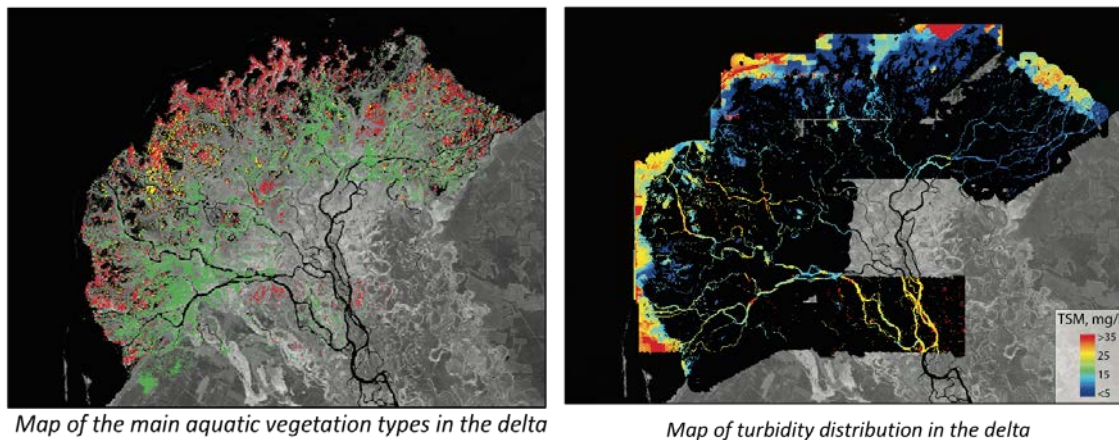


Figure 4.21: Maps of vegetation and turbidity in the delta of the Selenga river

Plant	Cr	Fe	Co	Cu	As	Mo	Pb
Small yellow pond-lily	191,0	111793,4	36602,3	142,0	88,3	20,4	25,1
Common reed	4,0	22060,4	5926,0	48,4	43,3	20,6	29,2
Pondweeds and watermilfoils	1466,9	1031032,2	485348,2	438,4	789,3	119,3	46,0

Table 4.3: Heavy metal concentrations accumulated in macrophytes (mg per sq m).

Satellite Positioning Performance Assessment for Road Transport, SaPPART COST Action TU 1302

P.-Y. Gilliéron¹ and U. Wild²

¹Ecole Polytechnique Fédérale de Lausanne

²Swiss Federal Office of Topography, swisstopo

Since end of 2013 Switzerland is involved in the COST Action TU 1302 on the Satellite Positioning Performance Assessment for Road Transport (SaPPART). As Swiss delegate of SaPPART, P.-Y. Gilliéron is also member of the chair of this Action. The main contribution of SaPPART is a better understanding and definition of the Global Navigation Satellite Systems (GNSS) within road transport and mobility services, with a particular focus on safety-related application (Figure 4.22). The road sector is estimated to represent more than 50% of the GNSS market and 75% when we consider the mobility services on smartphones. However, the current lack of a pan-European certification process underpinned by agreed standards is impeding the realisation of the expected benefits. The main reason for this is the complexity of defining and assessing GNSS performance which is highly influenced by the environment and operational scenario. Although standardisation activities have been initiated in Europe on this topic, many scientific issues are still open and require a common agreement. This Action brings together more than 80 leading experts in GNSS, ITS and mobility, from 22 countries, to address the open issues and guarantee the success of the standardisation for underpinning certification initiatives. The Action will provide 4 deliverables (White paper on GNSS for personal mobility and road transport; Handbook presenting the methodology; Guidelines for generic test procedures; Data sets) and will propose a unified framework for definition and assessment of performance for the GNSS-based positioning terminals. This framework is expected to pave the way for certified terminals, which is predicted to result in a significantly accelerated use of GNSS-based ITS and mobility applications.

Main objectives of the Action:

- To develop a framework for the definition of service levels for the GNSS-based positioning terminals, used in ITS and Personal Mobility applications, and the associated examination framework for certification purposes.
- To promote high-level educational and training programmes in the fields of GNSS, GNSS-based ITS and Personal Mobility applications.
- To promote the use of GNSS in general, and EGNOS and Galileo in particular, in ITS and Personal Mobility domains, for their common long-term development and deployment in Europe.

More specifically this Action has the following objectives:

- Capitalizing the main results of a number of National, European and International projects of the past 5 years that addressed the use of GNSS in the road sector.
- Coordinating European scientists to highlight problems and open issues, strength and weaknesses of GNSS solutions envisaged in different ITS applications.
- Developing a framework for the definition of service levels for the GNSS-based positioning terminals and the associated examination framework for certification purposes.

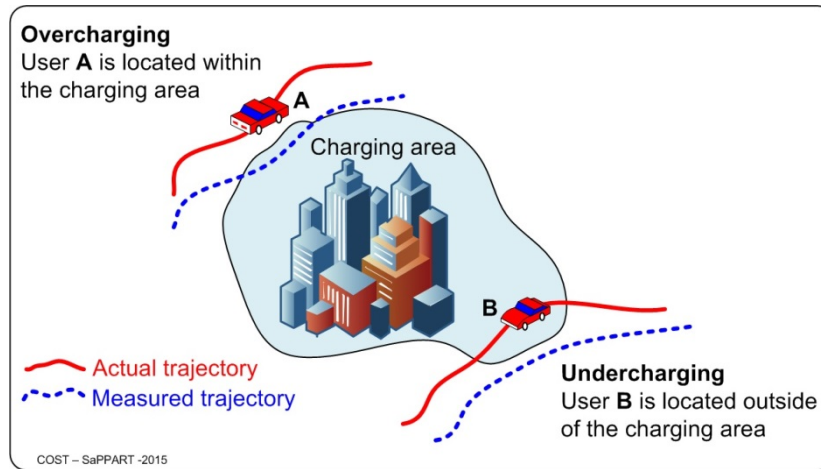


Figure 4.22: Road user charging is one example of road application based on GNSS signals. Positioning integrity plays a key role in such liability-critical application.

Bernese GNSS Software.

R. Dach¹, D. Arnold¹, C. Baumann¹², S. Bertone¹, H. Bock¹³, Y. Jean¹, A. Jäggi¹, S. Lutz¹², A. Maier¹, M. Meindl¹⁴, L. Mervart¹⁵, U. Meyer¹, E. Orliac¹, E. Ortiz-Geist¹⁶, L. Ostini¹, L. Prange¹, S. Schaer¹⁷, K. Sośnica¹⁸, D. Thaller¹⁹, P. Walser¹, A. Villiger¹, G. Beutler¹

¹Astronomical Institute, University of Bern

²Now with Federal Office of Topography, swisstopo

³Now with PosiTim UG

⁴Now with Institute of Geodesy and Photogrammetry, IGP, ETH Zurich

⁵Institute of Geodesy, Czech Technical University Prague

⁶European Space Operations Centre, Darmstadt

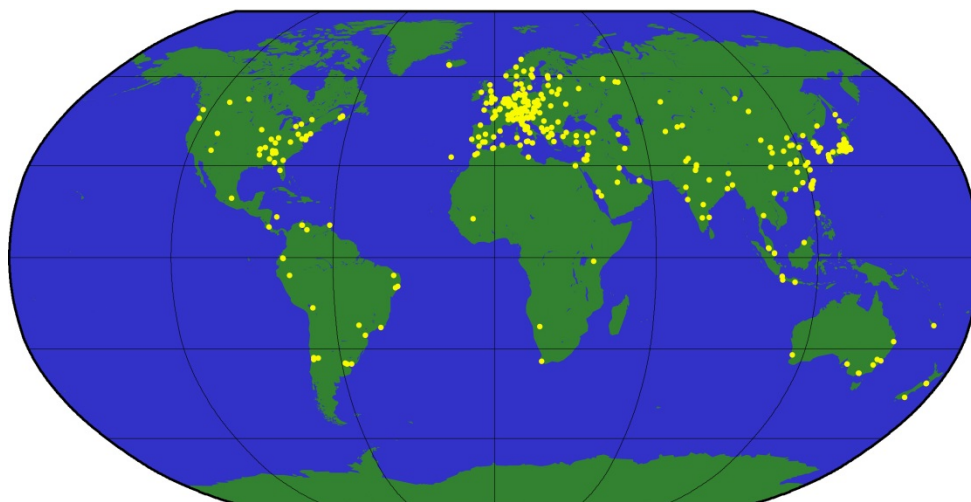
⁷Federal Office of Topography, swisstopo

⁸Now with Institute of Geodesy and Geoinformatics, Wrocław University of Environmental and Life Sciences

⁹Now with Federal Agency for Cartography and Geodesy, BKG

The Bernese GNSS Software (BSW, Dach et al., 2007) is the backbone for all activities of the satellite geodesy research group at AIUB: high performance processing of measurements, obtained by GNSS (Global Navigation Satellite Systems) and SLR (Satellite Laser Ranging), precise orbit determination for Low Earth Orbiting satellites (LEOs), and even gravity field determination. The software is also applied in the context of operational processing schemes, e.g., in the context of CODE (Center for Orbit Determination in Europe) since more than 20 years. CODE is a consortium of four institutions, namely the Astronomical Institute of University of Bern (AIUB, Switzerland), the Swiss Federal Office of Topography (swisstopo, Switzerland), the Bundesamt für Kartographie und Geodäsie (BKG, Germany), and the Ingenieurinstitut für Astronomische und Physikalische Geodäsie, Technische Universität München (IAPG/TUM, Germany). CODE's main functions are its activities as an Analysis Center (AC) of the International GNSS Service (IGS, GNSS standing for Global Navigation Satellite System), AC of the European Permanent Network (EPN), and as an Associated AC of the International Laser Ranging Service (ILRS).

The BSW is a high performance, high accuracy GNSS and SLR post-processing software package for the space-geodetic community. It is supported, maintained, and regularly updated by AIUB, considering the latest recommendations and models (e.g., IERS Conventions, Petit and Luzum, 2010) as well as technological advancements (e.g., new satellite systems and observables), offering the user a maximum of flexibility in customizing processing strategies and options. The BSW comes with a user-friendly interface, an online help system, and an extensive user manual. The so-called Bernese Processing Engine (BPE) allows for automated processing, which is especially useful for large network processing and reprocessing efforts. Nowadays the BSW consists of more than 100 programs and about 1300 modules and subroutines, is platform-independent, and is used by some hundred customers throughout the world (see Figure 4.23).



 2014 Aug 20 12:30:29 Geographical Distribution of Institutions using the Bernese GNSS Software

Figure 4.23: Worldwide distribution of the Bernese GNSS Software users as of February 2015.

As the support for BSW version 5.0 will end soon, most users meanwhile switched to the current version 5.2, which was released in late 2012. The major improvements of version 5.2 with respect to version 5.0 are:

- FODITS: Find Outliers and Discontinuities in Time Series (Ostini et al., 2008) – a tool dedicated to various types of time series (not only site coordinates).
- Algorithm for GLONASS ambiguity resolution (Schaer et al., 2009).
- Possibility to estimate GLONASS clock corrections (Dach et al., 2010).
- Precise Point Positioning (PPP) possible for GLONASS.
- GNSS-specific receiver antenna corrections (Dach et al., 2011a).
- New troposphere models: GMF/GPT (Boehm et al., 2006a, Boehm et al., 2006b) and VMF1 (Boehm et al., 2007) for microwave, and Mendes-Pavlis (Mendes and Pavlis, 2004) for SLR data processing.
- Modelling of higher order ionosphere correction terms (2nd, 3rd and ray bending) (Lutz et al., 2010).
- Handling of the quarter-cycle L2C shift.
- Update to IERS 2010 Conventions (DE405, OTL-CMC, mean pole, and many more).
- Geophysical (deformation) models can be introduced as grids and validated by estimating scaling factors (Dach et al., 2011b).
- Capability to process SLR-Range data (Thaller et al., 2009).
- Experimental Galileo and RINEX3 support (Prange et al., 2014).
- (the full list can be found at <http://www.bernese.unibe.ch>)

For the daily research at AIUB we continuously develop the software. Important enhancements are an improved radiation pressure modelling (Arnold et al 2015a, this volume), and the multi-GNSS capability (Prange et al. 2015, this volume) – of course accomplished by many improvements related to the latest scientific standards and background models. This version will be the bases for future versions provided to the user community.

CODE Contributions to Global Ionosphere Monitoring

S. Schaer^{1,2}, A. Villiger¹

¹Astronomical Institute, University of Bern

²Federal Office of Topography, swisstopo

CODE has been extracting information of the total electron content (TEC) from the International GNSS Service (IGS) tracking data since 1995. Since June 1998, related global ionosphere maps (GIM) have been generated in IONEX (Ionosphere Exchange) format and provided to the IGS to support variable applications, e.g., dealing with the ionosphere induced short-term signal variations or strong horizontal gradients.

In addition to this primary IONEX product, which is a product of the final analysis line, also corresponding rapid and predicted GIMs are generated at CODE on an operational basis. All GIM products are made available in form of IONEX and as ionosphere files in the internal format of the Bernese Software (Dach et al. 2007). Since July 2000, CODE has additionally been providing RINEX-formatted Klobuchar-style ionosphere coefficients (best fitting CODE's IONEX data).

In November 2014, the time resolution has been increased (from 2 hours) to 1 hour for all CODE GIM product lines (Schaer 2014). In order to manage the doubled number of GIM parameters, the final and rapid GIM computation procedures were completely redesigned and, furthermore, adjusted to latest NEQ processing standards. The new procedures turned out to be considerably faster than the previous procedures, even when applying it to the doubled number of GIM parameters.

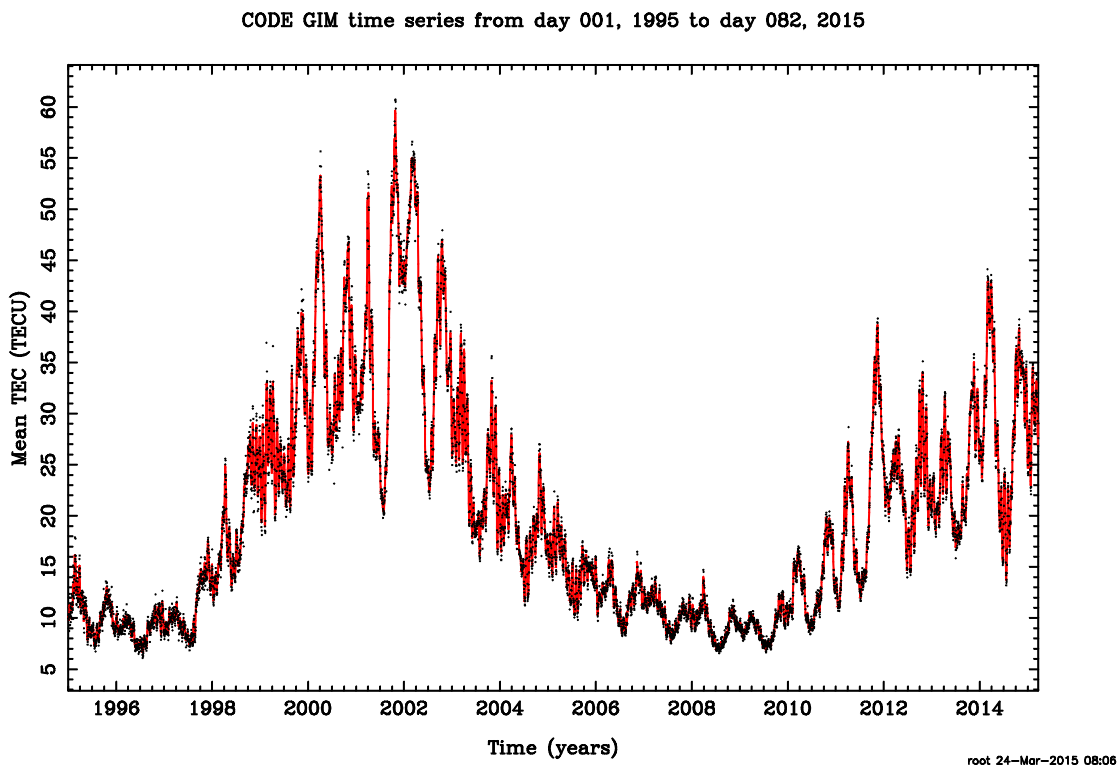
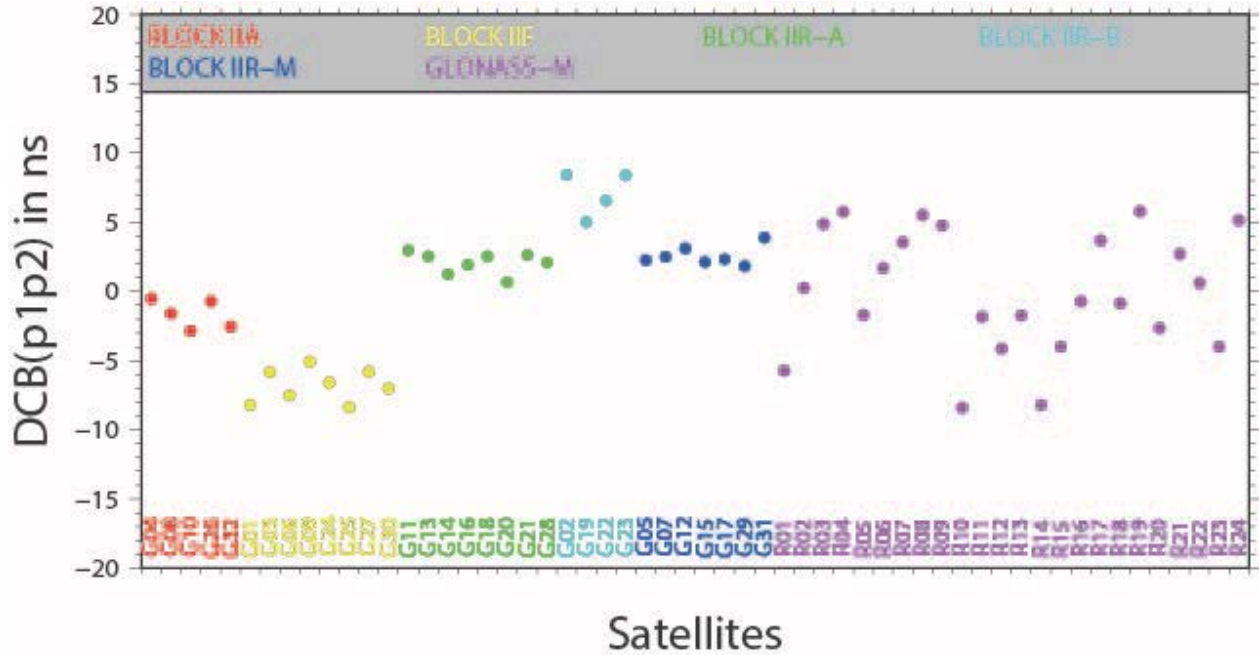


Figure 4.24: The time series of global mean TEC values extracted from the GIMs produced by CODE covers, with 20 years, almost two (11-year) solar cycles. Daily averaged mean TEC values, namely the zero-degree coefficients of the spherical harmonic expansion used to represent the global TEC, are shown. Annual

and semi-annual variations are visible. The ionospheric signal also includes very pronounced 27-day variations, caused by distinctive groups of sunspots co-rotating with the Sun.

P1-P2 DCBs (differential code biases) for GPS and GLONASS (satellites and receivers) are an essential by-product of the ionosphere analysis. Figure 4.25 shows corresponding bias results for the two satellite constellations and Figure 4.26 for the GNSS receiver components.



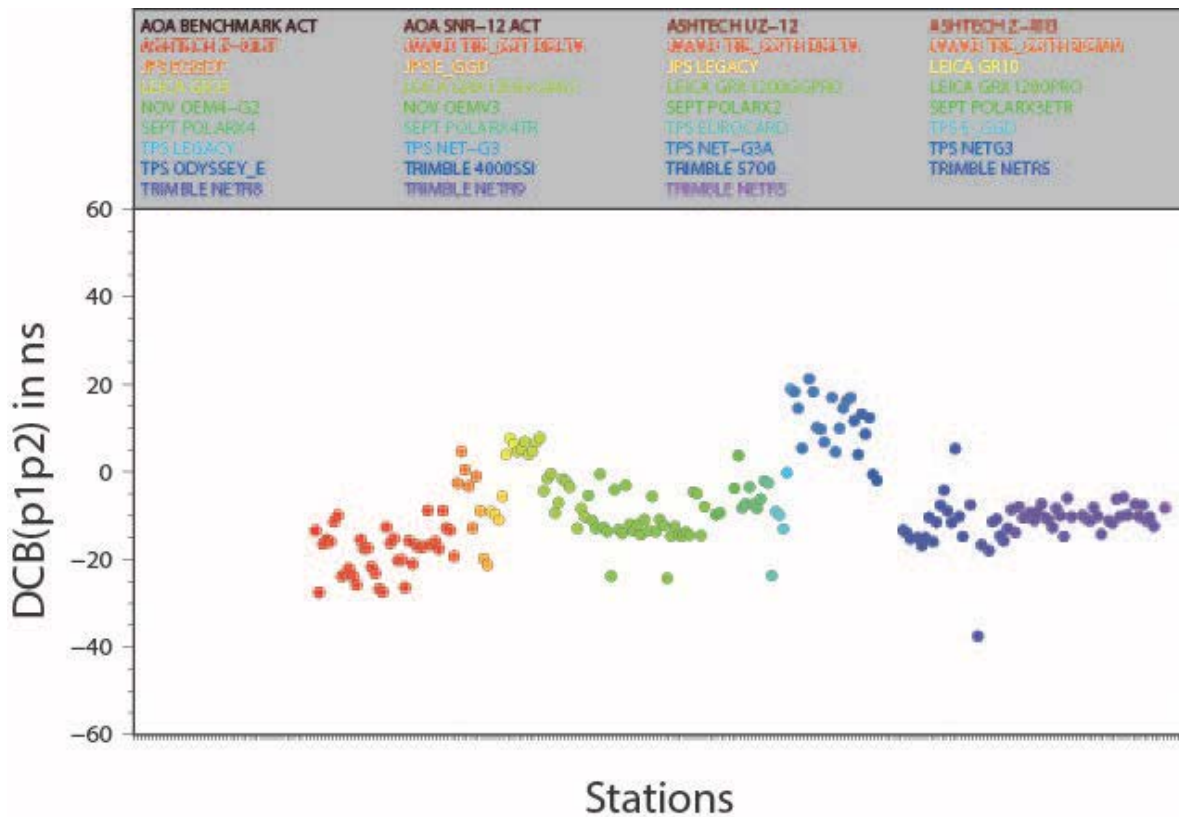
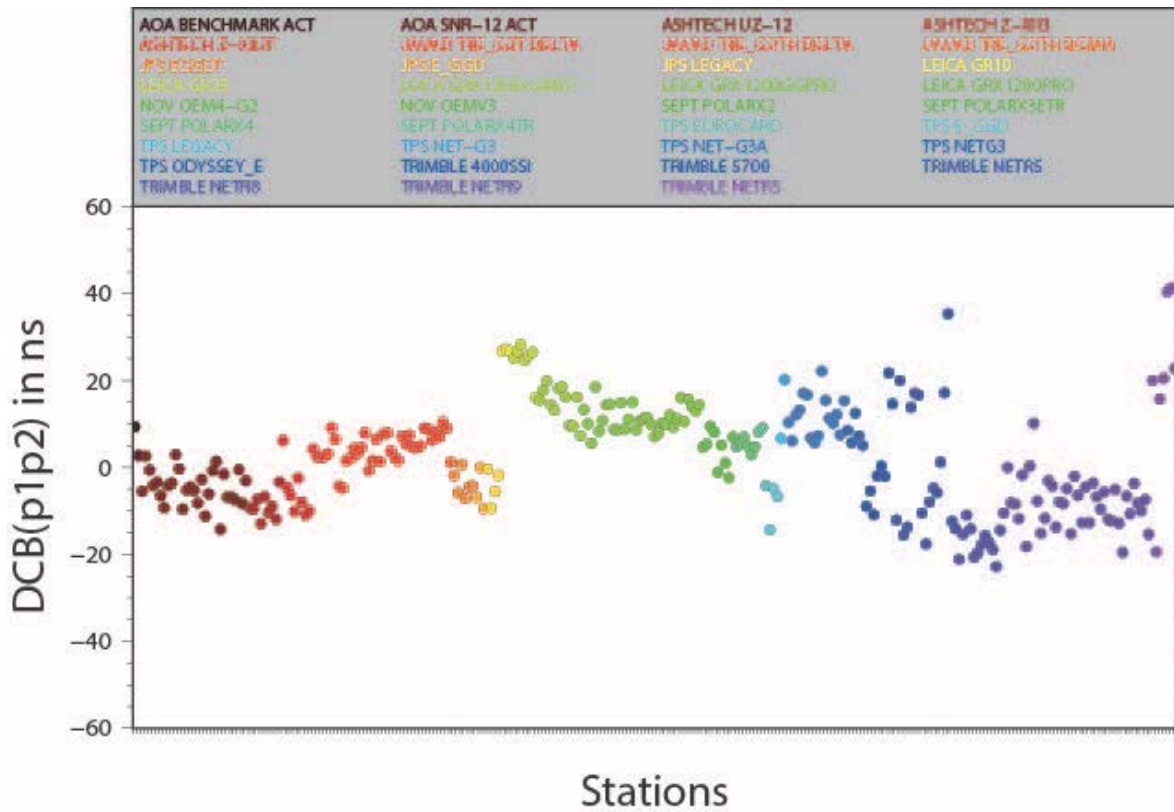


Figure 4.26: Monthly set of P1--P2 differential code biases for the GPS (top) and GLONASS (bottom) receiver components, for December 2014, computed at CODE.

Since the beginning of 2010, CODE has considered not only first-order but also higher-order ionosphere (HOI) and ray bending correction terms for the analysis of space geodetic observations in the operational contributions as well as for a future reanalysis of the data from IGS (Lutz et al. 2009, 2010). It should be mentioned that the previously introduced GIM products are of fundamental importance for computation of these higher-order ionosphere correction terms.

The Bernese GNSS Software was expanded with the ability to assign additional scaling parameters to the second and third order ionosphere term and to the ray bending term. This implementation concept allows switching on and off individually each HOI correction term on normal equation level. Corresponding scaling parameters may be set up globally or even specific to each ground station involved (in order to detect station anomalies and eventually refine HOI correction models). Moreover, the significance of each term may be verified on observation level for different ionosphere conditions.

In time periods with high ionosphere activity, higher-order ionosphere terms should be considered for global GNSS analysis. In times with low TEC levels, these correction terms are not significant. Depending on station latitude, elevation angle (an elevation mask angle of 3 degrees is used at CODE), and observation epoch, the second order HOI correction term of a single observation may reach few centimeters at extreme cases. Nevertheless, observation corrections due to HOI refraction effects are generally comparably small but the computation of the corresponding correction values is relatively CPU-time consuming. For global analysis, the impact on station positions (and consequently on the reference frame relied on) is of systematic nature and therefore has to be taken into account.

Ambiguity Resolution for GLONASS

S. Schaer^{1,2}

¹*Astronomical Institute, University of Bern*

²*Federal Office of Topography, swisstopo*

In June 1995, CODE was the first IGS AC that started to perform ambiguity resolution for GPS (for the global analysis). In February 2011, the same became true for GLONASS. As documented in the CODE analysis summary of GPS week 1625 (Schaer et al., 2011), ambiguity resolution was extended to GLONASS for three resolution strategies. CODE's extended GNSS ambiguity resolution scheme as performed in an operational mode may be summarized as follows:

- Up to 6000km (3000km in a first POD (precise orbit determination) step): Melbourne–Wübbena widelane and subsequent narrowlane ambiguity resolution (AR) are restricted to GPS only.
- Up to 2000 km: Quasi–Ionosphere–Free (QIF) L1/L2 AR for GPS and in addition for GLONASS DD ambiguities with the same frequency channel numbers.
- Up to 200 km: Phase–based widelane AR for GPS and GLONASS, including retrieval of GLONASS SD ambiguity initialization biases; narrowlane AR for GPS and GLONASS, considering the previously retrieved SD bias values.
- Up to 20 km: Direct L1/L2 AR for GPS and GLONASS, including retrieval of GLONASS SD ambiguity initialization biases. Optionally, the widelane–based SD bias retrievals could be considered as a priori bias information.

We consider the following rules essential for successful GLONASS ambiguity fixing:

- GNSS ambiguity parameters are generally treated at SD level.
- GNSS ambiguities are resolved at DD level (differences of SD ambiguities).
- The SD ambiguity parameters directly respond to (always) existing SD (ambiguity initialization) biases. Implicitly, they act as SD bias calibration parameters and thus may absorb present SD biases in the LS parameter adjustment.
- The initial singularity concerning all involved SD ambiguity parameters has to be eliminated by imposing loose constraints on these parameters. After fixing a first GLONASS DD ambiguity for a pair with unequal frequency channel numbers, SD ambiguity parameters become determinable.
- There are no extra bias parameters at DD level, apart from (unresolved) intersystem ambiguity parameters (see next item).
- GPS–GLONASS intersystem ambiguities are generally treated unresolved.
- A self–calibrating AR procedure (as used at CODE) is definitively indispensable.
- Our AR principles are also applicable to rapid static positioning using LAMBDA methods generalized for multi–GNSS (Schaer et al., 2009).

The benefit from the ambiguity resolution for the GLONASS observations is clearly visible in Figure 4.27. It is remarkable that this also did improve the orbits for the GPS satellites.

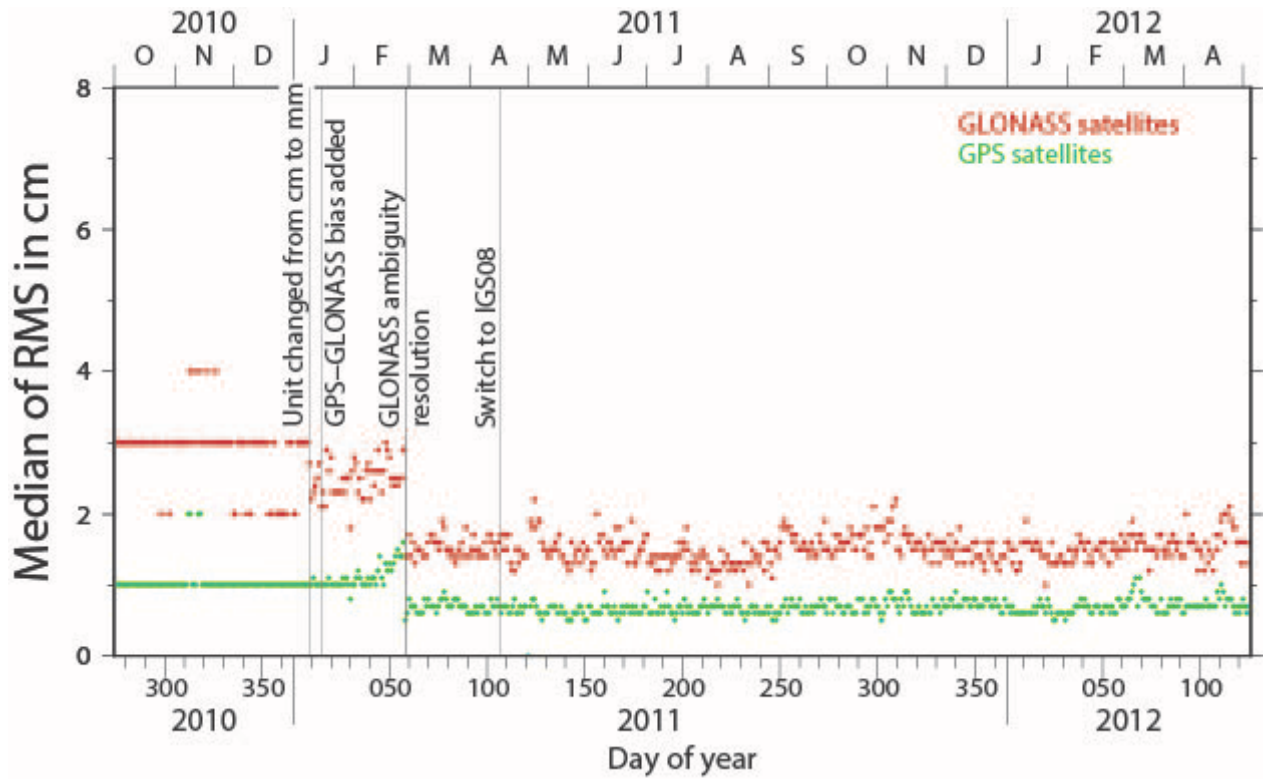


Figure 4.27: Median of the RMS from a three-day orbit fit.

Clock Modelling in GNSS Processing

E. Orliac¹, R. Dach¹

¹Astronomical Institute, University of Bern

Between 2010 and 2013, the Astronomical Institute of University of Bern (AIUB) took part to the “Satellite and station clock modelling for GNSS” ESA project, as the prime-contractor in a consortium consisting of AIUB, Technical University of Munich (TUM) and the Swiss Federal Institute of Technology of Zurich (ETH). The main objective of the project was to explore and use the stability of the best satellite and ground receiver clocks in Global Navigation Satellite System (GNSS) data processing, which is currently completely ignored in nowadays processing. This is due to the very high requirements put on the stability of the clocks to be useful in that direction: considering the ionosphere-free linear combination has a noise of 3 mm (i.e. 10 ps), the clock has to be stable to roughly 15 ps over the sampling rate of the processed data. This sampling rate can vary from several Hz to 300 s, as typically used for post-processing activities. Such stability is reached by the current best satellite clocks, such as the rubidium clocks onboard the GPS block IIF satellites or the H-Maser clocks of the Galileo satellites. Figure 4.28 illustrates the improved performances of the new generation of the rubidium clock driving the Block IIF satellites compared to the older generation ones equipping the GPS Block IIR-M satellites. On short averaging intervals, the stability is about one order of magnitude better.

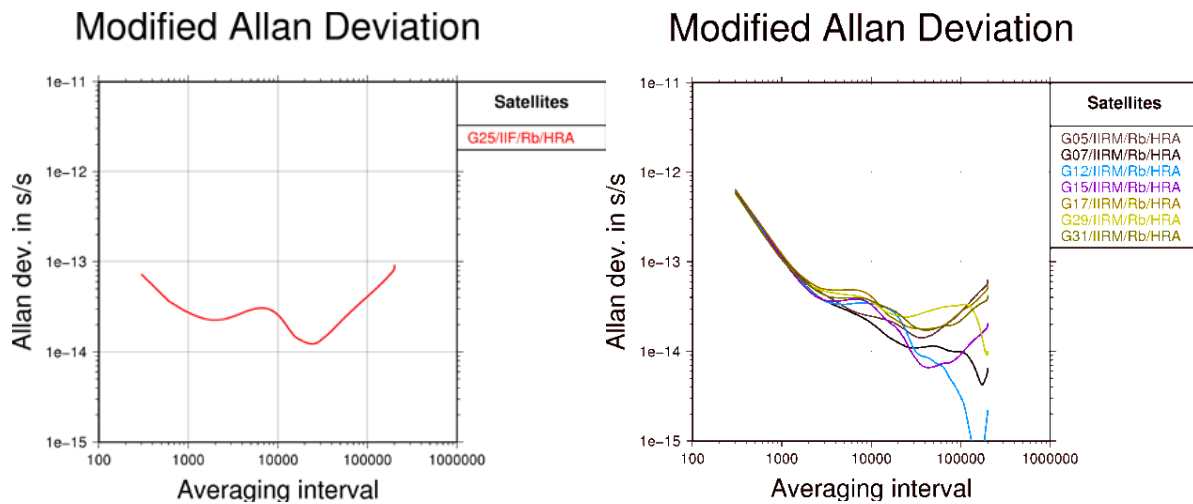


Figure 4.28: Comparison of the stability of older (left) and newer (right) GPS rubidium clock performances. The modified Allan deviation was computed on 7-day long time series with a sampling rate of 300 s.

Clock modelling is a very promising approach in GNSS data processing. It can potentially significantly reduce the number of parameters to be estimated as the epoch-wise satellite clock parameters could be replaced with a very basic model (e.g. 1st order polynomial) over the processed interval. This highly reduced parameterization would help stabilizing the solution in the short-term range (whereas the ambiguity resolution stabilizes the solution primary in the long-term range) if one thinks in terms of the other parameter types such as station height and troposphere which highly correlate with the clock parameters.

On the other hand, independent epoch-wise clock parameters are known for absorbing other model deficiencies, in particular solar radiation pressure modeling defects in orbit models. This lead to another very promising aspect of

better clocks in space: by monitoring their performances, one can directly judge about the orbit modeling for example. This was already demonstrated with the H-Maser clocks onboard the Galileo satellites.

The Bernese GNSS Software (BSW, [Dach et al., 2007]) was modified in order to allow clock modelling. Clock modelling was implemented as parameter transformation on the normal equation level. Different types of models are available, such as polynomials, cubic spline or periodic signals. So far, the impact of satellite clock modelling in global network solution appeared to be negligible, mainly because of the very limited number of satellites with clocks stable enough to allow clock modelling. But the situation is now evolving rapidly, thanks to the modernization of existing GNSS such as GPS, or the building up of new ones, such as QZSS or Galileo, where all satellites will be driven by H-Maser clocks, which nicely allow for clock modeling over one day with first or second order polynomials. Note that the typical bulge seen in the modified Allan deviation plot (see Figure 4.28) are due to deficiencies in the solar radiation pressure model. The Center for Orbit Determination in Europe (CODE) recently developed a model which significantly improves the situation [Arnold et al., 2015a].

Clock modelling will mainly benefit to kinematic objects processed with a high data sampling and real-time applications that require clock predictions. To illustrate the purpose, static ground GNSS sites driven by H-Maser clocks were processed in a kinematic mode over February 2011. The reference solution is the standard kinematic Precise Point Positioning (PPP) where receiver clocks were estimated independently every epoch. Then a series of solution based on deterministic clock modelling were derived, ranging from first and second order polynomial (solutions KIB and KIC in Figure 4.29) to cubic splines with node spacing of 30 and 15 minutes (solutions KIF and KIG in Figure 4.29). It is remarkable that the best improvement in term of station height stabilization was obtained with the most simple models, requiring only 2 and 3 parameters to represent the clock behavior over one day. The data was processed at a sampling rate of 300 s, meaning that the number of receiver clock parameters was reduced by a factor of up to 144.

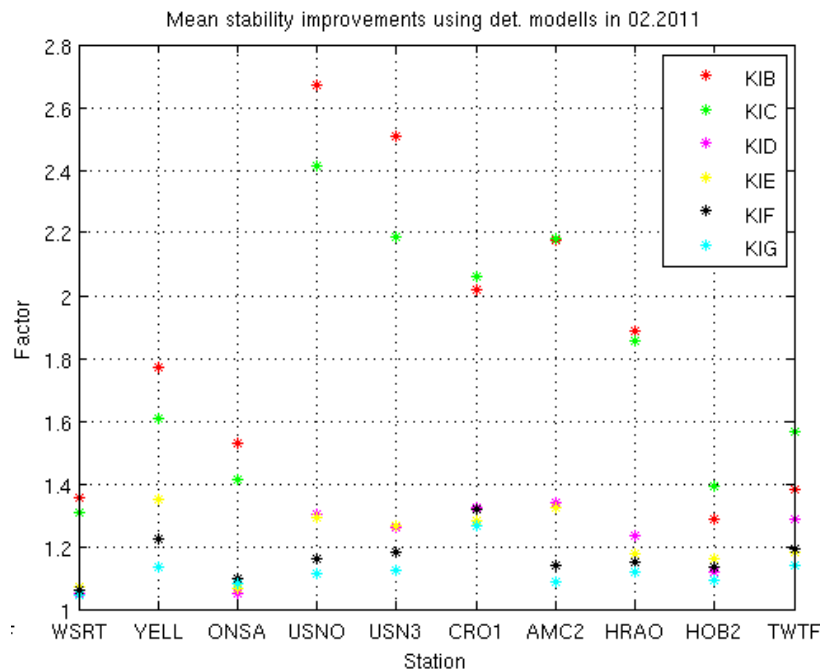


Figure 4.29: Mean PPP kinematic station height stabilization factors obtained for different deterministic clock models. Ten stations equipped with H-Maser were processed over February 2011.

GNSS data processing in the National Multi-Hazard Early Warning System in the Sultanate of Oman

D. Arnold¹, R. Dach¹, J. Steinborn², A. Kloth²

¹Astronomical Institute, University of Bern

²DiGOS Potsdam GmbH; successor of Space Tech's branch for terrestrial applications

After the disastrous tsunami on December 26, 2004 in the Indian Ocean, a lot of effort has been undertaken to plan and realize tsunami early warning systems. As one of the first reactions, already in 2005 the German Indonesian Tsunami Early Warning System (GITEWS, Falck et al., 2010) was initiated by the German government. Its establishment was coordinated by the German Research Centre for Geosciences Potsdam (GFZ) and it was successfully handed over to the Indonesian partner institutions in 2011.

In 2009, UNESCO signed an agreement with the Sultanate of Oman to establish a National Multi-Hazard Early Warning System (NMHEWS, <http://www.unesco.org/new/en/unesco/partners-donors/the-actions/sciences/national-multi-hazard-early-warning-system-nmhews/>). It is composed of several sensor networks, with seismic stations, GNSS stations, meteorological stations and tide gauges as the main components. The German company SpaceTech GmbH was commissioned to coordinate the setup of the GNSS sector, in cooperation with the GFZ and the Astronomical Institute of the University of Bern (AIUB). While SpaceTech carried out the system engineering, installation, training, initial operation and maintenance of the GNSS network with expertise contributed by GFZ, the AIUB provided the expertise for the GNSS data processing. The GNSS network consists of 10 permanent stations, equipped with Septentrio PolaRx4 receivers and NavXperience 3G+C antennas providing real-time data. Figure 4.30 shows the locations of the GNSS stations in Oman. The purpose of the network is the mid- and long-term monitoring of the tectonic plate movement of the Arabian Peninsula which can be used for analyzing Earthquake potential and the near real-time monitoring of crustal deformation to cross validate the possibility of a tsunami after a nearby submarine Earthquake. The data is streamed to a processing facility at a tsunami warning center in Muscat, where, with a delay of less than 2 minutes, the displacement vectors of the stations are computed. Due to current limitations of the communication bandwidth, only GPS data is streamed and processed.

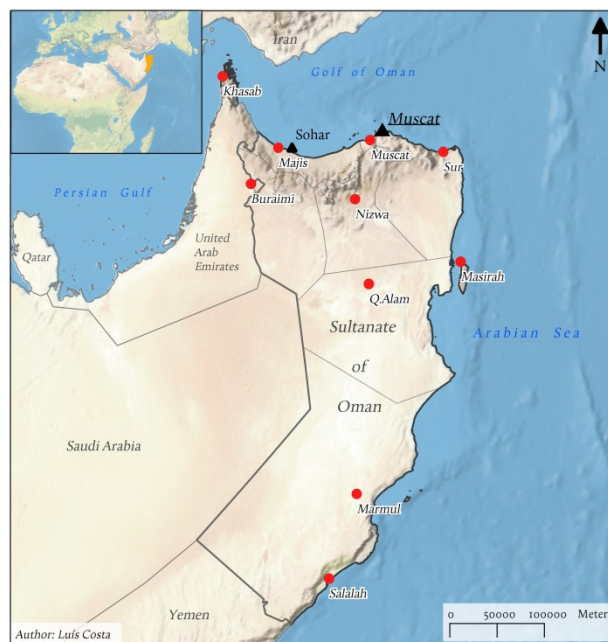


Figure 4.30: Locations of the GNSS stations (red dots) of the NMHEWS. By courtesy of Luís Costa.

The data is processed in a batch mode with the Bernese GNSS Software v5.2 (Dach et al., 2007), using the ultra-rapid orbits and Earth rotation parameters of the Center for Orbit Determination in Europe (CODE, Dach et al. 2014). To bypass the need of accurate near real-time satellite clock corrections for a precise point positioning and to make use of ambiguity resolution, the processing is based on double-differenced GNSS data, where baselines are formed with an algorithm to maximize the number of common observations.

The data processing is split up into two main steps: a datum step and a near real-time step. In the datum step (repeated once per hour) a solution for the ten warning stations together with external IGS reference stations is computed to monitor the stability of the warning stations w.r.t. the global reference frame. For this, a defined amount of the most recent data is used from the warning and the reference stations and ambiguities are resolved in an extended procedure. In the near real-time step (repeated every two minutes) only data from the warning stations is processed. To speed up the preprocessing, ambiguities are resolved in a single strategy suitable for the present baseline lengths and by using again a certain number of hours of the most recent data. For the last three minutes of the data, kinematic coordinates are estimated for the warning stations introducing the resolved ambiguities and using a no-net-translation condition for each epoch w.r.t. the coordinates computed for the warning stations in the most recent datum step. The ambiguity resolution success rate, the characteristics of consecutive coordinate batch overlaps and the processing time served as quality measures to develop and optimize the processing routines.

The processing of the GNSS data was established and assessed at AIUB in a test scenario, defined by a number of stations of the European Permanent Network (EPN, <http://www.epncb.oma.be/>) providing real-time data as well as IGB08 reference stations (Arnold et al., 2013). In addition, data from GITEWS, recorded during the May 2010 Northern Sumatra Earthquake, was analyzed using the developed procedures. Figure 4.31 shows the locations of the GNSS stations the data of which was processed, as well as the epicenter of the Earthquake. Figure 4.32 shows North, East and Up components of the kinematic coordinates of station Meulaboh (GITEWS station closest to the epicenter) on May 9, 2010 from 05:50 to 06:10 UTC. The vertical black line indicates the time of the Earthquake. The Figure reveals that the station suffered from a displacement of a few centimeters in all three directions and proves that the established processing scheme is capable to detect it.

In the meantime, the NMHEWS in the Sultanate of Oman is operational and working since January 2014. The maintenance of the GNSS networking is performed by the spin-off and successor of SpaceTech's branch for terrestrial applications company DiGOS Potsdam GmbH, which has been founded by former SpaceTech employees for terrestrial applications and now continues the engineering and development of geodetic observation systems.

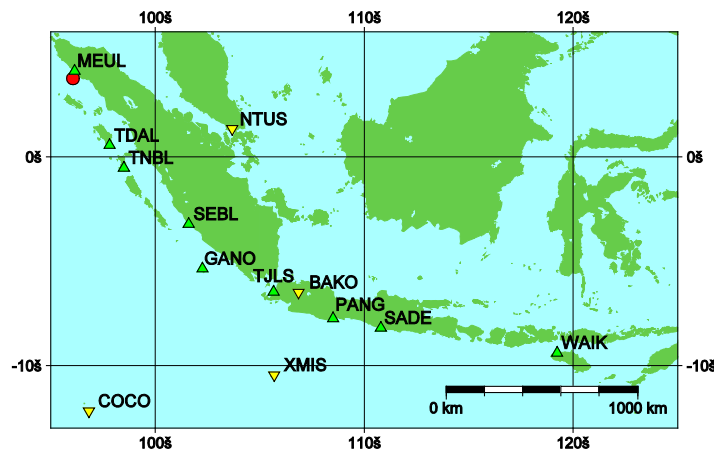


Figure 4.31: Green triangles: the 9 GNSS stations at tide gauges of the GITEWS. Yellow inverted triangles: IGS reference stations. Red circle: the epicenter of the May 2010 Northern Sumatra Earthquake.

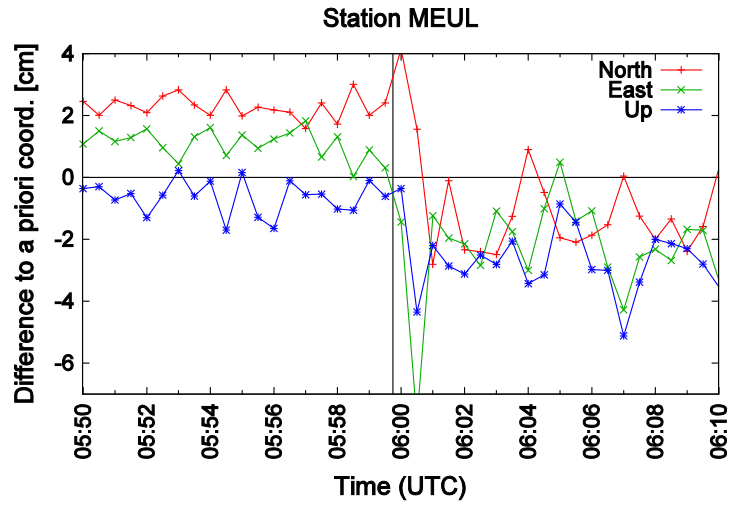


Figure 4.32: Kinematic coordinates of station MEUL on May 9, 2010. Vertical black line: time of the Earthquake.

Updating the IGS orbit combination for a Multi-System and multi-Frequency environment

E. Ortiz-Geist^{1,2}, R. Dach¹, E. Schönemann², W. Enderle²

¹*Astronomical Institute, University of Bern*

²*European Space Operations Centre, Darmstadt*

Motivation

The International GNSS Service (IGS, Dow et al. 2009) is well established as a scientific reference for GPS data processing since more than 20 years. The observations from a global tracking network are processed by a number of Analysis Centers (AC's, typically around ten nowadays) and combined to the official IGS products by the Analysis Center Coordinator (ACC) using an algorithm described by Beutler et al. (1995).

Some of the AC's have extended their activities to GLONASS, the Russian counterpart to GPS by a rigorously combined GPS and GLONASS solution. At the same time, the combination within the IGS takes place in two fully independent chains for GPS and GLONASS.

Extrapolating this current situation by the current development in the frame of IGS-MGEX (multi-GNSS experiment, Montenbruck et al. 2014) we will be faced in the future with inhomogeneous contributions by the different IGS AC's:

	GPS	GLONASS	Galileo	BeiDou	QZSS	IRNSS
AC1						
AC2						
AC3						
AC4						
AC5						

Figure 4.33: hypothetical scenario on the selection of constellations by IGS AC's

On top of this, with the modernization programs of the established Global Navigation Satellite Systems (GNSS) and the new systems under construction the manifold of frequencies and signals will significantly increase. This development is accomplished by an even more dramatic increase of signal tracking techniques indicated, what likely will increase the variability between the AC's contribution.

Emerging questions:

- What is the optimal combination strategy in order to
 - o keep the internal consistency between the systems from the contributing solutions into the combined products?
 - o obtain the optimal quality for the combined orbits of all satellites considering that the quality of the orbits from the different constellations may vary.
- In particular for the clock combination:
 - o How to consider the potential biases if each AC shall be free to choose any of the frequencies, signals and available observation types.

In order to answer these questions the Astronomical Institute, University of Bern (AIUB) and the European Space Operations Centre (ESOC) have established a PhD work in the frame of the Networking Partnership Initiative (NPI) program.

First Results:

As a first step the IGS final solutions from CODE and ESA have been compared, which are both generated to provide fully consistent GPS and GLONASS orbit products. This setup allows to get a first answer to the question to which extent the noisier orbit from GLONASS degrades the better GPS orbit in a combined combination scheme.

For this purpose we consider three different schemes to compare the two orbit products:

- 1) extracting only the GPS satellites,
- 2) considering only the GLONASS satellites,
- 3) taking all GPS and GLONASS satellites into account.

The comparison includes the 7-Helmert transformation parameters (scale, 3 rotation and 3 translation parameters) between the two set of orbits, one being CODE solution and the other one ESA solution. The Table 4.4 below shows the mean values and standard deviations of Helmert transformation parameters estimated from the orbit comparisons of one week.

	GPS-only		GLONASS-only		GPS+GLONASS	
	mean	std-dev.	mean	std-dev.	mean	std-dev.
Scale	0.23 ppb	0.05 ppb	0.35 ppb	0.10 ppb	0.28 ppb	0.07 ppb
Rotation x	0.04 mas	0.02 mas	0.04 mas	0.03 mas	0.04 mas	0.02 mas
Rotation y	0.01 mas	0.01 mas	0.06 mas	0.02 mas	0.03 mas	0.02 mas
Rotation z	0.04 mas	0.02 mas	0.08 mas	0.03 mas	0.02 mas	0.01 mas
Translation x	-0.2 mm	0.5 mm	-1.1 mm	1.6 mm	-0.1 mm	0.8 mm
Translation y	2.1 mm	0.7 mm	-1.1 mm	1.1 mm	0.7 mm	0.4 mm
Translation z	-7.1 mm	2.8 mm	21.7 mm	3.7 mm	5.5 mm	2.8 mm

Table 4.4: Transformation parameters when comparing the CODE and ESA contributions to the IGS final product during one week in January 2015 considering a subset or even all satellites; the values exceeding 3 times the standard deviation are indicated.

The scale and the translations in the Z direction are the two parameters where the two solutions show significant differences. The scale differences between the GPS-only and GLONASS-only comparison is about 0.1 ppb which corresponds to about 2.5 cm in the radial component at the height of the GPS and GLONASS satellites. In addition, the CODE and ESA GLONASS-only orbit products differ by about 3 cm in the Z translation.

Both discrepancies are reflected in the differences between the transformation parameters obtained by the single-system and the GPS+GLONASS approach. This is reflected in a degradation of the residuals, which affects the RMS after applying the transformation parameters to the orbit comparisons: the RMS of the orbit comparison increases by ~25% for the GPS and by ~9% for the GLONASS satellites, when applying the transformation parameters obtained from both GPS and GLONASS instead of separately derived ones.

With the current combination scheme both AC's would be «punished» by a reduction of their weight to the combined product when they are submitting multi-GNSS instead of single system contributions. These results confirm the need for an updated product combination scenario to consider the aspects of multi-GNSS solutions.

Local uplift rates in the Swiss Alps (Wildhorn-Decke¹)

B. Sievers

Institute of Geomatics Engineering, University of Applied Sciences and Arts Northwestern Switzerland FHNW

Motivation

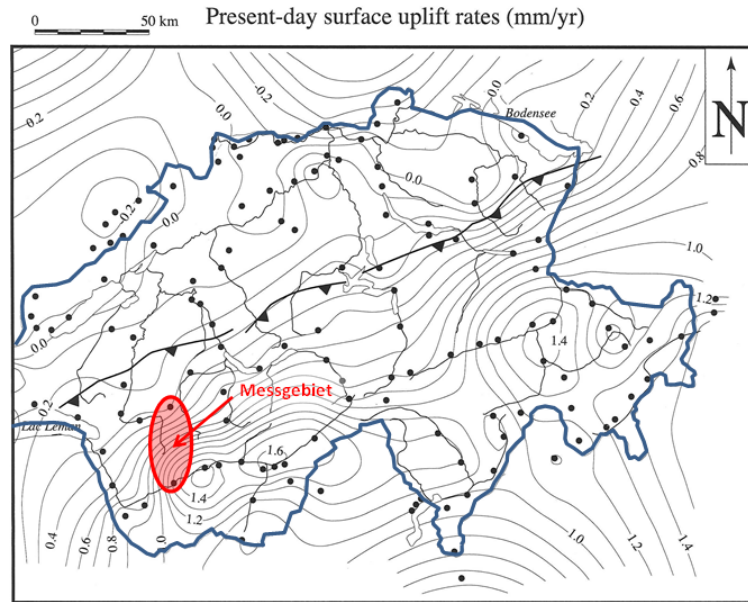


Figure 4.34: Elevation changes interpolated between points of the Swiss National Height Network, represented as contour lines with the project area in red. (Source: Institute of Geological Sciences, University of Bern)

The Alpine uplift rates of up to 1.6 mm per year are based on the following geological hypotheses: first, the melting of the ice after the last ice age and the compression of the earth's crust as a result of disk displacement with the bulging of the Alps. Second, a passive relief by erosion associated with a change of the height zero point with respect to the undeformed reference lithosphere (Condamin & Egli Oppliger 2013). The area (Saanen -) Gsteig - Sanetschpass - Sion is tectonically strongly folded and it is seismically active in the southern part. As accurately measured height points are missing in this area, surface uplift rates are interpolated between points of the Swiss National Height Network. The gradient is large (Figure 4.34). Therefore, the desire arose to develop this interpolated field with real points and thus to confirm the uplift rates.

Measurement area

From 2010-2012, eight points were sought in the project area and materialized permanently to the highest quality standards. Two points are first order points of the 1995 Swiss national control network (FHNW100 alias 1246.041 in Saanen, FHNW102 alias 1306.400 in Sion). Eleven surrounding permanent GNSS reference stations of the AGNES network (PAYE, ZIM2, SAA2, MAR2, HOH2, ZERM) and of the COGEAR / TECVAL networks (SANE, WEHO, EARTH, VARE, CRDM) were also included. The FHNW101 point in Gsteig was connected to the nearby national height points, BEO563 and BEO564. (Figure 4.35)

¹ a helvetic alpine nappe

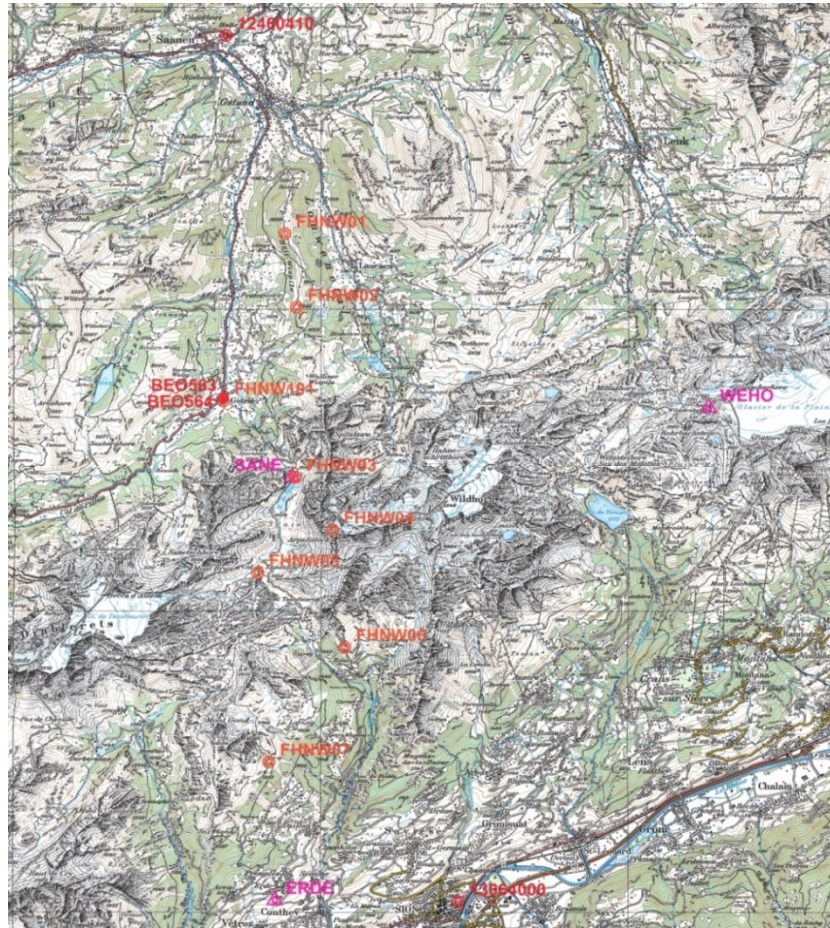


Figure 4.35: Measurement area with the mentioned points

Measurement campaigns

Two FHNW graduate students checked first the sensors and their accessories in the years 2012 and 2013. Then they measured the eight FHNW points and the two first order points with static GNSS in several daily sessions (in 2012 using Trimble 5700 Zephyr sensors of the Federal Office of Topography swisstopo and Leica 1200 GNSS sensors of FHNW; in 2013 only with Trimble Zephyr 5700 sensors). The local reference markers of five FHNW points were precisely measured with TPS (2012: Leica TM30, 2013: Leica TCRP 1201), and the connection of FHNW101 with the BEO height fix point group in Gsteig was levelled precisely using a Leica DNA03.

Measurement statistics:

Measurement campaign from ... to	10 July - 2 August 2012	8 - 26 July 2013
number of GNSS sensors	7 Trimble (T) + 6 Leica (L)	7 Trimble
number of measuring days	17	18
measured stations	21 GNSS + 5 TPS	12 GNSS + 5 TPS
medium stationing time per point [h]	53.8 T+ 75.2 L	124.7 T
GNSS epoch time	30"	30"
registered data [h] *)	591.8 T + 751.9 L	1'246.8 T
sets / directions / zenith angle	37 / 31 / 31	21 / 33 / 26
slope distances	23	24
levelling line [km] / height diff. [m]	0.328 / 16.8266	0.287 / 17.5066

*) without Continuously Operating Reference Station (CORS)



Figure 4.36: TPS measurement



GNSS measurement at the point FHNW04

Calculation

The GNSS baselines were calculated on the one hand using the Bernese GNSS Software Version 5.2 (Dach et al. 2013) obeying the procedural rules of the Swiss Permanent Network Analysis Center PNAC. The point positions of the frame network were estimated choosing the OBS-MAX strategy. Points with short distance baselines were integrated with a manually defined baseline.

On the other hand, the baselines were calculated with Leica Geo Office V8.2 or V8.3 (Leica Geosystems AG 2012): an L1 solution for the core network and an L3 solution for the frame network.

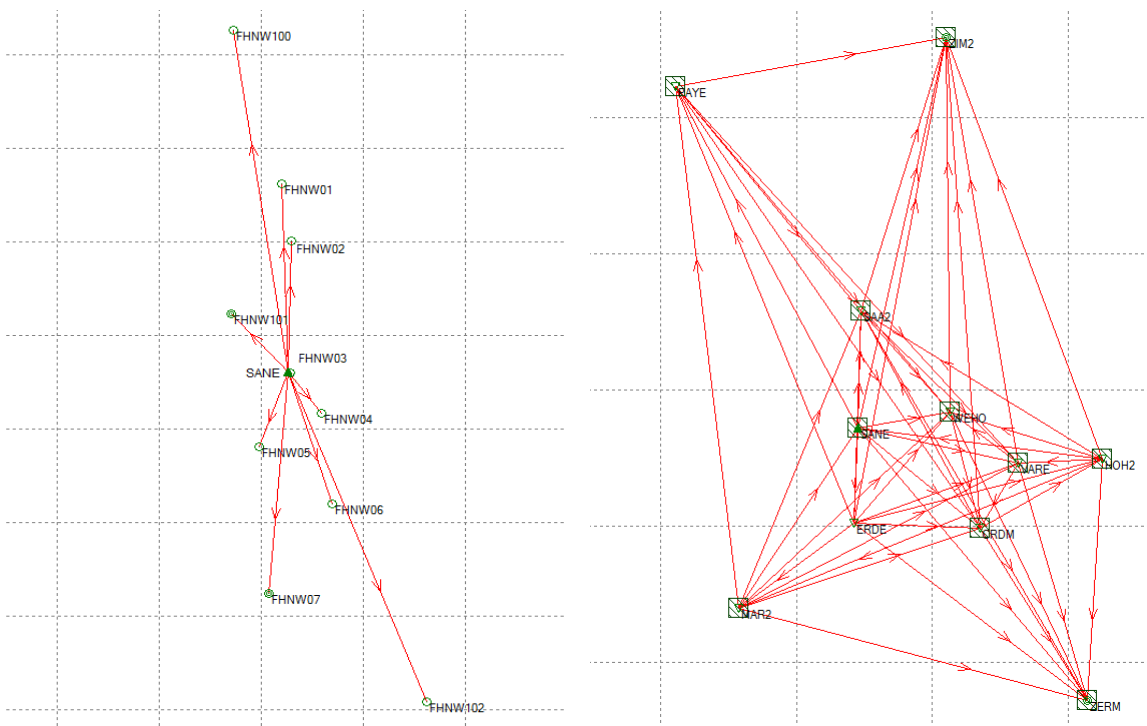


Figure 4.37: core network

frame network

Geometric height differences were calculated from precise levelling observations using the Maccsyl software.

The coordinates of the local reference markers and the height connection in Gsteig were calculated with TRINET+ V7.2 (Guillaume et al. 2009) in a strict three dimensional adjustment, together with the GNSS coordinate sets from LGO.

Results

Results from BSW

Dr. Elmar Brockmann (PNAC swisstopo) calculated these results with the Bernese GNSS software. The differences between the calculations in 2012 and 2013 were:

Frame network	BSW 2012			BSW 2013			differences [mm]			residuals [mm]	
	Point	E	N	height (ell.)	E	N	height (ell.)	ΔE	ΔN	ΔH (ell.)	position
CRDM	2'607'002.5904	1'119'785.8930	2'333.8540	2607002.5904	1119785.8944	2333.8462	0.0	1.4	-7.8	1.4	7.9
ERDE	2'588'525.8876	1'120'393.9678	730.7342	2588525.8866	1120393.9683	730.7257	-1.0	0.5	-8.5	1.1	8.6
HOH2	2'624'963.9223	1'129'829.0029	934.8374	2624963.9218	1129829.0028	934.8398	-0.5	-0.1	2.4	0.5	2.5
MAR2	2'571'556.8430	1'107'917.8958	592.1502	2571556.8397	1107917.8946	592.1488	-3.3	-1.2	-1.4	3.5	3.8
PAYE	2'562'243.5664	1'184'673.2764	498.3056	2562243.5681	1184673.2754	498.3063	1.7	-1.0	0.7	2.0	2.1
SAA2	2'589'460.3961	1'151'589.0909	1'368.7231	2589460.3966	1151589.0897	1368.7261	0.5	-1.2	3.0	1.3	3.3
SANE	2'589'054.0242	1'134'435.5193	2'025.6650	2589054.0237	1134435.5213	2025.6651	-0.5	2.0	0.1	2.1	2.1
VARE	2'612'626.9217	1'129'280.3625	652.2406	2612626.9201	1129280.3633	652.2363	-1.6	0.8	-4.3	1.8	4.7
WEHO	2'602'630.2823	1'136'743.0417	2'915.9300	2602630.2845	1136743.0418	2915.9241	2.2	0.1	-5.9	2.2	6.3
ZERM	2'622'726.0923	1'094'473.9053	1'879.5231	2622726.0938	1094473.9045	1879.5285	1.5	-0.8	5.4	1.7	5.7
ZIM2	2'602'011.9804	1'191'774.6051	906.6620	2602011.9803	1191774.6054	906.6627	-0.1	0.3	0.7	0.3	0.8

Core network	BSW 2012			BSW 2013			differences [mm]			residuals [mm]	
	Point	E	N	height (ell.)	E	N	height (ell.)	ΔE	ΔN	ΔH (ell.)	position
FHNW01	2'588'823.6614	1'142'488.0943	1'914.0143	2'588'823.6634	1'142'488.0937	1'914.0111	2.0	-0.6	-3.2	2.1	3.8
FHNW02	2'589'207.9288	1'140'052.2312	1'820.2903	2'589'207.9291	1'140'052.2314	1'820.2859	0.3	0.2	-4.4	0.4	4.4
FHNW03	2'589'150.4541	1'134'430.0063	2'051.7014	2'589'150.4545	1'134'430.0075	2'051.7020	0.4	1.2	0.6	1.3	1.4
FHNW04	2'590'380.6079	1'132'685.4072	2'968.9421	2'590'380.6082	1'132'685.4103	2'968.9416	0.3	3.1	-0.5	3.1	3.2
FHNW05	2'587'934.2864	1'131'264.7134	2'254.9427	2'587'934.2868	1'131'264.7167	2'254.9417	0.4	3.3	-1.0	3.3	3.5
FHNW06	2'590'782.4282	1'128'799.9051	1'981.4732	2'590'782.4285	1'128'799.9071	1'981.4759	0.3	2.0	2.7	2.0	3.4
FHNW07	2'588'321.9154	1'124'968.1284	1'908.1513	2'588'321.9167	1'124'968.1300	1'908.1492	1.3	1.6	-2.1	2.1	2.9
FHNW101	2'586'826.9586	1'136'958.0978	1'194.1982	2'586'827.7985	1'136'953.8698	1'194.5387	auxiliary point				
1306.4000	2'594'500.0917	1'120'353.0704	593.6703	2'594'500.0909	1'120'353.0753	593.6608	-0.8	4.9	-9.5	5.0	10.7
1246.0410	2'586'918.6921	1'149'063.3296	1'115.2238	2'586'918.6950	1'149'063.3321	1'115.2161	2.9	2.5	-7.7	3.8	8.6
SANE	2'589'054.0242	1'134'435.5193	2'025.6650	2'589'054.0237	1'134'435.5213	2'025.6651	-0.5	2.0	0.1	2.1	2.1

Table 4.5: Differences BSW 2013 minus BSW 2012

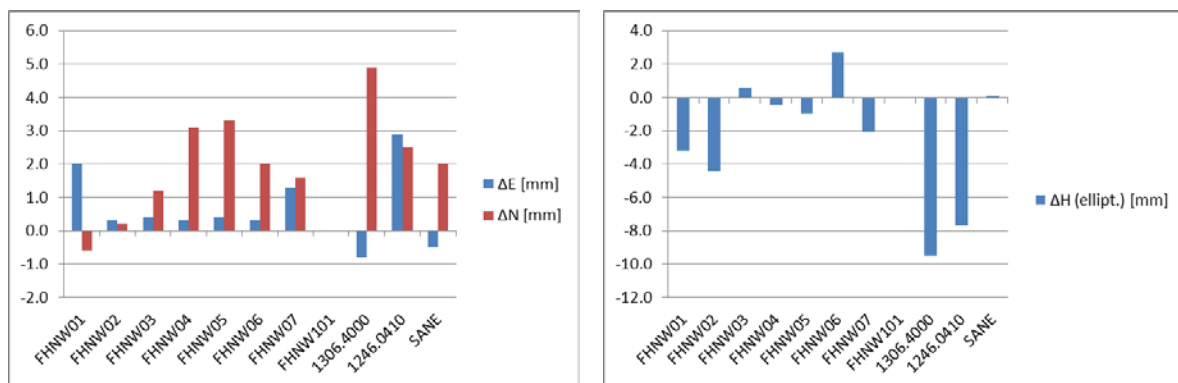


Figure 4.38: Core network, BSW differences in position und height (campaign 2013 minus 2012)

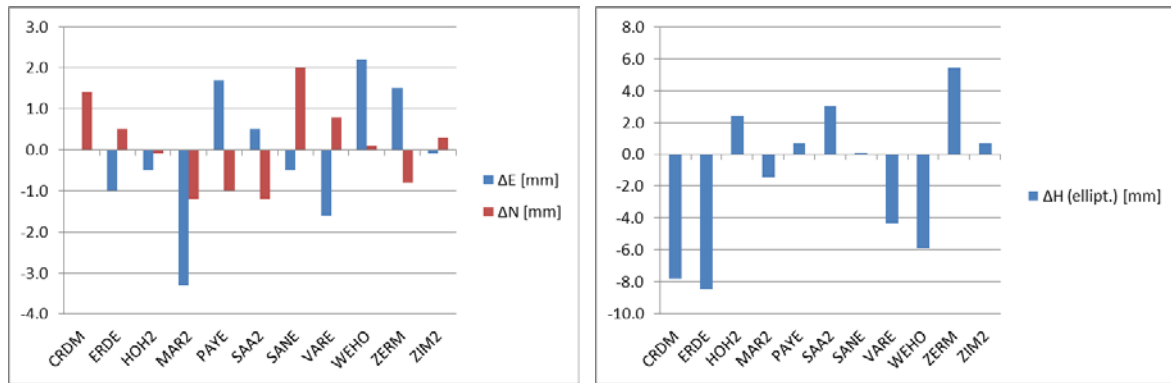


Figure 4.39: Frame network, BSW differences in position und height (campaign 2013 minus 2012)

Results from LGO

LGO fails to automatically calculate long time observed baselines: the tropospheric propagation delay is calculated in LGO, which masters only short-term changes, but not prolonged, as follows: "The Computed Tropo Model in LGO estimates the tropospheric zenith path delay with one parameter (and actually we only model the wet part of the zenith path delay), but we apply a random-walk for this parameter to model the difference from epoch to epoch. However, we allow only a small variance here to avoid this parameter drifting away too much over time. You cannot steer this parameter (would also be difficult for non-scientific users) and you cannot see the parameter variances over time anywhere in the report (as for the stochastic iono modelling).

Obviously, the Bernese software can do more here - it offers either fixed parameters valid for a certain period of time or also a random-walk type modelling, but one which you can control. So it is clear that if data is highly affected by troposphere or by a big change of troposphere over the observed time, you can get better results for the height in Bernese..." (e-mail Leica Support of 5 May 2011).

The troposphere variations of the Bernese GNSS software were consulted to build partial sessions with approximately constant tropospheric conditions for the core network (i.e. the wet delay parameter CORR_U in the vertical direction is estimated from measurements). These sessions were used to calculate baselines in LGO and to average them afterwards (LGO settings: absolute antenna calibration PCVs, precise ephemerides, frequency L1, troposphere "calculated", ionosphere "global / regional" from CODE).

The LGO solutions differed in height (ΔH) less than 6 mm from the BSW solutions. The positional deviations are less relevant in this project but confirm the quality of the solution.

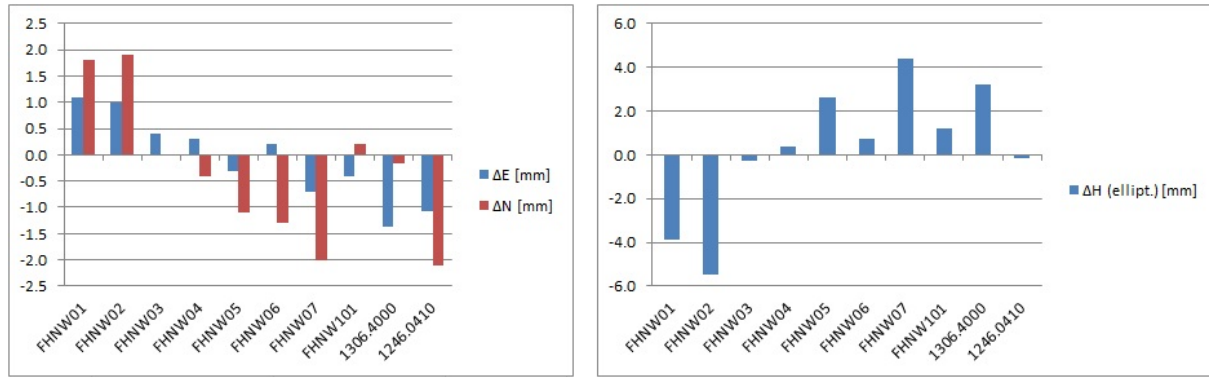


Figure 4.40: Core network, campaign 2012: Differences LGO minus BSW in position and height (reference point SANE)

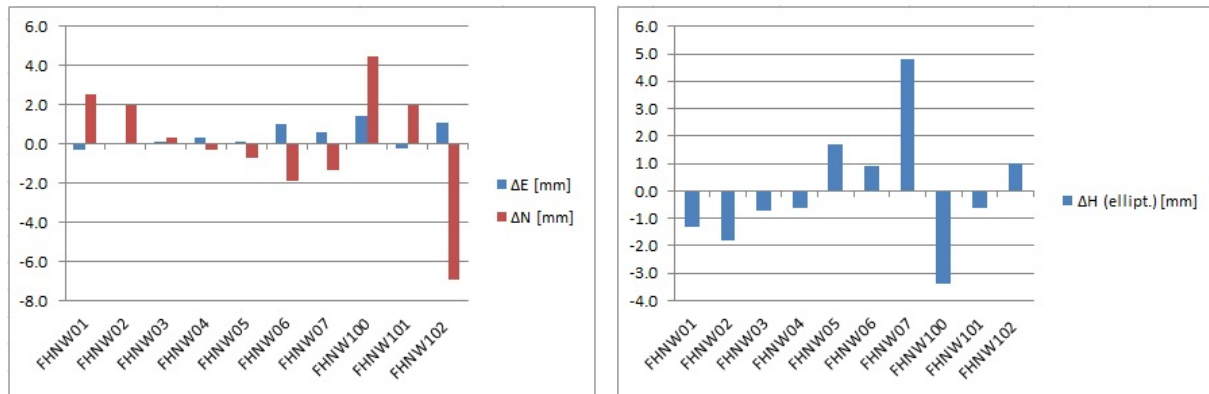


Figure 4.41: Core network, campaign 2013: Differences LGO minus BSW in position and height (reference point SANE)

The static baselines of the frame network were solved for both campaigns with LGO in a cast for various topologies: 1. star topology (manual), 2. all possible baselines (automatic), 3. all possible baselines (automatic) according to the 'independent set' criterion. In all cases, systematic deviations in height resulted in the Bernese solutions between 50 and 300 mm. They are caused by the improper modelling of tropospheric propagation delay. A partitioning into sub-sessions was omitted due to time constraints.

Results from TRINET+

With TRINET+ only the eccentric reinsurance markers were determined and the BEO height fix point group in Gsteig was integrated into the network. (Sterren 2014) describes this in more detail.

Conclusions

Temporally and geographically extensive measurement campaigns can currently be evaluated satisfactorily and reliably in Switzerland only with the Bernese GNSS software. LGO is geared to rapid and automated calculation of

many points of short series of measurements. Scientifically related variations scarcely exist. The tropospheric propagation delay is inadequately modelled in LGO and needs to be improved urgently.

With the two campaigns, a good basis for future campaigns has been established. The next one is scheduled for summer 2018. With increasing time, the significance of the height shifts can be evaluated.

(Condamin & Schwarzgruber 2013), (Bachofen & Tuchschnid 2013) and (Sterren 2014) describe the measurement and evaluation work in their bachelor theses in detail. ((Condamin et al. 2014) wrote a first published report on the project.

Acknowledgements

The work described was supported by the following institutions with funds, instrument loan, data deliveries and knowledge, for which they are gratefully acknowledged: University of Bern, Department of Geological Sciences Swiss Geodetic Commission, Zurich Federal Office of Topography swisstopo, Wabern University of Bern, Institute of Astronomy ETH Zurich, Institute of Geodesy and Photogrammetry.

Use of low-cost GNSS-R for limnometry

M. Kasser, E. Rodrigues

Haute Ecole d'Ingénierie et de Gestion du Canton de Vaud.

GNSS reflectometry (or GNSS-R) is a family of GNSS signal processing techniques based on an opportunistic use of reflected GNSS signals, more commonly known as multipath and generally considered as disturbances. If the reflector is a water surface, the GNSS receiver may become a gauge. The objective of this research is to examine to what extent this classical principle of GNSS-R gauge could also be successful with a low cost GNSS equipment.

Considering direct and reflected parallel signals, we are in a simple geometry and we may highlight the relationship between the height h , the satellite elevation ϵ and the additional path δ traveled by the reflected signal : $\delta = 2h \sin \epsilon$. A GNSS antenna, whatever its quality, never totally rejects multipath. It may simply reduce the intensity of a few dB, but the effect is still present. Thus, when a GNSS antenna is located close to water, the phase measurements are disturbed continuously by the reflected waves. We have worked on triple differences residues of a given pair of satellites, that include interferometric signals generated by the interaction between the direct and reflected waves from each satellite. But it is a very weak signal, and therefore difficult to measure.

Thus we have generated a series of theoretical interferometric signal for the possible values of the height of the antenna above water. They are calculated at regular steps (here every 10 cm), depending on the elevation of the observed satellite (master satellite) and for a fixed period (e.g.30 min) at a given time. Triple differences residuals are calculated over the same period between the master and pivot satellites. They are compared with theoretical correlation signals. The theoretical signal having the maximum correlation coefficient is identified as being the closest to the reality. Then, taking a few results in the vicinity of the latter, the result is refined using a 2nd degree polynomial regression. The height h can then be finely determined. To test this processing strategy, an algorithm has been developed and successfully tested on data from an acquisition campaign.

To obtain observations to test the concept, an acquisition campaign was undertaken on Neuchatel lake, the elevation of the water being measured by leveling. The material used is a u-blox LEA-6T chip (with phase measurement) with an SD card recording module. The antenna used is a Wireless Tallysman TW3430 fixed with its axis horizontal. The acquisition lasted 3 hours, with L1 GPS observations at 1 Hz.

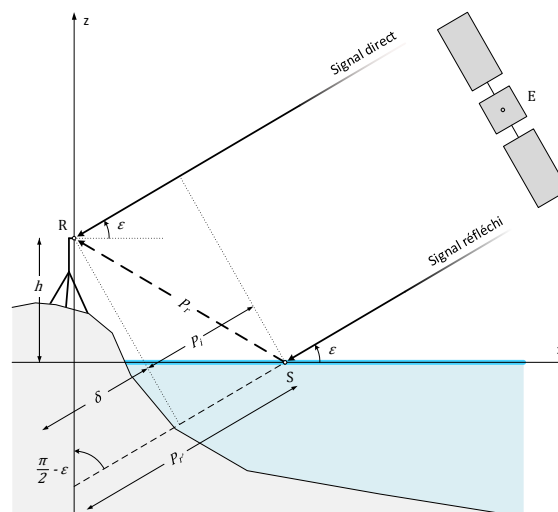


Figure 4.42: Principle of geometry of the GNSS reflectometry



Figure 4.43: The measurement site (Grandson harbor), the antenna axis being fixed horizontally.

Analysis of the results show that the elevation of the master satellite is a critical factor. The results are beginning to diverge around a 40° elevation (average elevation of the satellite during the observation period). Also the observation time is important: Tests conducted with 60 mn give very good results. This period may be reduced to 30 min of integration. Below, the results become quite random. By a combined analysis of geometric and temporal constraints, we see that there is a strong interaction between the two variables. Indeed, the lower the elevation, the lower the integration time required to calculate a good solution and vice versa.

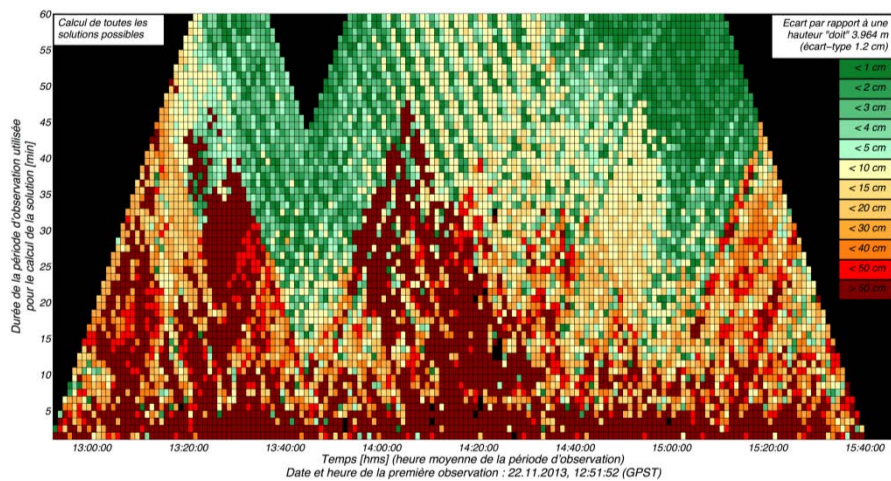


Figure 4.44: Quality of all solutions, calculated on all the data measured within the observation period. One solution per minute is calculated. The result is the mean value when there is more than one individual determination

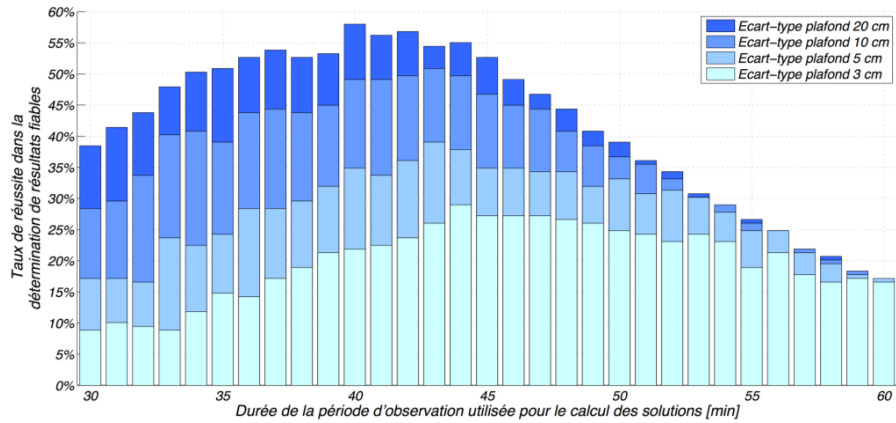


Figure 4.45: Success rate when calculating reliable water heights. This is the number of times when a reliable solution is calculated based on the total number of measurement epochs. The rate is calculated based on the observation period and used for four maximal standard deviations (3 cm, 5 cm, 10 cm and 20 cm), thus defining reliability.

Conclusions

Experiments conducted on data acquired in real situation show that it is possible to achieve centimeter accuracy water height within less than an hour measurements, precision and duration that easily will be improved by observing more constellations and frequencies with future hardware. This concept is based on a very cheap equipment, and has four advantages: its cost, no need for maintenance, quick and easy installation on existing structures, and absolute automatic georeferencing. We can imagine perfectly the use of such a system in conventional applications: reservoirs, lakes, rivers. But a particularly interesting application could be its use as an emergency level meter in the case of floods, fully autonomous if needed, and that can be set anywhere within a few minutes against a body of water.

Diachronic digital image correlation for monitoring of infrastructures.

M. Kasser, J. Compte

Haute Ecole d'Ingénierie et de Gestion du Canton de Vaud.

Diachronic image correlation is a technical measure of geometric differences, possibly very small, between images of an object taken at different times. Already used for tectonic deformation measurements, or for laboratory stress tests, it usually determines displacements with an accuracy of about one hundredth pixel or better with a single camera. The main goal of the research conducted at the HEIG-VD was to assess the opportunities of these techniques in the field of monitoring structures. This study summarizes the performances and limitations of this technique.

Now the available computing power, coupled with the availability of highly efficient open source correlation software (we used MicMac in this study) allows to exploit this tool without major limitations. It provides measurements over the entire surface, without contact, within a wide range of measuring scales. Correlation algorithms seek the maximum correspondence between small portions of images (subsets) whose size used for the calculation has great influence on the results (if small, short spatial wavelengths are well described, if large, the accuracy is better but the time calculation longer). The quality of the correlation also depends on the quality of images. The noise reduces the quality of the correlation. Thus one should work with the best possible dynamics images, and we are lucky to see that recent cameras often offer excellent signal / noise ratio.

Constraints and limitations of the method.

It is basically impossible to get rid of any phenomena having an isotropic effect on the image: such distortions cannot be measured with this technique. Under these conditions, instability of the focal length, or various thermal effects do not have to be fought, which allows to work with all current cameras and in all kinds of situations. But this is entirely satisfactory for most structures, where we will look for bending, shear, crack openings, etc., and where no isotropic deformation character usually has any interest.

Image distortion is well known in photogrammetry, where it is corrected by measuring it or by including it as unknown in the calculations. For a current device, when the camera is not aiming perfectly identically between the two shots, this induces an effect linked to the uncorrected distortion, direct consequence of misalignment.

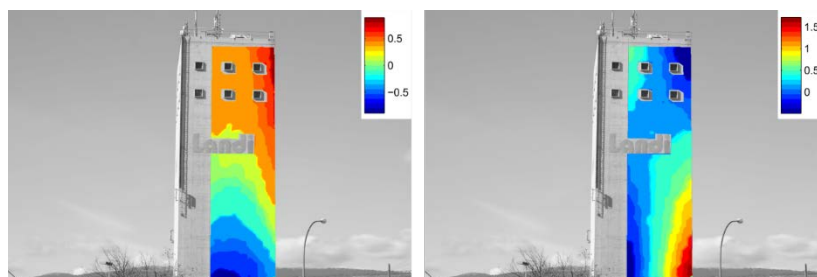


Figure 4.46: Effects (in pixels) of a target point modified of 280 pixels. Incorrect movements range to 2 px near the ends of the structure. With a 15 px misalignment effects are still up 0.1 px.

The sensor set-up orientation can easily reach a lower score of 5 px. Knowing that the distortion increases with the distance from the image center, the hundredth pixel can be achieved by using only the central portion thereof. But for cases in which the precise pointing is difficult to reproduce, distortion must be measured and corrected, which also allows working with images from different cameras if necessary.

In diachronic correlation identical camera set up over a point is not a problem, especially for a surveyor. But for the tilt, even a slight inclination of the sensor directly influences disparities measured between images.

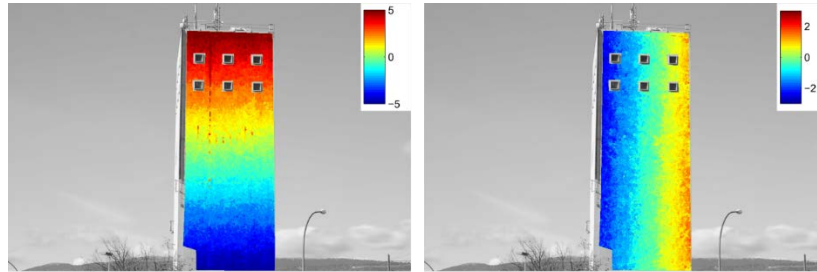


Figure 4.47: Horizontal (left) and vertical (right) components of the correlation between two images with rotation 0.2 gons of the camera between the two acquisitions, the colors are in pixels (1 px = 15 mm). The consequence of the tilt is highly visible and without corrections, makes the analysis of deformations impossible.

A tilt of 0.005 gons induces disparities close to 0.1 pixel. This artifact is only partially corrected by a posteriori calculation because the correlation between two subsets, one of which suffering from a small rotation, is degraded. Therefore one should recalculate, by resampling, an image without any rotation, and only then apply the diachronic correlation. In these conditions, the precision of 0.01 pixel is achievable.

The dynamic of the images is an essential element of the quality for the correlation. We must therefore adjust the image acquisition so that the histogram is as close as possible to saturation, without reaching it of course, so that the image has the best signal / noise ratio. But even so, the correlation coefficient can remain insufficient on some very smooth surfaces. However it is often possible, when the object deforms only very slowly, to make a summation of a set of images: if no deformation happens during the successive acquisitions, for each pixel of the image we sum the values obtained in successive images. For 64 summed images the dynamic improves of 6 bits, which can solve almost all situations, except those where the object is likely to move during acquisitions. But on natural concrete surfaces, the correlation coefficient is satisfactory with a single image for recent cameras, which often have more than 10 significant bits. Thus the bridge below allowed for a satisfactory correlation for unique pictures despite poor light, allowing to measure its flexural dynamic situation.

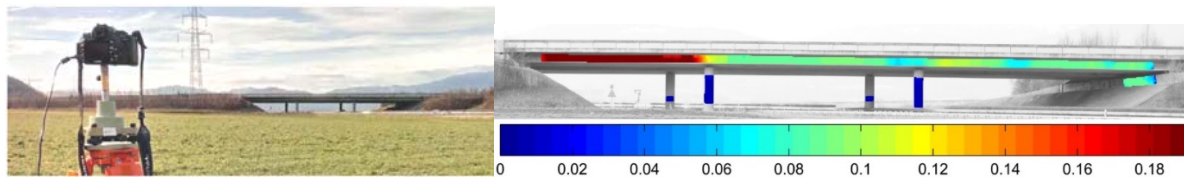


Figure 4.48: Overpass and vertical displacements observed at the passage of a vehicle, the colors are in pixels (1 px = 3cm).

Conclusions.

The ability to perform measurements without contact and without laying targets is of great interest. The generation of a vector field over the entire surface of a structure allows the analysis of most complex deformations. Nevertheless the only measured movements are those perpendicular to the viewing axis. And observations can be considered even at very large distances of the monitored item.

Approaching a measurement accuracy of 0.01 px allows to detect 0.1 mm in good conditions of acquisition. Measures with such an extreme precision, at high-speed (up to 10 im/s) and at very low cost should therefore make this methodology a popular tool for auscultation, now that the required calculations tools are accessible.

How this surface moves: the laser scanning as a surveillance tool

V. Barras, N. Delley, G. Chapotte, M. Jeanneret

Haute Ecole d'Ingénierie et de Gestion du Canton de Vaud.

Terrestrial laser scanners and lasergrammetry are increasingly present in the world of geomatics. They are used for architectural surveys and modeling of built environment or terrains.

Some specialized companies offer auscultation solutions through reflectorless measurement techniques. These new solutions allow, in many cases, to avoid the installation of reflectors, whether on built elements (bridges, dams ...) or on natural cliffs. The removal of this step, often costly in acrobatic works, simplifies the installation. But these virtual control points led to a new approach to the definition of the movements.

The laboratory of surveying of the G2C institute has worked on different methods:

Controls via one-off measures

Total stations that, as standard, now offer all the solutions for direct reflectorless measurements allow to survey a few points, rather regularly spaced, on a work. Such distance determinations are performed accurately and are not disturbed by changes in reflectivity. In addition the use of traditional tacheometric measures allows a high quality of referencing. But the number of points to be observed should remain limited to a few hundreds.

The principle is to define observations regularly distributed over the area to be monitored. In the next step, the instrument will be oriented with identical parameters to determine basically a distance variation. While processing, the modeling, through an identically arranged triangulation, allows to determine a change along the normal. By cons, any lateral slippage remains undetectable.

The arch of a bridge was monitored via this technique. Two very close states have validated that on this work, movements in the millimeter range are detectable.

Comparisons of clouds on meshes

Using the 3D scanning capacity of terrestrial laser scanners, it is also possible to monitor large areas. These instruments can provide an impressive point density, which offers the possibility of detecting erosions or local accumulations. Between 2 states, it is important to define and repeat the same established process so as to get similar systematic errors inherent to such rapid technical surveys. Georeferencing on targets or spheres also limit the accuracy of this method.

When processing, we will compare a detailed modeling of the reference state and the cloud of points of the auscultation campaign. When comparing the data sets, it is possible to detect erosion or accumulation. By cons, this treatment is quite dependent on measurement noise.

The spill ramp of Gebidem dam (VS) was observed after each spring purge. These experiments validate that for such a work (high-strength concrete), a ± 5 mm accuracy is achievable and very realistic.

Inspections between 3D models

Based on the same lasergrammetric work in the field, it is possible to modify the processing approach to reduce the effects of noise. Indeed, if we model the campaign of the reference year and of the new state with suitable smoothing parameters, it is possible to average the triangulated shapes to minimize inaccuracies in determination of each laser impact. By applying the same settings for each statement, the determination of precise movements of the model on

continuous surfaces is improved by a factor of 3 to 5. By cons, local irregularities (edges, cracks, deposits, ...) are erased by the processing and their interpretation gets difficult.

Some arches and part of a vaulted ceiling of the abbey of Payerne were monitored in this way. The test, conducted in parallel with traditional tacheometric measures, showed the importance of making 2 separate, but very close, campaigns when creating the reference survey. This dual approach allows to better adjust the many model parameters by searching for the lack of movement.

Always eager for new challenges, the Topometry Laboratory is now working to apply these methods on natural cliffs. The objective is to separate the significant and sometimes dangerous movements, from the natural vegetation changes. Another way is to move towards monitoring by laser scanning. These good prospects are expected to open a new way for reflectorless monitoring measurement.



Figure 4.49: tacheometric measures with reflectorless techniques



Figure 4.50: 3D terrestrial laser scanner

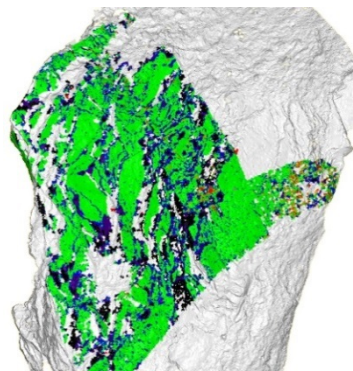


Figure 4.51: comparison

Low cost GNSS solution for landslide monitoring - GEOMON

P.-H. Cattin, M. Jeanneret

Haute Ecole d'Ingénierie et de Gestion du Canton de Vaud

The project led to developing a system of landslide monitoring through positioning measurements with a low cost GNSS-L1 equipment (GPS + GLONASS). GNSS receivers communicate by radio with a base station located on the site, which collects data, calculates the positions and sends them to a server via GPRS, Wi-Fi, Ethernet, etc.

The low cost system requires to choose and to assemble components which use very low energy. They are empowered by a small sized solar panel incorporated into the receiver box. In order to avoid operating costs and for precision of location of 1 to 3 cm, GNSS processing is performed with the free software RTKlib.

The results are performed by querying the server with special permissions (system manager, surveyor, geologist, mandatory, etc.). Informations are more or less detailed, with graphs illustrating the phenomena (displacements, velocities, acceleration profiles, etc.).



Figure 4.52: Geomon receiver

Valorization

Main innovations of the project are, on one hand the use of chips multi-system GNSS (GPS + GLONASS) communicating by radio medium-range (a few kilometers) with a low energy consumption and in GNSS processing with free software and the organization of the acquisition steps on the other hand to master energy consumption.

Two experimental sites allowed to refine and to validate the overall concept and architecture to optimize the GNSS receiver, the base station and the software part.

The purpose of the project led to the production and marketing of such equipment, and an offer of services by the company Infrsurvey, external project partner.

The current interest shown by professional in monitoring natural hazards demonstrates possible applications in auscultation of glaciers, permafrost and volcanoes, for example.

GEOMON system was developed in partnership with Infrsurvey Sàrl (external partner) and the Institute MIS (Prof. B. Hochet) HEIG-VD.

Contributions of swisstopo to GNSS Meteorology

E. Brockmann, D. Ineichen, S. Lutz and S. Schaer

Swiss Federal Office of Topography - swisstopo

Since 1999, swisstopo has been active in different projects covering the area of GNSS meteorology. swisstopo contributed on a routine basis to the European projects COST-716, TOUGH, E-GVAP I + II (with a product availability of more than 98%). Under the umbrella of EUMETNET, estimated troposphere parameters of more than 2500 permanent GNSS sites are provided by 10 analysis centers (totally 36 different solutions) with an averaged time delay of 1:30 hours (status April 2015; see Figure 4.53).

In October 2014 the number of processed sites was considerably increased (Figure 4.54) – this was motivated by having a quick monitoring of stations which are processed with a time delay in post-processing (especially re-processing). To keep the deadlines, several optimizations were implemented (e.g. clustering). Furthermore, since many years, also results of the real real-time system used for the Swiss positioning system swipos (only Swiss stations according to Figure 4.53) are provided to the meteo community. This solution is already submitted some minutes after the full hour.

Due to a memorandum of understanding between EUREF and EUMETNET, signed in 2007, radiosonde data of more than 200 stations can be provided also to the geodetic community. Many of them are closer than 20-30 km to the next GNSS site, allowing comparisons between these collocated sites. Totally 13 sites out of the GNSS sites processed at swisstopo have collocations with radiosonde data. In Switzerland, the so-called super site PAYE is processed by all analysis centers. Comparisons of troposphere parameters are also displayed on swisstopo's monitoring web pages (see Figure 4.55).

The troposphere parameters are also provided to the STARTWAVE database maintained by the Institute of Applied Physics (IAP) at the University of Berne.

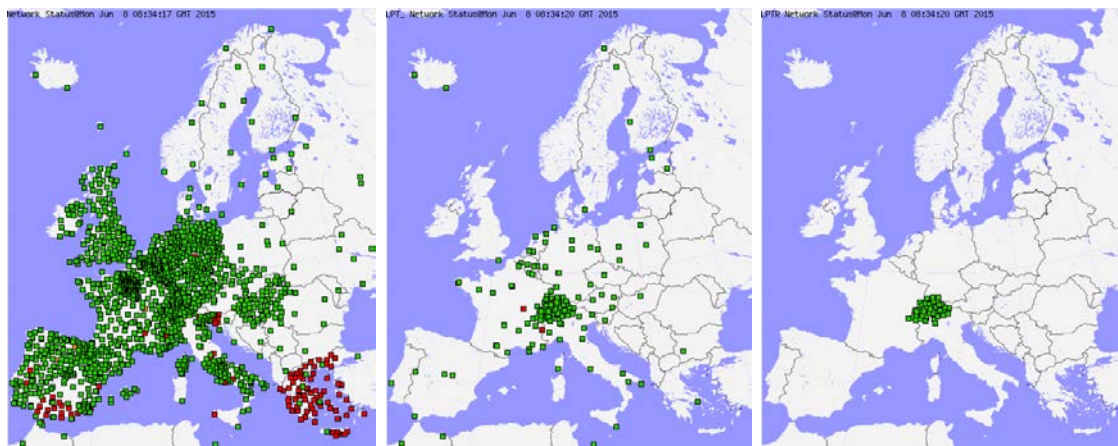


Figure 4.53: GNSS permanent sites processed by all analysis centers (left), processed at swisstopo in near real-time (middle) and processed in real real-time (right) on April 1, 2015 monitored within the E-GVAP project of EUMETNET.

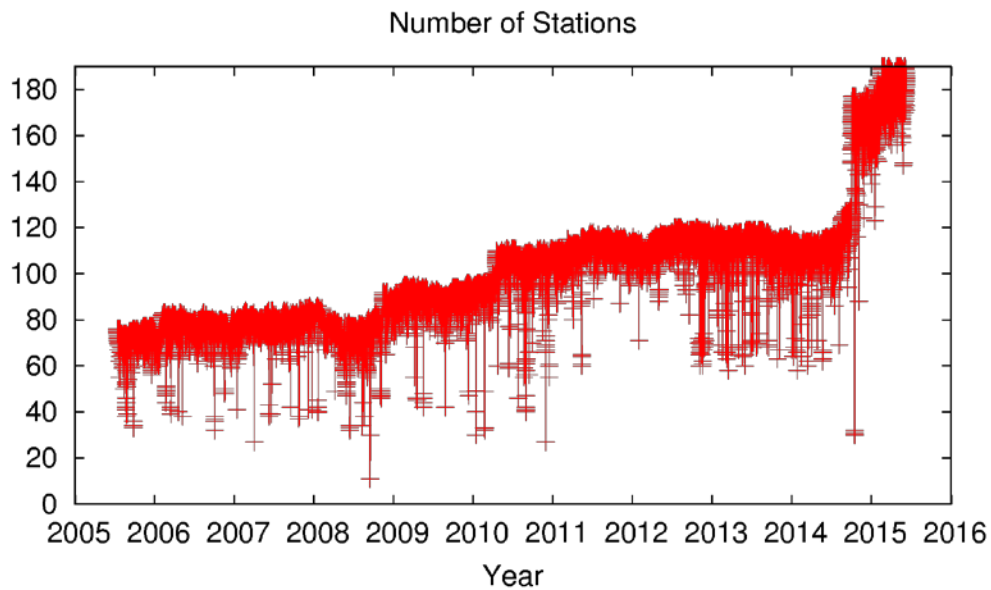


Figure 4.54: Number of sites processed by swisstopo in near real-time.

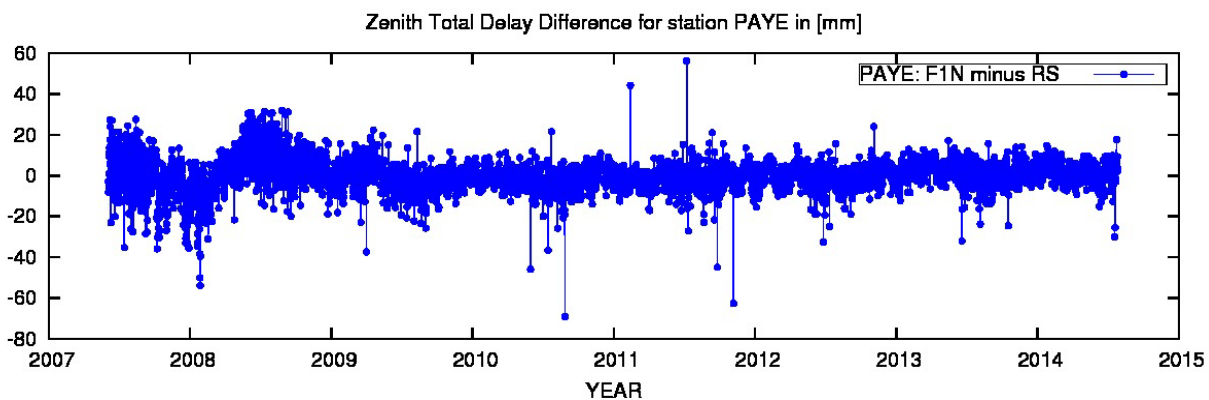


Figure 4.55: Difference between troposphere parameters estimated from GNSS post-processing and troposphere parameters derived from radiosonde data for station PAYE. A new humidity sensor was used for radiosonde launches after May 2009.

Contributions of swisstopo to GNSS climatology: COST Project GNSS4SWEC

E. Brockmann, D. Ineichen, S. Lutz and S. Schaer

Swiss Federal Office of Topography, swisstopo

swisstopo is joining the COST project GNSS4SWEC which started successfully in 2013 after several years of preparation. Main focus of the project is:

1. Severe weather forecasting: new GNSS products are required to provide more information on the spatial heterogeneity and rapid temporal variability of humidity in the troposphere.
2. Nowcasting: providing rapid updates in the analysis of the atmospheric state requires a transition from near real-time GNSS network processing (as implemented in E-GVAP) to real-time PPP processing.
3. Multi-GNSS analysis combining data from GPS, GLONASS, and Galileo in the future is expected to provide improved tropospheric products. Processing algorithms need to be modified and impact of use of additional observations needs to be assessed.
4. Climate monitoring through the evaluation of trends and variability in IWV for which the quality of reprocessed GNSS data and homogenized IWV estimates need to be assessed. The goal is to establish a new climate data record, taking benefit of more than 15 years of reprocessed ZTD estimates from hundreds of global and regional GNSS stations.

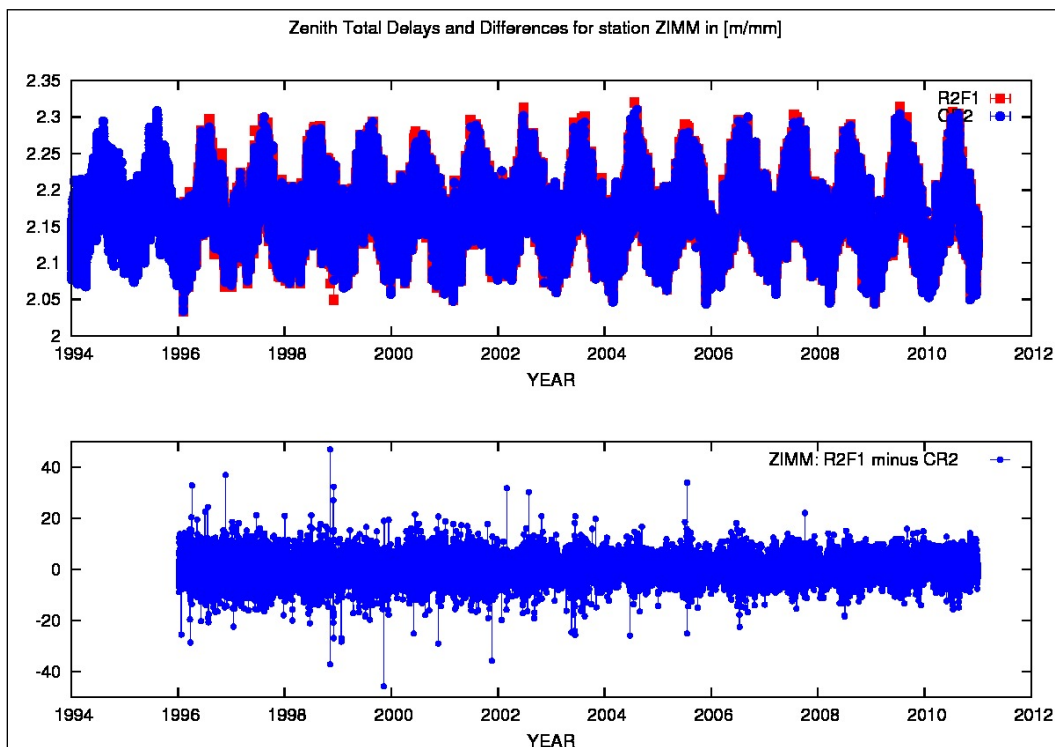


Figure 4.56: Troposphere estimates for station ZIMM derived from the swisstopo reprocessing (R2F1) and the global reprocessing of the CODE analysis center (CR2). The difference of both estimates is plotted below.

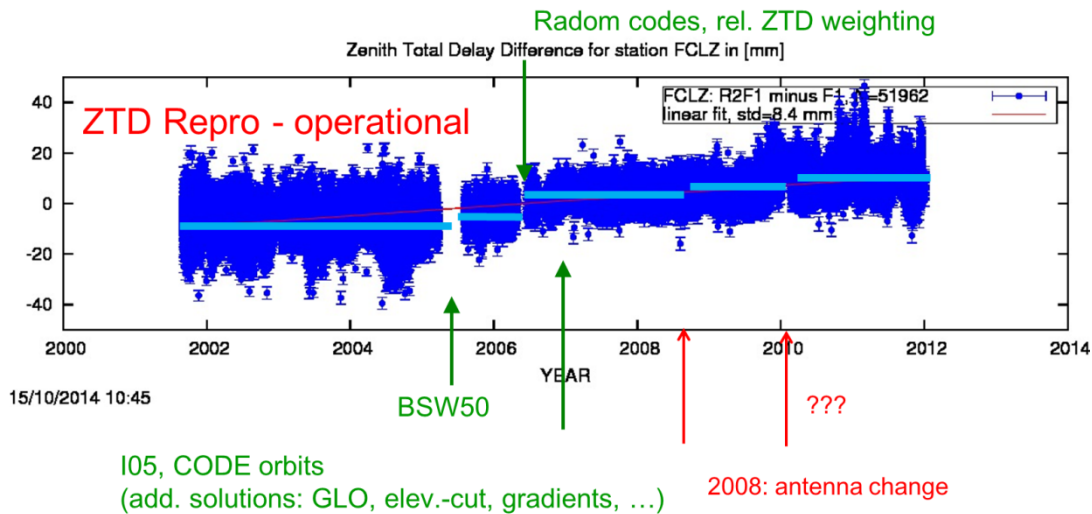


Figure 4.57: Difference of troposphere estimates for station FCLZ derived from the swisstopo reprocessing (R2F1) and the operational swisstopo processing.

ZTD comparison	Time span	# stations	$\bar{\Delta}$ Diffs/Station	$\bar{\Delta}$ std [mm]	$\bar{\Delta}$ bias [mm]	$\bar{\Delta}$ rate [mm / 10yrs]
CODE Repro2 - swisstopo Repro 2	1996 - 2011	39	52765	4.1	-0.1	0.8
swisstopo Repro 2 - operational	1996 - 2011	68	61423	5.5	-1.1	10.1

Table 4.6: Statistical values of the comparison of different troposphere time series (summarizing a larger set of stations).

swisstopo is basically interested in all of the project objectives. Main contribution is expected to topic 4 – the climate monitoring based on the swisstopo re-processing activities. The homogeneously processed time series allow investigating the development of the troposphere and especially the greenhouse gas “water vapor” on the long-term.

Figure 4.56 shows the troposphere estimates for station ZIMM derived from the swisstopo reprocessing based on an European-wide network and the global re-processing of the CODE analysis center. The difference of both time series shows a remarkable agreement and especially no jumps or trends. Comparing the re-processed series to operational troposphere results (Figure 4.57) shows the huge impact of software changes, changes in the antenna radom code handling, etc. This demonstrates quite impressively the sensitivity of the troposphere estimates on the data modelling in the processing. Inconsistently processed data would lead to artificial values of derived troposphere rates (see Table 4.6).

The project logo for the COST activity was evaluated by swisstopo's young cartographers (Figure 4.58).



Figure 4.58: Logo competition: proposals by the swisstopo young cartographers. Winner was the second left logo.

Swiss Positioning Service (swipos)

U. Wild, D. Andrey, C. Biberstein-Pedroni, L. Kislig and Chr. Misslin

Swiss Federal Office of Topography, swisstopo

The Automated GNSS-Network Switzerland (AGNES) has experienced some minor changes during the years 2011 – 2015. Due to local instabilities the stations Andermatt (ANDE) and Sargans (SARG) have been moved in 2011 by a few meters to new foundations (resulting in new station names AND2 and SAR2). Because the new station AND2 showed the same annual variations of the station coordinates as the old station ANDE, the station AND2 has finally been moved in 2014 to a new location on the Oberalp Pass (OALP).

Because our Italian partner IREALP (= Istituto di Ricerca per l'Economia e l'Ecologia Applicate alle Aree Alpine) was not willing to renew the contract in 2013 we were forced to look for a new partner in order to be able to integrate Italian real-time stations into swipos. In 2013 a new contract was established with Leica Geosystems Italy, which operates a network of about 200 stations under the name SmartNet/ItalPos. We finally were able to integrate the stations Varese (VARE) and Colico (COLI) into the swipos services. Unfortunately other stations of interest such as Tirano or Aosta could not be integrated for technical reasons. As a substitute for the Tirano station a private Swiss GNSS reference station in Poschiavo (POSC) could be integrated in swipos.

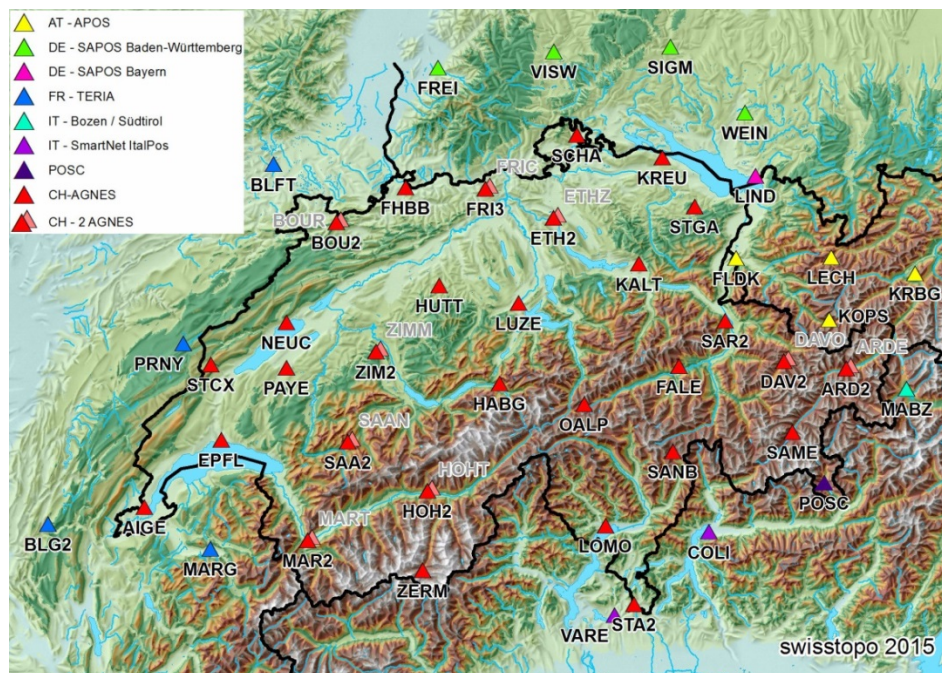


Figure 4.59: Station Map

In 2011 a new control center for AGNES/swipos has been built up. The new central is hosted by BEGASOFT AG and consists of 12 virtual servers and is divided in a production and a test environment (see Fig. 4.63). The production environment is fully redundant, i.e. all servers are permanently up and running (hot stand-by).

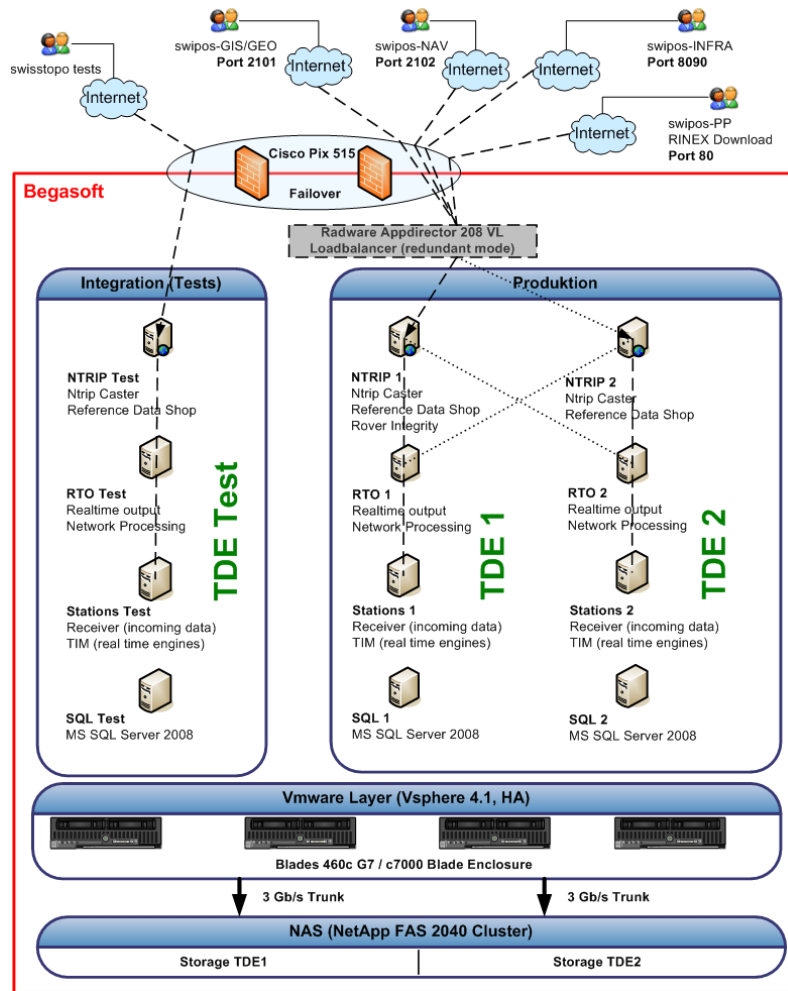


Figure 4.60: AGNES/swipos control center

The new Trimble VRS3Net software has been installed, which is adapted to the use on distributed environments (TDE = Trimble Distributed Environment). In addition the software runs as Windows services and is therefore much more stable than classical applications. In 2013 the software has been upgraded to the so called Trimble Pivot Platform (TPP).

During late 2011 extensive field tests of the new VRS3Net software have been carried out by measuring 30 points of the national first order network LV95. The results showed a good coincidence with the old software GPSNet, the mean absolute differences to the official coordinates were 8 mm in the horizontal and 18 mm in the vertical component. After these successful field tests the new central became operational in spring 2012 and the customers were migrated to the new services.

New rack-mounted controller modules for the AGNES stations have been designed and procured in 2011. The first module contains the power supply and the high-voltage protection elements, the second one the switches for the different devices (GNSS receiver, router etc.). The stations are operated internally on 24 V DC. The station PC's have been removed, except for the AGNES double stations. The roll-out of the new station controller modules took place in late 2011 / early 2012.

The main key figures for the performance of the swipos service are availability and precision. The availability is measured by an external company by accessing the service every 4 minutes and checking the availability of the data streams. The availability of the service varied between 99.8% and 99.9% during the years 2011-2015. The precision of the service is accessed by the “integrity monitoring” option of the software Trimble Pivot Platform, where a receiver located at the swisstopo office is used to simulate a customer of the service by comparing every 10 seconds the RTK fixed solution with the known reference position. The mean accuracy (1 sigma) of the horizontal component is about 1 cm, the vertical component about 2 cm.

The steady increase of the number of licensed swipos users during the period 2011-2015 is shown in Figure 4.61. A new business model has been introduced in 2014, where the customers are directly charged by our swipos resellers. The resellers are the local representatives of the GNSS receiver manufacturers (e.g. Leica, Topcon, Trimble etc.) and participate to a certain percentage in the revenues of the service. The main advantage for the customers is the “single point of selling” for GNSS rovers and the swipos service, as well as the professional support.

swipos: Lizenzenwachstum

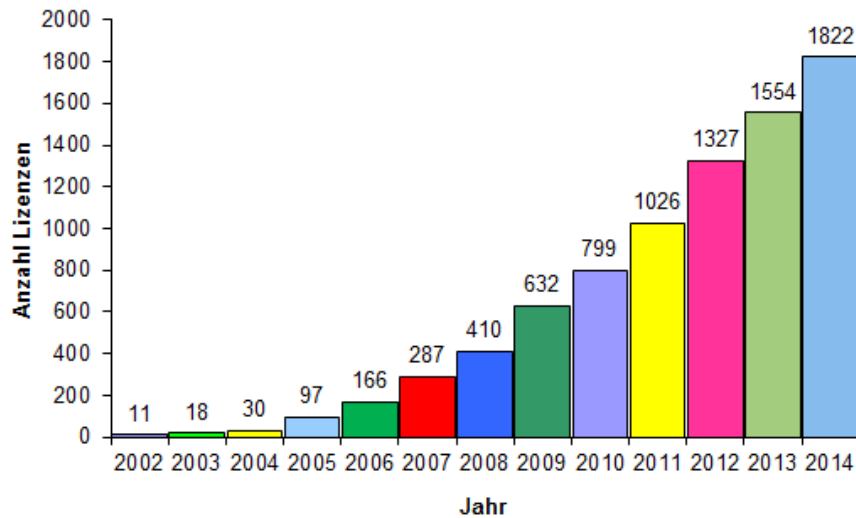


Figure 4.61: Number of swipos licences 2002 – 2014

In 2013 two new projects have been started for the further improvement and development of the swipos services.

The project AGNESIII aims to enhance AGNES and swipos with new GNSS constellations such as Galileo and BeiDou. By the end of 2014 new Trimble NetR9 receivers have been procured, the roll-out of the receivers was started in early 2015. In mid-2015 the new multi-GNSS software Trimble RTXNet will be installed in the central.

In the frame of the project POSTECH the potential of Precise Point Positioning (PPP) technologies for real-time services is studied. In a first phase a static PPP client software was developed, which in a second phase shall be enhanced with ambiguity resolution in order to achieve a shorter convergence time.

Geodetic Dam Monitoring

A. Wiget and M. Kistler

Federal Office of Topography, swisstopo

In the 1920s the engineers of the Federal Office of Topography swisstopo introduced geodetic methods like triangulation and levelling for the monitoring of dams (see e.g. W. Lang, 1929). Over the years and with new technologies and instruments the techniques and practices have changed. Till today swisstopo participates in these developments. The advances can be applied in the surveying campaigns and analyses of the dozen dams for which swisstopo is responsible for the safety control. For instance, end of the 1980s swisstopo introduced GPS measurements to strengthen and extend the control-networks to stations in geologically stable surroundings, not affected by water level changes. Moreover, swisstopo is improving the self-developed software tools and their adaption for dam monitoring.

The knowledge and the experiences are regularly shared with other institutions, especially in the Swiss Committee on Dams (e.g. Wiget, 2014). The basic concepts and recommendations for geodetic deformation measurements for dam control are described in (Darbre et al., 2013).

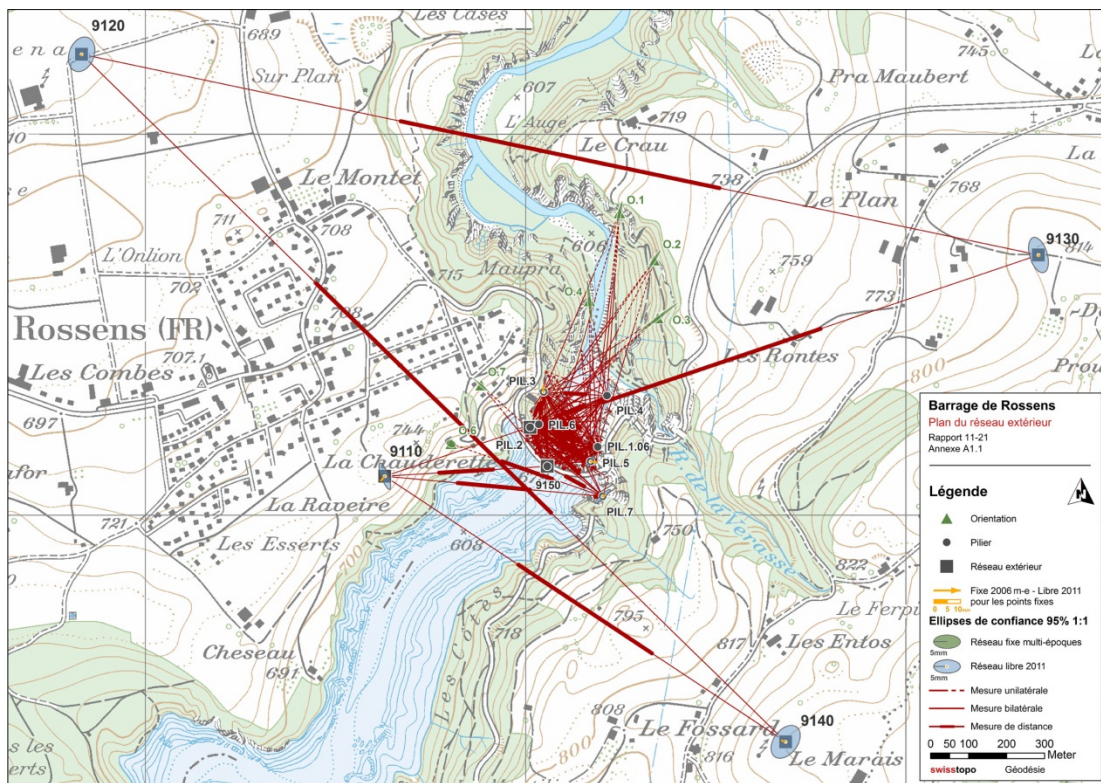


Figure 4.62: Water dam "Rossens" in the western part of Switzerland with the interior and external geodetic control network including the residuals at the datum definition points and their confidence ellipses.

GNSS Interference Detection with Helicopter Flights:

M. Scaramuzza, M. Troller, H. Wipf

skyguide, Swiss Air Navigation Services Ltd., Switzerland

With the introduction of GNSS based navigation procedures for civil aviation within Switzerland a number of special issues have been identified. Special interest is on the probability of an aerial vehicle being affected by GNSS Radio Frequency Interference (RFI). A project called Helicopter Recording Random Flights (HRRF) was launched, which objective is to install quick access recorders on board of three dozen helicopters operated by the Rega, the main Swiss Helicopter Emergency and Medical Service (HEMS), and the Swiss Air Force. Global Positioning System (GPS), Flight Management System (FMS) and Attitude and Heading Reference System (AHRS) data of every flight are recorded during a period of three years and under daily operation conditions. By this way large parts of Switzerland are randomly covered. Common to all of these helicopter operations are low flight altitudes. Therefore it is expected, that the probability of them being exposed to RFI of GPS signal is higher than for fixed wing vehicles flying at higher altitudes. Any exposure of this kind can be detected through the recorded GPS carrier to noise (C/N₀) measurements or position losses. The additional recorded data supports more in depth analysis of this kind of occurrences.



Figure 4.63: EC-635 of the Swiss Air Force (© VBS).

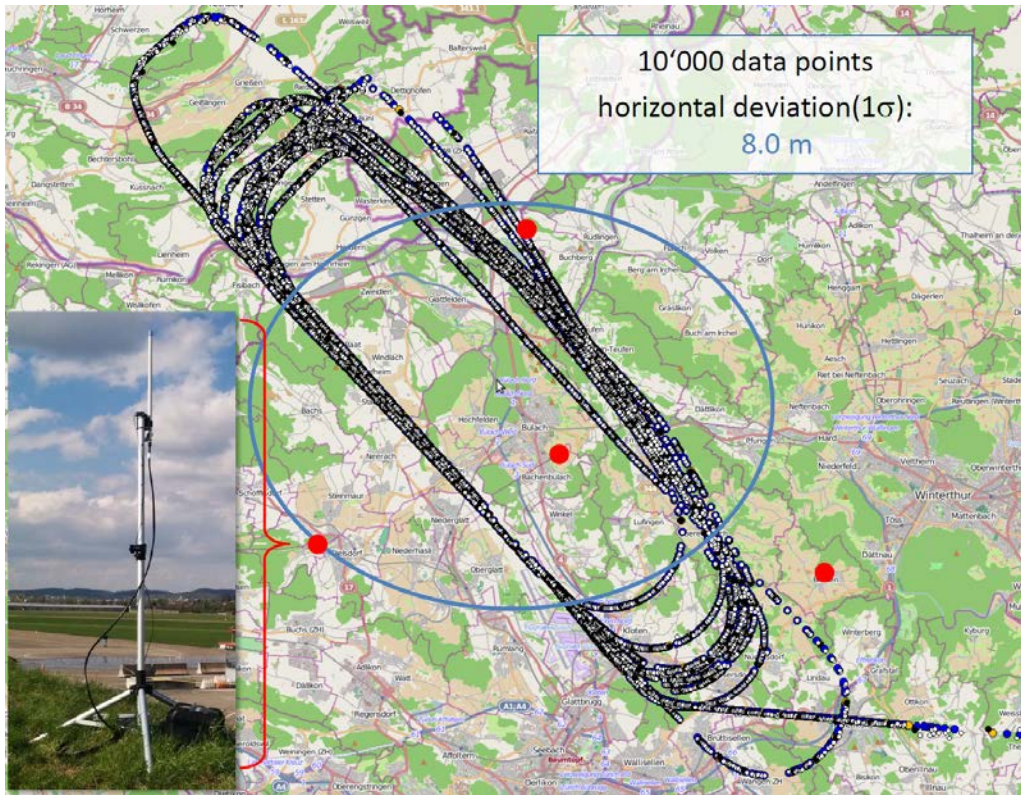


Figure 4.65: Flight trials with a dedicated airplane for mobile MLAT testing.

GNSS Performance Model

M. Scaramuzza¹, H. Wipf¹, A. Geiger²

¹skyguide, Swiss Air Navigation Services Ltd., Switzerland

²ETH Zürich, Switzerland

Within aviation GNSS enables navigation in regions where conventional navigation cannot be used. In conjunction with the mountainous topography the GNSS performance for aerial vehicles is of central importance for flight safety and operations efficiency. It is therefore fundamental to model these specific situations in order to estimate the limits of the system performance. A model is derived which assumes simplified topography, GNSS satellites constellation and GNSS performance parameters. Verification of the model is done by simulation. Adopting this model to a specific mountainous region leads finally to an optimum trajectory selection.

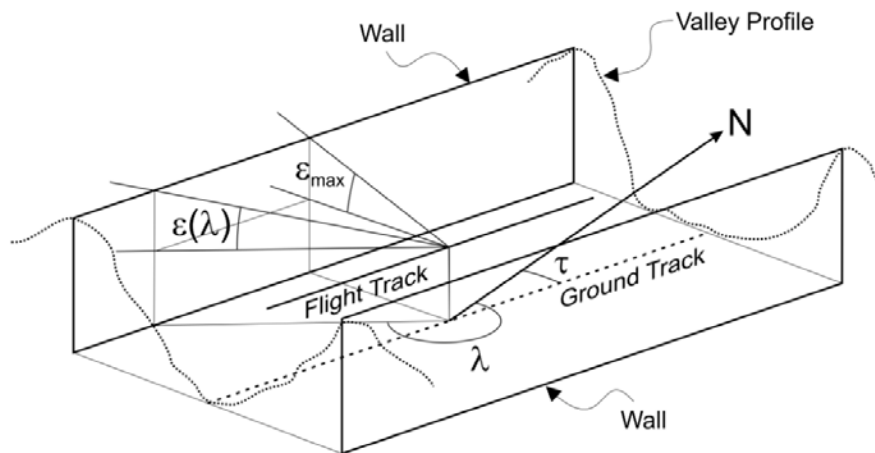
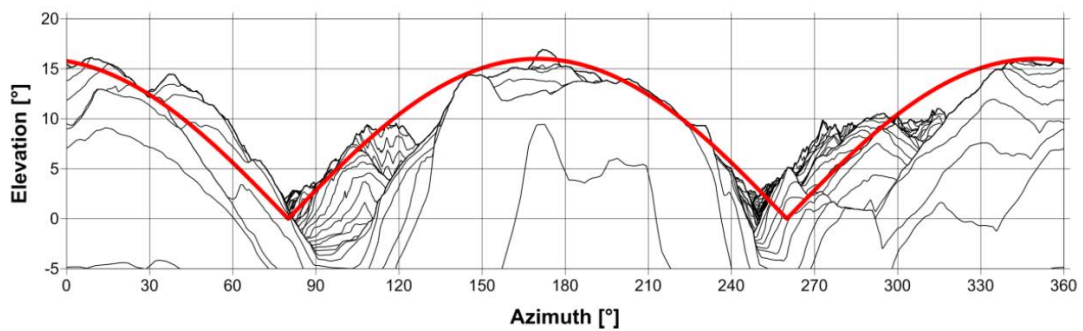


Figure 4.66: Valley modeled by two walls in order to represent the topography.

The Cube Satellite Mission CubETH

D. Willi, Ch. Hollenstein, B. Männel, M. Rothacher

Geodesy and Geodynamics Lab, Institute of Geodesy and Photogrammetry, ETH Zurich

Introduction

CubETH is a Swiss nanosatellite currently being developed by a collaboration of ETH Zurich, EPF Lausanne, the Swiss Space Center and several Swiss universities of applied sciences and companies. The tiny satellite with a size of 10 x 10 x 10 cm, to be launched in 2017, has the goal to demonstrate the use of low-cost single-frequency GNSS receivers for orbit and attitude determination. More specifically, the science goals include:

1. Investigation and assessment of precise orbit determination strategies by using observations from single receivers;
2. attitude determination based on data from three to four receivers on short baselines;
3. in space comparison and combination of different GNSS (GPS and GLONASS, and possibly others);
4. further experimental measurements such as S/N studies for satellites at very low elevations (occultation) and atmospheric density estimation

Therefore, the payload of the satellite consists of five GNSS antennas, each connected to two receivers thus increasing the redundancy of the instrumentation and enabling the simultaneous recording of GPS and GLONASS phase and code observations. Four antennas are mounted on the zenith-facing side and one antenna is located on the side (see Figure 4.67 (a)). In addition, CubETH will carry three very small retro-reflectors for Satellite Laser Ranging (SLR) measurements required for validation purposes.

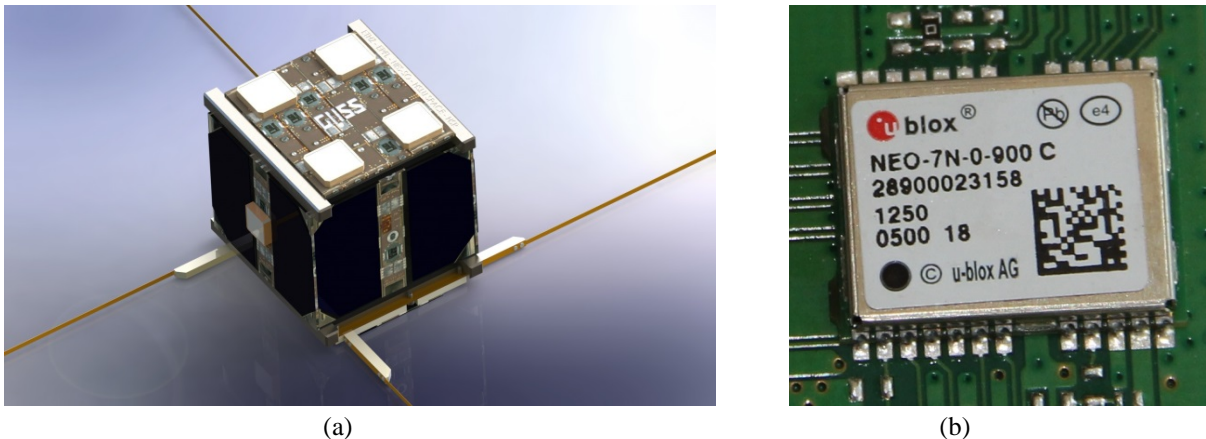


Figure 4.67: (a) 3D model of CubETH [R. Wiesendanger, SSC]; four GNSS antennas in the corners of the upper side and one on a side panel are shown; the laser retro-reflectors on the nadir side are not visible here. (b) u-blox NEO-7N receiver

Project partners

- ETH Zürich, Geodesy and Geodynamic Lab (GGL): PI, scientific leadership, responsible for payload and payload data processing software (PDS)
- EPF Lausanne, Swiss Space Center (SSC): Mission project management and responsible for the realization of the satellite bus, including the sub-systems CDMS (control and data management system), ADCS (attitude determination and control system), COM (communication subsystem), EPS (energy and power subsystem) and the satellite structure

- Hochschule Luzern (HSLU), Technik & Architektur: responsible for payload board hardware, payload control software (PCS) and ground station for satellite communication
- Hochschule Rapperswil (HSR), Institute for Communication Systems: responsible for GNSS antennas and collaborating in GNSS receiver and antenna testing
- Haute Ecole Spécialisée de Suisse Occidentale (HES-SO): collaboration in satellite bus work
- u-blox AG: supply of GNSS receivers, firmware adaptations and advisory service
- RUAG Space: providing test facilities, space expertise, and review of documents
- Saphyrion: support of work related to the satellite bus and GNSS receivers for space

Current project status and first results

The work performed so far was focused on developing mission requirements as well as specifications, in performing concept studies and on testing the GNSS receivers.

During the GNSS receiver testing, the behavior of u-blox receivers (see Figure 4.67 (b)) in the anticipated space environment, the quality and integrity of the receiver output and the accuracy of the receiver results were assessed. As the receivers are commercial off-the-shelf (COTS) products with just a few adaptations in the firmware (primarily redefinition of speed/height limits and consideration of the higher Doppler range), they are not space-proof, nor space-qualified. Therefore, the GNSS receivers were subjected to various tests (in particular radiation, temperature, vacuum, and GNSS simulator tests).

Several receivers were radiated at a proton beam facility while tracking GPS, simulating the expected radiation conditions in the orbit. The receivers were tested for both, a total ionizing dose (TID) as well as single electron events (SEE). Two of the devices under TID test were permanently affected, but no receiver was completely broken, no memory damage occurred and a remarkable autonomous error detection and recovery behavior of 82% for SEE could be observed.

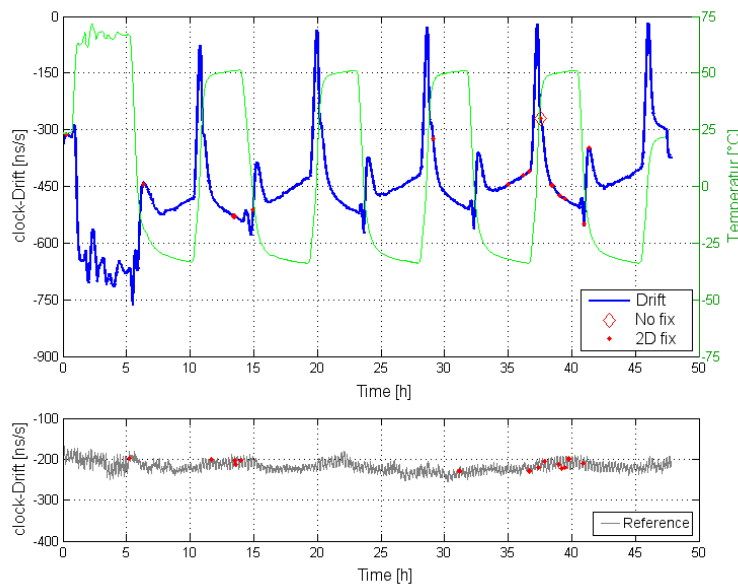


Figure 4.68: Clock drift of a u-blox receiver under thermo- vacuum cycling test. The blue line shows the clock drift, the green line is the temperature curve. The lower part (grey line) shows the clock drift of a reference receiver outside the thermo- and vacuum-chamber.

Tests concerning effects of extreme temperature conditions and vacuum were carried out. The receivers survived vacuum and extensive temperature cycles without major problems and tracked GNSS signals continuously. Increased

clock drift variations were observed at high temperature variations (Figure 4.68), while very low temperatures were associated with excessive clock drift values. Furthermore, autonomously recovered losses of phase lock at temperature jumps were observed.

GPS simulator tests, in which the GPS signals were simulated for a LEO orbit with a height of 450 km above the Earth, revealed accuracies of the code-based internal u-blox navigation solution of about 3m in position and <10cm/s in velocity. In summary, the results of the tests carried out so far led to the conclusion that the u-blox receivers are usable for space applications in low Earth orbits as planned in the CubETH project, if latch-up protection and redundant receivers are included in the payload design.

Position and attitude estimation

Currently, emphasis is put on developing and testing the on-board as well as the post-processing software. Specific filter algorithms for the position estimation and the attitude determination on board the satellite have to be implemented and tested. For that purpose, software simulations as well as hardware-in-the-loop simulations will be performed.

The on-board position estimation will rely on a code-only solution, directly available from the receiver. In order to enhance this solution, the receiver output is processed within a Kalman-filter. The propagation relies on a simple dynamical model and considers the different ionospheric conditions in the orbit.

A total of four GNSS receivers, resulting in three baselines, is available for the GNSS attitude determination. A carrier-phase single-difference approach is used to determine the orientation of the satellite within a filter process. The shortness of the baselines, less than 10 cm, conditions the whole estimation process. On the one hand, baseline length dependent errors nearly cancel and the ambiguity searching space reduces to a few candidates per single-difference. On the other hand, the achievable angular accuracy suffers from the shortness of the baselines. For practical reasons, mainly hardware robustness in space, no physical synchronisation between the receivers will be realized. The receiver clock error is known a posteriori and output by the receiver with an accuracy of about 50 ns and can amount to up to 1 ms. Therefore, the satellite position has to be extrapolated to the reference epoch in order to account for the displacement of the satellite within this 1-ms synchronisation error, which represents roughly 7 m of satellite motion. Ultimately, the attitude determination accuracy is limited by the carrier-phase noise, multipath and antenna phase centre offsets and variations.

The post-processing on the ground will rely on the well-established Bernese GNSS Software. Due to the lack of a second frequency, a linear combination of code and phase is used. This approach eliminates the first order ionospheric errors. The Bernese GNSS Software will strengthen the results using a full dynamical model, including a high-degree gravity field, air drag and solar radiation pressure, preserving the information content of the measurements including stochastic pulses. This results in a so-called reduced-dynamic orbit. Using highly accurate orbit products, sub-meter level accuracy can be expected for the position estimation in post-processing.

Active Debris Removal (GSTP 5.4)

K. Wang, Ch. Hollenstein, M. Rothacher

Geodesy and Geodynamics Lab, Institute of Geodesy and Photogrammetry, ETH Zurich

According to the data collected by the European Space Agency (ESA), a large amount of space debris (over 20000 trackable objects larger than 10 cm in size) is becoming an essential problem for diverse space missions due to the enormous velocities of the objects. In order to prevent disasters, different techniques were tested to remove large space debris. The ESA GSTP activity "CubeSat Active Debris Removal Experiment" (CADRE) led by the Swiss Space Center at EPFL is aimed to provide a feasible approach for an "In-orbit demonstration" of these techniques.

Within this project, the GGL provided expertise regarding the application of GNSS receivers on such a demonstration satellite. It performed a survey of available receiver types, also describing the necessary hardware and software integration efforts, and provided information on orbit determination accuracies when applying GNSS in a relative measurement setup. Furthermore, a Matlab Tool simulating the position and clock errors of a Low Earth Orbit (LEO) satellite receiving observations from GNSS satellites was developed based on the satellite geometry. Figure 4.69 shows the simulated real-time position and clock errors for a LEO satellite like GRACE-A on February 13, 2012. Pseudorange measurements with measurement error of about 1 m were used for the simulation.

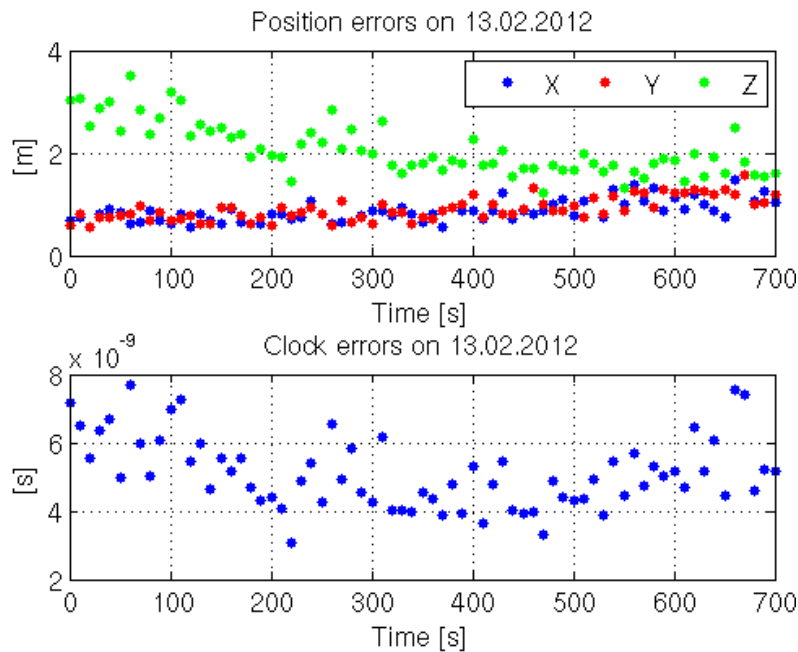


Figure 4.69: Simulated position and clock errors of a LEO satellite like GRACE-A with noise level of 1 m for pseudorange measurements.

Skyplots of GNSS satellite visibility from a LEO satellite were generated based on the satellite geometry and the antenna orientation on the LEO satellite. Figure 4.70 shows the skyplot of the GPS and the GLONASS satellites for GRACE-A, when the GNSS antenna is pointing towards the Earth. The magenta circle represents the Earth, while the red and the green circles represent the holes, where no GPS and GLONASS satellites are available because of their orbit inclinations. The 3D satellite configuration with the antenna directed towards the open sky is shown in Figure 4.71.

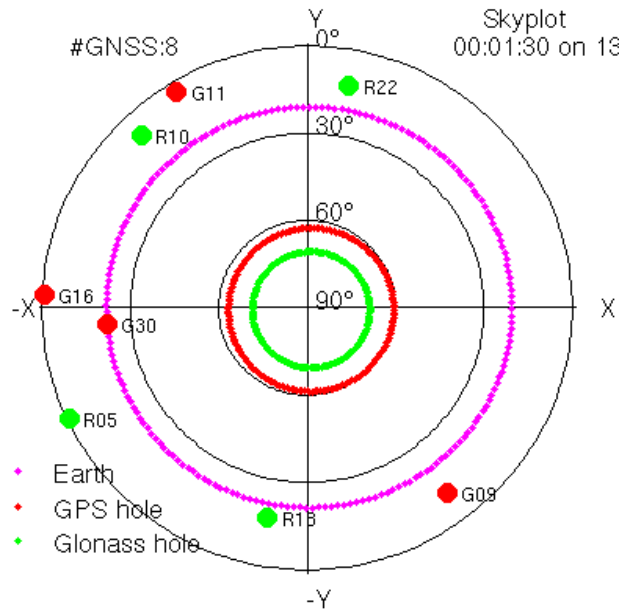


Figure 4.70: Simulated skyplot of the GPS and the GLONASS satellite visibility for GRACE-A with the antenna pointing towards the Earth.

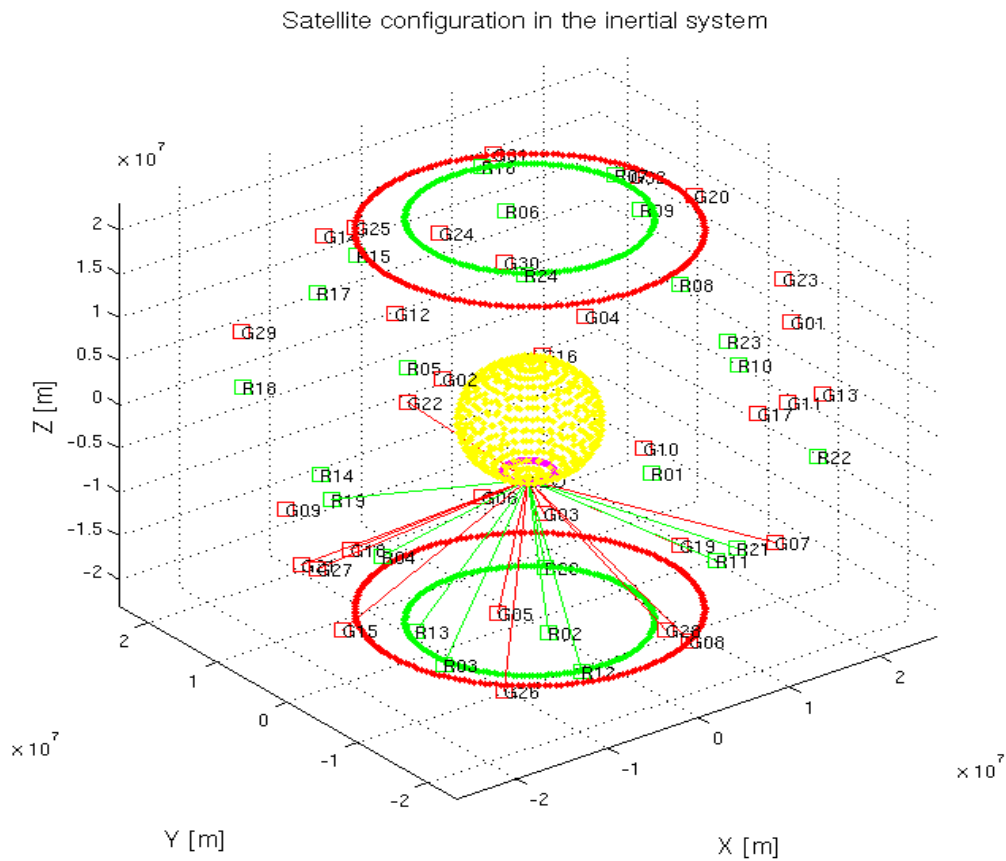


Figure 4.71: Simulated 3D satellite configuration of the GPS and the GLONASS satellites for GRACE-A with the antenna pointing towards the open sky.

Ionosphere Gradients for GBAS

K. Wang¹, M. Meindl¹, A. Geiger¹, M. Rothacher¹, M. Scaramuzza², M. Troller² and P. Truffer²

¹Geodesy and Geodynamics Lab, Institute of Geodesy and Photogrammetry, ETH Zurich

²Skyguide - Swiss Air Navigation Services Ltd.

The ionospheric delays are mostly considered to be significantly reduced in differential GNSS processing, especially for short baselines. However, they have to be considered and evaluated for applications with high safety requirements, e.g., the positioning during the approach and landing process of aircrafts in a Ground Based Augmentation System (GBAS) network, especially during stormy days of the ionosphere.

In order to assess the single-difference ionosphere residuals and spatial gradients in Switzerland, we have used GPS observations of around 40 stations of swisstopo's Automated GNSS Network for Switzerland (AGNES) to generate an overview of the regional ionosphere situation. Based on the dual-frequency GPS phase measurements of the AGNES stations and the global ionosphere maps provided by the Center for Orbit Determination in Europe (CODE), an automated processing using the Bernese GNSS Software (see Dach et al. 2007) was performed from 1999 to 2013 (see Wang et al. 2014).

Figure 4.72 shows the distribution of the AGNES stations on June 16, 2013. 41 stations were used for the processing in total.

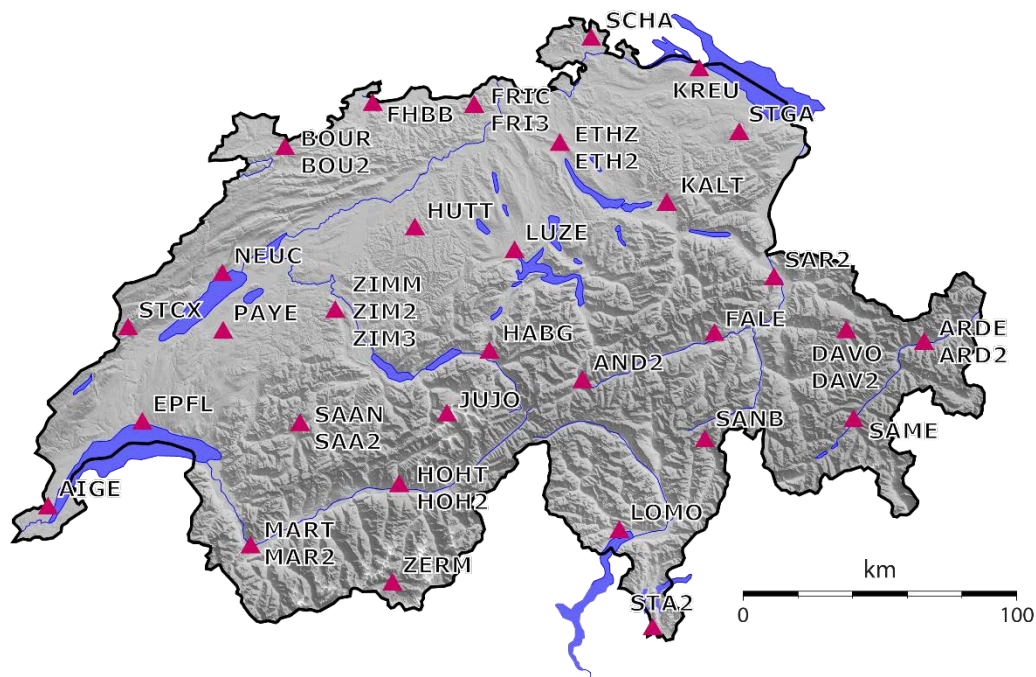


Figure 4.72: Swisstopo's AGNES stations used for the processing on June 16, 2013.

The estimated daily maximum slant ionospheric gradients, which were calculated with the single-difference slant ionospheric delays and the Ionosphere Pierce Point (IPP) distances from 1999 to 2013, are plotted in Figure 4.73 with respect to the IPP distances, the Central European Time (CET) and the mean elevation angles from the corresponding baseline to the satellite. The maximal ionospheric gradient of 81 mm/km is observed in October 2001. We also see that most of the daily maximum gradients appear at local noon of Switzerland and at low elevation angles.

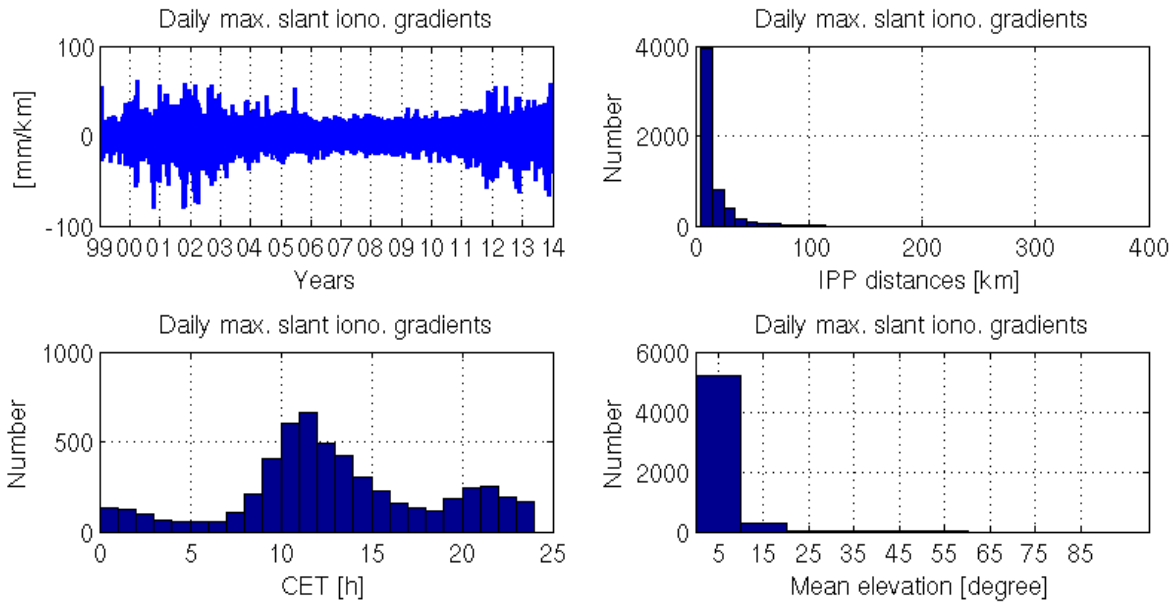


Figure 4.73: Daily maximum ionospheric gradients from 1999 to 2013.

An extended study to gradually decrease the filtering effects during phase pre-processing (removal of relevant observations at low elevation) and to analyze data with critical quality is on-going work.

This work has been financed by Flughafen Zürich AG as part of the Skyguide (Swiss Air Navigation Services Ltd.) project "Impact of Ionospheric Activities onto GNSS Signal during Approach and Landing" within the frame of the Swiss-wide program to implement new technologies (CHIPS).

GNSS-LoC

K. Wang, M. Meindl and M. Rothacher

Geodesy and Geodynamics Lab, Institute of Geodesy and Photogrammetry, ETH Zurich

In kinematic Precise Point Positioning (PPP), modelling high-performance receiver clocks, e.g. H-Masers, is helpful to stabilize the vertical component of the kinematic receiver coordinates derived from phase measurements due to the high correlation between epoch-wise clock and height parameters (see Wang and Rothacher, 2013a). In the same way, modeling receiver clocks with lower costs and less stability, e.g., rubidium clocks, should also be able to improve the vertical component of the kinematic solutions using pseudo-range observations. Due to the higher noise level of the pseudo-range measurements the sensitivity of the clocks to the measurement environment is much less critical and this also increases the mobility of the receiver (see Figure 4.74).

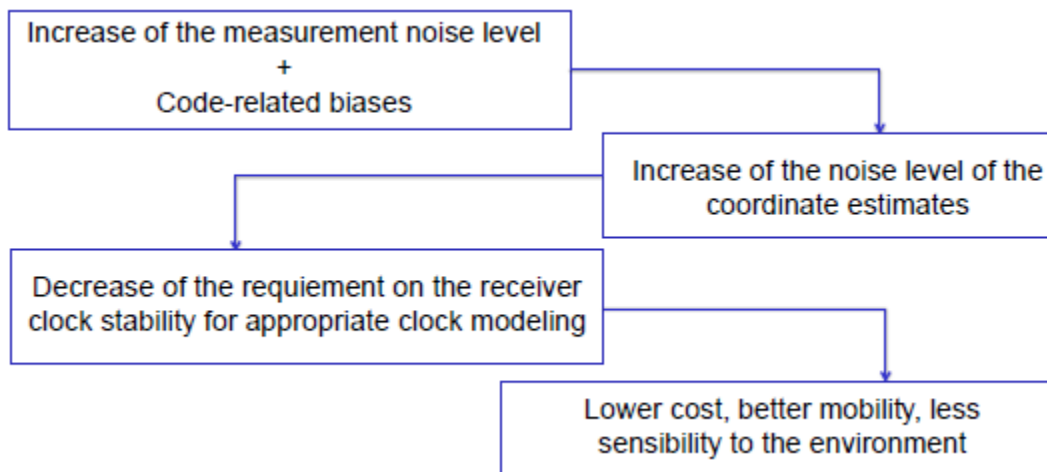


Figure 4.74: Modelling low-cost receiver clocks in pseudo-range kinematic PPP solutions.

Figure 4.75 shows the RMS of the height component of simulated kinematic pseudo-range solutions applying a linear polynomial as the deterministic model and different relative constraints between subsequent epochs for different receiver clocks. Dual-frequency pseudo-range observations with a noise of 0.5 m on both, L1 and L2, were used in the simulations to form the ionosphere-free (IF) linear combination. Real clock data of different clock types connected to stations of the International GNSS Service (IGS) were collected from the Center for Orbit Determination in Europe (CODE) and used as receiver clock errors in the simulations. Apart from that, data of crystal oscillators (SPT1, SPT5, SPT6) and rubidium clocks (SPT2, SPT3, SPT4) provided by Spectratime were also used in the simulations. The legend is sorted by the corresponding clock qualities. “PERF” represents a perfect clock, namely a linear polynomial.

From Figure 4.75 we see that the improvement of the height component of the receiver coordinates increases with the clock quality. The improvement reaches about a factor of 3.6 for the perfect receiver clock in the simulation.

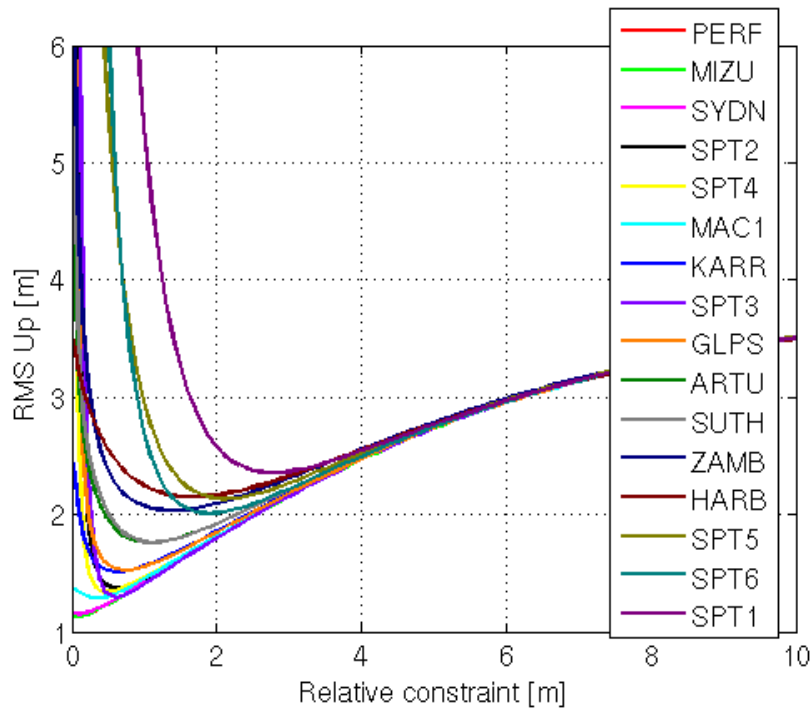


Figure 4.75: RMS of the estimated kinematic heights of the receiver using simulated pseudo-range measurements applying different clock models for different receiver clock types.

Triple-frequency ambiguity resolution

K. Wang and M. Rothacher

Geodesy and Geodynamics Lab, Institute of Geodesy and Photogrammetry, ETH Zurich

Due to the continuously increasing number of the GNSS satellites sending signals on more than two frequencies (e.g., GPS Block IIF satellites and Galileo In Orbit Validation (IOV) satellites), different studies were performed in the last ten years to reduce or eliminate GNSS-related errors using multi-frequency linear combinations (see Hatch, 2006; Henkel and Günther, 2012). In this study, we have concentrated on forming geometry-free (GF) and ionosphere-free (IF) linear combinations using triple-frequency code and phase measurements to resolve the ambiguities. The combined noise level after forming the linear combinations is minimized with the assumption that the phase noise is equal (in cycles) on all the three frequencies and the code noise is equal (in meters) to the product of a constant noise value and a scaling factor, which can vary with the frequency and is defined as input parameter (see Wang and Rothacher, 2013b).

To minimize the combined noise level of the triple-frequency linear combination described above, the six weighting coefficients before the code and phase measurements have to fulfill fixed relationships defined by the three frequencies, the code scaling factors and the integer coefficients, which provide the connection between the single ambiguities and the combined ambiguities of the linear combination. Testing with different sets of integer coefficients that vary in a pre-defined range and that are linearly independent to each other, the best and the second best triple-frequency GF and IF linear combination with minimized noise level can be found for a given frequency triplet.

Figure 4.76 shows the combined measurements using the best (n_x) and the second best (n_y) triple-frequency GF and IF linear combination for station CUT2 and CUTA in Australia (see Raziq et al., 2012) and Beidou satellites C01 and C03 on March 21, 2014. The raw code measurements were pre-processed to reduce the noise and the mean values of the combined measurements were removed from the plot. We can observe standard deviations of both combined measurements smaller than 0.4 cycles and we also see that the noise level of the second best linear combination is slightly larger than that of the best linear combination.

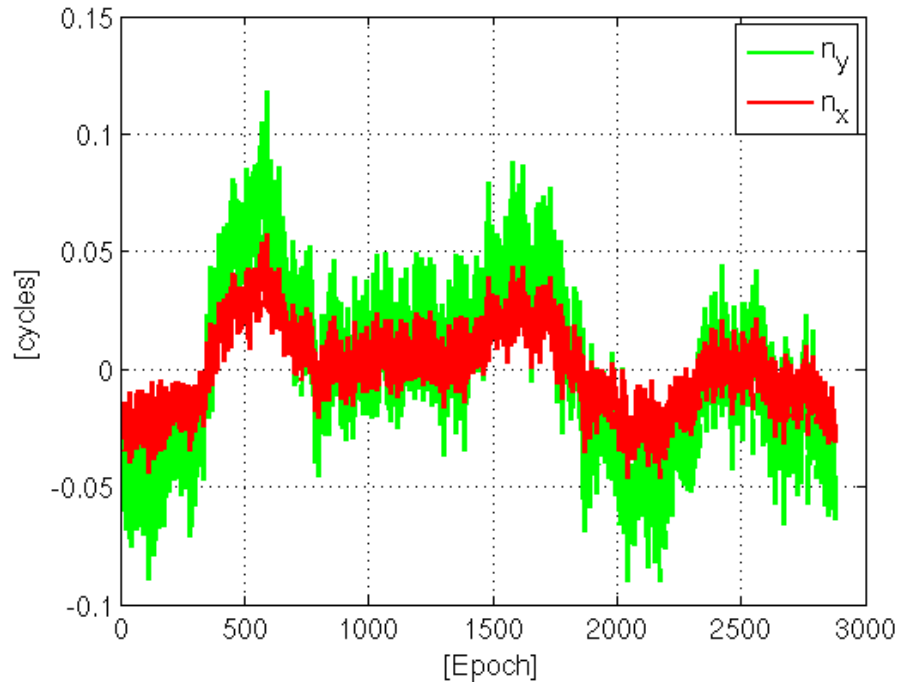


Figure 4.76: The combined measurements for the best and the second best GF and IF linear combination for station CUT2 and CUTA and Beidou satellites C01 and C03.

Since it is difficult to find a third linear combination, which is independent of the best two linear combinations and has a relatively low noise at the same time, we gave up to use the code observations and used the ambiguity-corrected observation instead (see Li et al., 2010). The resulting fractional parts of the combined ambiguity are still relatively large due to the strong amplification of the remaining biases. Further information about phase-related biases, like Phase Center Variations (PCVs) or multipath, needs to be considered to successfully resolve the ambiguities on each of the three frequencies.

Tropospheric sounding with GNSS and water vapour distribution

F. Hurter¹, A. Geiger¹, D. Perler¹, K. Wilgan²

¹*ETH Zurich, Geodesy and Geodynamics Lab, Schafmattstr. 34, HPV G53, 8093 Zürich, Switzerland*

²*Wroclaw University of Environmental and Life Sciences, Institute of Geodesy and Geoinformatics, Grunwaldzka 53, 50-357 Wroclaw, Poland*

Over the recent years the so-called GNSS-Meteorology has experienced an increasing importance within the context of the atmospheric research and weather forecasting. Newly installed, continuously running, and densely distributed GNSS receivers brought forward the applications of satellite geodetic methodologies in research and practice. The approaches and methods, devised at the institute of geodesy and photogrammetry of ETHZ, for the determination of water vapor concentration in the atmosphere by GNSS have been further developed and analyzed in detail.

Main methods consist of tomographic approaches and parameterized estimations with stochastic 4D interpolation. In addition the work features extensive and detailed investigations in an especially designed, dense alpine measurement network, where verifications and analyses with meteoswiss' numerical weather model COSMO-2 were carried out. Extensive theoretical aspects of data correlation have been studied with concretely available meteo- and GNSS data. In particular a test network 'Zermatt' has been established where also special balloon soundings were launched, from which the very interesting, sometimes debated theme on the comparison of balloon soundings and GNSS results is discussed. It is shown that the balloon soundings are not of unproblematic use and there offsets to GNSS (path delay estimations) might be at least partially attributed to the soundings themselves.

In this study we have reconstructed total refractivity profiles over a western part of Switzerland using the least-squares collocation software COMEDIE (Collocation of Meteorological Data for Interpretation and Estimation of Tropospheric Pathdelays). Different datasets were included into collocation algorithms: total refractivity calculated from meteorological parameters at ground-based SwissMetNet sites as well as GNSS derived ZTDs and horizontal gradients of ZTD from Automated GNSS Network for Switzerland (AGNES). The refractivity fields were compared to the reference radiosonde station in Payerne. We are also investigating the application of collocation algorithms to improve modeling of refractivity field in Poland and Australia.

We presumed that introducing the horizontal gradients will improve the interpolation, but for the vertical interpolation case study in Switzerland at Payerne the refractivity field from the dataset with gradients was worse by about 0.5 ppm than the interpolation without gradients. Currently we are actively researching the reason for results degradation (gradient noise, orography of Switzerland, parameterization problems).

The presented work is part of a series of activities in GNSS meteorology at the Institute of Geodesy and Photogrammetry at ETH Zürich and of the Swiss Geodetic Commission.

In parallel to the tomography approach a more statistical method has been pursued. Further development was made on our least-squares collocation software COMEDIE (Collocation of Meteorological Data for Interpretation and Estimation of Tropospheric Pathdelays) to include additional data sets. The following datasets were included into the collocation algorithms: total refractivity calculated from meteorological parameters at ground-based SwissMetNet sites as well as GNSS derived ZTDs and horizontal gradients of ZTD

We have reconstructed the total refractivity profiles over western part of Switzerland using the software COMEDIE. Ground-based SwissMetNet data as well as GNSS derived ZTDs and horizontal gradients of ZTD from Automated GNSS Network for Switzerland (AGNES, swisstopo) were used. The refractivity fields were compared to the reference radiosonde station in Payerne. We are also investigating the application of collocation algorithms to improve modeling of refractivity field in Poland and Australia. We presumed that introducing the horizontal gradients will improve the interpolation, but for the vertical interpolation case study in Switzerland at Payerne the refractivity field from the dataset with gradients was worse by about 0.5 ppm than the interpolation without

gradients. Currently we are actively researching the reason for results degradation (gradient noise, orography of Switzerland, parameterization problems).

The studies were partially funded by the Competence Center Environment and Sustainability of the ETH Domain (CCES) in the frame of the project APUNCH.

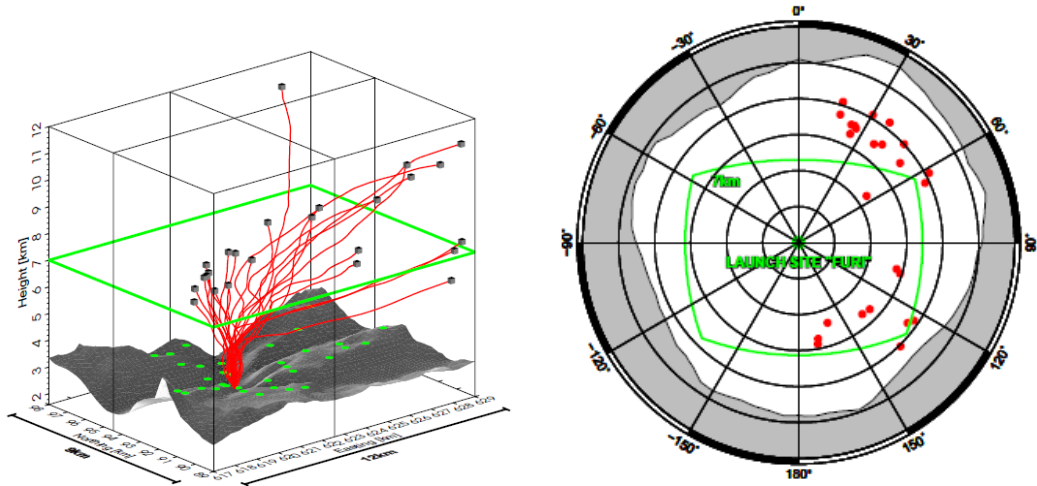


Figure 4.77: (left) Radiosonde tracks calculated from sonde wind information. The tracks start at Furi and leave the research area at the small gray boxes. The additional grid lines are placed at the easting and northing of the launch site at Furi and divide the field into quadrants. The green dots are the campaign's GNSS stations. The green square denotes the height of 7 km. (right) Skyplot of radiosonde leaving positions. The sonde tracks have been calculated with sonde wind information. Gray shading shows the visibility horizon at Furi calculated from the digital height model DHM25 (from Hurter, 2014)

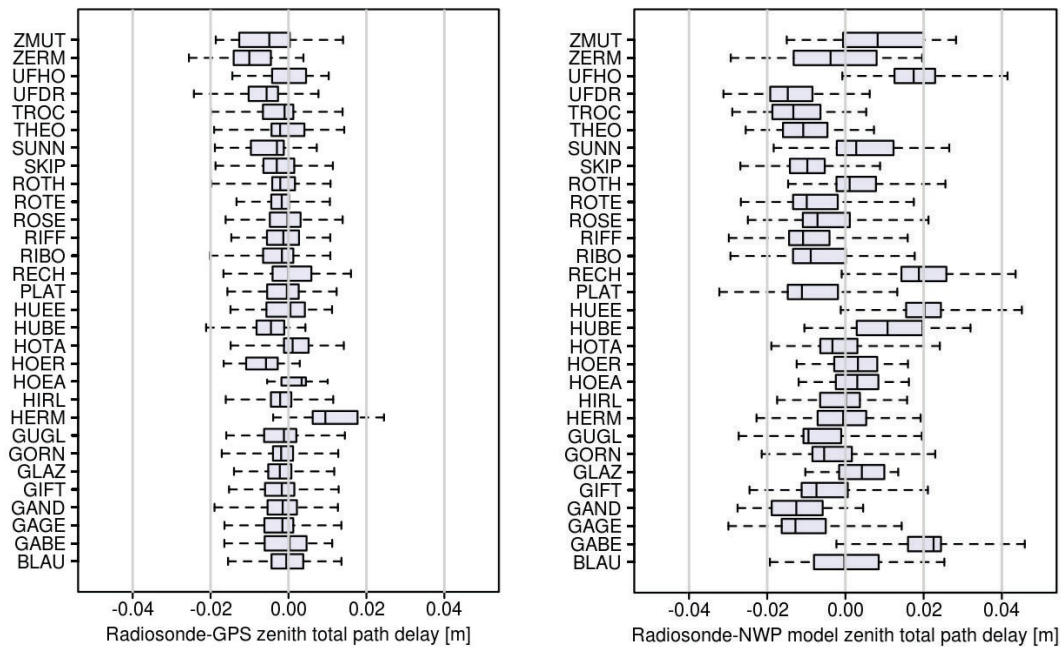


Figure 4.78: Boxplots comparing total zenith path delays at different stations calculated from radiosonde launches (RS) with (left) GPS path delays and (right) calculated path delays from numerical weather prediction (NWP) model data (from Hurter, 2014).

Atmospheric Water Vapour Sensing by means of Solar Lunar Absorption Spectroscopy using a Compact High-Resolving NIR Spectrograph

S. Münch¹, B. Bürki¹, M. Rothacher¹, A. Geiger¹, P. Sorber¹, St. Florek², H. Becker-Ross², M. Okruss², R. Tischendorf²

¹*Institute of Geodesy and Photogrammetry, ETH Zürich*

²*Leibniz-Institute of Analytical Sciences (ISAS), Berlin*

Various scientific disciplines, ranging from climatology through meteorology to space geodesy, rely on correct information on the atmospheric humidity. Due to the vast number of factors influencing the highly dynamic spatial and temporal distribution of tropospheric water vapour, all attempts to create sufficiently accurate models are rendered futile to the present day. Owing to the need for proper water vapor concentration values, a substantial number of measuring methodologies have emerged over the last decades, predominantly in the field of remote sensing, including both, ground-based and space-borne techniques, see (Kämpfer, 2013).

The analysis of the atmosphere's chemical composition through evaluation of molecular absorption signatures in the spectrum of a broadband light source, such as the Sun or also artificial illuminants, is an established procedure in atmospheric sciences, especially for trace gas investigations. The applicability of the approach to determine local water vapor slant concentrations has been verified in different projects at ETH (Sierk, 2001; Somieski 2005).

The Solar Lunar Spectrometer for Atmospheric Research (SOLUSAR), jointly developed by ETH Zürich, the Leibniz-Institute of Analytical Sciences (ISAS) in Berlin and the GFZ German Research Centre for Geosciences in Potsdam, is a highly integrated instrument using a custom-designed mirror telescope for light gathering and a coupled spectrally high-resolving NIR spectrograph (Littrow configuration with an echelle grating as main dispersing element, see Figure 4.79).

For the first time measurements have been conducted using the Moon as background radiation source (at phase angles clearly below 90°). The results confirm the potential of compact high-étendue spectrometers to obtain night-time concentration values with reasonable accuracy, however, with substantially decreased time resolution (Münch, 2013).

The construction of two identical instrument prototypes allowed to study the internal precision of the methodology, while external validation using an independent approach (GNSS meteorology) shed light on the integrity of absolute measurement values: The current hardware and software set-up yields excellent results regarding precision. Furthermore, the assumption that the approach could become a viable independent validation tool for other measurement techniques is supported by the findings. However, a number of different issues will have to be addressed to reach said objective, such as the enhancement of the algorithms to determine the reference intensity or the improved monitoring of the apparatus influence.

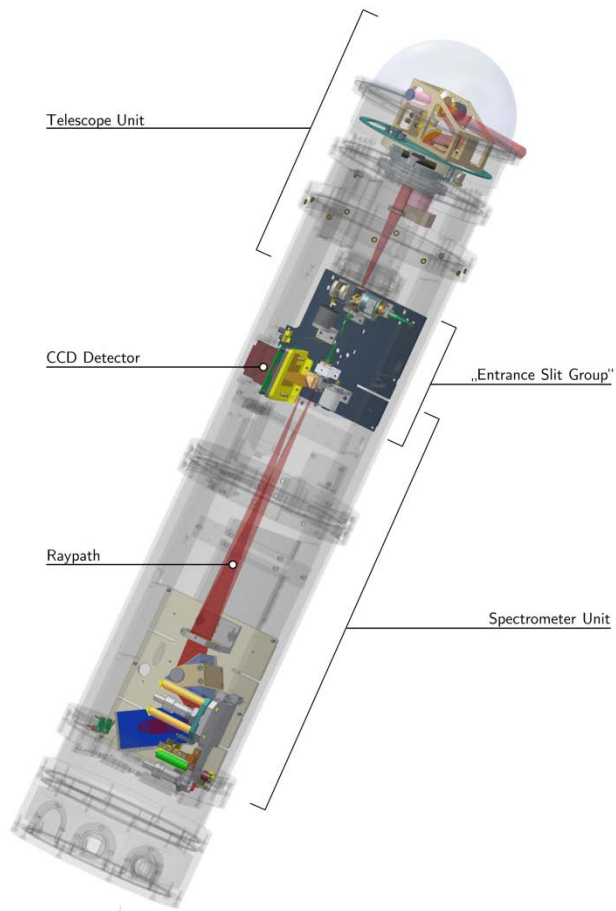


Figure 4.79: Overview of the optical layout of the SOLUSAR instrument. The radiation is gathered by a heliostat-type Sun-tracking telescope at the top. The light is guided to the entrance slit, where it enters the echelle spectrograph, which produces a two-dimensional solar/lunar spectrum image, a portion of which is recorded by a CCD detector.

Image Based Geomonitoring

F. Neyer, Ph. Limpach, A. Geiger

Geodesy and Geodynamics Lab, Institute of Geodesy and Photogrammetry, ETH Zurich, Switzerland

At ETH Zurich, the Geodesy and Geodynamics Lab (GGL) of the Institute of Geodesy and Photogrammetry is involved in several interdisciplinary projects and activities related to mountain permafrost (X-Sense, X-Sense2, PERMOS). Its major field of activities is the monitoring of displacements and deformations with continuously operated GPS stations, and especially the geodetic processing of GPS data (P. Limpach, A. Geiger, S. Su, R. Hohensinn). In the framework of the X-Sense project, GGL has developed algorithms for automated image processing from digital cameras (F. Neyer, A. Geiger). Feature motions are estimated by applying least-squares matching and image rectification procedures. Two cameras (J. Beutel, T. Gsell) have been installed at the Grabengufer Rock Glacier to monitor the displacement field. For immediate image processing capability, the permanent camera installations are connected to a developed wireless sensing technology, allowing also the remote control of almost all camera settings as well as to change the image capture timer. Because the installation area did not allow placing the cameras onto the bedrock, each camera installation is equipped with a GPS to accurately measure its displacement. As the motion of the camera might be critical for the accurate estimation of the motion of the target object, the continuous camera position measurements are included in our procedure.

The advantage of areal displacement information is tested in terms of resolution and accuracy to complement the GPS data. In a first attempt, we demonstrate that our robust feature tracking method accurately estimates displacements up to a level of 0.05 pixels. To correctly scale the displacements, either digital elevation models or 3D position estimates with multiple cameras are used. The latter procedure is preferred especially in cases where rays project in a critical angle, i.e., where small errors in the elevation model cause large errors in the estimated scale.

A product of the image pre-processing is the detection of snow cover. With respect to image point tracking, it is important to exclude all areas affected either by strong radiation differences (shadow) or by snow. In case snow only partially covers a point of interest, feature tracking may fail due to the strong image gradients introduced by the snow borders. Small patches of snow or changing surface structures are automatically detected by our robust matching strategy thus are not critical. Good snow detection however can also be used for estimating correlations between water input (weather station) and observed displacements of a glacier.

Remote sensing with optical off-the-shelf cameras is also a promising field for ice glacier monitoring. Depending on the flow speed and dynamical characteristics of an ice glacier, special care must be taken for the fast changing topography, for example ice break offs and crevasses that do not necessarily represent the true velocity of the ice package. Figure 4.80 shows an example of image based feature tracking of a rapidly changing unit of ice.

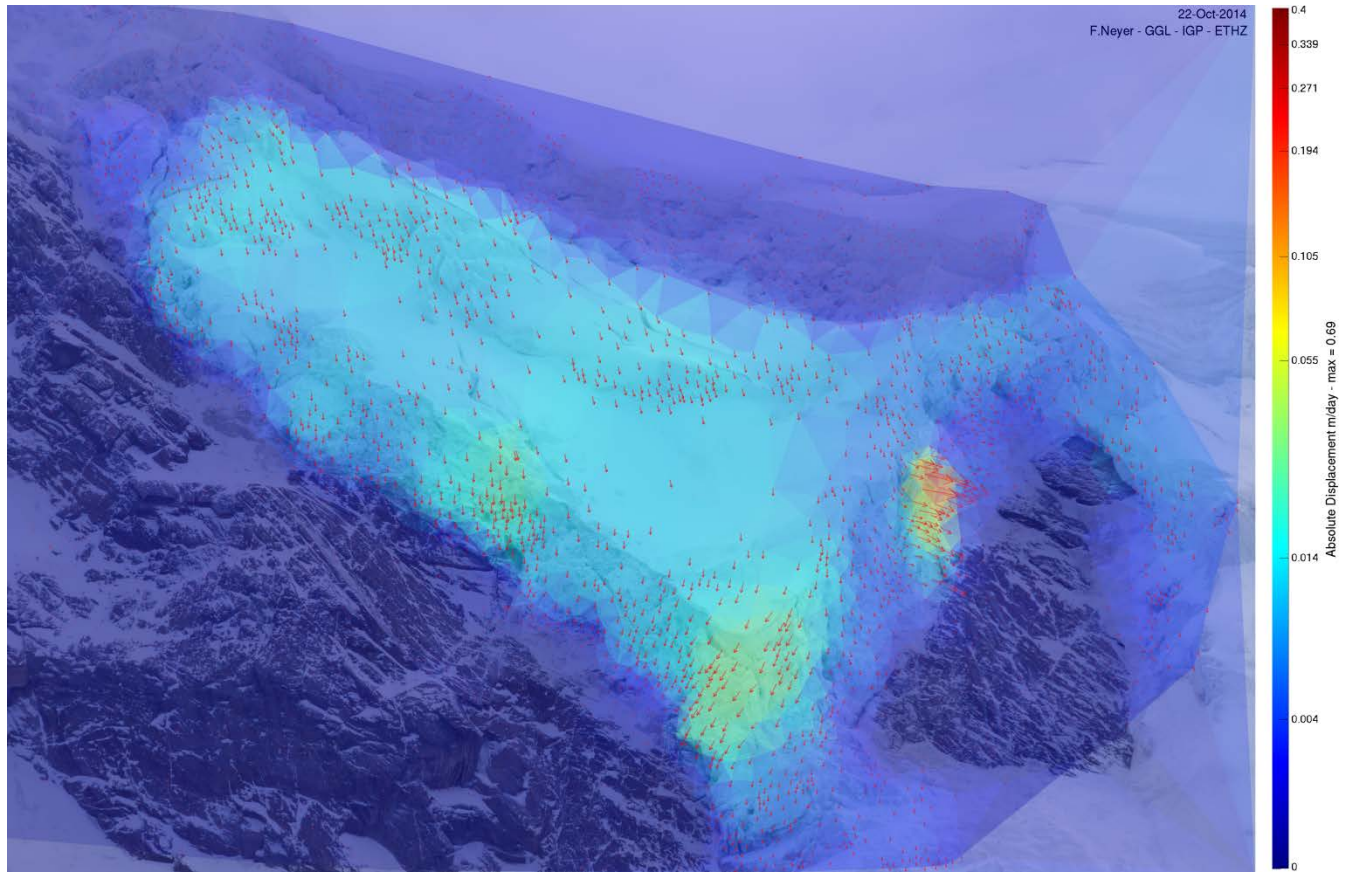


Figure 4.80: *Imaged based estimates of displacements at one ice unit that disconnected from the main part of the Triftglacier (Valais, Switzerland). Maximum displacements measured during the late autumn period in 2014 reached up to 1 meter per day.*

GNSS for Deformation and Geohazard Monitoring in the Swiss Alps

P. Limpach and A. Geiger

Geodesy and Geodynamics Lab, Institute of Geodesy and Photogrammetry, ETH Zurich

The Geodesy and Geodynamics Lab (GGL) is involved in several interdisciplinary projects and activities related to alpine mass movements. Within these projects, our major field of activities is the monitoring of displacements and deformations with continuously operated GNSS stations, and especially the geodetic processing of the GNSS data. The GNSS data allows the precise monitoring of rock glaciers, slope instabilities and rock instabilities with a high temporal resolution. With continuous observations over several years, it was possible to analyze the temporal variations of the displacements and the displacement rates. At present, the data of more than 30 GNSS stations from various projects in Switzerland are operationally processed at GGL. A large number of these stations were deployed by the X-Sense project since 2011, where a network of permanent single frequency GNSS stations has been set up in the Matter Valley, Switzerland. X-Sense is an interdisciplinary project for monitoring alpine mass movements at multiple scales, funded by the Swiss federal program Nano-Tera, involving partners from the Computer Engineering and Networks Lab (ETH Zurich), the Department of Geography (University of Zurich) and the Federal Office for the Environment (FOEN). In collaboration with FOEN, GNSS data was used to validate results from interferometric radar observations. Another project aims to quantify seasonal ground deformations of bedrock around an active glacier, and investigate long-term trends associated with ongoing ice retreat. This project is part of an interdisciplinary cooperation lead by the Engineering Geology Group of ETH Zurich. Two GNSS stations are continuously operated at the Great Aletsch Glacier (Swiss Alps) since October 2013 (Figure 4.81 (a)). A new type of compact and rugged stations has been designed at GGL to work as self-sustaining units under harsh environmental conditions. They are equipped with single frequency GNSS receivers. Power is provided by solar modules and data is transmitted by GPRS/UMTS. Similar GNSS stations have been deployed in 2014/2015 at a slope instability close to the Great Aletsch Glacier (Figure 4.81 (b)), in collaboration with FOEN, and at a landslide in canton Glarus, Switzerland. In another project, single-frequency GNSS receivers are operated in an experimental set up at the Weissfluhjoch test site of the Institute for Snow and Avalanche Research (SLF) in Davos, Switzerland, with the goal investigate the potential of GNSS to monitor snow water equivalent and snow depth.

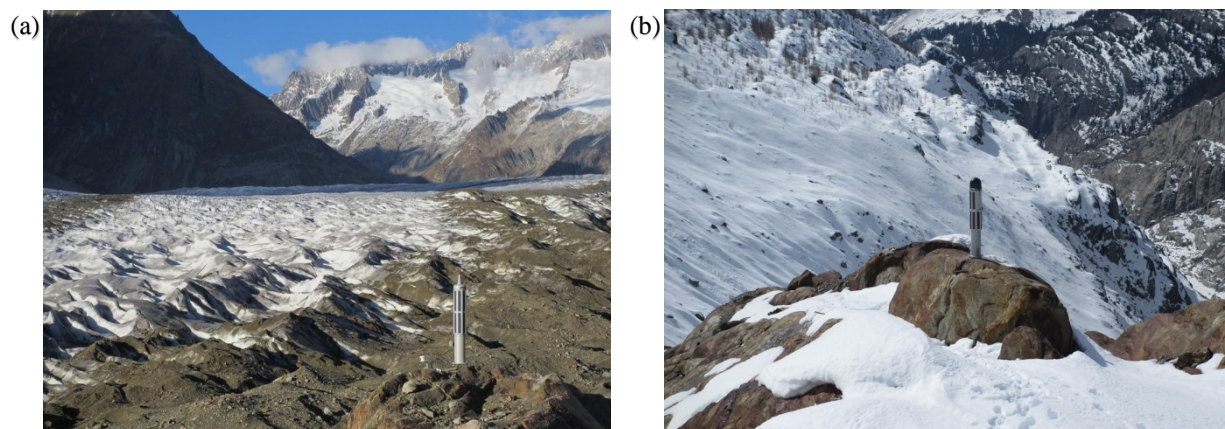


Figure 4.81: (a) Single frequency GNSS station for bedrock deformation monitoring at the Great Aletsch Glacier. (b) Single frequency GNSS station for slope failure monitoring at the Great Aletsch Glacier.

Fast detection of sudden movements with GNSS in view of hazard monitoring

R. Hohensinn, A. Geiger

Geodesy and Geodynamics Lab, Institute of Geodesy and Photogrammetry, ETH Zurich

The framework of this PhD thesis is formed by the SNF project X-Sense 2, which aims, amongst others, at the development of an early warning system in high-risk alpine regions in view of a reliable and fast detection of hazardous events like landslides and rockfalls. The project is led by the Computer Engineering and Networks Laboratory (TIK) of ETH Zurich. Further partners are: Group of Micro and Nanosystems (ETHZ), Institute of Geography (University of Zurich) and Institute of Geodesy and Photogrammetry (ETHZ). The task of the Geodesy and Geodynamics Lab (GGL) of the Institute of Geodesy and Photogrammetry is to develop an efficient algorithm, once a Global Navigation Satellite System (GNSS) receiver is awakened by acoustic triggering, to rapidly assess the motion of the sensors' underground. On the one hand this shall be achieved by a further development of the G-MoDe (GPS Movement Detection) algorithm, which was developed at the GGL and aims at the detection of small and rapid movements in GPS time series of relative displacements. The goal is to develop this algorithm towards a tool for detecting small movements on different scales by estimating the receiver velocity and relative displacements right from sensor start-up. On the other hand, movement detection from start-up could also be achieved by detecting motions from precise position coordinates, gained by advanced GNSS signal processing methods. In this case, the key lies in almost instantaneous resolution of the GNSS phase ambiguities. Nevertheless, for both cases filter algorithms have to be set up to separate a movement from measurement noise and other drifts and offsets arising from the different effects affecting the GNSS measurements.

At the moment an algorithm for the movement detection in the velocity domain is under development. A preliminary version of the algorithm was tested for GPS Doppler observations (on the first satellite carrier frequency) of a shake table experiment, measured with a geodetic-grade JAVAD dual frequency receiver, sampled at 100 Hz. Therefore, a sub-dataset of a quiet period, followed by an oscillation with a period of 10 s and an amplitude of 0.05 m was extracted. The ground truth of displacement and velocity as well as the shake table instrumental setup is shown in Figure 4.82.

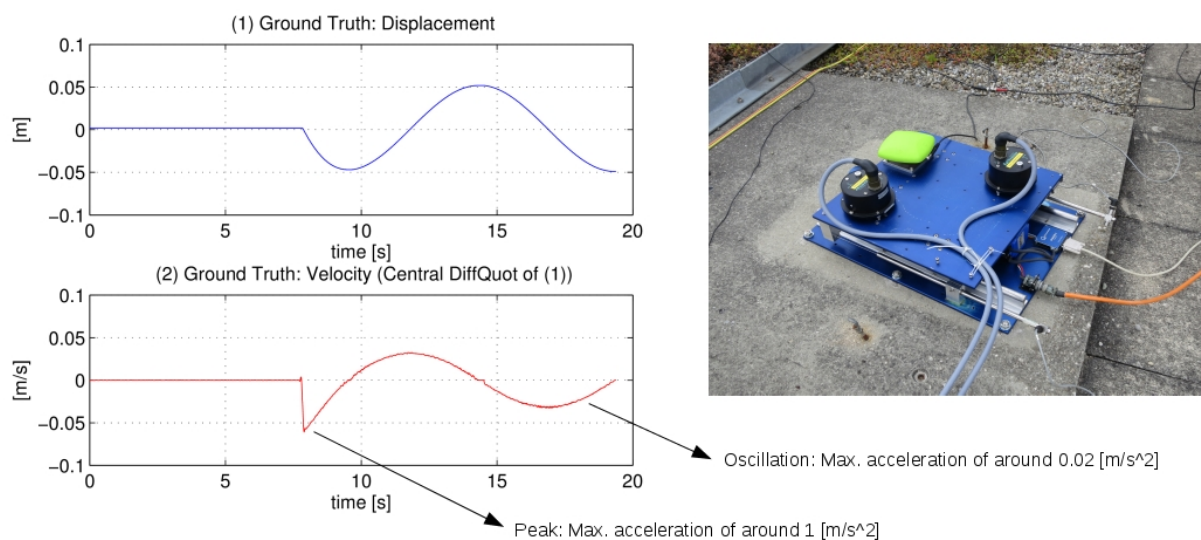


Figure 4.82: Ground truth (displacement and velocity) and instrumental set up for the shake table experiment

To characterize the movement, a second-order kinematic model for a Kalman filter was chosen. Figure 4.83 compares filter results for the x and y component of the receiver velocity for two different values of the system noise versus ground truth and an epoch-wise least squares estimation.

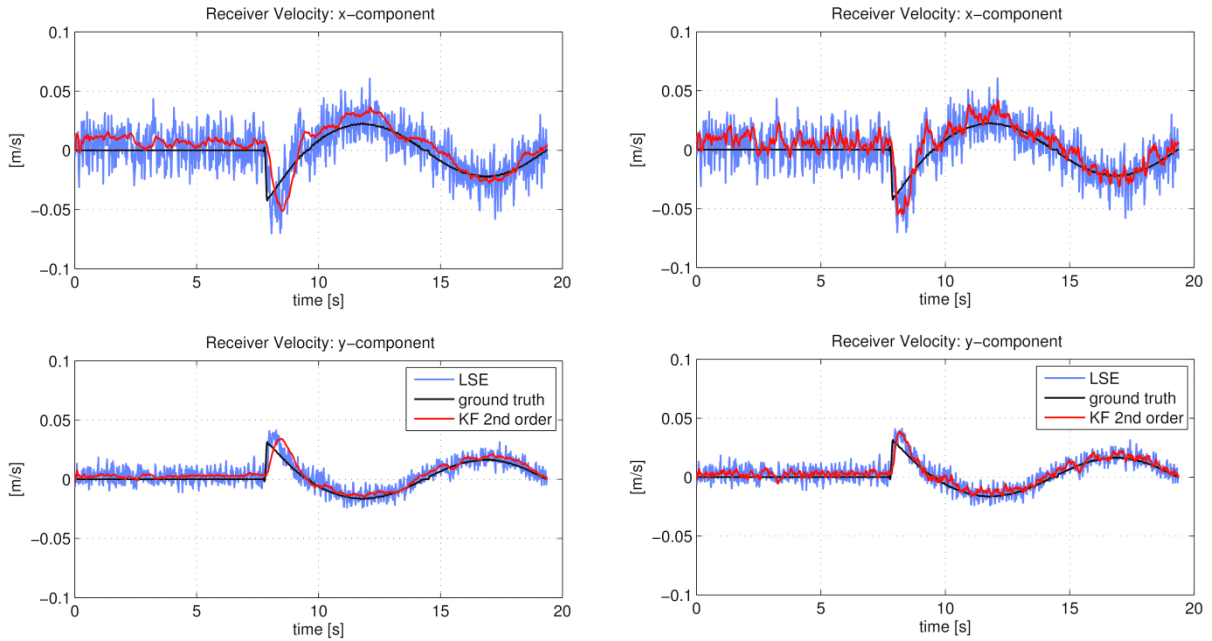


Figure 4.83: Velocity components for the sub-dataset of the shake table experiment: Results of the epoch-wise least squares estimation, ground truth and Kalman filter estimates for two different process noise densities of the filter ($0.0001 \text{ m}^2/\text{s}^5$ on the left-hand-side and $0.01 \text{ m}^2/\text{s}^5$ on the right-hand side)

As there is low dynamics, the results for the lower system noise better correspond to the oscillation, whereas the performance of the filter with higher system noise does a better job for high system dynamics, which is the case at the initialization of the oscillation. Both filter results exhibit a significant improvement w.r.t. noisier epoch-by-epoch least squares estimation of the receiver velocity and demonstrate the potential ability of GNSS for motion detection in the velocity domain even for movements which exhibit quite low dynamics and small magnitude.

GNSS Remote Sensing of Snow Coverage on Ground and Glacier Surfaces

L. Steiner¹, P. Limpach¹, A. Geiger¹, M. Rothacher¹, M. Huss²

¹Institute of Geodesy and Photogrammetry, ETH Zurich

²Laboratory of Hydraulics, Hydrology and Glaciology, ETH Zurich

Knowledge of snow cover depth and characteristics is an important basis for climatology, natural hazards forecasting, early-warning systems, and hydro-energy industries. The extensive amount of water stored in snow covers has a high impact on flood development during snow melting periods. Snow depth and type are important parameters in avalanche formation. In climatology, changes in glacier mass balance due to snow accumulation and ice melt over a glacier surface are important parameters to better understand glacier response to climatic forcing.

Extensive observations of snow water equivalent (SWE) and snow depths are challenging due to the heterogeneity of snow distribution caused by mountainous terrain and environment. Global navigation satellite system (GNSS) remote sensing techniques are capable to provide reliable, accurate, efficient, and continuous observations independent of weather conditions.

The project “GNSS Remote Sensing of Snow Coverage on Ground and Glacier Surfaces” funded by the Swiss National Science Foundation is carried out in coordination with the Laboratory of Hydraulics, Hydrology and Glaciology at ETH Zurich (VAW-ETHZ). The main objective of this project is the thorough investigation of the contribution of GNSS remote sensing techniques to mountainous snow and glacier applications, such as snow pack characterization and quantification of snow depth and SWE. For this investigation, GNSS remote sensing from reflected signals will be combined with GNSS signals received by antennas underneath the snow pack. Based on the path extension of reflected signals compared to direct signals, the analysis of multipath GNSS signals will lead to estimations of snow depth. The analysis of directly received GNSS signals below the snow surface allows the estimation of SWE based on the refraction of the GNSS signals during its propagation in the snow cover. The spatial distribution of SWE and snow depth will be estimated within an area of several square meters around the antenna. The study is carried out at the WSL Institute for Snow and Avalanche Research SLF test-site “Weissfluhjoch” above Davos (Figure 4.84). The GNSS measurements will be compared to SWE ground truth data from snow pillow and snow scale measurements as well as to snow depth ground truth data from laser distance sensors at the test-site.

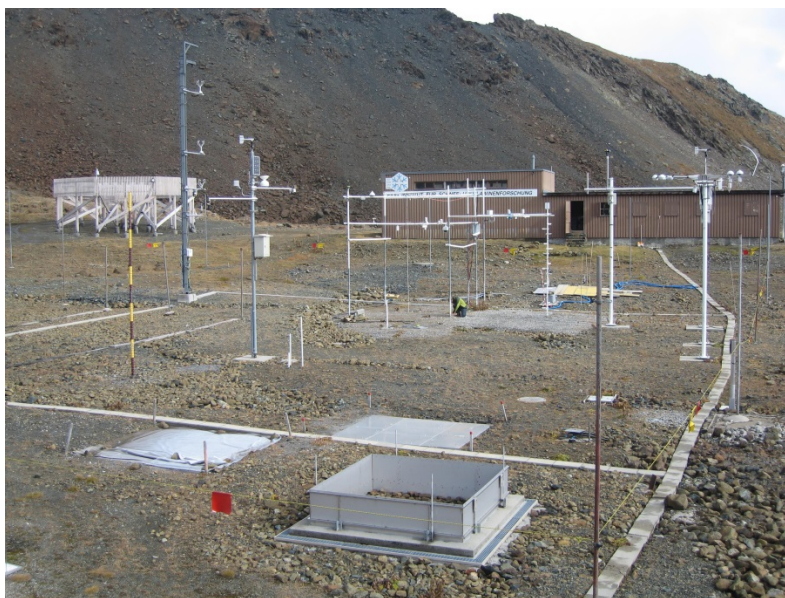


Figure 4.84: SLF test-site “Weissfluhjoch” above Davos, Switzerland.

QDAEDALUS: A versatile usable digital clip-on measuring system for total stations

S. Guillaume, B. Bürki, A. Wolf, P. Sorber, H-P. Oesch, and A. Geiger

Geodesy and Geodynamics Lab, Institute of Geodesy and Photogrammetry, ETH Zurich

QDaedalus is a measurement system developed at the Institute of Geodesy and Photogrammetry at ETH Zurich (Bürki 2010). It is composed of both, hardware and software developments (Figure 4.85). The basic idea is to replace the eye-piece of an existing total station by a CCD camera in a non-destructive way in order to measure fully automatically very accurate spatial directions to visible objects without using corner-cube targets as in standard Automatic Object Recognition (ATR). In addition to the CCD camera and the total station, the hardware is composed of a motorized focuser and a small electronic interface, including a low-cost GNSS receiver, for precise absolute time referencing and hardware synchronization of several systems. The dedicated software of QDaedalus is based on a user-friendly graphical interface and controls all sensors including the total station. Furthermore it allows calibrating the system properly before starting the measurement of the targets. These measurements are based on different optical target object recognition (OTR) and extraction algorithms like template least-squares matching, center of mass operator, robust circle and ellipse matching thus allowing a fully automatic acquisition of numerous kinds of objects (Figure 4.86).



Figure 4.85: Main hardware components of the QDaedalus system.

Applications

Since the first developments, various kind of applications were successfully applied:

- **Astrogeodetic Measurements:** deflections of the vertical with a precision between 0.15-0.2 arcsec can be obtained after 30 minutes of automatic observation and online processing (Hauk 2014). Furthermore, it is possible to determine astronomical azimuths at nighttime (with stars) and even at daytime (with sun or bright planets) with a precision between 0.5 to 1 arcsec after 20 minutes of observation.
- **Automatic Microtriangulation:** Optical micro-triangulation is an extremely powerful technique for measuring automatically 3D objects very precisely without touching them. The basic principle is to measure horizontal directions and zenith angles of well-defined targets from at least two different locations in order to determine a micro geodetic network by means of three-dimensional intersections. A concrete application of this technique was applied at the European Organization for Nuclear Research (CERN) for the

determination of 3D coordinates of 8mm ceramic spheres fixed on accelerating components (1x4x1 meters) of a future linear particle collider (*Guillaume 2012*). The results obtained reveal a 3D-accuracy at a level better than 10 microns (Figure 4.87 and Figure 4.88).

- **Real-Time deformation and Vibration Analysis:** thanks the possibility to push the rate of data acquisition to several tenths of Hertz and the capability to synchronize several systems, 3D deformation and vibration measurements of indoor and outdoor objects are possible. In collaboration with the Institute of Structural Engineering of ETH Zurich, this technique was applied for the determination of the 3D position's response of a wood structure excited with an appropriate shaker at different frequencies. Two leds were placed at extremities (12m separation) and observed at 60 Hz by synchronized 4 QDaedalus systems (Figure 4.89). The results show that it was possible to obtain 3D high-rate kinematic position time series of the leds with a precision of a few hundreds of mm (Figure 4.90).
- **High precision optical automated tracking of flying objects:** the system QDaedalus is also capable to track and measure, in a pure passive manner, flying objects (Conzett 2014, Hildebrandt 2014, Nüssli 2014, Salzgeber 2014). First experiments show that 3D trajectories of aircrafts at 5 kilometers can be obtained at 20 Hertz with a precision of about 1-2 meters (Figure 4.91).

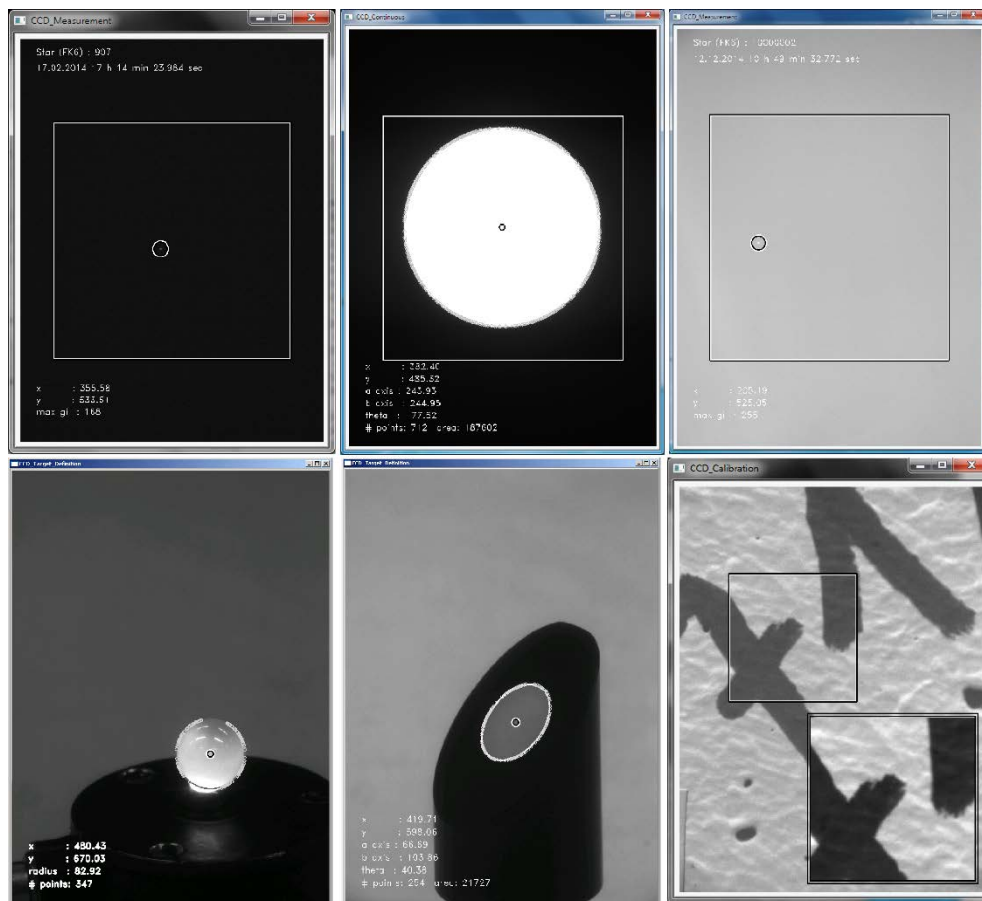


Figure 4.86: Various objects extracted in QDaedalus system. (Upper, left) Polaris, (upper, center) sun, (upper, right) Venus daylight, (lower, left) ceramic sphere, (lower, center) photogrammetric target, (lower, right) arbitrary template.

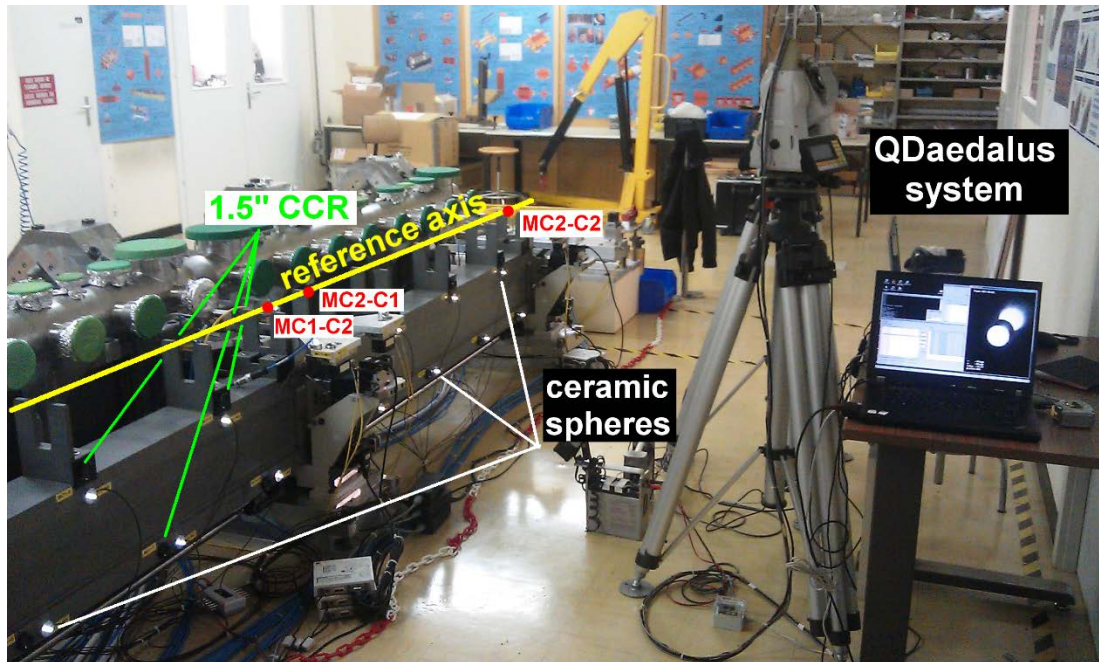


Figure 4.87: Accelerating components (1x4x1 meters) of the future linear particle collider CLIC at CERN and QDaedalus systems ready for microtriangulation measurements.

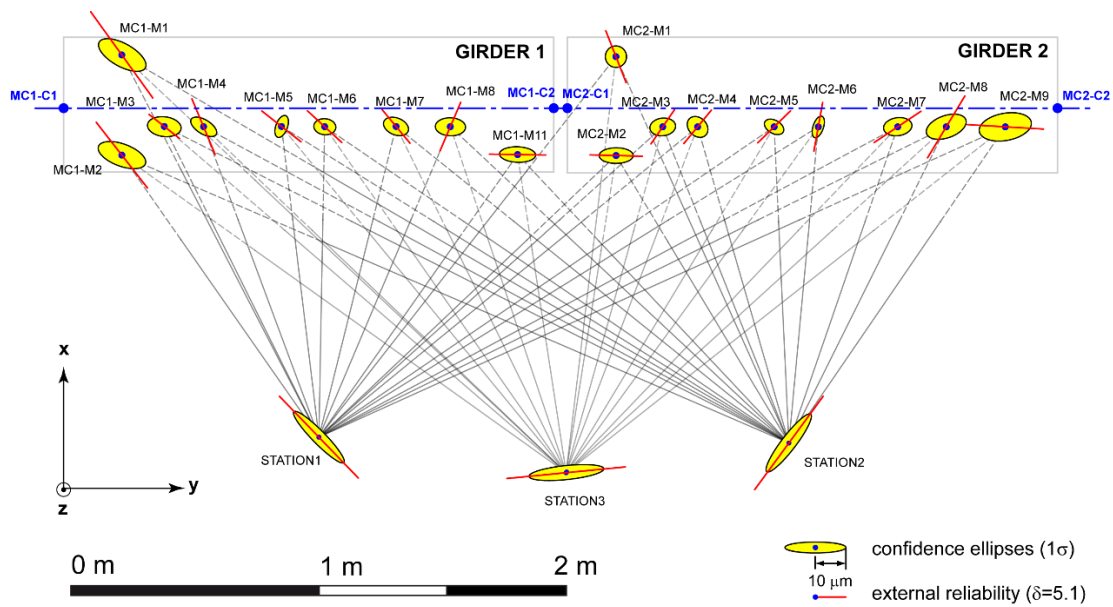


Figure 4.88: Results of the geodetic network adjustment of the microtriangulation experiment at CERN.



Figure 4.89: Wood structure and 4 synchronized QDaedalus systems ready for 3D high-rate kinematic position measurements.

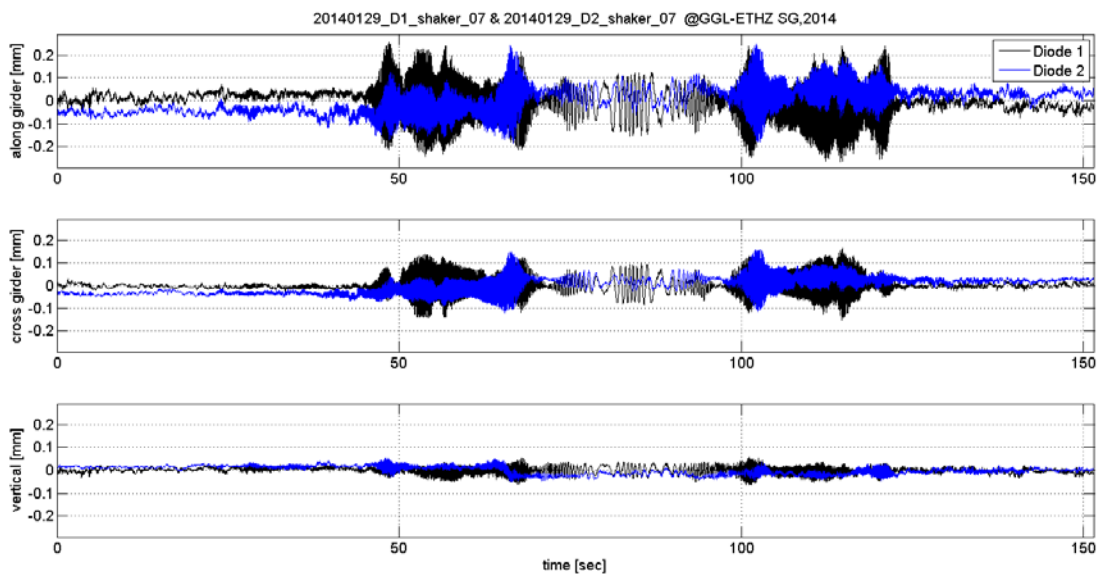


Figure 4.90: 3D time series of 2 led measured at 60 Hz by 4 synchronized QDaedalus systems.



Figure 4.91: Aircraft tracked and measured at Zürich airport by a QDaedalus system.

Laser Alignment Multipoint Based Design Approach LAMBDA project

G. Stern^{1,2}, A. Geiger¹, H. Mainaud-Durand², S. Guillaume¹

¹Geodesy and Geodynamics Lab, Institute of Geodesy and Photogrammetry, ETH Zurich.

²European Organization for Nuclear Research (CERN), Geneva, Switzerland.

The Compact Linear Collider study has set challenging requirements for the pre-alignment of beam related components. In some parts of the future particles accelerator, the required alignment accuracy should be 10 μm over 200 m. In order to validate, complete and possibly replace existing systems based on stretched wires or water level, a new alignment system based on laser beam as straight line reference is currently under study at CERN (European Organization for Nuclear Research). The name of the project is LAMBDA which is an acronym standing for Laser Alignment Multipoint Based Design Approach. Laser based alignment systems have already been developed in other research centers, e.g. SLAC (Stanford Linear Accelerator Center), KEK (the High Energy Accelerator Research Organization of Japan) and DESY (Deutsches Elektronen-Synchrotron) but their estimated alignment accuracies did not meet CLIC requirements. Compared to these systems, the LAMBDA project proposes a new type of sensor to measure the positions of the components with respect to the laser beam. The LAMBDA sensor is made of a camera and an open/close shutter. A measurement works as follows: (1) attach the LAMBDA sensor on the component to be measured, (2) close the shutter, (3) take a picture of the laser spot on the closed shutter with the camera, (4) determine the coordinates of the laser spot by image processing, (5) deduce the position of the component attached to the LAMBDA sensor and (6) open the shutter and let the laser beam propagate until the next closed shutter. In a first iteration, we tested the performance of the LAMBDA sensor at short distance and found standard deviations of the laser spot coordinates of 10 μm at 3 m. In a second iteration, we tested the sensor over long distance (Stern et al., 2013). We found that the standard deviations increase with the distance of propagation (up to 2 mm at 200 m). Since these values are much above CLIC requirements, we performed an additional test with laser beam under vacuum which gave standard deviations of 8 μm at 35m.

The detection and determination of the laser beam's position on the shutter is performed by a further developed center of mass and elliptic form detection algorithm. To further validate the micrometric positioning sensors, several parameters are examined. E.g. the most appropriate reference targets on the shutter have to be selected in terms of implementation and measurement of targets, as well as the laser pointing stability is analyzed in conjunction with different types of shutter surfaces. Experiments are carried out with paper, metal and ceramic surfaces.

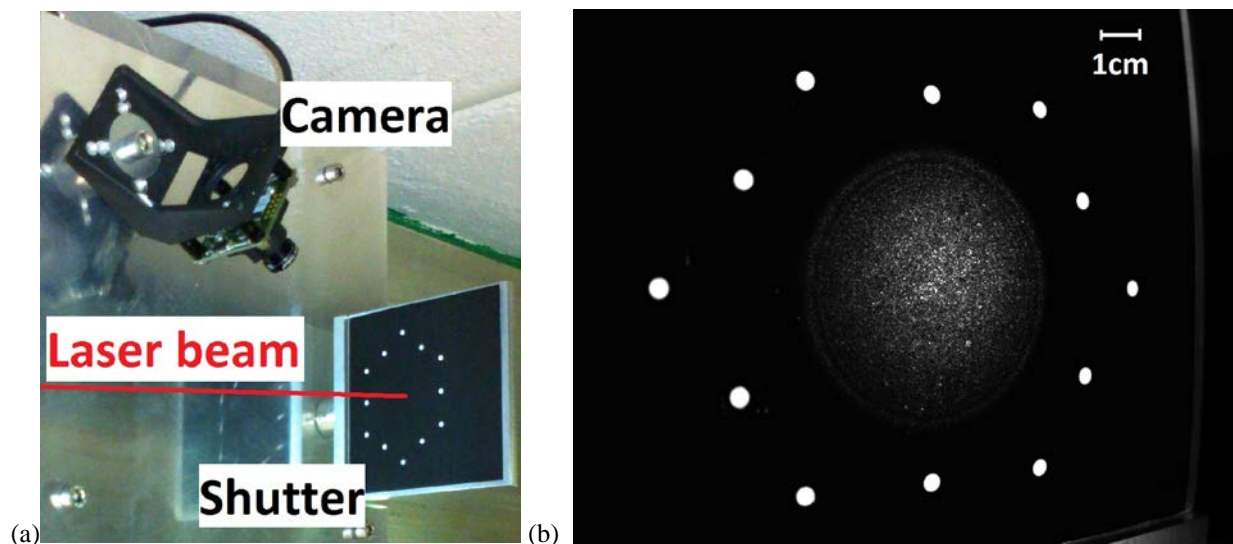


Figure 4.92: (a) LAMBDA sensor (from Stern et al., 2013); (b) Shutter with laser spot in the middle and targets around (paper surface) (from Stern et al., 2013)

FSI and Micro-Triangulation Study for the Pre-alignment of CLIC in the PACMAN Project

S. W. Kamugasa and V. Vlachakis

CERN, Geneva, Switzerland and Geodesy and Geodynamics Lab, Institute of Geodesy and Photogrammetry, ETH Zurich, Switzerland

The alignment precision of linear colliders is extremely demanding owing to the very narrow beam size at the collision point. Unlike circular colliders, particles in linear colliders have only one chance to collide and are hence tightly focused to maximise the number of interactions per collision. CLIC (Compact Linear Collider) is a site-independent feasibility study aiming at the development of realistic technology at an affordable cost for an electron-positron linear collider. This multi-TeV (nominal 3 TeV) collider will expand the knowledge of particle physics in the post-Large Hadron Collider (LHC) era (Aicheler et al., 2012). One of the main technical challenges of this nearly 50 km long collider is the very tight alignment requirements, which will require the pre-alignment of its 20'000 modules at the level of 10 μm over a 200 m sliding window (Becker et al., 2013). The pre-alignment is a 3-step process involving firstly fiducialisation, which is the determination of the position of external targets with respect to the reference axis of a component. The second step is the alignment of components on a common support and finally, the alignment of the support in the tunnel.

PACMAN (Particle Accelerator Components Metrology and Alignment to the Nanometre scale) is a Marie Curie Initial Training Network, implemented as Innovative Doctoral Program (IDP), hosted by CERN. The project provides training to 10 Early Stage Researchers in a variety of disciplines like beam instrumentation, metrology, micrometric alignment, magnetic measurements, nano-positioning and high precision engineering (PACMAN, 2015). This is being done in collaboration with 8 industrial partners and 8 universities which will provide technical training and academic instruction, respectively. The technical goal of PACMAN is to develop very high accuracy metrology and alignment tools and integrate them in a single automatic test stand. In PACMAN, the magnetic centre of the quadrupole magnets will be determined by magnetic measurements and will be materialised by a stretched 0.1 mm diameter Copper Beryllium (CuBe) wire. As such, a study is being conducted within this project to develop a contactless measurement head for the Leitz Infinity CMM (Coordinate Measuring Machine). This CMM will then be able to measure the stretched wire and hence perform the fiducialisation of the magnet and Beam Position Monitor (BPM) whose electromagnetic centre will also be materialised by the CuBe wire. With an accuracy of 0.3 μm +1 ppm, the Leitz Infinity is currently the most accurate means of performing fiducialisation and alignment of components on a common support. However, this CMM is immobile and has a limited measurement volume (1200 x 1000 x 700 mm), whereas some elements will be 2 m long and some measurements may be required on site.

Two alternatives are being developed in PACMAN (Kamugasa and Vlachakis, 2014) to overcome these limitations, one based on FSI multilateration and the other on Micro-Triangulation. FSI realized by Etalon AG's Absolute Multiline system (Etalon, 2015) and Micro-Triangulation implemented by QDaedalus system developed at ETH Zurich (Bürki et al., 2010) offer a precision of 0.5 $\mu\text{m}/\text{m}$ and 2.4 $\mu\text{m}/\text{m}$, respectively. However, these systems need to be improved in order to provide the necessary geometric information via distance measurements (multilateration) and angle measurements (triangulation), respectively.

QDaedalus, a contactless angle measurement system, will be improved by developing an algorithm to detect the CuBe wire, extract angle measurements and reconstruct the wire's 3D position. FSI on the other hand will be transformed into a system that can accurately determine 3D coordinates through multilateration. These two systems will be compared for accuracy, reliability and robustness and will then be validated by the Leitz Infinity. They will be extrapolated into portable solutions in order to be able to make measurements on site.

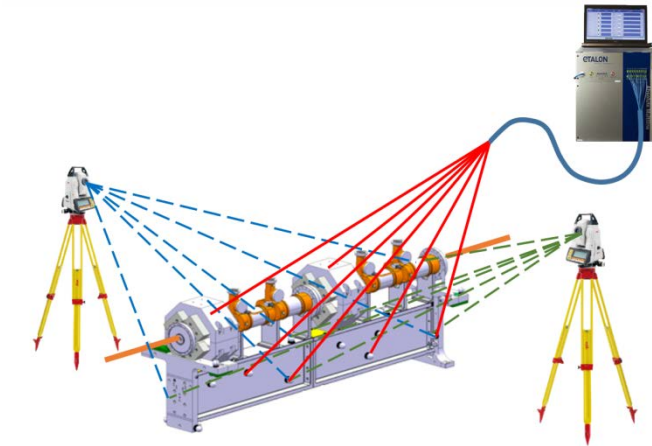


Figure 4.93: Illustration of Micro-triangulation and FSI arranged about a CLIC module.

The successful integration of both fiducialisation and alignment of the components on a common support, will lead to a lower cost, time efficient and more precise pre-alignment. FSI and Micro-Triangulation can then be valuable not only in the CLIC pre-alignment measurements and installation, but also in other geodetic metrology applications at CERN and especially in hazardous environments, where automation is needed.

Bibliography Commission 4

- Aicheler, M., Burrows, P., Draper, M., Garvey, T., Lebrun, P., Peach, K., Phinney, N., Schmickler, H., Schulte, D., and Toge, N. (2012): A Multi-TeV Linear Collider Based on CLIC Technology: CLIC Conceptual Design Report", CERN-2012-007, CERN, Geneva, Switzerland, ISBN 978-92-9083-379-62014.
- Akhtman, Y., Constantin, D., Rehak, M., Nouchi, V.M., Bouffard, D. et al. Leman-Baikal (2014): Remote sensing of lakes using an ultralight plane. 6th Workshop on Hyperspectral Image and Signal Processing, Lausanne, Switzerland.
- Akhtman, Y., Constantin, D., Rehak, M., Nouchi, V.M., Shinkareva, G. et al (2014): Télédétection multi-échelle des lacs depuis un aéronef ultraléger motorisé. In Géomatique Suisse, vol. 9, num. 395-398, 2014.
- Arnold, D., Lutz, S., Dach, R., Jäggi, A., Steinborn, J. (2013): Near real-time coordinate estimation from double-difference GNSS data. A case study for the National Multi-Hazard Early Warning System in the Sultanate of Oman. IAG Symposia Series (in press).
- Arnold, D., Beutler, G., Sošnica, K., Meindl, M., Lutz, S., Dach, R. (2015a): Updating the empirical CODE orbit model and validation of GPS and GLONASS orbits using Satellite Laser Ranging data, this volume
- Arnold, D., Meindl, M., Beutler, G., Dach, R., Schaer, S., Lutz, S., Prange, L., Sosnica, K., Mervart, L., and Jäggi, A. (2015b): CODE's new solar radiation pressure model for GNSS orbit determination. Journal of Geodesy, doi:10.1007/s00190-015-0814-4
- Bachofen, N. and Tuchschnid, T. (2013): Lokale Hebungsdaten in den Schweizer Alpen (Wildhorndecke). Bachelor Thesis 2013/01. Muttenz: Fachhochschule Nordwestschweiz.
- Barras, V., Delley, N., and Chapotte G. (2013) : Analyses aux limites des scanners laser terrestres, Parties 1 et 2 Alter 2 : auscultation via scanner laser terrestre. Revue XYZ N°. 137 – 4ème trimestre 2013 : 19-31
- Barras, V., and Jeanneret, M. (2013) : Surveillance par vidéotachéométrie, à la limite de l'optique. Veille technologique géosuisse, Yverdon-les-Bains, 19.03.2013
- Barras, V., and Chapotte, G. (2015): Auscultation sans réflecteur: diverses méthodes et techniques. Veille technologique géosuisse, Yverdon-les-Bains, 28.01.2015
- Becker, F., Coosemans, W., Pittin, R., and Wilson, I.H. (2013): An Active Pre-Alignment System and Metrology Network for CLIC, CLIC Note 553, CERN.
- Beutel, J., Buchli, B., Gruber, S., Gsell, T., Lim, R., Limpach, P., Sutton, F., Walser, C., Weber, S., and Wirz, V. (2013): The X-Sense Wireless GPS Network in Matter Valley, 4th Annual Plenary Meeting of Nano-Tera.
- Beutler, G., Kouba, J., Springer T. (1995): Combining the orbits of the IGS analysis Centers. Bulletin geodesique, volume 69 number 4 pages: 200-222
- Beyerle, G., Grunwaldt, L., Heise, S., Köhler, W., König, R., Michalak, G., Rothacher, M., Schmidt, T., Wickert, J., Tapley, B.D., and Giesinger, B. (2011): First results from the GPS atmosphere sounding experiment TOR aboard the TerraSAR-X satellite, Atmospheric chemistry and physics, 11, 6687–6699, doi:10.5194/acp-11-6687-2011.
- Blaha, M., Eisenbeiss, H., Grimm, D., and Limpach, P. (2011): Direct Georeferencing of UAVs. International Archives of the Photogrammetry, Remote Sensing and Spatial Information Sciences, Vol. XXXVIII-1/C22, UAV-g 2011, Conference on Unmanned Aerial Vehicle in Geomatics, September 14-16, 2011, Zurich, Switzerland. ISSN 1682-1777.
- Boehm, J., Niell, A., Tregoning, P., and Schuh, H. (2006a): Global Mapping Function (GMF): a new empirical mapping function based on numerical weather model data. Geophysical Research Letters, 33:L07304. doi:10.1029/2005GL025546.
- Boehm, J., Werl, B., and Schuh, H. (2006b): Troposphere mapping functions for GPS and very long baseline interferometry from European Centre for Medium-Range Weather Forecasts operational analysis data. Journal of Geophysical Research 111:B02406. doi:10.1029/2005JB003629.

- Boehm, J., Heinkelmann, R., and Schuh, H. (2007): Short note: a global model of pressure and temperature for geodetic applications. *Journal of Geodesy* 81(10):679–683. doi:10.1007/s00190-007-0135-3
- Botteron, C., Dawes, N., Leclere, J., Skaloud, J., and Weijs, S.V. (2013): Soil moisture & snow properties determination with GNSS in alpine environments: Challenges, status, and perspectives, *Remote Sens.*, vol. 5, no. 7, pp. 3516–3543, 2013.
- Brockmann, E. (2010): swisstopo (LPT) E-GVAP report. Expert group meeting in Oslo, 22.-23.9.2010
- Brockmann, E. (2011): swisstopo (LPT) E-GVAP report. Expert group meeting in Toulouse, 20.-21.10.2011
- Brockmann, E., Bock, O., Dach, R., Dick, G., Dousa, J., Hugentobler, U., and Pacione, R. (2014): Reprocessing Activities as possible contribution to GNSS4SWEC”, GNSS4SWEC workshop, Munich, February 25-28, 2014.
- Brockmann, E. (2014): Intercomparison of ZTD solutions: operational – reprocessed (global, kontinental), GNSS4SWEC workshop, Varna, September 9-13, 2014.
- Brockmann, E. (2014): Status of the working progress in Switzerland, GNSS4SWEC workshop, Varna, September 9-13, 2014.
- Brockmann, E. (2014): swisstopo Report for EGVAP 2014, EGVAP expert meeting, Exeter, October 2014.
- Bürki, B., Guillaume, S., Sorber, P., and Oesch, H.-P. (2010): DAEDALUS: A versatile usable digital clip-on measuring system for Total Stations, International Conference on Indoor Positioning and Indoor Navigation (IPIN), Zürich, IEEE.
- Charalampous, E., Psimoulis, P., Guillaume, S., Spiridonakos, M., Klis, R., Bürki, B., Rothacher, M., Chatzi, E., Luchsinger, R., and Feltrin, G. (2014): Measuring sub-mm structural displacements using QDaedalus: a digital clip-on measuring system developed for total stations, *Applied Geomatics*, Springer Berlin Heidelberg, doi: 10.1007/s12518-014-0150-z, pp. 1-11.
- Clausen, P., Skaloud, J., Gilliéron, P.-Y., Merminod, B., and Perakis, H. et al. (2015): Position Accuracy with Redundant MEMS IMU for Road Applications. European Navigation Conference GNSS, Bordeaux, France, April 7-10, 2015.
- Clenet, H., Constantin, D., and Rehak, M. et al. (2015): UAV based multispectral imaging over a lagoon with corals in Reunion Island. EARSel 2015, Luxembourg. April 2015.
- Comte, J., and Kasser, M. (2014): Performances et limitations de la corrélation diachronique d’images pour les ouvrages d’art; *Géomatique Suisse* 11/2014, pp. 488-492.
- Comte J., and Kasser M. (2014): Performances et limitations de la corrélation diachronique d’images pour les ouvrages d’art; *Septembre 2014, XYZ N° 140*, pp. 29-34.
- Condamin, S., and Egli Oppliger, R. (2013): Hebungsdaten in den Schweizer Alpen - Bestimmung der lokalen Hebungsdaten in einem Testgebiet in den Schweizer Alpen, Muttenz: Fachhochschule Nordwestschweiz (FHNW)
- Condamin, S., and Schwarzgruber, J. (2013): Lokale Hebungsdaten in den Schweizer Alpen (Wildhorndecke). Bachelor Thesis 2012/03 (überarbeitet). Muttenz: Fachhochschule Nordwestschweiz.
- Condamin, S., Schwarzgruber, J., and Sievers, B. (2014): Lokale Hebungsdaten in den Schweizer Alpen (Wildhorndecke). *Geomatik Schweiz*, 112(1), S.12–15.
- Constantin, D., Rehak, M., Akhtman, Y., and Liebisch, F. (2015): Hyperspectral remote sensing of crop properties with Unmanned Aerial Vehicles. EARSel 2015, Luxembourg. April 2015.
- Conzett, K. (2014): Tracking of Fast Moving Objects Using Video Tachymetry, ETH Zürich, Institute of Geodesy and Photogrammetry, Semester Work.
- Cubero-Castan, M., Constantin, D., and Akhtman, Y. (2015): A new smoothness based strategy for semi-supervised atmospheric correction: application to the Léman-Baïkal campaign. 6th Workshop on Hyperspectral Image and Signal Processing, Tokyo, Japan. September 2015.

- Dach, R., Hugentobler, U., Fridez, P., and Meindl, M. eds. (2007): Bernese GPS Software, Version 5.0. Astronomical Institute, University of Bern.
- Dach, R., Schaer, S., Bock, H., Lutz, S., and Beutler, G. (2010): CODE's New Combined GPS/GLONASS Clock Product. IGS Workshop 2010, Newcastle upon Tyne, England, 28 June - 2 July, 2010.
- Dach, R. et al. (2011): Bernese Software, 25th International Union of Geodesy and Geophysics General Assembly (IUGG 2011).
- Dach, R., Beutler, G., Jäggi, A., Schildknecht, T. (2011): GNSS-Forschungsarbeiten am Astronomischen Institut der Universität Bern . Geomatik Schweiz, vol. 109(6), pp. 280-283.
- Dach, R., Böhm, J., Lutz, S., Steigenberger, P., and Beutler, G. (2011b): Evaluation of the impact of atmospheric pressure loading modeling on GNSS data analysis. *Journal of Geodesy*, vol. 85(2), pp. 75-91, doi:10.1007/s00190-010-0417-z.
- Dach, R., Schmid, R., Schmitz, M., Thaller, D., Schaer, S., Lutz, S., Steigenberger, P., Wübbena, G., Beutler, G. (2011a): Improved antenna phase center models for GLONASS. *GPS Solutions*, vol. 15(1), pp. 49-65, doi:10.1007/s10291-010-0169-5.
- Dach, R. et al. (2013): Bernese GNSS Software, Version 5.2, Bern: Universität Bern, Astronomisches Institut. Available at: <http://www.bernese.unibe.ch/>.
- Dach, R. et al. (2013): Center for Orbit Determination in Europe (CODE), IGS Central Bureau.
- Dach, R., Schaer, S., Lutz, S., Baumann, C., Bock, H., Orliac, E., Prange, L., Thaller, D., Mervart, L., Jäggi, A., Beutler, G., Brockmann, E., Ineichen, D., Wiget, A., Weber, G., Habrich, H., Söhne, W., Ihde, J., Steigenberger, P., and Hugentobler, U. (2014): Annual Center Reports: Center for Orbit Determination in Europe (CODE). pp. 21 - 34. International GNSS Service, Technical Report 2013, R. Dach, Y. Jean, Astronomical Institute, University of Bern (edts.), printed by IGS Central Bureau, Pasadena, California (USA).
- Darbre, G., Kolly, J.-C., Lutz, M., Walser, F., and Wiget, A. (2013): Geodäsie für die Überwachung von Stauanlagen. Empfehlungen des Schweizerischen Talsperrenkomitees STK für den Einsatz der geodätischen Deformationsmessung bei Stauanlagen (in German and French). Schweizerisches Talsperrenkomitee – Comité suisse des barrages – Swiss Committee on Dams, 2013.
- Diessongo, H.T., Bock, H., Schüler, T., Junker, S., Kiroe, A. (2012): Exploiting the Galileo E5 Wideband Signal. *Inside GNSS*, pp. 64-73
- Dow, J. M., Neilan, R. E., and Rizos, C. (2009): The International GNSS Service in a changing landscape of Global Navigation Satellite Systems. *Journal of Geodesy*, 83(3), 191–198. doi:10.1007/s00190-008-0300-3.
- Durand, H. M., Missiaen, D.P., and Stern, G. (2013): Alignment Challenges for a Future Linear Collider, 4th International Particle Accelerator Conference (IPAC 2013).
- Etalon AG (2015): web site <http://www.etalon-ag.com/?lang=en> .
- Eissa, L., and Kasser, M. (2011): Représentation cartographique des déformations de la croûte terrestre par des tenseurs régulièrement répartis. *Bulletin d'Information de l'IGN*, pp. 53-56, 2011.
- Falck, C., Ramatschi, M., Subarya, C., Bartsch, M., Merx, A., Hoeberechts, J., and Schmidt, G. (2010): Near real-time GPS applications for tsunami early warning systems. *Nat. Hazards Earth Syst. Sci.*, 10, 181-189.
- Filliger, R., Stebler, Y., Skaloud, J., and Hug, K. (2013): Autarktic and inertial measurement based low-cost reconstruction of motorcycle forward speed, in *Proceedings of the ENC-GNSS*, Vienna, Austria, 2013.
- Gazeaux, J., Williams, S., King, M., Bos, M., Dach, R., Deo, M., Moore, A.W., Ostini, L., Petrie, E., Roggero, M., Teferle, F.N., Olivares G. and Webb, F.H. (2013): Detecting offsets in GPS time series: first results from the Detection of Offsets in GPS Experiment. *J. Geophys. Res. Solid Earth*, 118, L23602, DOI 10.1002/jgrb.50152.
- Geiger, A., Perler, D., Hurter, F., and Rothacher, M.. (2011): Ground-Based GNSS Tomography: Challenges in Mountainous Regions (invited) *IGARSS IEEE Int. Geoscience and Remote Sensing Symposium*, 24-29 July, 2011, Vancouver, CDN.

- Geiger, A., Perler, D., Hurter, F., Rothacher, M. (2011): Ground based GNSS tropospheric tomography: Next steps. (invited), Int. workshop on GNSS Remote Sensing for Future Missions & Sciences, 7.-9. August, 2011, Shanghai, China.
- Geiger, A., Wipf, H., and Scaramuzza, M. (2014): Simplified GNSS Positioning Performance Analysis, PLANS 2014, Monterey, 2014, 978-1-4799-3320-4/14/ IEEE, p.708-711.
- Geiger, A., Scaramuzza, M., and Wipf, H. (2014): Simplified GNSS Positioning Performance Analysis. PLANS 2014, IEEE / US ION, Monterey, USA, Proceedings. Presentation and publication.
- Gilgien, M., Spörri, J., Kröll, J., Crivelli, P., Chardonens, J., Limpach, P., Geiger, A., Cabri, J., Müller, E., Kröll, J., Lindinger, S.J., Pfusterschmied, J., and Stöggli, T. (2013): Global Navigation Satellite Systems in alpine skiing: Method validity and applications, 6th International Congress on Science and Skiing.
- Gilgien, M., Spörri, J., Limpach, P., Geiger, A., and Müller, E. (2014): The effect of different global navigation satellite system methods on positioning accuracy in elite alpine skiing, *Sensors*, 14, 18433–18453, doi:10.3390/s141018433.
- Gilgien, M., Spörri, J., Chardonens, J., Kröll, J., Limpach, P., Müller, E. (2015): Determination of the centre of mass kinematics in alpine skiing using differential global navigation satellite systems, *Journal of Sports Sciences*, 33, 960–969, doi:10.1080/02640414.2014.977934.
- Gilliéron, P.-Y. (2014): Intégrité du positionnement dans le transport routier, in *Strasse und Verkehr*, vol. 09, num. 09-14, p. 14-17, 2014.
- Gilliéron, P.-Y., and Peyret, F. (2014): SaPPART - Satellite Positioning Performance Assessment for Road Transport. 5th TRA - Transport Research Arena, Paris, F, April, 14-17, 2014.
- Guerrier, S. (2009): Improving accuracy with multiple sensors: study of redundant MEMS-IMU/GPS configurations,” presented at the ION GNSS 2009, Savannah, Georgia, USA, 2009.
- Guerrier, S., Stebler, Y., Skaloud, J., and Victoria-Feser, M.-P. (2012): Improving modeling of MEMS-IMUs operating in GNSS-denied conditions, in *Proceedings of the Position Location and Navigation System (PLANS) jointly organized by IEEE-Aerospace and Electronics Systems Society (AESS) and Institute of Navigation (ION)*, 2012.
- Guerrier, S., Skaloud, J., Stebler, Y., and Victoria-Feser, M.-P. (2013): Wavelet-variance-based estimation for composite stochastic processes, *J. Am. Stat. Assoc.*, vol. 108, no. 503, pp. 1021–1030, 2013.
- Guerrier, S., Molinari, R., Skaloud, J., and Victoria-Feser, M.-P. (2013): An algorithm for automatic inertial sensor calibration, in *ION GNSS+*, Nashville, Tennessee, USA, 2013.
- Guillaume, S., Muller, C., and Cattin, P.-H. (2009): TRINET+ - Logiciel de Compensation de Reseaux 3D, Yverdon-les-Bains: Haute Ecole d'Ingénierie et de Gestion du Canton de Vaud (HEIG-VD).
- Guillaume, S., Jones, M., Bürki, B., Geiger, A., Rizos, C., and Willis, P. (2011a): Determination of High Precision Underground Equipotential Profiles for the Alignment of a future Linear Collider, IAG General Assembly : Earth on the edge: Science for a sustainable planet.
- Guillaume, S., Jones, M., Bürki, B., Geiger, A., Rizos, C., and Willis, P. (2011b): Measurement of underground variations in the deflection of the vertical with a high precision interferometric deflectometer, *Proceedings of the IAG General Assembly*.
- Guillaume, S., Jones, M., Bürki, B., and Geiger, A. (2011c): Ultra precise geoid determination for a new generation of future linear collider: A feasibility study at CERN, XXV General Assembly of the International Union of Geodesy and Geophysics.
- Guillaume, S., Geiger, A., and Forrer, F. (2012): G-MoDe Detection of Small and Rapid Movement by Single GPS Carrier Phase Receiver. *Proceedings of The VII Hotine-Marussi Symposium Rome, 6-10 June, 2009 Series: International Association of Geodesy Symposia*, Springer, volume 137, Sneeuw, N.; Novák, P.; Crespi, M.; Sansò, F. (Eds.), DOI 10.1007/978-3-642-22078-4_21, pp. 141-145.
- Guillaume, S., and Bürki, B. (2012): QDAEDALUS ein CCD-Zusatzmodul für automatisierte optische Objektmessungen mittels Totalstationen, *Workshop Videotachymetrie TU München*.

- Guillaume, S., Jones, M., Bürki, B., and Geiger, A. (2012a): Determination of High Precision Underground Equipotential Profiles for the Alignment of a future Linear Collider at CERN in Geneva, International Symposium on Gravity, Geoid and Height Systems GGHS 2012.
- Guillaume, S., Bürki, B., Griffet, S., Mainaud Durand, H. (2012b): QDaedalus: Augmentation of Total Stations by CCD Sensor for Automated Contactless High-Precision Metrology, FIG Working Week 2012: Knowing to manage the territory, protect the environment, evaluate the cultural heritage, Rome, Italy, 6-10 May 2012.
- Guillaume, S., Jones, M., Bürki, B., and Geiger, A. (2012): Determination of High Precision Underground Equipotential Profiles for the Alignment of a future Linear Collider, International Association of Geodesy Symposia. Ref.: Ms. No. IAGS-D-12-00051R1, accepted on 22-05-2012.
- Guillaume, S., Jones, M., Bürki, B., and Geiger, A. (2012): Measurement of Underground Variations in the Deflection of the Vertical with a High Precision Interferometric Deflectometer, International Association of Geodesy Symposia. Ref.: Ms. No. IAGS-D-12-00052R1, accepted on 01-07-2012,
- Guillaume, S. (2015); Determination of a Precise Gravity Field for the CLIC Feasibility Studies, Ph.D. thesis, ETH Zurich.
- Häberling, S., and Geiger, A. (2011c): GPS-Gyro, 25th International Union of Geodesy and Geophysics General Assembly (IUGG 2011).
- Harrington, J., Peltzer, G., Leprince, S., Ayoub, and F., Kasser, M. (2011): Surface Deformation Associated With a Historical Diking Event in Afar From Correlation of Space and Air-Borne Optical Images. AGU Fall Meeting Abstracts, Vol. 1, P. 2226.
- Hashemi, A., Kalantari, M., and Kasser, M. (2013): Direct Calculation of the Parameters of Orientation and Position of a Set of Images. Appl. Math. Inf. Sci. 7, No. 4, pp. 1375-1382.
- Hatch, R.R. (2006): A New Three-Frequency, Geometry-Free, Technique for Ambiguity Resolution. In Proceedings of the 19th International Technical Meeting of the Satellite Division of The Institute of Navigation (ION GNSS 2006), Fort Worth, TX, September 2006, pp. 309-316.
- Hauk, M., Hirt, Ch., and Ackermann, Ch. (2014): Erprobung des astrogeodätischen Messsystems QDaedalus zur Bestimmung von genauen Lotabweichungen, Technische Universität München, Master Thesis.
- Henkel, P., and Günther, C. (2012): Reliable Integer Ambiguity Resolution: Multi-Frequency Code Carrier Linear Combinations and Statistical A Priori Knowledge of Attitude, J. Ins. Nav., 59 (1): 61-75, Spring 2012, doi: 10.1002/navi.6.
- Hiltebrand, K. (2014): Automated high precision optical aircraft tracking: Different methods of point extraction, ETH Zürich, Institute of Geodesy and Photogrammetry, Semester Work.
- Hollenstein, C., Männel, B., Scherer, L., Hiltebrand, K., Rothacher, M., Geiger, A., Kehl, P., Kronig, L., Ivanov, A., Kluser, M., Fleischmann, P., and Mathis, H. (2013): Evaluation of a Low-Cost GNSS Receiver for CubeSat Missions, 5th European CubeSat Symposium.
- Hollenstein, C., Männel, B., Serantoni, E., Scherer, L., Rothacher, M., Kehl, P., and Ivanov, A. (2014a): Concepts and testing of low-cost GNSS receivers for CubeSat orbit and attitude determination, 7th ESA Workshop on Satellite Navigation Technologies and European Workshop on GNSS Signals and Signal Processing (NAVITEC 2014).
- Hollenstein, C., Männel, B., Serantoni, E., Scherer, L., Rothacher, M., and Kehl, P. (2014b): Testing of low-cost GNSS receivers for CubeSat orbit and attitude determination, 6th European CubeSat Symposium, Estavayer-le-Lac, Switzerland.
- Hurter, F., and Geiger, A. (2011a): Geodetic contribution to the process understanding and prediction of hydrological extremes and complex hazards (APUNCH), 25th International Union of Geodesy and Geophysics General Assembly (IUGG 2011).
- Hurter, F., Geiger, A., and Perler, D. (2011b): Geodetic water vapor monitoring campaign in Zermatt, summer 2010, 9th Swiss Geoscience Meeting.

- Hurter, F., Geiger, A., Perler, D., and Rothacher, M. (2012): GNSS water vapor monitoring in the Swiss Alps. IEEE International Geoscience and Remote Sensing Symposium proceedings (2012), ISBN 9781467311601, DOI: 10.1109/IGARSS.2012.6351115 Munich, Germany.
- Hurter, F., and Maier, O. (2013): Tropospheric profiles of wet refractivity and humidity from the combination of remote sensing data sets and measurements on the ground, Atmospheric measurement techniques, 6, 3083–3098, doi:10.5194/amt-6-3083-2013.
- Hurter, F. (2014): GNSS meteorology in spatially dense networks, ETH-Zürich.
- IERS Conventions (2010): Petit, G. and Luzum, B. (eds.). (IERS Technical Note ; 36) Frankfurt am Main: Verlag des Bundesamts für Kartographie und Geodäsie, 2010. 179 pp., ISBN 3-89888-989-6
- Ivanov, A., Masson, L.A., Rossi, S., Belloni, F., Wiesendanger, R., Gass, V., Rothacher, M., Hollenstein, C., Männel, B., Fleischmann, P., Mathis, H., Klaper, M., Joss, M., and Styger, E. (2014): CubETH: low cost GNSS space experiment for precise orbit determination, Proc: Small Satellites Systems and Services Symposium, Porto Petro, Majorca, Spain.
- Kämpfer, N., editor (2013): Monitoring Atmospheric Water Vapour: Ground-Based Remote Sensing and In-situ Methods (ISSI Scientific Report Series). Springer, 2013 edition.
- Kamugasa, S. W., and Vlachakis, V. (2014): PACMAN study of FSI and Micro-Triangulation for the pre-alignment of CLIC, <http://indico.ihep.ac.cn/event/4156/session/38/material/2/0.pdf>, IWAA 2014, Beijing, China.
- Kasser, M., Touze, T., and De Joinville, O. (2011) : Le projet Z-Earth, étude des aspects géométriques et radiométriques de la mission. Septembre 2011, Rapport final du contrat CNES 4700031324/SIER490, 86 p.
- Kasser, M. (2011): Le GPS : utilisation en positionnement et surveillance. Techniques de l'Ingénieur, R 1384v2. 8 p.
- Kasser, M. (2012) : Auscultation des ouvrages d'art, la surveillance au fil du temps. Septembre 2012, Géomètre, pp. 30-39.
- Kasser, M. (2012) : Un impressionnant nouvel arrivant dans l'imagerie spatiale. Septembre 2012, Géomatique Suisse, pp. 436-438.
- Kasser, M. (2013) : Systèmes GNSS, la plénitude ? Des applications scientifiques originales. Mai 2013, Géomètre N° 2103, pp. 44-45.
- Kasser, M. (2013) : Systèmes GNSS, la plénitude ? La stabilisation d'un paysage plein de vitalité. Mai 2013, Géomètre, pp. 30-38.
- Kasser, M. (2013) : Topographie, topométrie, géodésie. Techniques de l'Ingénieur, C 5010v2. 20 p.
- Kasser, M. (2014) : Les nouveaux débouchés de la photogrammétrie. Mars 2014, Géomètre N° 2112, pp. 46-48
- Kirchner, G., Grunwaldt, L., Neubert, R., Koidl, F., Barschke, M., Yoon, Z., Fiedler, H., and Hollenstein, C. (2013): Laser Ranging to Nano-Satellites in LEO Orbits: Plans, Issues, Simulations, 18th International Workshop on Laser Ranging.
- Klaper, M., Lussi, M., Jordan, M., Bucher, M., Rohrer, T., Willener, Y., Hollenstein, C., Rothacher, M., Ivanov, A., Kronig, L., and Reinhard, R. (2013): Software framework for measurement campaigns on a CubeSat payload, 5th European CubeSat Symposium.
- Le Dantec, N. et al. (2014) : Morphological analysis of the upper reaches of the Kukuy Canyon derived from shallow bathymetry. In Proceedings of the "Bringing Together Selenga Baikal Research" (2014). Leipzig, Germany, September 2014.
- Leica Geosystems AG (2012): Leica Geo Office, Heerbrugg: Leica Geosystems AG. Available at: http://www.leica-geosystems.com/de/Leica-Geo-Office_4611.htm [accessed July 14, 2014].
- Li, B., Feng, Y., and Shen, Y. (2010): Three carrier ambiguity resolution: distance-independent performance demonstrated using semi-generated triple frequency GPS signals, GPS Solut., 14 (2): 177-184, doi: 10.1007/s10291-009-0131-6.

- Limpach, P. (2011a): Permanent GPS monitoring of slope instabilities: Case study at Dirru rockglacier, Mattertal, Jahrestagung der Schweizerischen Geomorphologischen Gesellschaft.
- Limpach, P., Geiger, A., Beutel, J., Buchli, B., Wirz, V., and Gruber, S. (2011b): Permanent monitoring of rock glaciers with low-cost GPS, Abstract Volume 9th Swiss Geoscience Meeting, p.373-374. Swiss Academy of Sciences (Ed.). November 2011, Zurich, Switzerland.
- Limpach, P., Geiger, A. (2011c): Permanente GNSS-Beobachtungen am Matterhorn. Geomatik Schweiz, Vol. 109, Issue 6, pp. Titelseite+257, ISSN 1660-4458.
- Limpach, P., Neyer, F., Geiger, A., Mueller-Gantenbein, J., Wiget, A., Marti, U., Rothacher, M., and Gilliéron, P.-Y. (2011d): X-Sense: Monitoring Alpine Mass Movements at Multiple Scales, XXV General Assembly of the International Union of Geodesy and Geophysics.
- Limpach, P. (2011f): Permanent GPS monitoring of slope instabilities: case study at Dirru rockglacier, Mattertal. Poster Presentation at the annual meeting of the Swiss Geomorphological Society (SGmG) 2011: "Mattertal – ein Tal in Bewegung". 29-30 June 2011, St. Niklaus, Switzerland.
- Limpach, P., Kretz, A., Villiger, A., and Geiger, A. (2012): Verdichtung des AGNES-Netzes im Wallis & Ueberwachung von Rutschgebieten mit low-cost GPS Sensoren, oral presentation at the Swiss4D Colloquium, swisstopo, January 2012, Bern, Switzerland.
- Limpach, P., Su, Z., and Geiger, A. (2013a): Continous monitoring of alpine slope instabilities with GPS sensors, 4th Annual Plenary Meeting of Nano-Tera.
- Limpach, P., Geiger, A., Gschwend, F., Ruesch, M., and Dawes, N. (2013b): Monitoring of snow height and snow water equivalent with GPS, Geophysical Research Abstracts, Vol. 15, EGU2013-11920, 2013, EGU General Assembly 2013, ISSN 1029-7006.
- Limpach, P., Su, Z., and Geiger, A. (2013c): Permanent monitoring of alpine slope instabilities with L1-GPS, Geophysical Research Abstracts, Vol. 15, EGU2013-13519, 2013, EGU General Assembly 2013, ISSN 1029-7006.
- Limpach, P., Gschwend, F., and Geiger, A. (2013d): How Snow Cover Affects the Positioning and Monitoring. GNSS 2013, ION-US, Nashville, TN.
- Limpach, P., Steiner, L., and Geiger, A. (2014a): GPS Zeitreihen am Aletschgletscher, Presentation at AHORN 2014 - der Alpenraum und seine Herausforderungen, November 2014, Graz, Austria
- Lutz, S., Schaer, S., Meindl, M., Dach, R., and Steigenberger, P. (2009): Higher-order ionosphere modeling for CODE's next reprocessing activities. AGU 2009 Fall Meeting, San Francisco, CA, USA, December 14-18, 2009.
- Lutz, S., Schaer, S., Meindl, M., Dach, R., and Steigenberger, P. (2010): Higher-Order Ionosphere Modelling for CODE's Next Reprocessing Activities. IGS Workshop 2010, Newcastle upon Tyne, England, 28 June - 2 July, 2010.
- Maier, O., and Hurter, F. (2012): Accuracy of Boundary Layer Humidity Profiles retrieved by GNSS Meteorology and Microwave Radiometry, 9th International Symposium on Tropospheric Profiling (ISTP 2012).
- Manning, T., Rohm, W., Zhang, K., Hurter, F., Wang, C., Rizos, C., and Willis, P. (2011): Determining the 4D dynamics of wet refractivity using GPS tomography in the Australian region, IAG General Assembly.
- Manning, T., Zhang, K., Rohm, W., Choy, S., and Hurter, F. (2012): Detecting Severe Weather using {GPS} Tomography: An Australian Case Study, Journal of Global Positioning Systems, 11, 58–70, doi:10.5081/jgps.11.1.58.
- Meindl, M., Wang, K., Geiger, A., and Rothacher, M. (2014): Single-difference ionospheric residuals in a regional network, IGS Workshop 2014.
- Mendes, V. B., and Pavlis, E.C. (2004) : High-accuracy zenith delay prediction at optical wavelengths. Geophys. Res. Let., 31, L14602, doi:10.1029/2004GL020308.
- Molina, P., Colomina, I., Victoria, T., Silva, P.F., Stebler, Y., Skaloud, J., Kornus, W., and Prades, R. (2011): EGNOS-based multi sensor accurate and reliable navigation in search-and-rescue missions with UAVs, Int. Arch. Photogramm. Remote Sens. Spat. Inf. Sci., vol. 38–1, no. C22, p. 7, 2011.

- Molina, P., Colomina, I., Victoria, T., Freire, P., and Skaloud, J. (2011): CLOSE-SEARCH: Accurate and safe EGNOS-SOL Navigation for UAV-based low-cost SAR operations, presented at the International Geomatic Week 2011, Barcelona, Spain, 2011.
- Molina, P., Colomina, I., Victoria, T., Skaloud, J., Kornus, W., Prades, R., and Aguilera, C. (2012): Drones to the rescue!, *GNSS*, vol. July/August, pp. 36–47, 2012.
- Molina, P., Colomina, I., Victoria, T., Skaloud, J., Kornus, W., Prades, R., and Aguilera, C. (2012): Searching lost people with UAVS: The system and results of the CLOSE-SEARCH project, *Int. Arch. Photogramm. Remote Sens. Spat. Inf. Sci.*, vol. 39–B1, pp. 441–446, 2012.
- Montenbruck, O., Hugentobler, U., Dach, R., Steigenberger, P., Hauschild, A. (2011): Apparent clock variations of the Block IIF-1 (SVN62) GPS satellite. *GPS Solutions*, vol. 16(3), pp. 303-313, DOI 10.1007/s10291-011-0232-x.
- Montenbruck, O., Steigenberger, P., Schönemann, E., Hauschild, A., Hugentobler, U., Dach, R., Becker, M. (2012): Flight Characterization of New Generation GNSS Satellite Clocks. *NAVIGATION: Journal of The Institute of Navigation* vol. 59(4), Winter 2012, pp. 291-302.
- Montenbruck, O., Steigenberger, P., Khachikyan, R., Weber, G., Langley, R., and Mervart, L. (2014): Preparing the ground for Multi-Constellation (GNSS) Science. *Inside GNSS*, number 1, pages: 42-49, volume: 9
- Münch, S., Bürki, B., Rothacher, M., Kahle, H.-G., Sorber, P., Becker-Ross, H., Florek, S., Okruss, M., and Tischendorf, R. (2011): Determination of Atmospheric Water Vapor Abundance using Solar Lunar Spectrometry, 25th International Union of Geodesy and Geophysics General Assembly (IUGG 2011).
- Münch, S. (2013): Atmospheric Water Vapour Sensing by means of Differential Absorption Spectroscopy using Solar and Lunar Radiation. PhD thesis, ETH Zürich. Diss. ETH No. 21491.
- Neyer, F., and Delaloye, R. (2011a): Displacement detection on rock glaciers using webcam images: A case study in the Mattertal, 9th Swiss Geoscience Meeting.
- Neyer, F., Delaloye, R., and Geiger, A. (2011b): Temporal Displacement detection on rock glaciers using webcam images: A case study in the Mattertal, Imst, Austria, Ahorn 2011
- Neyer, F., Limpach, P., Su, Z., Geiger, A., Strozzi, T., and Raetzo, H. (2011c): Getting the Most Accurate velocity Fields: Data Fusion of GPS and InSAR, Jahrestagung Schweizerische Geomorphologische Gesellschaft „Mattertal - ein Tal in Bewegung“, St. Niklaus, June, 2011.
- Neyer, F., and Geiger, A. (2012): Visualizing vector data: Clustering noisy displacement fields, 10th Swiss Geoscience Meeting.
- Neyer, F., Su, Z., Limpach, P., Delaloye, R., Raetzo, H., Beutel, J., and Gruber, S. (2012): The Potential of Merging Multiscale Data Sequences, 3rd Annual Plenary Meeting of Nano-Tera.
- Neyer, F., Limpach, P., and Geiger, A. (2013): Monitoring Rock Glaciers with GPS and High-Resolution Cameras, Presentation at the 2nd Joint International Symposium on Deformation Monitoring (JISDM), September 2013, Nottingham, UK.
- Neyer, F., Limpach, P., Gsell, T., Geiger, A., and Beutel, J. (2014): Permanent rock glacier monitoring with a stereo pair of optical cameras, Abstract Volume, 12th Swiss Geoscience Meeting, Fribourg, November 2014, p. 381.
- Nüssli, T. (2014): Automated high precision optical aircraft tracking: Determination of 3D trajectories, ETH Zürich, Institute of Geodesy and Photogrammetry, Semester Work.
- Ostini, L., Dach, R., Meindl, M., Schaer, S., and Hugentobler, U. (2008): FODITS: A New Tool of the Bernese GPS Software to Analyze Time Series. In *Proceedings of EUREF 2008 Symposium*, Brussels, Belgium, June 18-21, 2008.
- Ostini, L. (2012): Analysis and Quality Assessment of GNSS-Derived Parameter Time Series. PhD thesis of the Philosophisch–naturwissenschaftlichen Fakultät of the University of Bern.
- PACMAN project (2015): web site <http://pacman.web.cern.ch/pacman>

- Perler D., Hurter, F., Brockmann, E., Leuenberger, D., Ruffieux, D., Geiger, A., and Rothacher, M. (2010): GNSS meteorology: Activities in Switzerland. Paper presented at the COST Action ES0702 EG-CLIMET meeting Nov 16-19, 2010, Cologne, Germany.
- Perler, D., Geiger, A., and Hurter, F. (2011a): 4D GPS water vapor tomography: New parameterized approaches, *Journal of Geodesy*, 85, 539–550, doi:10.1007/s00190-011-0454-2.
- Perler, D., Geiger, A., and Rothacher, M. (2011b): Determination of the 4D-Tropospheric Water Vapor Distribution by GPS for the Assimilation into Numerical Weather Prediction Models, AGU Fall Meeting 2011.
- Perler, D., and Geiger, A. (2011c): GPS-Tomography and Assimilation in Numerical Weather Models (GANUWE), 25th International Union of Geodesy and Geophysics General Assembly (IUGG 2011).
- Prange, L., Dach, R., Lutz, S., Schaer, S., and Jäggi, A. (2014): The CODE MGEX orbit and clock solution. In: Willis, P. (Ed.), IAG Potsdam 2013 Proceedings. International Association of Geodesy Symposia. Springer, accepted for publication.
- Prange, L., Orliac, E., Dach, R., Schaer, S., and Sośnica, K. (2015): CODE five system solution for IGS MGEX, this volume
- Psimoulis, P. A., and Stiros, S.C. (2012): A supervised learning computer-based algorithm to derive the amplitude of oscillations of structures using noisy GPS and robotic theodolites (RTS) records, *Computers & structures*, 92-93, 337–348, doi:10.1016/j.compstruc.2011.10.019.
- Rehak, M., Skaloud, J., and Mabillard, R. (2013): A micro-UAV with the capability of direct georeferencing, in UAV-g, Rostock, Germany, 2013.
- Rehak, M., Mabillard, R., and Skaloud, J. (2014): A micro aerial vehicle with precise position and attitude sensors, *Photogramm. Fernerkund. Geoinformation PFG*, vol. 4, no. August, pp. 239–251, 2014.
- Rodrigues, E., and Kasser, M. (2014a): Limnimétrie par réflectométrie GNSS à faible coût. Août 2014, *Geomatik Schweiz* 8/2014, pp. 349-354.
- Rodrigues, E., and Kasser, M. (2014b) : Limnimétrie par réflectométrie GNSS à faible coût. Juin 2014, *XYZ N°* 139, pp. 51-58.
- Röösli, C., and Rothacher, M. (2011): First Galileo Data Processing, 25th International Union of Geodesy and Geophysics General Assembly (IUGG 2011).
- Rothacher, M. (2012b): Precise Point Positioning (PPP); Spezielle Aspekte: Mehrdeutigkeitslösungen und Real-Time, Informationsnachmittag „PPP“, Hochschule für Technik Rapperswil (HSR).
- Salzgeber, R. (2014): Automated high precision optical aircraft tracking: Software Development in C++, ETH Zürich, Institute of Geodesy and Photogrammetry, Semester Work.
- Scaramuzza, M., Wipf, H., and Geiger, A. (2013a): GNSS Navigation Performance versus Aerial Vehicle's Trajectory in Mountainous Terrain, International Symposium on Precision Approach and Performance Based Navigation (ISPA) 2013, proc. paper, Braunschweig
- Scaramuzza, M., Wipf, H., and Geiger, A. (2013b): GNSS Navigation Performance versus Aerial Vehicle's Trajectory in Mountainous Terrain. ISPA 2013, DGON, Berlin, Germany, Proceedings, pp 203-209. Presentation and publication.
- Scaramuzza, M., Wipf, H., Troller, M., Leibundgut, H., Wittwer, R., and Rämi, S. (2014): GNSS RFI Detection in Switzerland based on Helicopter Recording Random Flights. IFIS 2014, Oklahoma City, USA, Proceedings. Presentation and publication.
- Schaer, S., Brockmann, E., and Meindl, M. (2009): Rapid Static Positioning Using GPS and GLONASS. In: Ihde, J. and H. Hornik (Eds): Subcommission for the European Reference Frame (EUREF), Firenze, 2009.
- Schaer, S. et al. (2011): IGSREPORT #19560: Wk 1625 COD Analysis Report. <https://igsceb.jpl.nasa.gov/pipermail/igsreport/2011-March/019572.html>.
- Schaer, S. (2014): CODE GIM products with 1-hour resolution, IGSMail-6993, IGS Central Bureau Information System.

- Schwendener, M., Scaramuzza, M., and Leibundgut, H. (2014): Flight Inspection of Helicopter Procedures in a Challenging Topographic Environment. IFIS 2014, Oklahoma City, USA, Proceedings. Presentation and publication.
- Scirè Scappuzzo, F., Bürki, B., Geiger, A., Kahle, H.-G. (2011): Analysis and corrections of non-hydrostatic effects on GNSS observations and antenna errors for accurate GPS and Galileo IWV estimates, 25th International Union of Geodesy and Geophysics General Assembly (IUGG 2011).
- Sierk, B. (2001): Solar Spectrometry for Determination of Tropospheric Water Vapor. PhD thesis, ETH Zürich. Diss. ETH No. 13850.
- Skaloud, J., and Schaer, P. (2012): Automated assessment of digital terrain models derived from airborne laser scanning,” *Photogramm. Fernerkund. Geoinformation PFG*, vol. 2, pp. 105–114, 2012.
- Skaloud, J., Rehak, M., and Lichti, D. (2014): Mapping with MAV: Experimental study on the contribution of absolute and relative position control, *Int. Arch. Photogramm. Remote Sens. Spat. Inf. Sci.*, vol. 40–3/W1, pp. 123–129, 2014.
- Skaloud, J., Rehak, M., and Clausen, P. (2014): Ein Mikroflugzeug zur genauen Kartierung ohne Passpunkte am Boden, *Geomatique Suisse*, vol. 9, pp. 376–380, 2014.
- Somieski, A. (2005): Geodetic Mobile Solar Spectrometer. PhD thesis, ETH Zürich. Diss. ETH No. 15881.
- Stebler, Y., Guerrier, S., Skaloud, J., and Victoria-Feser, M.-P. (2011): Constrained expectation-maximization algorithm for stochastic inertial error modeling: study of feasibility, *Meas. Sci. Technol.*, vol. 22, no. 8, p. 12, 2011.
- Stebler, Y., Guerrier, S., Skaloud, J., and Victoria-Feser, M.-P. (2012) : A Framework for inertial sensor calibration using complex stochastic error models, in *IEEE-ION Position Location and Navigation Symposium (PLANS)*, Myrtle Beach, SC, USA, 2012.
- Stebler, Y., Filliger, R., and Skaloud, J. (2012): Event analyzer for accident reconstruction, EPFL, 2012.
- Stebler, Y., Guerrier, S., Skaloud, J., and Victoria-Feser, M.-P. (2014): The generalized method of wavelet moments for inertial navigation filter design, *IEEE Trans. Aerosp. Electron. Syst.*, vol. 50, pp. 2269–2283, 2014.
- Stern, G., Lackner, F., Mainaud Durand, H., Piedigrossi, D., and Geiger, A. (2012): Feasibility Study of Multipoint Based Laser Alignment System for CLIC, 12th International Workshop on Accelerator Alignment (IWAA 2012), Fermilab, Batavia, U.S.A, September 10-14.
- Stern, G., Kemppinen, J., Lackner, F., Mainaud-Durand, H., Piedigrossi, D., Sandomierski, J., Sosin, M., Geiger, A., and Guillaume, S. (2013): Development and validation of a multipoint based laser alignment system for CLIC, 4th International Particle Accelerator Conference (IPAC 2013).
- Stern, G. (2014a): Laser Based Alignment Systems for CLIC, *Advanced Low Emittance Rings Technology (ALERT 2014)*, Workshop.
- Stern, G. (2014b): LAMBDA project, Mini Workshop Laser Based Alignment Systems at CERN.
- Stern, G. (2014c): Summary and Conclusions of the Mini Workshop on Laser Based Alignment Systems, CLIC Workshop at CERN.
- Stern, G., Mainaud-Durand, H., Piedigrossi, D., Sandomierski, J., Sosin, M., Geiger, A., and Guillaume, S. (2014): Experiments of Laser Pointing Stability in Air and in Vacuum to Validate Micrometric Positioning Sensor. In *Proceedings of 5th International Particle Accelerator Conference (IPAC14)*, Dresden, June 15-20, 2014.
- Stern, G., Mainaud-Durand, H., Piedigrossi, D., Sandomierski, J., Sosin, M., Geiger, A., Guillaume, S., and Ruland, R. (2014): Experiments of Laser Pointing Stability on Different Surfaces to Validate Micrometric Positioning Sensor, 13th International Workshop on Accelerator Alignment, Beijing, October 13-17.
- Sterren, J. (2014): Re-Processing lokale Hebungsdaten 2012-2013 in den Schweizer Alpen (Wildhorndecke). Bachelor Thesis 2014/02. Muttenz: Fachhochschule Nordwestschweiz.

- Stiros, S. C., and Psimoulis, P.A. (2012): Response of a historical short-span railway bridge to passing trains: 3-D deflections and dominant frequencies derived from Robotic Total Station (RTS) measurements, *Engineering structures*, 45, 362–371, doi:10.1016/j.engstruct.2012.06.029.
- Su Z., Limpach, P., Rothacher, M., and Geiger, A. (2011): Improving sub-daily solutions of single-frequency GPS using antenna PCV, 9th Swiss Geoscience Meeting.
- Su, Z., Geiger, A., and Limpach, P. (2012): Investigation on the performance of low-cost single-frequency GPS, 3rd International Conference on Machine Control and Guidance, March 27-29, 2012, Stuttgart, Germany
- Su, Z., Geiger, A., Rothacher, M., and Limpach, P. (2013a): Carrier phase multipath identification, modeling and mitigation: Application to short baselines used in L1 low-cost GPS monitoring, International Association of Geodesy Scientific Assembly 2013.
- Su, Z., Limpach, P., and Geiger, A. (2013b): Real Time Geomonitoring with Low-cost L1 GPS, Nano-Tera Annual Plenary Meeting 2013: Virtual Edition.
- Su, Z., Geiger, A., Limpach, P., Beutel, J., Gsell, T., Buchli, B., Gruber, S., Wirz, V., and Sutton, F. (2014a): Online monitoring of alpine slope instabilities with L1 GPS Real Time Kinematic Positions, *Geophysical Research Abstracts*, Vol. 16, EGU2014-7733, EGU General Assembly 2014, ISSN 1029-7006.
- Su, Z., Sun, B., Geiger, A., and Rothacher, M. (2014b): The potential benefits of Multi-constellation GNSS, Abstract Volume 12th Swiss Geoscience Meeting, 12, 361–361.
- Tarasov, M., Shinkareva, G., Constantin, D., Akhtman, Y. et al. (2015): Investigation of heavy metals distribution in suspended matter and macrophytes of the Selenga river delta using airborne hyperspectral remote sensing. EARSel 2015, Luxembourg. April 2015
- Thaller, D., Mareyen, M., Dach, R., Beutler, G., Gurtner, W., Richter, B., and Ihde, J. (2009): Preparing the Bernese GPS Software for the analysis of SLR observations to geodetic satellites. 16th International Workshop on Laser Ranging, Poznan, Poland, October 13-17, 2008, vol. 1, pp. 143-147.
- Thaller, D., Dach, R., Seitz, M., Beutler, G., Mareyen, M., and Richter, B. (2010): Combination of GNSS and SLR observations using satellite co-locations. Accepted for publication in *Journal of Geodesy*, doi:10.1007/s00190-010-0433-z.
- Troller, M., Scaramuzza, M., Truffer, P., Wipf, H., and Raemi, S. (2012): Performance Impact of Mountainous Topography for Cloud Break GNSS Procedure. ION GNSS 2012, US ION, Nashville, USA, Proceedings. Presentation and publication.
- Troller, M., Germann, R., Friik, A., Bertschi, M., Truffer, P., and Scaramuzza, M. (2013): Curved Approach Segments for Noise Abatement. ION GNSS 2013, US ION, Nashville, USA, Proceedings. Publication.
- Troller, M., Scaramuzza, M., and Germann, R. (2013): RF Leg for Departures: One Year of successful experience. ISPA 2013, DGON, Berlin, Germany, Proceedings. Presentation and publication.
- Waegli, A., Skaloud, J., Guerrier, S., and Pares, E. (2010) : Noise reduction and estimation in multiple micro-electromechanical inertial systems, *Meas. Sci. Technol.*, vol. 21, pp. 065201–065212, 2010.
- Wang, K., and Rothacher, M. (2012): Ionosphere-free and geometry-free triple-frequency combinations for ambiguity resolution: theory and first results with real data: Theory and first results with real data, AGU Fall Meeting 2012.
- Wang, K., and Rothacher, M. (2013a): Ambiguity resolution for triple-frequency geometry-free and ionosphere-free combination tested with real data, *Journal of Geodesy*, 87, 539–553, doi:10.1007/s00190-013-0630-7.
- Wang, K., and Rothacher, M. (2013b): Satellite track-to-track ambiguity resolution for GNSS dual- and triple-frequency linear combinations, European Geoscience Union General Assembly 2013.
- Wang, K., and Rothacher, M. (2014): Modeling of low-stability GPS receiver clocks and its impact on pseudo-range kinematic coordinates, European Frequency and Time Forum (EFTF 2014).
- Wang, K., Meindl, M., Geiger, A., Rothacher, M., Scaramuzza, M., Troller, M., and Truffer, P. (2014): Assessment of Single-difference Ionospheric Residuals in a Regional Network for GBAS, 27th International Technical Meeting of The Satellite Division of the Institute of Navigation (ION GNSS+ 2014), Tampa, Florida, September 2014, 2384–2393.

- Wang, K., Meindl, M., Geiger, A., Rothacher, M., Scaramuzza, M., Troller, M., Truffer, P. (2015): Non-ionosphere biases in the single-difference ionospheric residuals, Proc., European Navigation Conference, ENC15, Bordeaux, 2015 (submitted).
- Weber, S., Beutel, J., Buchli, B., Gruber, S., Gsell, T., Lim, R., Limpach, P., Raetzo, H., Su, Z., Sutton, F., Walser, C., Wirz, V., and Vieira, G. (2014): PermaSense L1-GPS for kinematic monitoring, 4th European Conference on Permafrost: Book of Abstracts, June 2014, Évora, Portugal, pp. 186-187.
- Wiget, A. (2014): Satellitengestützte Messungen (GNSS) in der Staumauerüberwachung – Mesures par satellites (GNSS) pour la surveillance des barrages. Vortrag an der Fachtagung des Schweizerischen Talsperrenkomitees (in German and French). Chamonix, 12./13. Juni 2014. Veröffentlichung geplant in – to be published in «Wasser, Energie Luft».
- Willi, D., and Skaloud, J. (2014): Prediction of phase ambiguity resolution based on signal intensity and geometry, GPS Solut., pp. 1080–5370, 2014.
- Wirz, V., Limpach, P., Beutel, J., Geiger, A., and Gruber, S. (2011a): Investigating diverse phenomena of slope movement in mountain areas, XVIII INQUA-Congress: Quaternary sciences – the view from the mountains.
- Wirz, V., Beutel, J., Buchli, B., Limpach, P., Gruber, S., and Su, Z. (2011b): Temporal characteristics of various cryosphere-related slope movements in high mountains: GPS measurements and analysis, Abstract Volume 9th Swiss Geoscience Meeting, p.282, Swiss Academy of Sciences (Ed.), November 2011, Zurich, Switzerland.
- Wirz, V., Gruber, S., Beutel, J., Buchli, B., Limpach, P., and Geiger, A. (2011c): Temporal characteristics of different mountain cryosphere-related debris slope movements. The Second World Landslide Forum - Abstract Book, p. 672, 3-9 October 2011, FAO, Rome, Italy, ISPRA. ISBN 978-88-448-0515-9.
- Wirz, V., Beutel, J., Buchli, B., Gruber, S., Limpach, P. (2013): Temporal Characteristics of Different Cryosphere-Related Slope Movements in High Mountains. *Landslide Science and Practice*, Vol. 4, pp. 383-390.
- Zeiner, A. (2012): Umweltforschung mit Leica GRX1200, *Leica Reporter*, das Magazin der Leica Geosystems, Vol. 66, p. 10-11.
- Zhe, L., Geiger, A., Guillaume, S., Su, Z., Häberling, S., and Psimoulis, P. (2012): Small and Fast Motion Detection using GPS receiver Single-Frequency Carrier Phase Observations, 10 th Swiss Geoscience Meeting.